COMPUTER-AIDED SIMULATION AND OPTIMISATION OF ROAD VEHICLE SUSPENSION SYSTEMS

by

Alwyn Francois Naudé

Submitted in partial fulfilment of the requirements for the degree

PHILOSOPHIAE DOCTOR (MECHANICAL ENGINEERING)

in the Faculty of Engineering, the Built Environment and Information Technology

University of Pretoria
Pretoria

University of Pretoria

2001

COMPUTER-AIDED SIMULATION AND OPTIMISATION OF ROAD VEHICLE SUSPENSION SYSTEMS

Alwyn Francois Naudé

Promoter: Prof J.A. Snyman
Department: Mechanical and Aeronautical Engineering
Degree: Philosophiae Doctor (Mechanical Engineering)

Abstract

Problems were experienced during the development of a military three-axle vehicle weighing 22 tons. These problems included premature axle and suspension failures. In trying to solve these problems full three-dimensional parametric studies were performed using commercially available computer-aided vehicle dynamic simulation programs. Performing these parametric simulation studies proved to be a cumbersome task. The need for a computationally economic computer-aided simulation program coupled to a systematic optimisation process for the optimisation of the vehicle's suspension system therefore arose.

After the presentation of an overview of relevant work that has been done in the field of suspension optimisation, this study continues with the development of a two-dimensional multi-body vehicle dynamics simulation program that is to be linked to a robust mathematical optimisation algorithm. The optimisation algorithm selected is the gradient based LFOPC algorithm for constrained optimisation. With this algorithm the design space can be systematically searched for a set of design variables that optimises the suspension system with respect to ride-comfort.

For the above purposes a two-dimensional vehicle dynamics simulation program Vehsim2d is developed here. In order to enable the optimisation of non-linear suspension characteristics, a six piece-wise continuous linear approximation is used for representing spring, damper, bump stop, tyre stiffness and tyre damping characteristics. With this approach twelve design variables are used to describe the characteristic of each of the suspension components. The simulation results of the Vehsim2d program are qualified by comparing them with that of the more advanced DADS program and by comparison with experimentally measured values on a real military vehicle.

A comprehensive case study is presented in which the damper characteristics for the three axle military vehicle is optimised. Three different route profiles are selected as representative terrain over which the vehicle is to prove its mobility. One of the road profiles used is a dirt road profile of length 2.2 km and is specifically selected because the major suspension failures on the vehicle occurred on similar road profiles. An objectively determined ride-comfort value at the driver, centre of gravity, rear passenger and for pitch movement of the vehicle is used as the objective function for the optimisation. From the optimisation results an improvement of up to 40% in ride-comfort is obtained. These results were again qualified by means of DADS simulations.

In conclusion this study proves that the Vehsim2D/LFOPC modelling and optimisation system is a valuable tool for vehicle designers.

Keywords: *vehicle suspension optimisation, passive suspension, mathematical programming, gradient based optimisation algorithm, two-dimensional vehicle model*

REKENAARGESTEUNDE SIMULASIE EN OPTIMERING VAN PADVOERTUIG SUSPENSIESTELSELS

Alwyn Francois Naudé

Promotor: Prof J.A. Snyman
Departement: Meganiese en Lugvaartkundige Ingenieurswese
Graad: Philosophiae Doctor (Meganiese Ingenieurswese)

Samevatting

Probleme is tydens die ontwikkeling van 'n drie-as militêre voertuig, met massa 22 ton, ondervind. Die probleme het onder andere vroeë faling van die voertuig aste en suspensiekomponente ingesluit. Tydens pogings om hierdie probleme op te los, is volle drie dimensionele parametriese studies met kommersieël beskikbare voertuig dinamika simulasie pakkette uitgevoer. Die uitvoer van hierdie parametriese studies was omslagtig. Die behoefte aan 'n numeries ekonomiese rekenaargesteunde simulasie program wat gekoppel word aan 'n sistematiese optimeringsproses vir die optimering van die voertuigsuspensie het dus ontstaan.

Na die aanbieding van 'n oorsig oor relevante navorsing in verband met suspensie optimering, gaan die studie voort met die ontwikkeling van 'n twee dimensionele voertuig dinamika simulasie program wat aan 'n robuuste wiskundige optimeringstegniek gekoppel word. Die optimeringsalgoritme wat vir hierdie doel gekies is, is die gradiënt gebaseerde LFOPC algoritme vir begrensde optimeringsprobleme. Met hierdie optimeringstegniek kan 'n ontwerpgebied sistematies deursoek word om die ontwerpsveranderlikes te vind wat die voertuig suspensie ten opsigte van ritgemak sal optimaliseer.

Vir bogenoemde doel is 'n twee dimensionele voertuigdinamika simulasiepakket Vehsim2d ontwikkel. Ten einde die optimering van die nie-linieêre karakteristiek van suspensiekomponente te kan uitvoer, word 'n ses-stuksgewyse kontinue linieêre benadering gevolg vir die beskrywing van die karakteristieke van die vere, dempers, deurstampstoppe, bandstyfheid en banddemping. Met hierdie benadering word twaalf ontwerpsveranderlikes gebruik vir beskrywing van die karakteristiek van elke suspensiekomponent. Die simulasieresultate is gekwalifiseer deur die simulasieresultate te vergelyk met simulasieresultate van die meer gevorderde program DADS asook eksperimenteel gemete waardes op 'n werklike militêre voertuig.

'n Uitgebreide gevallestudie waartydens die demperkarakteristieke van die drie-as militêre voertuig ge-optimeer is, word gegee. Drie verskillende padprofiele is vanaf die voertuig se mobiliteitsvereistes geselekteer as verteenwoordigende terrein waaroor die voertuigmobiliteit bewys moet word. Een van die padprofiele is 'n grondpad met lengte 2.2 km en is spesifiek ingesluit aangesien die meeste van die falings op soortgelyke terrein ondervind was. Objektiewe bepaalde ritgemak waardes by die bestuurder, massamiddelpunt, agterste passsasier en vir heibeweging van die voertuigromp is as doelfunksie tydens die optimering gespesifiseer. Vanuit die optimeringsresultate is gevind dat daar tot 'n 40% verbetering in die ritgemak verkry kan word. Hierdie resultate is weereens gekwalifiseer deur die uitvoer van simulasies met die program DADS.

Ten slotte bewys hierdie studie dat die Vehsim2d/LFOPC modellering- en optimeringstelsel 'n waardevolle gereedkapstuk vir voertuigontwerpers is.

Sleutelterme: voertuig suspensie optimering, passiewe suspensie, wiskundige programmering, gradient gebaseerde optimerings-algoritme, twee-dimensionele voertuig model

Acknowledgements

I would like to express my sincere thanks to the following for their contribution during this study:

- Prof. J.A. Snyman for his professional leadership and willingness to help with any problem experienced.
- Dr. S. Nell and mr. C. Giliomee of Land Mobility Technologies for their support with DADS simulations and the supply of data and information.
- Mr. F.J. Beetge of Armscor, the project leader on the Okapi vehicle project, for arranging financial support from Armscor for this study.
- My wife, Annalene, for her support and encouragement.
- My heavenly Father for giving me the health and capabilities to perform this work.

Contents

1. Introduction

A vehicle's suspension has a primary influence on its ride characteristics. Most of the literature available on this subject concentrates on four-wheel vehicles and in particular on passenger cars. When designing vehicles for other specialised applications, in particular for armoured personnel carriers, many of the standard design parameters may change because of the following considerations:

i. high mass and inertia may arise due to the armour and land mine protection used,
ii. high centre of gravity may occur due to the characteristic V shape hull used,
iii. use of more wheels for increased mobility may be required in order to reduce the average ground pressure to be applied,
iv. the vehicles may be required to operate over a wide range of terrain, from on-road to extreme off-road conditions, and
v. reliability is to be of utmost importance.

A specific example of such a vehicle is the Okapi 6x6 vehicle developed by Armscor, Truckmakers, Reumech Ermetek and Vickers OMC. The vehicle weighs 22 tons, uses three axles, carries electronic equipment and personnel. The vehicle uses a solid axle suspension with leaf springs. Four dampers on each of the front and rear axles and two dampers on the middle axle are used. Figure 1.1 shows the Okapi vehicle.

Figure 1.1: The Okapi vehicle.

During the development of the Okapi axle failures were experienced on the front axle of the vehicle [1, 2]. The axles used on the Okapi vehicle were the same as that used on other vehicles with similar static axle loads. In order to explain the axle failures, experimental evaluations of the Okapi vehicle and two other military vehicles, the Withings and Kwêvoël were performed. Both the Withings and Kwêvoël vehicles use similar axles as the Okapi. These vehicles were driven over the same terrain and at the same speed as the Okapi. Strain gauge measurements indicated that although the Okapi vehicle did not experience the highest axle forces, it was subjected to more severe force reversals and that the axles on the Okapi vehicle failed due to fatigue of the axles. At that stage this phenomenon could only be explained due to the specific axle configuration and suspension used on the Okapi.

An upgrade on the axles of the Okapi vehicle was performed. Higher load rating axles from a different supplier were used. At the same time a suspension upgrade was done based on the results of computer simulations. Computer-aided vehicle dynamic simulations were done with different spring and damper stiffness combinations. In successive simulations the spring stiffnesses in the vehicle were decreased and the damper configurations were changed. Due to time constraints only a limited parametric study could be performed [2].

Vehicle tests were conducted with the upgraded axles and the new suspension. During these tests damper failures were experienced. Investigation of the failed dampers indicated that too high damper deflection rates and forces were experienced during vehicle operation.

Since the start of the Okapi project it was already clear that designing a 6x6 suspension would not be a simple task. Although complete three dimensional vehicle simulation studies had been performed by the Laboratory for Advanced Engineering using GENRIT [3], and by Reumech Ermetek and Vickers OMC using DADS [4], it was realised that to fully understand the 6x6 vehicle suspension and to improve the suspension would be a difficult and cumbersome task. This would be so mainly due to the large number of variables involved and the limit on available computational time.

The need for the present study arose in parallel with experiencing the above problems with the Okapi vehicle suspension. Clearly a simple but yet effective systematic vehicle suspension modelling and optimisation system, enabling improvement of vehicle suspensions was required. The program should be such that it can be used by the project manager and the design team to simulate the vehicle suspension and to determine the parameters to be adjusted so as to improve certain evaluation criteria. In addition the system should be robust, user friendly and easy to implement without the need to simulate the vehicle in the finest detail. For these first order simulations, required during the design stage, it is suggested that a two-dimensional vehicle dynamic simulation program would be appropriate. Although the specific vehicle example is a 6x6 (three axle) vehicle, the same problems occur during the concept design of 4x4 (two axles) and 8x8 (four axles) vehicles.

In a study by Etman [5] a suspension optimisation was performed during the design of a stroke dependent damper for the front axle suspension of a truck. The first optimisation was done using a quarter car model. Due to its simplicity the quarter car model is not highly accurate [5] and a great deal of the dynamic behaviour of the truck is not included. A second optimisation study was done using a full-scale (3-D) DADS model of the truck with a total of 34 degrees of freedom. In his conclusion Etman [5] states that the step from a quarter car model to a full-scale model "has been pretty large" and suggests that possibly a six degree of freedom model should rather be used.

In the remainder of this chapter the basic principles of vehicle suspension are described and a brief literature survey of optimisation of vehicle suspensions is presented. Finally the achievements and shortcomings of the existing studies will be discussed and the specific goal of the present study will be outlined.

1.1 Primary functions of the vehicle suspension

According to Gillespie [6] the primary functions of a vehicle suspension system are:

i. to provide vertical compliance so the wheels can follow the uneven road, isolating the chassis from roughness in the road,
ii. to maintain the wheels in the proper steer and camber attitudes to the road surface,
iii. to react to control forces produced by the tyres,
iv. to resist roll of the chassis, and
v. to keep the tyres in contact with the road with minimal load variations.

The importance of the suspension system in order to provide suitable ride and handling have long been known, for example Sternberg [7] states that: "*The suspension provides a cushioning means between the axle and the frame and therefore is important in providing suitable ride qualities, as well as providing suitable cushioning properties for the cargo. Improved riding qualities are becoming of greater importance and, therefor, the role of suspensions in providing improved cushioning for both the driver and the cargo will receive more attention in the future.*"

Gillespie [6] further states the following regarding the vehicle suspension: "*The properties of a suspension important to the dynamics of the vehicle are primarily seen in the kinematic (motion) behaviour and its response to the forces and moments that it must transmit from the tyres to the chassis. In addition, other characteristics considered in the design process are cost, weight, package space, manufacturability, ease of assembly and others*".

As can be seen from Sternberg and Gillespie the importance of the vehicle suspension in regard to the vehicle quality, ride comfort, handling, driver perception, etc. are of primary consideration during

the development and design of vehicles. This is also apparent from the huge amount of research that has been done in this regard (see references).

In general improvement of vehicle suspension will give the following:

i. improvement of vehicle ride quality,
ii. increased vehicle mobility, and
iii. increased component life.

The specific requirements for the vehicle suspension are directly coupled to the mobility requirements and the application of the vehicle. For example in some instances ride comfort may be sacrificed to improve handling or visa versa.

1.2 Vehicle suspension systems

Vehicle suspension systems can be divided into two groups, namely solid axle and independent suspensions [6, 7, 8, 9]. Figures 1.2 and 1.3 show the difference between the two types of suspension systems.

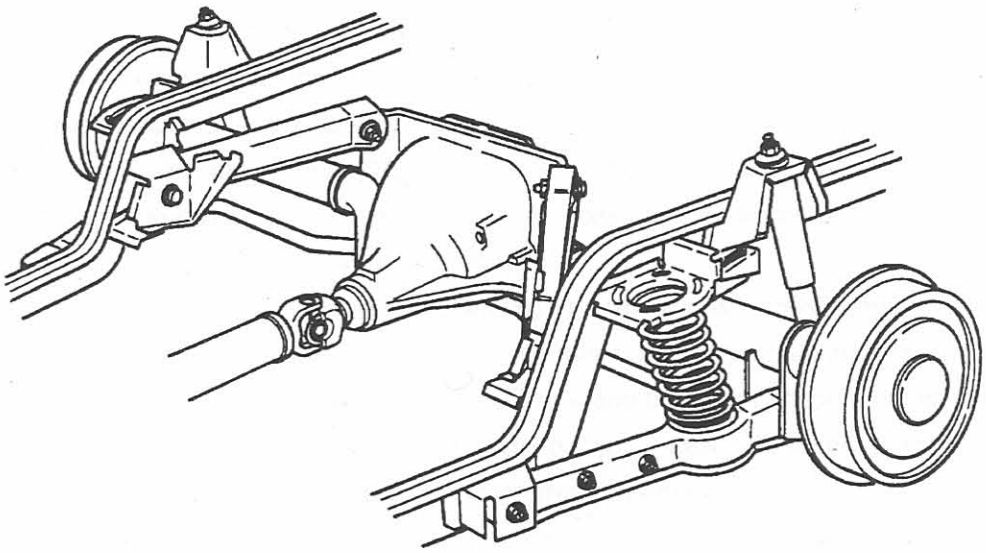

Figure 1.2: Example of a solid axle suspension (after Gillespie [6]).

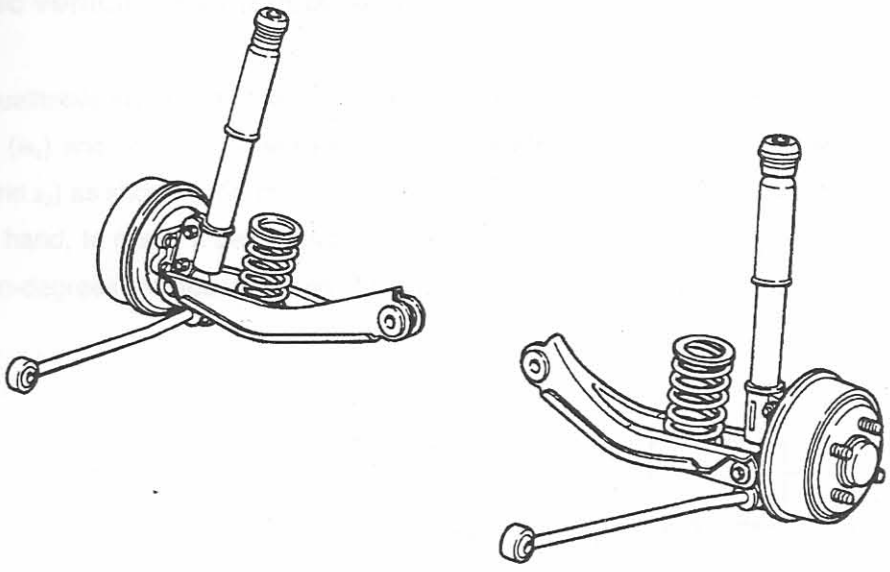

Figure 1.3: Example of an independent suspension system [6].

Many variations of these two suspension systems exist [6, 7, 8, 9]. The main components of a suspension system are the following:

i. Geometrical components. Examples are: connecting rods, swing arms, Panhard rods, links, trailing arms, sliding tubes etc. The functions of these components are to connect the wheels/axles to the vehicle body and to keep the tyres in the proper camber and steer attitude.

ii. Springs. The springs of the suspension can be divided into leaf springs, coil springs, torsion bars, rubber springs and air springs. The function of the springs are explained by Nunney [8]: *"When the road wheels rise and fall over surface irregularities, the springs momentarily act as energy storage devices and thereby greatly reduces the magnitude of loading transmitted by the suspension system to the vehicle structure".*

iii. Dampers. According to Gillespie [6]: *"Damping in suspensions comes primarily from the action of hydraulic shock absorbers. Contrary to their name, they do not absorb the shock from road bumps. Rather the suspension absorbs the shock and the shock absorber's function then is to dissipate the energy put into the system by the bump."* Telescopic shock absorbers have been used almost exclusively for damping in automotive suspensions.

iv. Bump stops. These are in principle secondary springs that limit the total suspension deflection. Generally bump stops consists of a rubber stop.

1.3 Basic vehicle ride models [6, 9]

To obtain a qualitative insight into the functions of the suspension and in particular of the effects of the sprung mass (m_s) and unsprung mass (m_{us}) on vehicle vibration, a linear model with two degrees of freedom (z_1 and z_2) as shown in figure 1.4, may be used. This is the so-called quarter car model [5, 6]. On the other hand, to reach a better understanding of the pitch and bounce of the vehicle body, an alternative two-degrees of freedom (z and θ) model as shown in figure 1.5 may be preferable.

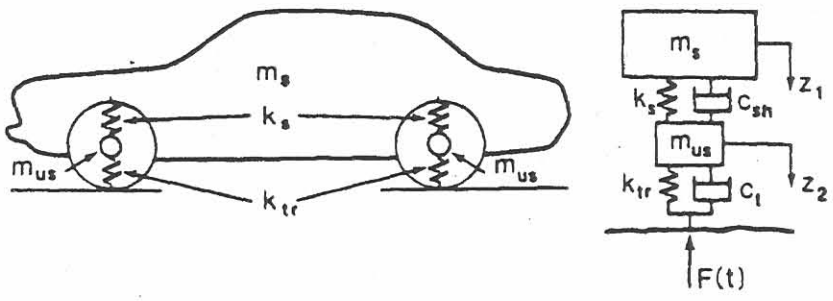

Figure 1.4: A two-degrees of freedom ride model for the sprung and unsprung mass (after Wong [9]).

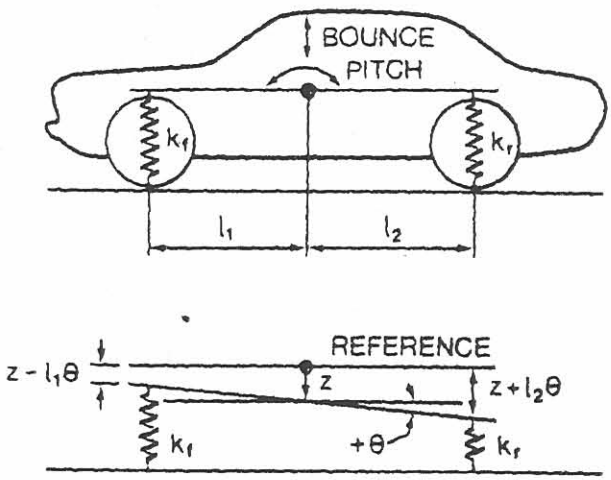

Figure 1.5: A two-degrees of freedom model for pitch and bounce of the sprung mass [9].

1.3.1 The quarter car model for sprung and unsprung masses

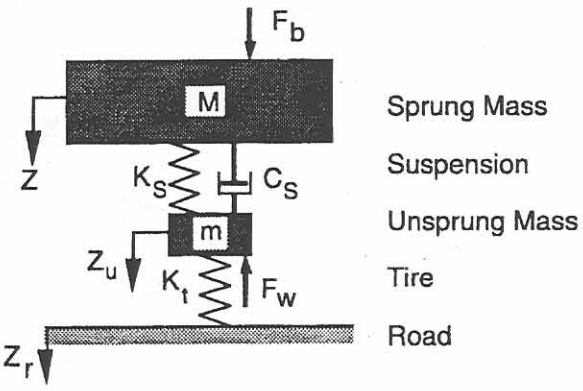

Figure 1.6: Quarter car model (after Gillespie [9]).

The two degrees of freedom quarter car model shown in figure 1.6 includes an unsprung mass m consisting of the wheels and associated components, and a sprung mass M representing the vehicle body. The respective displacements of the masses M and m in the vertical direction are denoted by Z and Z_u, with origins at the static equilibrium positions. Using Newton's second law and neglecting the effect of the tire damping, the equations of motion for the system can be obtained [6,9]:

for the sprung mass:

$$M\ddot{Z} + C_s(\dot{Z} - \dot{Z}_u) + K_s(Z - Z_u) = F_b \tag{1.1}$$

and for the unsprung mass:

$$m\ddot{Z}_u + C_s(\dot{Z}_u - \dot{Z}) + K_s(Z_u - Z) + K_t(Z_u - Z_r) = -F_w \tag{1.2}$$

where

Z = *sprung mass displacement [m]*
Z_u = *unsprung mass displacement [m]*
Z_r = *road displacement [m]*
F_b = *external force on the sprung mass [m]*
F_w = *external force on the unsprung mass [m]*
C_s = *damping coefficient of the suspension shock absorber [Ns/m]*
K_s = *spring rate of the suspension spring [N/m]*
K_t = *spring rate of the tyre [Ns/m]*

The above equations can be solved analytically or by numerical methods. The typical response properties are shown in figure 1.7

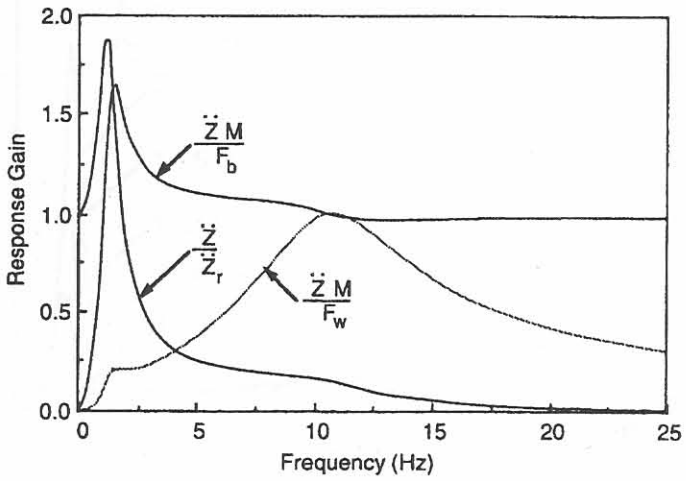

Figure 1.7: Quarter car model response to road, tire/wheel and body inputs [6].

The natural (undamped) frequencies (Hz) of the sprung and unsprung mass are given by [6, 9]:

$$f_{n,s} = \frac{1}{2\pi}\sqrt{\frac{K_s K_t / (K_s + K_t)}{M}} \tag{1.3}$$

and

$$f_{n,us} = \frac{1}{2\pi}\sqrt{\frac{K_s + K_t}{m}} \tag{1.4}$$

When damping is present the damping ratio is given by [6]:

$$\varsigma = \frac{C_s}{\sqrt{4K_s M}} \tag{1.5}$$

and the damped natural frequency for the sprung mass by [6]:

$$f_{d,s} = f_{n,s}\sqrt{1-\varsigma^2} \tag{1.6}$$

For acceptable ride comfort the damping ratio normally falls between 0.2 and 0.4. Within this range the damped natural frequency is close to the undamped natural frequency. The undamped natural frequency is commonly used to characterise the vehicle suspension.

1.3.1.1 Suspension stiffness

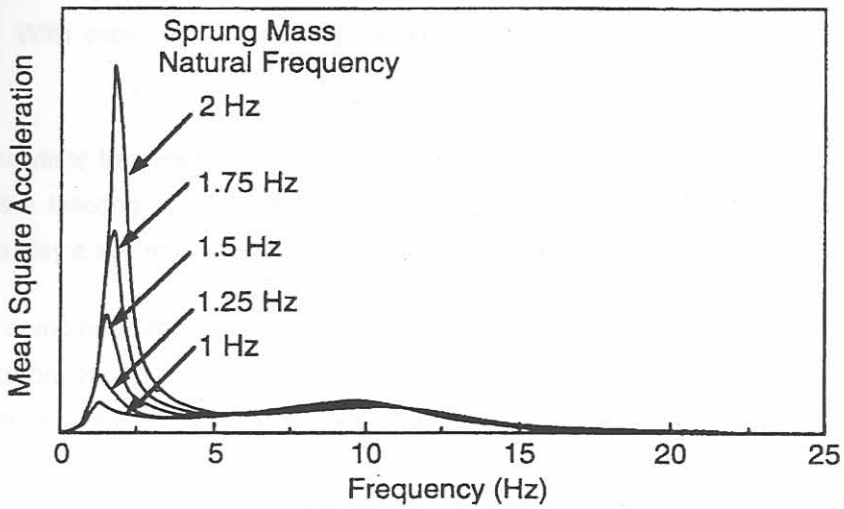

Figure 1.8: Effect of suspension stiffness [6].

The effect of the suspension stiffness (higher stiffness - higher natural frequency) on the mean square acceleration of the sprung mass is shown in figure 1.8. While this analysis clearly shows the benefits of keeping the suspension soft for ride isolation, the practical limits of stroke that can be accommodated within a given vehicle size constrain the natural frequency for most cars to a minimum of 1 to 1.5 Hz. Performance cars, for which ride comfort is sacrificed for handling benefits, have stiff suspensions with natural frequencies of 2 to 2.5 Hz [6].

1.3.1.2 Damping

The nominal effect of damping is shown in figure 1.9.

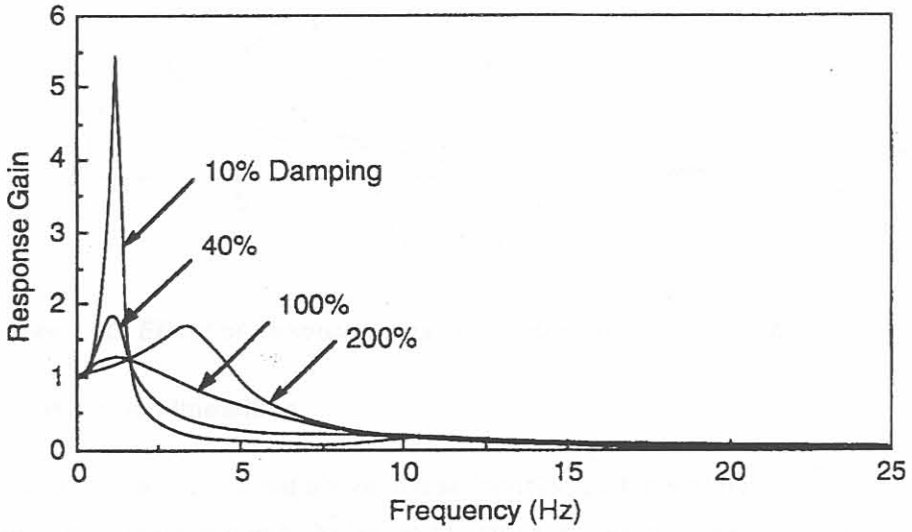

Figure 1.9: Effect of damping on suspension isolation behaviour [6].

At light damping (10%) the response is dominated by a very high response at the natural frequency. The 40% damping (damp ratio = 0.4) is representative of most cars. At 100% damping (critical damping) the natural frequency bounce motion will be controlled but with penalties at higher frequencies. With even higher damping the vehicle bounces on the tires resonating at a higher frequency.

While this analytical treatment provides a simplified illustration of the ride effect of damping in the suspension, the tailoring of dampers to achieve optimum performance is much more complicated. Dampers also play a key role in keeping good tire-to-road contact for road holding and safety.

Normally the damping in the jounce (compression) and rebound (extension) directions are not equal due to the fact that during compression damping aids in the transmission of forces to the sprung mass and is thus undesirable. Typically a three-to-one ratio is used between rebound and jounce damping. The damping for typical dampers is also non-linear.

For a realistic treatment of the dampers in ride analysis the damper must be treated as a non-linear element.

1.3.1.3 Wheel hop

Figure 1.10 indicates the effect of the unsprung mass on the response gain of the sprung mass. As can be seen from figure 1.10 it is best to keep the unsprung mass as light as possible.

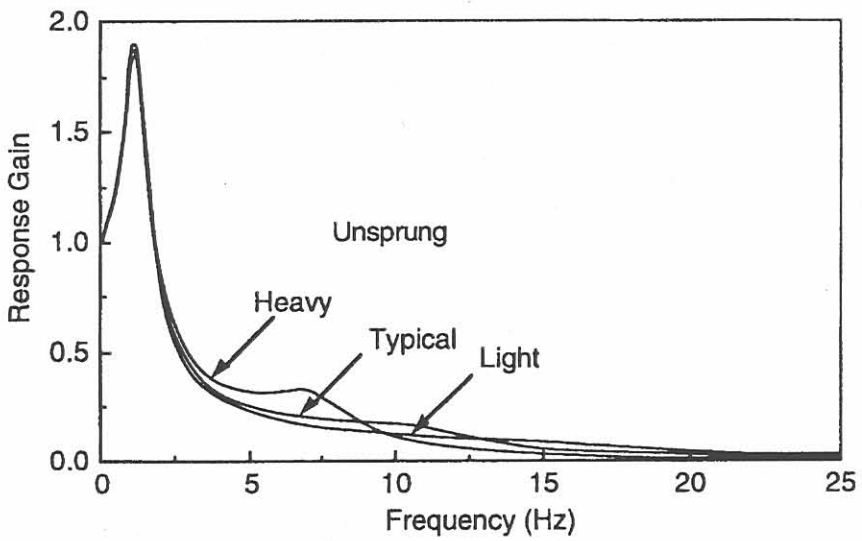

Figure 1.10: Effect of unsprung mass on suspension isolation behaviour [6].

1.3.1.4 Suspension non-linearities

In practice, contrary to that assumed above, the suspension systems of many vehicles are not linear. Non-linearities are introduced due to friction in the struts, bushings, interleaf friction in a leaf spring and other design aspects. In figure 1.11 the solid line indicates the force versus deflection

relationship as measured for a particular leaf spring. Due to non-linearities in the spring, especially friction, a hysteresis loop is obtained rather than a single line. The dotted lines indicate the nominal stiffness for the different deflection ranges. From figure 1.11 it can be seen that the effective spring rate for a leaf spring at small deflections can be typically three times the nominal rate.

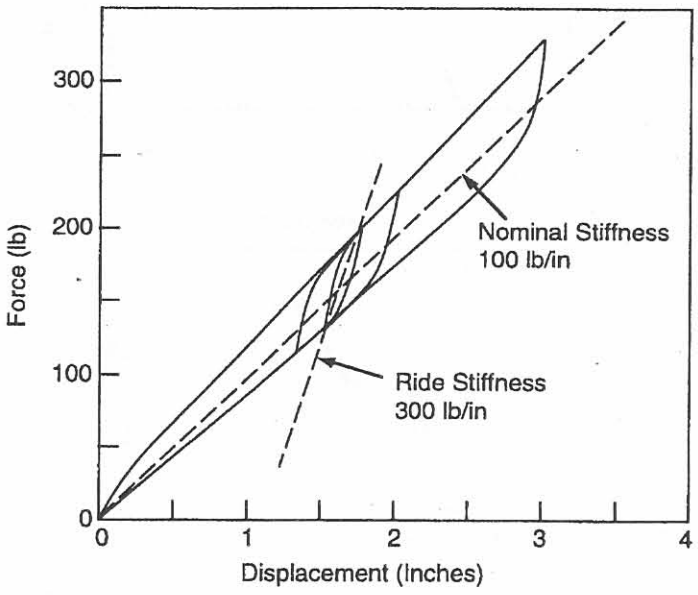

Figure 1.11: Load-deflection characteristics of a hysteretic leaf spring [6].

Figure 1.12 indicates the effect of suspension non-linearities on the response gain for roads with the same frequency content, but at high (rough) and low (smooth) amplitudes. The top figure (for the smooth road) in figure 1.12 shows that the natural frequency of the sprung mass is higher (± 2.3 Hz) than that for the rough road (bottom figure, ± 1.6 Hz). The response gain at the sprung mass natural frequency is also higher for the smooth road than that for the rough road. Both these observations point to the higher nominal stiffness experienced by the leaf spring at smaller deflections on the smooth road. The same tendency can be seen at the unsprung mass natural frequency (± 10 Hz).

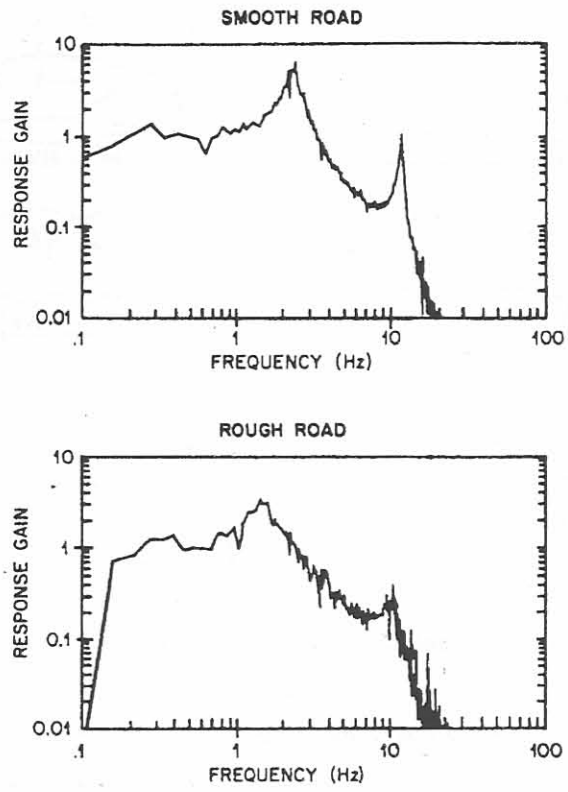

Figure 1.12: Response of a quarter car model with a hysteretic suspension [6].

1.3.2 Two-degrees of freedom model for pitch and bounce

Obviously the simple mechanics of the quarter car model does not fully represent the rigid-body motion that may be experienced by a motor vehicle. Because of the longitudinal distance between the axles, it is a multi-input system that responds with pitch motions as well as vertical bounce. The discussion of the combination of pitch and bounce that follows in this section is also mainly taken from Gillespie [6]. Figure 1.13 indicates this phenomena for different sinusoidal inputs of varying wavelength. As can be seen in the left figure in figure 1.13 pure bounce is induced at integer spatial frequencies and pure pitch in between (right figure in figure 1.13). At any other spatial frequency both pitch and bounce will be induced.

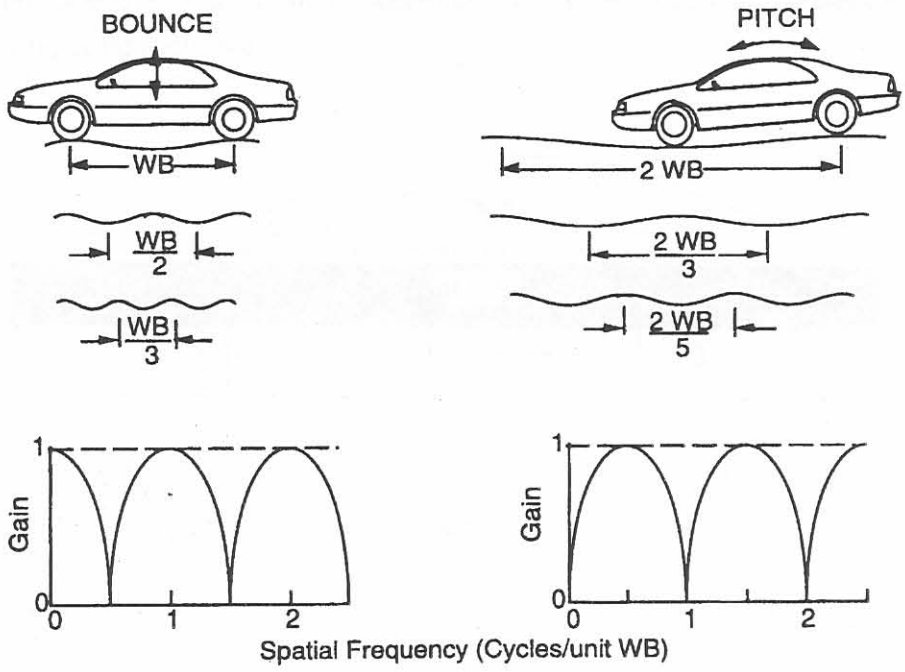

Figure 1.13: The wheelbase filtering mechanism [6].

The combination of pitch and bounce as well as the position on the vehicle will also alter the response gain, as shown in figure 1.14.

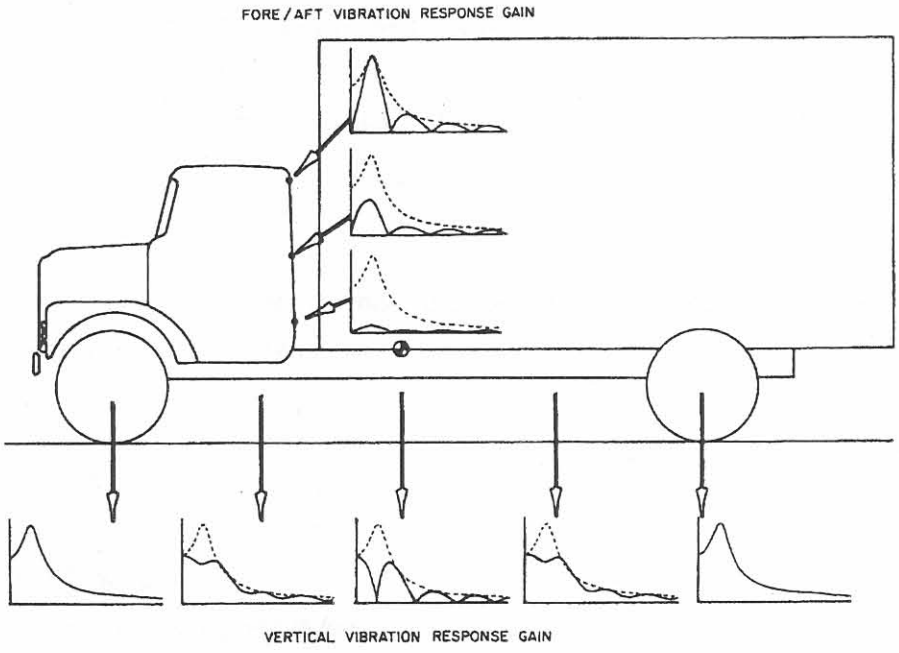

Figure 1.14: Effect of wheelbase filtering on the response gain of a truck [6].

Because of the wide separation of the natural frequencies of the sprung and unsprung mass, the up and down motion (bounce) and the angular motion (pitch) of a vehicle body and the motion of the

wheels may be considered to exist almost independently. Figure 1.15 shows the basic model with the effect of damping being neglected.

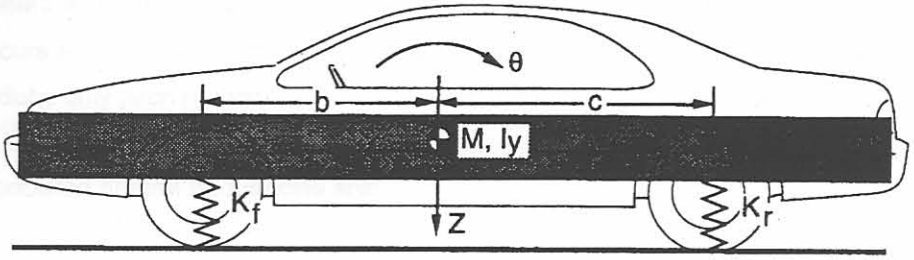

Figure 1.15: Pitch plane model for a motor vehicle [6].

The following parameters are defined:

$$\alpha = (K_f + K_r) / M$$
$$\beta = (K_r c - K_f b) / M \qquad (1.7)$$
$$\gamma = (K_f b^2 + K_r c^2) / (Mk^2)$$

where

K_f = *front ride rate [N/m]*

K_r = *rear ride rate [N/m]*

b = *distance from the front axle to the CG [m]*

c = *distance from the rear axle to the CG [m]*

I_y = *pitch moment of inertia about CG [kgm^2]*

k = *radius of gyration about CG [m]*

M = *mass of vehicle body [kg]*

Neglecting the mass of the wheels the ride rate, i.e. the effective spring stiffness due to the tyre stiffness and spring stiffness clearly is:

$$K = \frac{K_s K_t}{K_s + K_t} \qquad (1.8)$$

where

K = *ride rate [N/m]*

K_s = *suspension spring rate [N/m]*

K_t = *tire spring rate [N/m]*

The governing differential equations, for free vibrations for bounce Z and pitch θ motions, can respectively be written as:

$$\ddot{Z} + \alpha Z + \beta\theta = 0$$
$$\ddot{\theta} + \beta Z / k^2 + \gamma\theta = 0 \qquad (1.9)$$

Only β appears in both equations and is therefor called the coupling coefficient. When $\beta = 0$ no coupling occurs and a vertical force at the CG produces only bounce and a pure torque applied to the chassis produce only pitch motion.

The two associated natural frequencies are:

$$f_1 = \frac{1}{2\pi}\sqrt{\frac{(\alpha+\gamma)}{2} + \sqrt{\frac{(\alpha-\gamma)^2}{4} + \frac{\beta^2}{k^2}}}$$
$$f_2 = \frac{1}{2\pi}\sqrt{\frac{(\alpha+\gamma)}{2} - \sqrt{\frac{(\alpha-\gamma)^2}{4} + \frac{\beta^2}{k^2}}} \qquad (1.10)$$

The positions of the two oscillation centres from the CG are given by:

$$\ell_1 = \frac{\beta}{(2\pi f_1)^2 - \alpha}$$
$$\ell_2 = \frac{\beta}{(2\pi f_2)^2 - \alpha} \qquad (1.11)$$

When the centre distance is positive it is ahead of the CG and if negative behind the CG. When the centre lies outside the wheel base the motion is predominantly bounce and the associated frequency is the bounce frequency. For the centre within the wheel base, the motion will be predominantly pitch and the associated frequency the pitch frequency. These two cases are illustrated in figure 1.16.

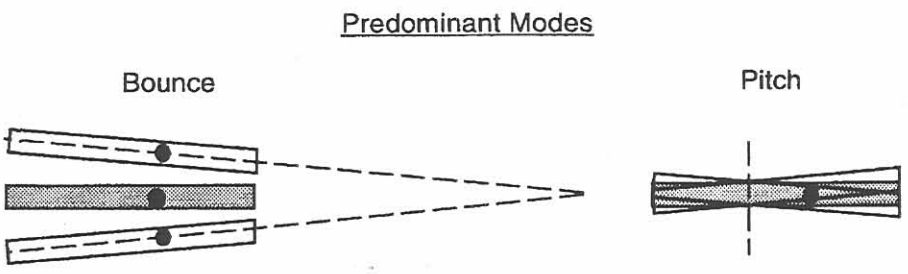

Figure 1.16: The two vibration modes of a vehicle in the pitch plane [6].

For acceptable ride comfort the so-called Olley criteria are suggested:

i. The front suspension should have a lower natural frequency than the rear suspension. Pitching is more annoying than bouncing. The desirable ratio of front frequency to rear-end frequency depends on the wheel base of the vehicle, the average driving speed and the road conditions.
ii. The pitch and bounce frequencies should be close together.
iii. Both frequencies must be smaller than 1.3 Hz.

The Olley dynamic index is defined as:

$$DI = \frac{k^2}{bc} \qquad (1.12)$$

The following special cases for the value of the dynamic index and for the other parameters are of particular importance:

i $DI = 1$

In this case the oscillation centres are located at the front and the rear axles. This is desirable for good ride if Olley's criteria are also satisfied. There is no interaction between the front and rear suspensions.

ii $\beta = 0$ (uncoupled motion)

The pitch and bounce oscillations are totally independent. Poor ride results because the motions can be very irregular. Coupling tends to even out ride.

iii $\beta = 0$ and $DI = 1$

This condition results in equal bounce and pitch frequencies. The ride is inferior because there is essentially no pattern to the road-generated motion; it is quite unpredictable.

1.4 Human response to vibration

According to Gillespie [6]: *"Ride is a subjective perception, normally associated with the level of comfort experienced when travelling in a vehicle"*. Although ride, ride quality or ride comfort is a subjective concept, it is nevertheless necessary to attempt a measurement of this quality so as to be able to evaluate the ride comfort of the vehicle objectively.

A guide to defining the human tolerance to whole-body vibration has been developed by the International Organization for Standardization and published as ISO 2631 [10]. The limits for the vertical and transverse directions are respectively shown in figure 1.17(a) and (b). These limits are for decreased proficiency, which are related to the preservation of working efficiency, and apply to such tasks as driving a road vehicle or tractor. Figure 1.17(a) indicates the proficiency boundaries for vertical vibration, which are defined in terms of root mean square values of acceleration as a function of frequency for various exposure times. It can be seen that as the average daily exposure time increases, the boundary lowers. Figure 1.17(b) indicates the boundaries for the transverse direction, i.e. for side-to-side or chest-to-back vibration.

The tolerance curves shown in figure 1.17 are generally determined from sinusoidal inputs, while the actual ride environment in a motor vehicle contains all frequencies over a broad spectrum. Thus in the application of the above information to obtain objective measurements of ride vibration on the seat of a car or truck, it is necessary to overcome this deficiency. One method is to filter the acceleration data in inverse proportion to the selected tolerance curve, i.e. to accentuate acceleration that occurs at frequencies for which lower tolerance levels exists. The inverse filtering then allows the resultant acceleration spectrum to be viewed as if all frequencies are equally important. In this approach the fore and aft vibration must be evaluated separately.

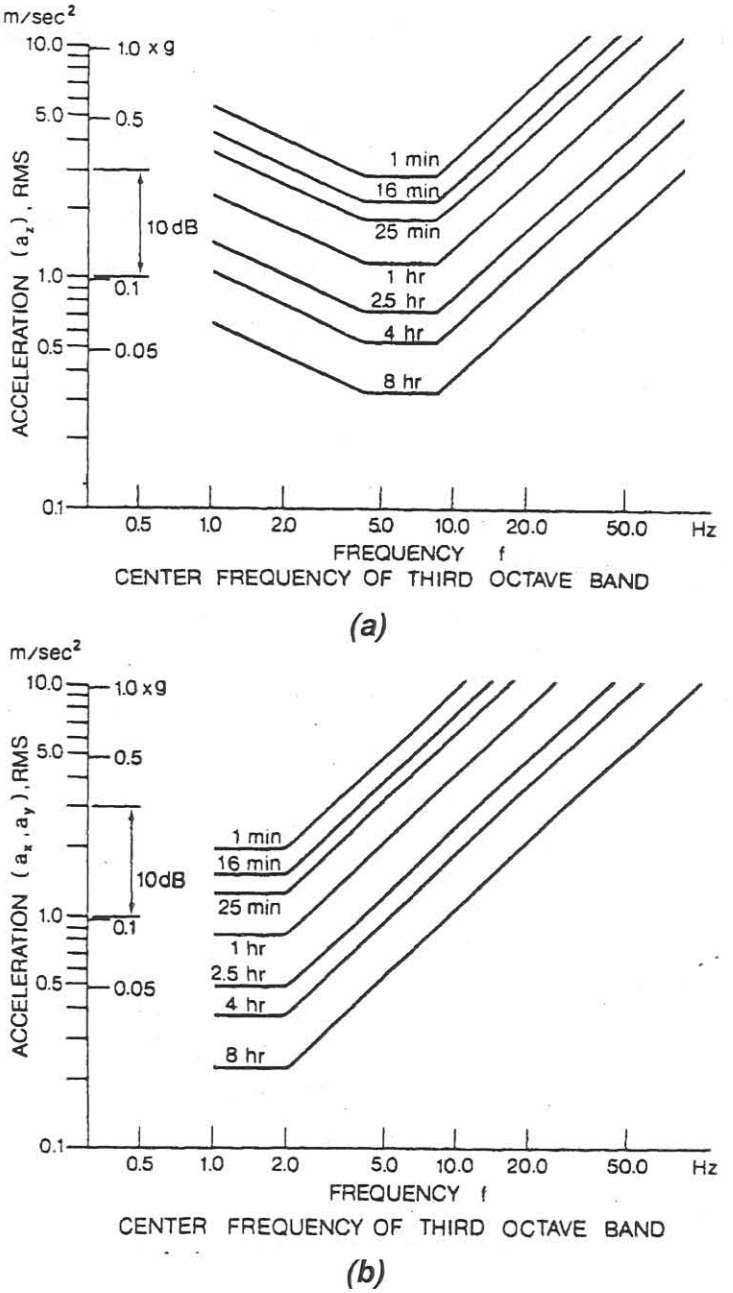

Figure 1.17: ***Limits of whole-body vibration for fatigue or decreased proficiency in:***
(a) ***vertical direction and***
(b) ***transverse direction, as recommended by ISO2631 [10].***

According to the study done by Nell [11], the ISO2631 criterion has certain limitations in measuring the ride comfort of vehicles. One of these limitations is that the limit curves only extend to 1 Hz, whereas many off-road vehicles have suspension resonance frequencies around 1 Hz. Responses below this frequency are therefore also important. A more fundamental measure is the average absorbed power (*AAP*) technique [11, 12]. Here it is assumed that the level of discomfort is related to the vibration power being dissipated in the subject's body, whether vertical, fore/aft, or lateral (side to

side) inputs. In this method the tolerance curves are used to weigh accelerations so as to arrive at an absorbed power for each direction and the power quantities are then simply added [11].

Another method used to evaluate ride comfort is to determine the vibration dose value (VDV) as calculated according to BS 6841 [11, 13]. For crest factors (defined as the modulus of the ratio of the maximum instantaneous peak value of the frequency weighted acceleration signal to its root mean square (rms) value) of more than 6, the following relationship is used:

$$VDV = \{ \int_0^T [a_w(t)]^4 \, dt \}^{0.25} \tag{1.13}$$

where

$a_w(t)$ = the instantaneous frequency-weighted acceleration and

T = the duration of the measurement.

The weighted acceleration is obtained by filtering the actual acceleration with a frequency function that is prescribed according to the specific direction of the acceleration. The vibration dose value can also be transformed to an equivalent 4-hour vibration dose value for linear and rotational acceleration by using:

$$VDV = (\frac{t_0}{t_1} VDV_1^{\,4})^{0.25} \tag{1.14}$$

where

t_0 = the total period of vibration duration (4 hours for the 4-hour VDV),

t_1 = the duration of one representative period, and

VDV_1 = the vibration dose value calculated for one representative period.

The 4-hour VDV is then equivalent to the VDV that would have been obtained if the specific vehicle response was experienced for a duration of 4-hours.

In a local study by Els [14] comparison of measured criteria for ride-comfort were compared with the subjective evaluations of different people. In the experiment a 14 ton, 4x4 mine protected military vehicle (see figure 1.18) was driven over different terrain, at various speeds and tyre pressures. The terrain was chosen to be representative of typical South African operating conditions and such that it excites a significant amount of body roll, pitch and yaw motion. Seven groups, each consisting of 8 or 9 people were used for determining subjective comments while, simultaneously, recording acceleration data required for the objective analysis. People of different postures, age groups and experience were used. Figure 1.19 indicates the subjective response of the different groups to the different tests. A high value in the subjective comment corresponds to poor ride-comfort experienced. Figure 1.20 indicates the correlation for the 4-hour VDV value with the subjective value. In the

conclusion of his study Els states: "*The conclusion from this investigation is that any of the four methods under consideration, namely ISO2631, BS6841, AAP and VDI2057, can be used to objectively determine ride comfort for the vehicles and terrain of importance similar to those used in this study*". **Accordingly, in this study the vibration dose value (*VDV*) will be used as an objective indication of the ride-comfort of a vehicle.**

Figure 1.18: Test vehicle for ride comfort evaluation used by Els [14].

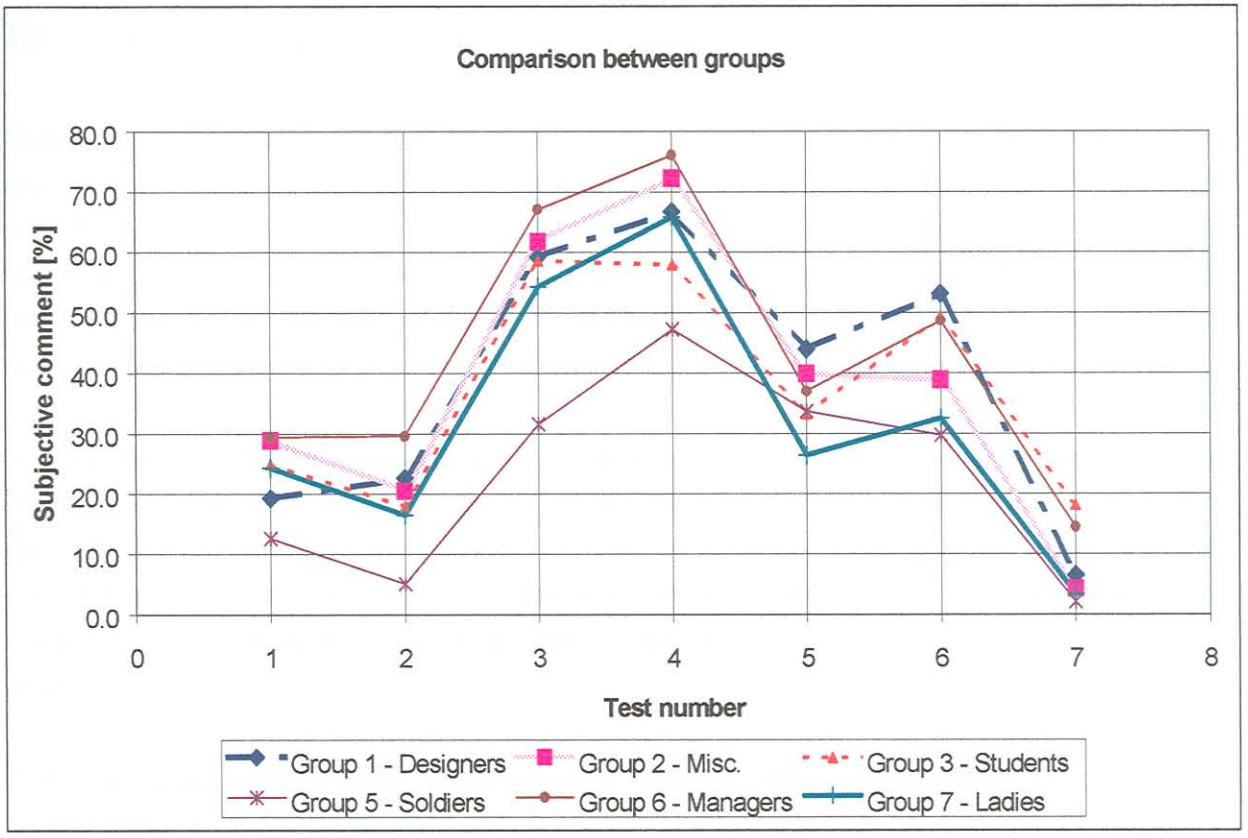

Figure 1.19: Comparison between groups [14].

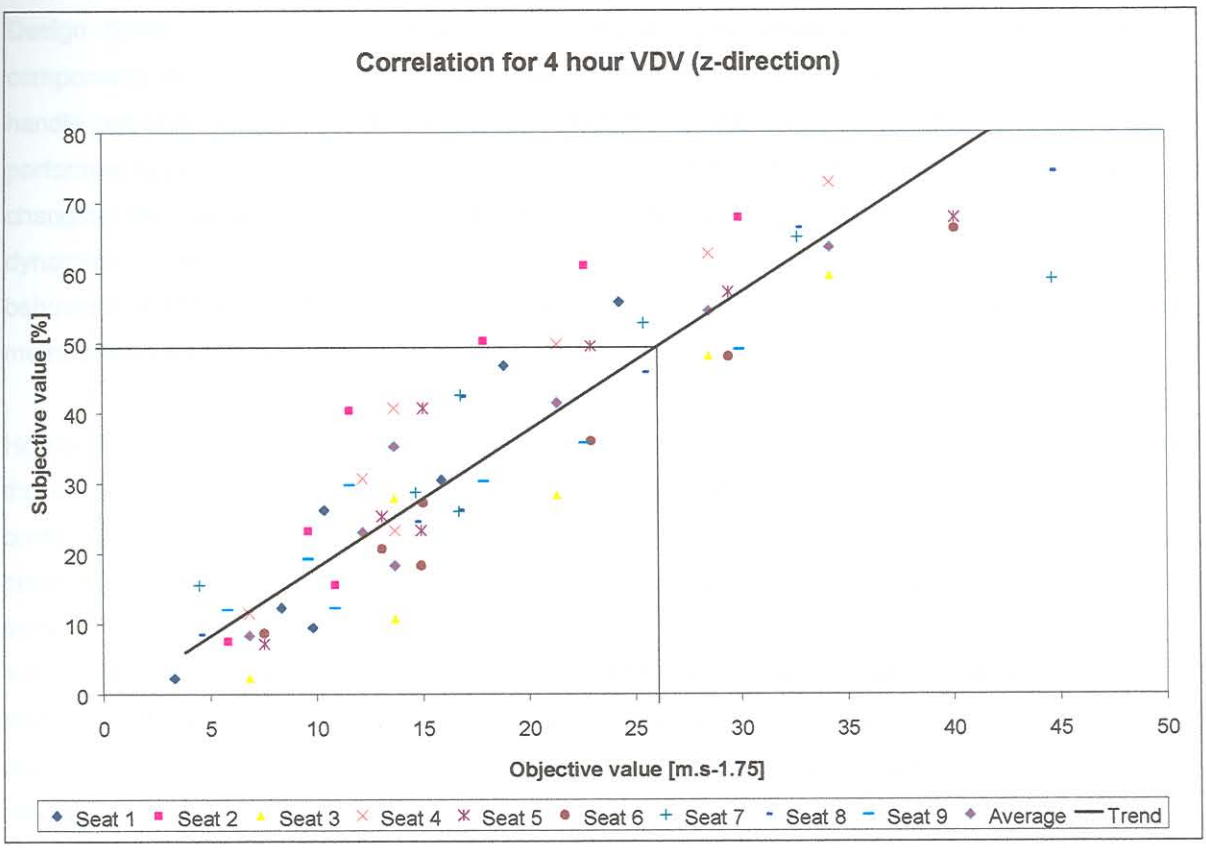

Figure 1.20: Correlation for 4 hour VDV values [14].

1.5 Suspension optimisation

Suspension optimisation is the process through which decisions are made on the specific choices of characteristics for the suspension components such that certain prescribed design objectives or evaluation criteria are fulfilled. These criteria may be the attainment of a certain level ride-comfort over specified terrain and vehicle speed, or the reduction of the maximum accelerations of the cargo to acceptable values, or any other specified criteria, subject to the vehicle complying to prescribed mobility criteria.

The first step in deciding on the suspension criteria to be applied is normally to use basic vehicle models, of the type described in 1.3, to obtain first order computed indications of suitable spring and damper constants for the specific vehicle. A good reference for such criteria can be found in the publication: Magic numbers in design of suspensions for passenger cars [15]. Although these "magic numbers" are specifically prescribed for passenger cars they can be applied to other type of vehicles as well.

The initial basic approximation models usually assume linear characteristics for suspension components such as the springs and dampers. The second step is to perform a more extensive and detailed analysis of the vehicle concerned. This can be done by performing vehicle simulations using vehicle dynamic simulation programs such as, for example, GENRIT [3], DADS (Dynamic Analyses

Design System) [4] or ADAMS/Car [16]. In these more advanced programs the suspension components are normally prescribed using two-dimensional tabular data and these programs can also handle non-linear suspension characteristics. Once the vehicle model is available, simulations can be performed to evaluate the vehicle ride dynamics over different specified route profiles and speeds. By changing the suspension characteristics the influence of these parameters on the vehicle ride dynamics can be assessed. The parameters may then be adjusted accordingly until acceptable ride behaviour is obtained. A brief overview now follows of some reported projects where this design methodology was applied.

Heyns et.al. [17] describe the design of the suspension system for a container carrier. The author of the current study was part of this project team. This carrier is used to carry different types of containers, such as a mobile operating theatre, x-ray equipment, etc. For this type of cargo it is obviously required that low acceleration levels must be maintained when travelling over any kind of terrain. A GENRIT simulation model of the vehicle was built. Using different lay-outs for the suspension system as well as different characteristics for the suspension components, the carrier motion was simulated over different terrain and at various speeds. The suspension lay-out and characteristics varied were those for the suspension at the fifth wheel of the truck-tractor, and for the rear suspension of the trailer. A combination with dual axles at the rear of the trailer was also included in the study. Subjective and objective evaluations of the acceleration experienced by the cargo were then used to determine the "optimum", or rather, the best configuration from those for which simulations were performed. Figure 1.21 depicts the side view of the carrier and figure 1.22 gives a schematic of the GENRIT simulation model used in this study.

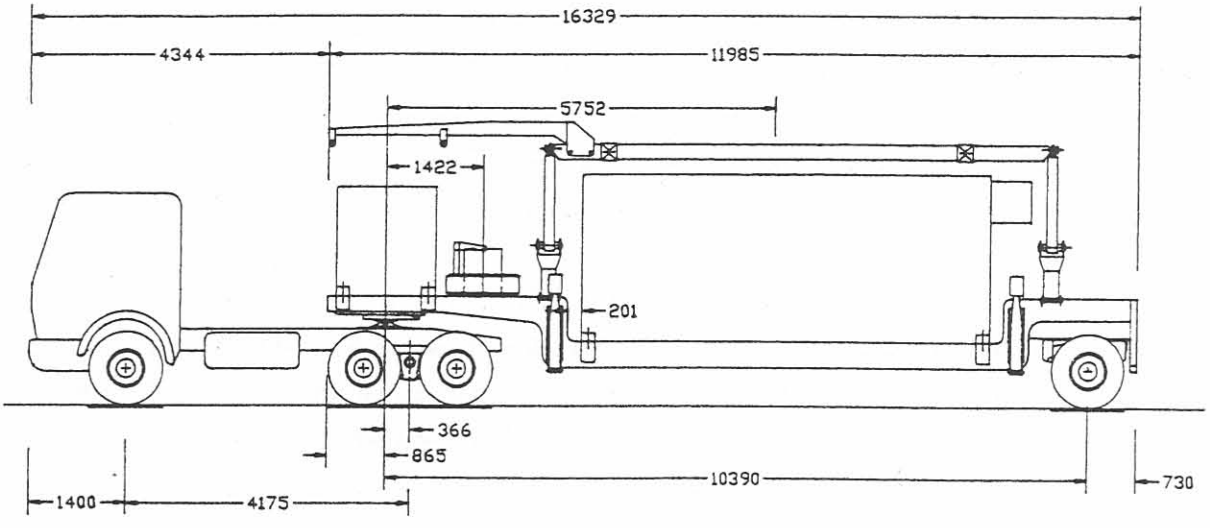

Figure 1.21: Side view of the container carrier for suspension optimisation [17].

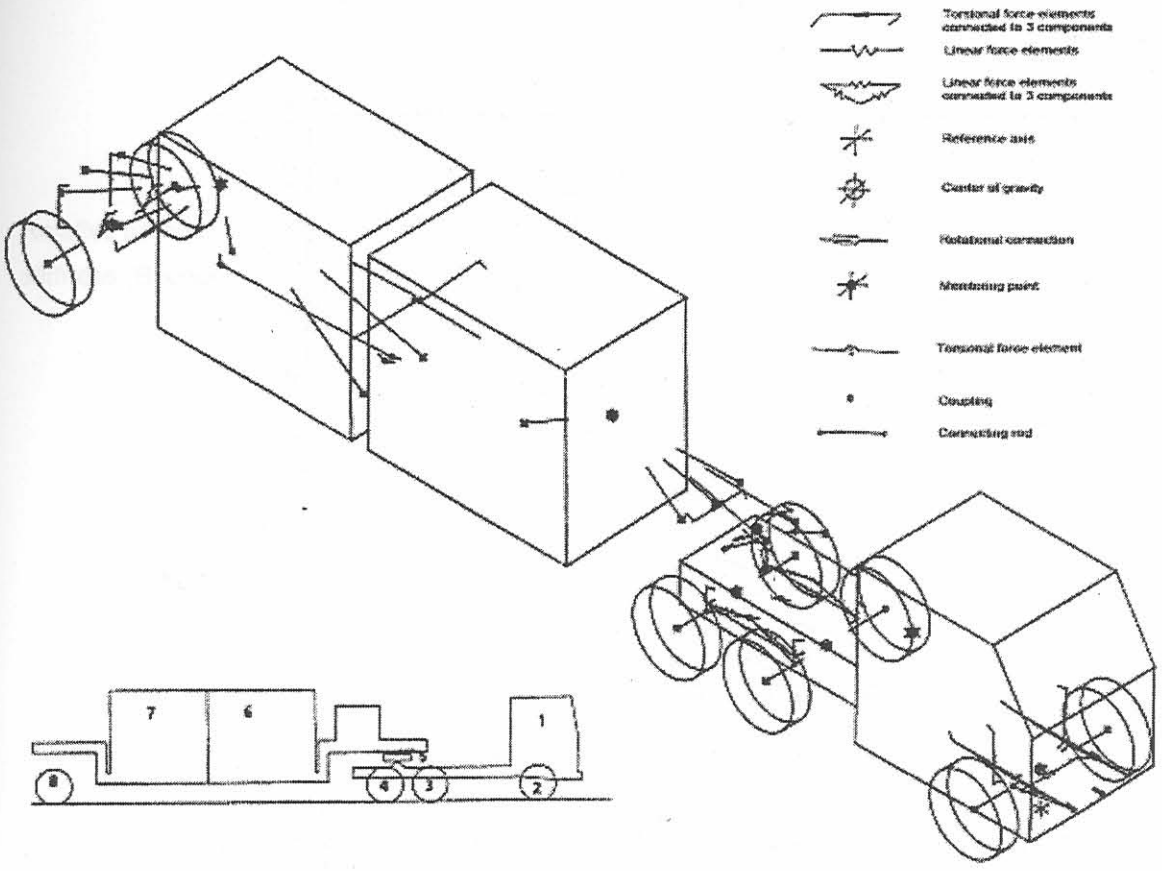

Figure 1.22: Schematic of the GENRIT simulation model used in the suspension optimisation study of a container carrier [17].

The author of the present study (Naudé) was also involved in the optimisation of the suspension characteristics of the Mingwe vehicle [18]. The Mingwe vehicle is a four-wheeled armoured personnel carrier (see figure 1.18). The simulation program GENRIT was used for simulating the dynamics of the Mingwe vehicle. In this study the suspension characteristics of the dampers in the bounce and rebound direction where changed by a certain percentage, the vehicle motion was then simulated over a certain route profile and the vibration dose value at a specific point of interest was calculated. The results were drawn on a two dimensional contour plot which indicates the percentage improvement in the vibration dose value for the different damper stiffness combinations. An example of such a plot, for a specific terrain and speed, can be seen in figure 1.23. A positive percentage indicates an improvement in the ride comfort for the specific terrain and speed. The point (1.0, 1.0) indicates the original design.

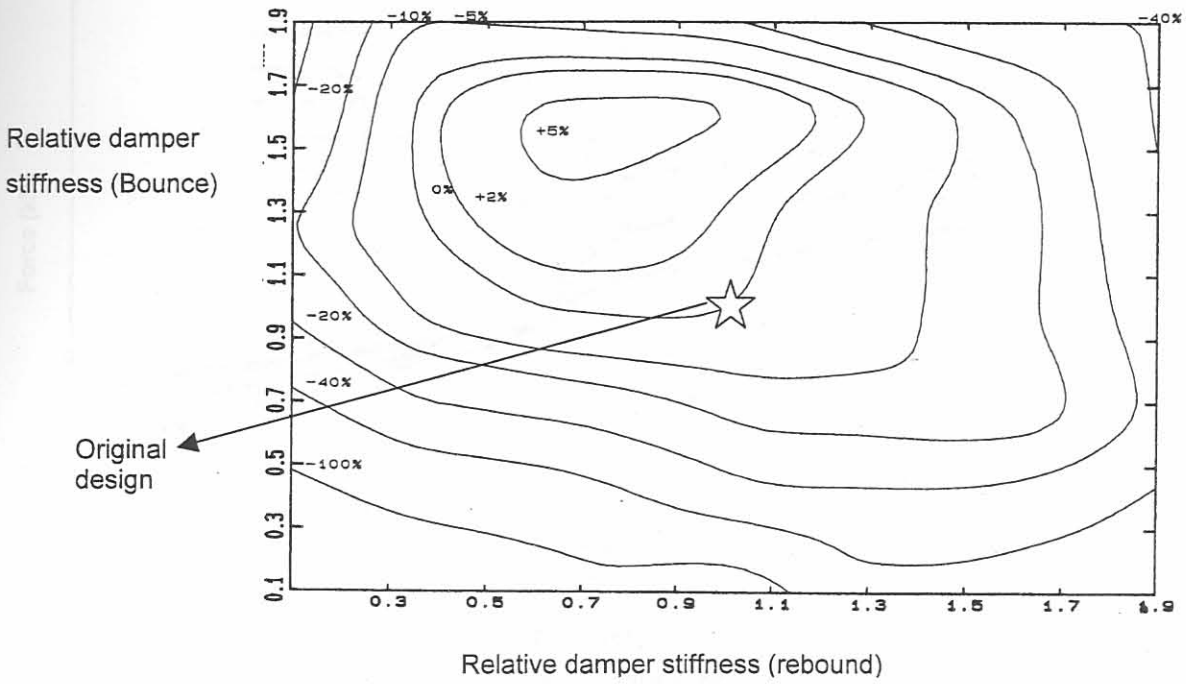

Figure 1.23: Improvement of ride comfort for the Mingwe vehicle as function of the damper stiffness in bounce and rebound [18].

In a study done by Heui-bon Lee et al. [19] a similar approach to that of Naudé [18] was used. Using DADS the ride quality for a medium truck was simulated for different spring stiffness of the front/rear suspension and damping characteristics of the shock absorbers. Examples of the damper characteristics used can be seen in figure 1.24. In figure 1.24 the thick lines indicate the damper characteristics used for the front axles and the thin lines that for the rear axle. As can be seen the configurations used have damper stiffness two and three times the stiffness of the baseline (the solid line). Using power spectrum density (PSD) plots of the truck body acceleration and pitch motion a decision was made regarding the configuration with the "best" characteristics. The configuration chosen was the one giving the lowest PSD plot.

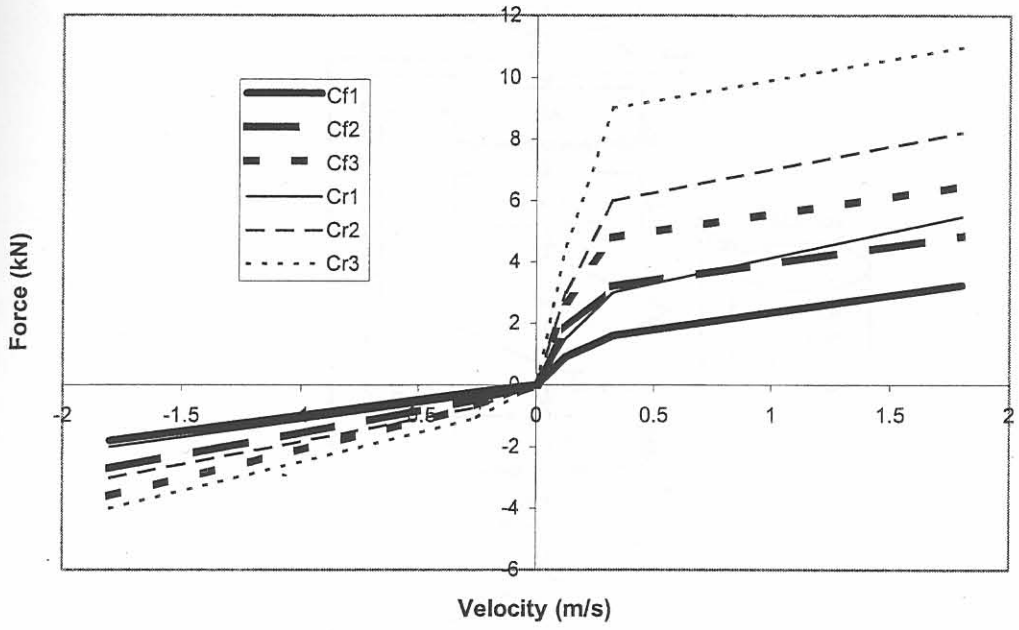

Figure 1.24: Example of discrete changes in damper characteristics used during suspension optimisation [19].

In more recent studies the concept of Multidisciplinary Design Optimisation (MDO) has been proposed in which a more formal mathematical optimisation methodology is adopted in performing the optimisation. Some examples of this approach are presented below.

Motoyama et al. [20] performed an optimal automobile suspension design using a formal optimisation technique. In their study a kinetic analysis of double wishbone independent vehicle suspension system was used in conjunction with a Genetic Algorithm (GA) to determine the optimum values of 18 design variables, specifying the location of the suspension attachment points. The objective function minimised was the change in the toe angle over a stroke of 100 mm of the wheel. ADAMS/Car was used as the simulation program by means of which the objective function was evaluated. Figure 1.25 gives a schematic representation of the "optimisation system" used in the study. Using this optimisation methodology and, for specified sets of starting values for the geometry of the suspension, an optimum configuration was obtained with an average change in the toe angle of 0.06 ° over the 100mm stroke. The original configuration gave a change in the toe angle over the 100mm stroke of – 2 ° to +5.6 °. The optimum was obtained after five thousand simulations! To improve the computational economy a Response Surface Methodology (RSM) was implemented to construct approximations to the behaviour of the system. With these approximations the influence of the design variables on the change in the objective function could more economically be evaluated. This method enabled the design engineer to change the design variables, and economically determine the tendency of the toe curve without excessive calling of the simulation program.

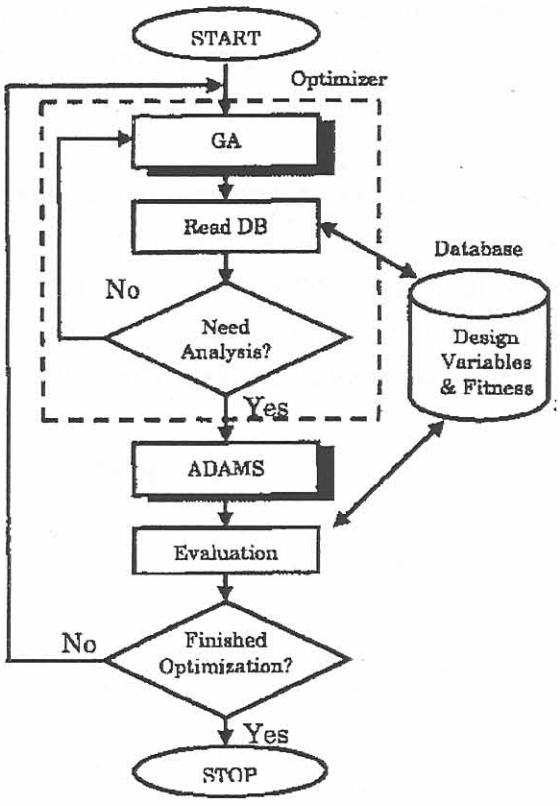

Figure 1.25: The "optimisation system" used by Motoyama et al. [20]

Lee et al. [21] performed a fuzzy multi-objective optimisation of a train suspension also using a response surface model. The dynamic analysis program VAMPIRE was utilised to optimise 58 responses of the suspension with respect to 26 design variables using optimisation applied to a response surface model. A fuzzy decision-making algorithm was used to investigate the engineer's confidence level in the optimisation process. Every first order response surface model of 58 responses was constructed from Taguchi's L_{32} 2 orthogonal array, and these were generated and simulated 32 times by using VAMPIRE. With this system Lee and his co-workers claim that they obtained an optimum design for the suspension of a train.

Although not directly applicable to vehicle suspension systems, Botkin [22] performed a structural optimisation of automotive body components based upon parametric solid modelling. A Convex linearisation technique was used in conjunction with Nastran Solution 200 to perform eight case studies for optimisation of an automotive front structure component. Mass reduction of up to 64% was obtained using composite constructions.

Etman [5] coupled optimisation software to commercial multi-body analysis packages such as MECANO, MADYMO and DADS using approximation concepts. With specific application to vehicle suspensions a stroke dependant damper for the front axle suspension of a truck was optimised. Various optimisation runs were performed for a two degree of freedom model, as well as for a full-scale truck model, using single-point linear approximations. Etman states that: "*This application*

clearly showed that the final optimum design heavily relies on the choices made by the designer." He also concludes that: "*The ultimate goal is to integrate multibody analysis and optimisation into one general purpose design tool.*"

As can be seen from the abovementioned examples, as well as other investigations reported in the literature [23, 24, 25, 39-50], optimisation and analysis of a vehicle suspension can be complex, expensive and time-consuming. These factors force the design engineer to take a more pragmatic approach summarised by the statement of Esat [26]: ***"The important goal of optimisation is improvement and attainment of the optimum is much less important for complex systems".***

1.6 Active / semi-active suspensions

From the reported suspension optimisation studies it is evident that the so-called "optimum" vehicle suspension characteristics are dependant on the particular evaluation criteria set, i.e., on the objective function used, and on the specific route and speed over which the vehicle is to be driven. Thus as the criteria and conditions change, so the "optima" will vary. In general, however, the following tendencies are evident:

i. ride-quality can be improved over moderate, i.e. low amplitude input terrain by lowering both the spring stiffness and the damping,
ii. low spring stiffness and low damping require more suspension deflection, which are limited for practical reasons, and
iii. higher spring stiffness and higher damping are required for improved road holding.

One way of accommodating these conflicting suspension requirements is to use an active suspension. A fully active suspension system incorporates actuators, normally hydraulic actuators, to generate the desired forces in a suspension system to satisfactorily deal with changes in road conditions. External power is required to operate the system. Semi-active suspensions contain spring and damping components, the properties of which can be changed by external control. A signal or external power is supplied to these systems for the purpose of changing the properties. In passive suspension systems conventional springs and dampers are used. These component properties are time-invariant.

Due to the fact that the suspension characteristics in semi-active or active suspensions can be changed according to the terrain requirements, these types of suspension systems can improve ride quality over a wide spectrum of terrain. These improvements come at the penalty of increased complexity and higher cost. A large amount of research has been done on control algorithms for such suspension systems [27-38].

Due to the associated higher cost and increased complexity, semi-active suspension systems and active suspension system are still relatively rare and confined to the more expensive car segments. Some of the newest military vehicles also make use of semi-active suspensions. **This study will, however, be limited to the optimisation of passive suspension systems.**

1.7 Multidisciplinary design optimisation

In search of better designs parametric studies have in the past been performed as part of a general design process. However, a more effective and efficient design method is demanded in order to reduce the time to design and develop products. Design optimisation techniques in which a systematic mathematical approach is adopted is considered to be a better way to search for good designs in comparison to performing parametric studies. Due to the high performance demands and multiple requirements of products, design teams need mathematical optimisation techniques that can reliably optimise complex systems. This need has resulted in the concept of multidisciplinary design optimisation (MDO) [51].

Multidisciplinary design optimisation can be described as the development of general mathematical optimisation algorithms that may universally be applied to design problems arising in various different disciplines. Basic to this approach is the systematic adjustment of the values of the design variables so that they will minimise an objective function subject to constraints. Typical examples of design problems solved in the way include [51]:

i. the minimisation of traffic noise over an irregular wall,
ii. optimal tundish design using CFD with inclusion modelling,
iii. minimum cost design of welded structures,
iv. optimisation of engine mountings,
v. sound and vibration optimisation of carillon bells and MRI scanners,
vi. shape optimisation for crashworthiness, and
vii. optimisation of heat sinks.

Often the problem requires the use of a computer simulation program to enable the determination of the influence of the design variables on the objective function. As stated by Papalambros [52]: *"Design optimisation is now a discipline in high technology product development and a natural extension of the ever-increasing analytical capabilities of computer-aided engineering."*

For many engineering problems, multi-body analysis routines are used to calculate the kinematic and dynamic behaviour of the mechanical design. In these cases the values of the objective function and constraint functions follow from the numerical simulation. Therefor, to solve the optimisation problem, the multi-body code has to be coupled to a mathematical programming algorithm. Such a coupling may be difficult to implement and can lead to high computational cost [23].

Several classes of optimisation algorithms have been developed. The most important classes are [51]:

i. Mathematical programming methods (including gradient based methods such as, for example, Sequential Quadratic Programming [SQP],
ii. Lipschitzian and deterministic optimisation and
iii. Genetic algorithms (GA's).

Engineering optimisation problems where simulation programs are used in computing the objective functions present unique challenges because of

i. *the presence of noise* in the objective and/or constraint functions due to numerical inaccuracies in the simulations that result from discretisation and round-off errors, and the use of not fully converged solutions, and
ii. *the presence of discontinuities* in the objective/constraint functions arising from formulations of the optimisation problem in forms convenient for engineers, e.g., by the use of absolute value objective functions and by using penalty function formulations for constrained problems.

These aspects, presently of great world-wide interest to design engineers, have been addressed by Snyman [53, 54]. Central and essential to his tackling of the above difficulties has been the development of novel optimisation algorithms suitable for engineering problems. This required both the construction of new algorithms, and the testing of these methods on appropriate standard, and new, engineering design problems. A particular successful development has been the "leap-frog" trajectory methods [53,54]. These methods fall within the class of gradient based mathematical programming methods.

The leap-frog unconstrained optimisation algorithms were originally proposed in the early eighties [53, 54]. These algorithms have the unique characteristics, for gradient based methods, that only the gradient of the objective function is used and that no explicit line searches are performed. These algorithms were later refined and extended to constrained problems [55]. The methods were found to be extremely reliable and robust. In particular, the methods are relatively insensitive to problems where discontinuities and noise are present. Since it is expected that the latter problems occur in the numerical simulation of suspension systems, the leap-frog method is the method of choice for this study where reliability and robustness of the proposed Suspension Optimisation System is of prime importance. The most current version of the leap-frog code for constrained optimisation, is called LFOPC [55].

1.8 Summary: purpose of study

The need for a Suspension Optimisation System evolved from difficulties experienced during the design of a 6x6 armoured personnel carrier. Although parametric studies, using complete three dimensional simulation programs, were performed in the design of the vehicle, problems and failures continued to occur on the suspension system. While the need for suspension optimisation was demonstrated for the particular vehicle investigated, the same requirement arises during the design of any other vehicle, especially for vehicles for specialised applications such as armoured personnel carriers. The optimisation methodology needs to be applied during the vehicle concept design stage, at which time little geometrical information regarding the vehicle and its suspension is available. It is proposed that the initial optimal design may be done by coupling a sufficiently representative two-dimensional vehicle dynamic simulation program to a suitable optimisation algorithm.

An outline of a linear quarter car model and of the associated pitch and bounce analysis for vehicle suspensions are given. Although this model can be used in obtaining a first order estimation of the suspension behaviour, it does not, of course, provide a complete description of the non-linear suspension characteristics. Due to the fact that almost all suspension component characteristics, especially that of dampers, are non-linear the model to be used in the optimisation must contain non-linear characteristics.

In an overview of work done in the field of suspension optimisation it is shown that first order optimisation has been done through parametric studies. The latest developments are, however, the application of mathematical optimisation algorithms, in conjunction with computer aided simulation of the vehicle system, to determine values for the design variables that a minimises an objective function related to certain desirable design criteria. The development and application of multidisciplinary design optimisation techniques to almost every engineering field, spurred the application of these techniques in the field of vehicle design. The reported work done in this field all achieve specific design optimisation goals but are not general enough to be directly applicable to the problem at hand. Furthermore the reported methods are numerically extensive and either require a specific code for the particular problem or specific hardware.

By using an active or semi-active suspension it is in principle be possible to incorporate "suspension optimisation" into the suspension system of the vehicle. In this instance the suspension characteristics can be "programmed" to change as required in real-time. The changing of the suspension characteristics is controlled by a control strategy. For the active or semi-active suspension system this control strategy also needs to be optimised. Due to the higher cost and complexity of semi-active suspension systems, **the current study is limited to the optimisation of passive suspension systems**.

The literature reveals several classes of optimisation algorithms. All of these classes have successfully been applied to engineering optimisation problems. One of the mathematical programming algorithms that is singled out here is the LFOPC algorithm [55]. This algorithm is very robust and particularly suited for use in problems where numerical noise and discontinuities may occur, as is typically experienced in the computer aided analysis of mechanical systems. This algorithm is to be used in this study.

The specific overall objective of this study is summarised as **the application of a formal mathematical approach to the optimisation of vehicle suspension characteristics.** The methodology is to be embodied in a Computerised Suspension Optimisation System for which the following requirements are set:

i. The system must be general enough to be applicable to different single body vehicles with up to four axles.
ii. The optimisation must be able to optimise non-linear suspension characteristics for the different suspension components: springs, dampers, bump-stops and tyres. The specific design variables used must be user configurable.
iii. The specific objective function used must be user configurable.
iv. The optimisation system is to be used during the concept design stage of the vehicle. During this stage only limited geometrical information for the specific vehicle and suspension is available. This obviates the need for a full three-dimensional multi-body simulation. A representative two-dimensional simulation is required and will suffice for concept stage evaluation of the objective function.
v. The system must be user friendly and usable by the project manager, who may have limited vehicle dynamic analysis background and experience.

Finally, although the need for this Computerised Suspension Optimisation System arose from problems experienced locally, the same need exists internationally. Etman [5] suggests that in performing vehicle suspension optimisation greater benefit may be obtained by using a simpler vehicle model than a full-scale 3-D model. He also mentions that: "*A serious difficulty is that the designer often does not precisely know how to mathematically formulate the multibody design problem beforehand. It is very likely that during optimization he wants to remove or change* [the] *objective function, constraints and design variables. Therefore, graphical means have to be available, not only for modelling, but for optimization purposes as well.*" He thus stresses the importance of **an interactive computer design tool for successful design optimisation**. The development of the latter versatile and flexible tool, specifically for a vehicle suspension system, is therefore indeed the main objective of this study.

CHAPTER 2:

MATHEMATICAL MODEL AND OPTIMISATION ALGORITHM

2. Mathematical model and optimisation algorithm

In chapter 1 the need for a two-dimensional vehicle dynamic simulation program was motivated. In this chapter the basic mathematical model for a two-dimensional vehicle dynamic simulation is developed. The requirements for this model can be summarised as follows:

i. A single body vehicle with up to four axles must be modelled.
ii. The basic kinematics of the vehicle suspension must be taken into consideration. For this purpose an equivalent trailing arm suspension analysis is to be used.
iii. The suspension is to consist of a spring, damper and bump stop, where all of these component characteristics may be non-linear.
iv. Geometrical input should be a minimum since only the basic geometry of the vehicle and suspension is available during the concept design phase.
v. The vehicle motion is to be simulated over rough terrain and therefore a realistic tyre model, that includes both the effects of tyre stiffness and damping, must be used.

This chapter is concluded with the presentation of the basic principles of the mathematical optimisation approach to design. The properties of the LFOPC optimisation algorithm, which will be used in conjunction with the vehicle model to optimise the suspension system, will also be briefly described.

2.1 Six degree of freedom vehicle model

Figure 2.1 shows a schematic of a two-dimensional vehicle body and four axles.

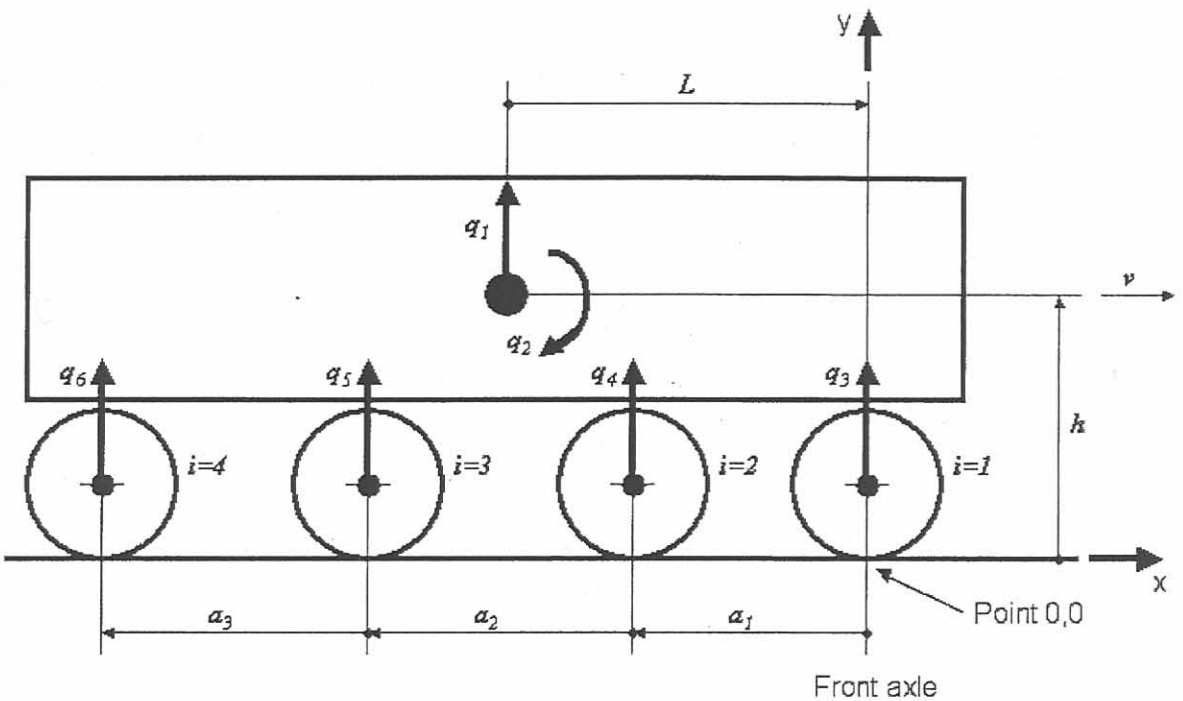

Figure 2.1: Schematic of the vehicle model (in the initial prescribed position)

The vehicle system consists of five solid body components, i.e. the vehicle body and four axles. The vehicle body represents the sprung mass and each axle an unsprung mass associated with the specific wheel station i. A reference co-ordinate system is defined as the point on the road surface vertically underneath the front wheel centre (point 0,0 in figure 2.1). This is also the reference position for the start of the simulation at time zero specified in seconds by $t = 0$. The initial position of the vehicle at $t = 0$, is the static equilibrium position (or as close as possible to the equilibrium position) and is called the *initial prescribed position* of the vehicle on a level road. The exact equilibrium position will be determined before the simulation starts.

Section A1 of Appendix A gives a complete list of all the parameters and variables used for the vehicle model. A basic description of the model is provided by the following specified parameters (*for the initial prescribed position*):

m_1 = mass of the vehicle body (the sprung mass),

m_{i+1} = mass of the unsprung mass associated with each axle i, $i = 1,2,3,4$,

I = pitch inertia of the sprung mass about its centre of gravity,

L = horisontal distance between the sprung mass centre of gravity and the centre of the front axle,

h = height of the centre of gravity with respect to the reference point 0,0,

v = horisontal (forward) vehicle speed at the centre of gravity of the vehicle body, and

a_i = distances between axles as indicated in figure 2.1, $i = 1,2,3$.

Six degrees of freedom, measured relative to the *initial prescribed position*, are defined as follows:

q_1 = vertical displacement at the centre of gravity of the vehicle body,

q_2 = pitch displacement of the vehicle body, and

q_{i+2} = vertical displacement at the wheel centre of axle i, $i = 1,2,3,4$.

Displacements are defined as positive vertically upwards and positive pitch displacement indicates a nose down pitch motion of the vehicle. In the initial prescribed position all the degrees of freedom have a value of zero, i.e. $q_i = 0$, $i=1,2,...,6$.

The corresponding velocity values for these six degrees of freedom are denoted by $\dot{q}_i$, $i = 1,2,...,6$, and the associated accelerations by $\ddot{q}_i$, $i = 1,2,...,6$.

The suspension of each of the axles is modelled by an equivalent trailing arm suspension, although the vehicle may not actually be fitted with a trailing arm suspension. In this approximation the axle is connected to a trailing arm that rotates about an axis (at the trailing arm instant centre) that is connected to the vehicle body. More details of this modelling are given in section 3.10. For each axle the total effect of the springs, dampers and bump stops is simulated by an equivalent suspension connecting the centre of the axle vertically upward to the vehicle body. This is shown in figure 2.2, which gives a schematic representation of this model for one of the axles in the *initial prescribed position*.

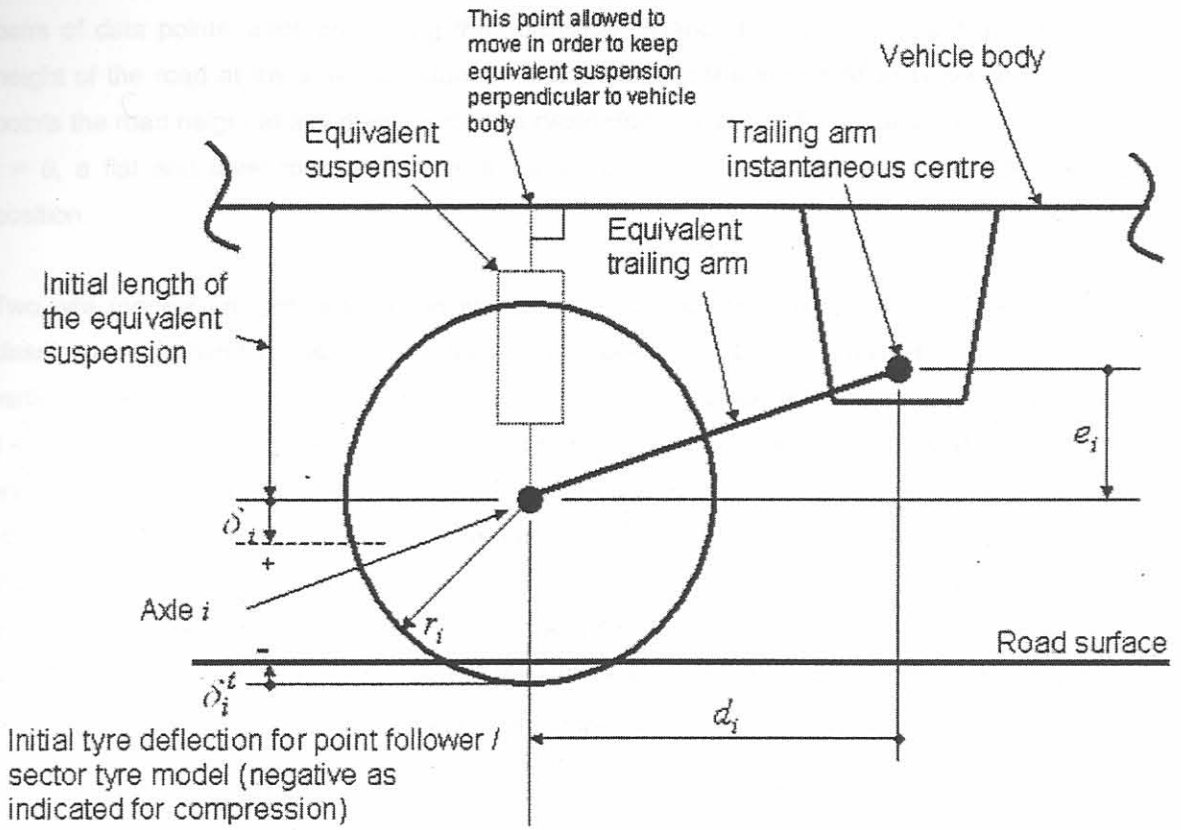

Figure 2.2: Schematic of the axle showing the equivalent trailing arm and suspension (in the initial prescribed position)

The following values are assumed known for the model *initial prescribed position*:

d_i = horisontal length of the equivalent trailing arm,

e_i = vertical height of the equivalent trailing arm, and

r_i = rolling radius of the tyre, $i = 1,2,3,4$.

The deflection of the equivalent trailing arm suspension is given by δ_i, $i = 1,2,3,4$ and is determined by the change in the length of the equivalent suspension as shown in figure 2.2. A negative value for δ_i indicates compression of the equivalent suspension. At the initial prescribed position of the vehicle $\delta_i = 0$, $i=1,2,3,4$. In this position however the actual spring, bump stop and tyre deflection correspond to the initial deflection for these components, namely:

δ_i^s = initial spring deflection,

δ_i^b = initial bump stop deflection, and

δ_i^t = initial tyre deflection, with negative values indicating compression, $i=1,2,3,4$.

The input road profile for the model is given by a discrete two-dimensional data array consisting of pairs of data points, each pair giving the horizontal distance from point 0,0 and the corresponding height of the road at the specific distance. Using cubic spline interpolation between the prescribed points the road height at any distance can be determined. To simplify the calculation of equilibrium at $t = 0$, a flat and level road surface is assumed underneath the wheels at the reference starting position.

Two tyre models are proposed for inclusion in the overall suspension model. The first being the classic point follower model, where the tyre is represented by an equivalent spring and damper, vertically placed between the wheel centre and the road surface and similar to that shown in figure 1.4. This type of tyre model works fine for smooth road surfaces, such as a sinusoidally shaped road with a long wavelength. In instances where the road is rough and the vehicle behaviour for extreme obstacles needs to be simulated, such as for a half round obstacle as shown in figure 2.3, the point follower tyre model does not give realistic results. In such cases the second tyre model, a sector tyre model, should be used. For this sector tyre model the tyre / wheel is divided into a number of sectors and the deflection for each sector, due to the road input, is determined. Finally the deflections of all the sectors are used together to determine respectively the resultant tyre force f_i^w and resultant deflection δ_i^w, $i = 1,2,3,4$. These force and deflection vectors are shown in figure 2.3. Clearly the resultant tyre force is not necessarily vertical as in the case of the point follower, but may be applied at an angle φ_i, also shown in figure 2.3. The sector tyre model to be used in this study is similar to that used in the more comprehensive vehicle dynamic simulation program GENRIT [3]. The current author developed this model [3] for improved simulation accuracy when using GENRIT. This sector tyre model will not be discussed in detail here.

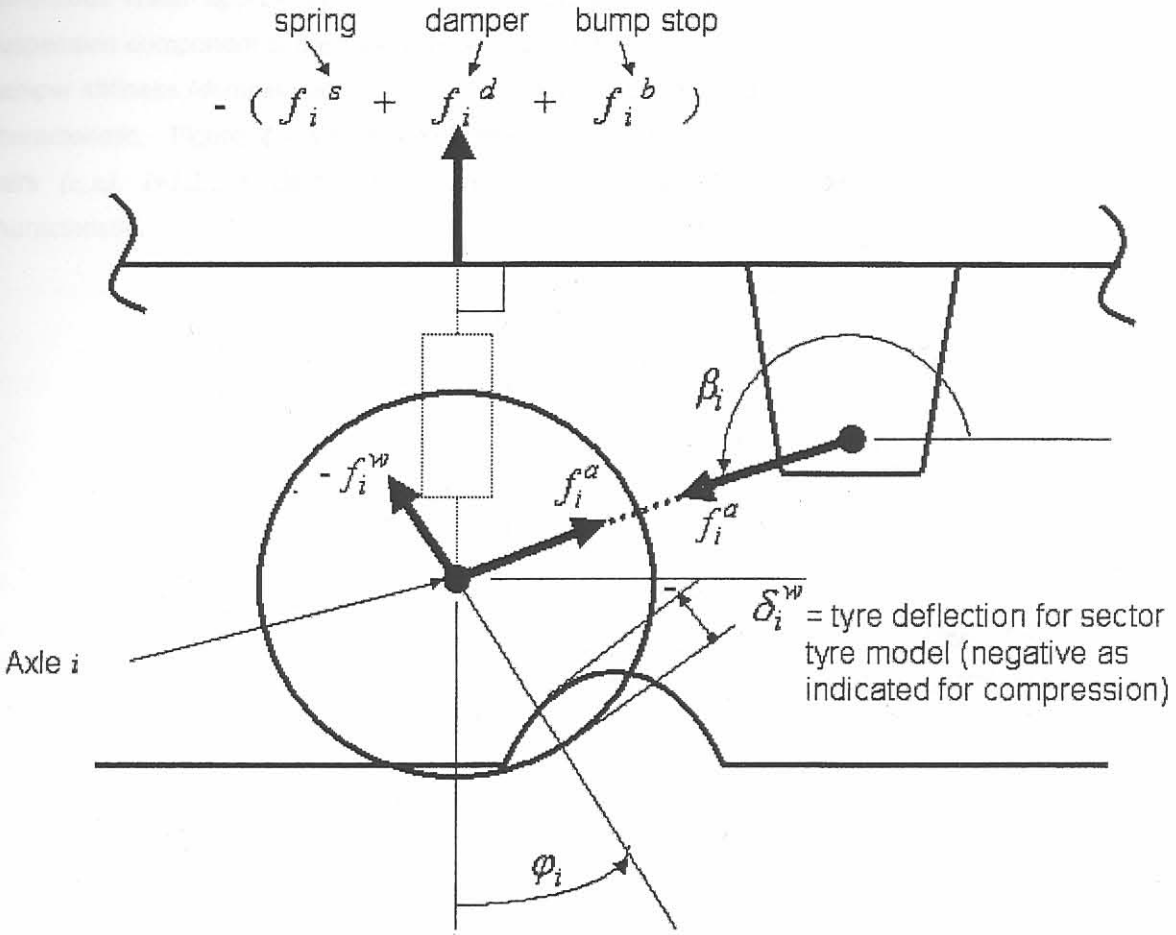

Figure 2.3: Schematic of the axle showing the road profile and suspension forces

The suspension forces on the vehicle body (and opposite and equal on the axle) due to each axle i, $i = 1,2,3,4$, consist of the following four forces shown in figure 2.3:

f_i^s = equivalent spring force,

f_i^d = equivalent damper force,

f_i^b = equivalent bump stop force, and

f_i^a = force in the equivalent trailing arm.

The first three forces are defined to be negative for compression (associated with negative deflections), and therefore the upward force on the vehicle is obtained by multiplying their respective values by minus one. The angle β_i is the angle of the equivalent trailing arm measured as indicated in figure 2.3

The non-linear characteristics of the suspension and tyres need to be modelled. In order to be able to describe the non-linear force characteristics of these components it was decided to use six piece-wise

continuous linear approximations. In this approach the approximation of the characteristic of a suspension component is described by twelve parameters. For example, for a particular damper six damper stiffness (damping coefficient) values and six corresponding deflection rate values define the characteristic. Figure 2.4 shows a schematic for damper characterisation. Clearly the parameter pairs (c_i,x_i), $i=1,2,...,6$ define the piece-wise continuous linear representation of the damper characteristic.

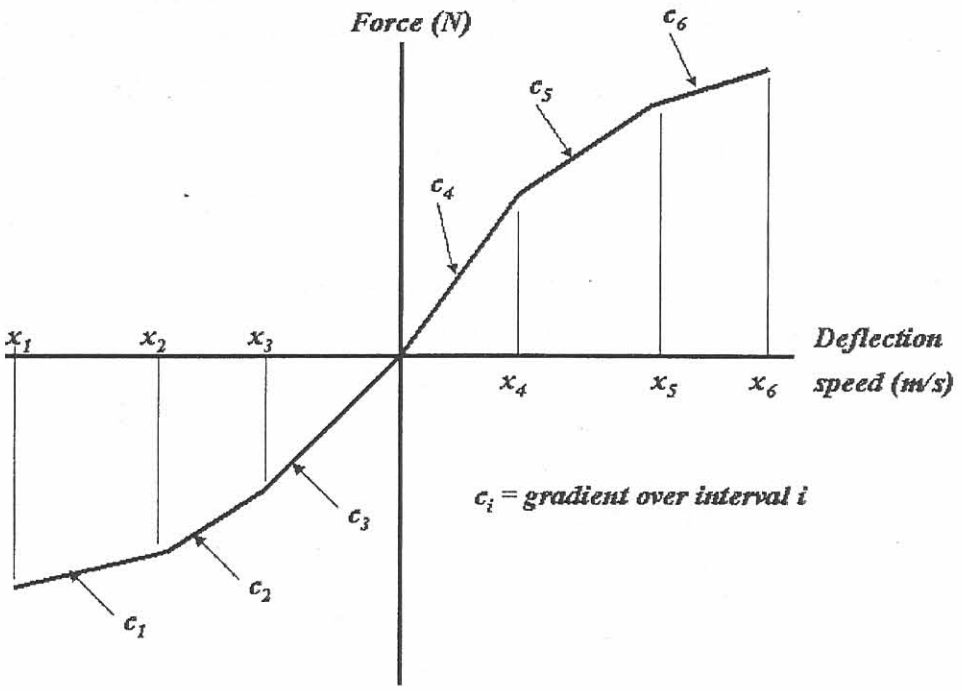

Figure 2.4: The six piece-wise continuous linear approximation for suspension force characterisation

Using this six piece-wise linear approximations the damping force, F, at any deflection rate x, is explicitly and analytically given as follows:

For $x < x_2$:	$F = c_3x_2 + c_2(x_2 - x_3) + c_1(x - x_2)$	(2.1)
For $x_2 < x < x_3$:	$F = c_3x_2 + c_2(x - x_3)$	(2.2)
For $x_3 < x < 0$:	$F = c_3x$	(2.3)
For $0 < x < x_4$:	$F = c_4x$	(2.4)
For $x_4 < x < x_5$:	$F = c_4x_4 + c_5(x - x_4)$	(2.5)
For $x > x_5$:	$F = c_4x_4 + c_5(x_5 - x_4) + c_6(x - x_5)$	(2.6)

The characteristics for the other suspension components, i.e. for the springs, bump stops and tyres are handled in a similar manner. In the case of spring, tyre and bump stop deflections the data pairs represent the force versus deflection characteristic of the respective components. The deflections

used for these components include the initial deflections and the deflections due the equivalent trailing arm deflection (see 2.1.1.2) for more detail.

2.1.1 Equations of motion of the vehicle system

Newton's second law can be applied separately to each solid body component of the vehicle system to determine the respective accelerations. The first step in computing the accelerations is to determine all the forces acting on each body at a particular time instant, denoted by the simulation time t. At the start of the simulation $t = 0$.

2.1.1.1 Tyre forces

In order to determine the wheel forces, the tyre deflections need to be calculated. Figure 2.5 gives a schematic for a part of the vehicle at a particular instant in time. (Note that the angle θ as indicated in the figure is for negative pitch of the vehicle and is therefore negative. Similarly δ_i is negative as shown.)

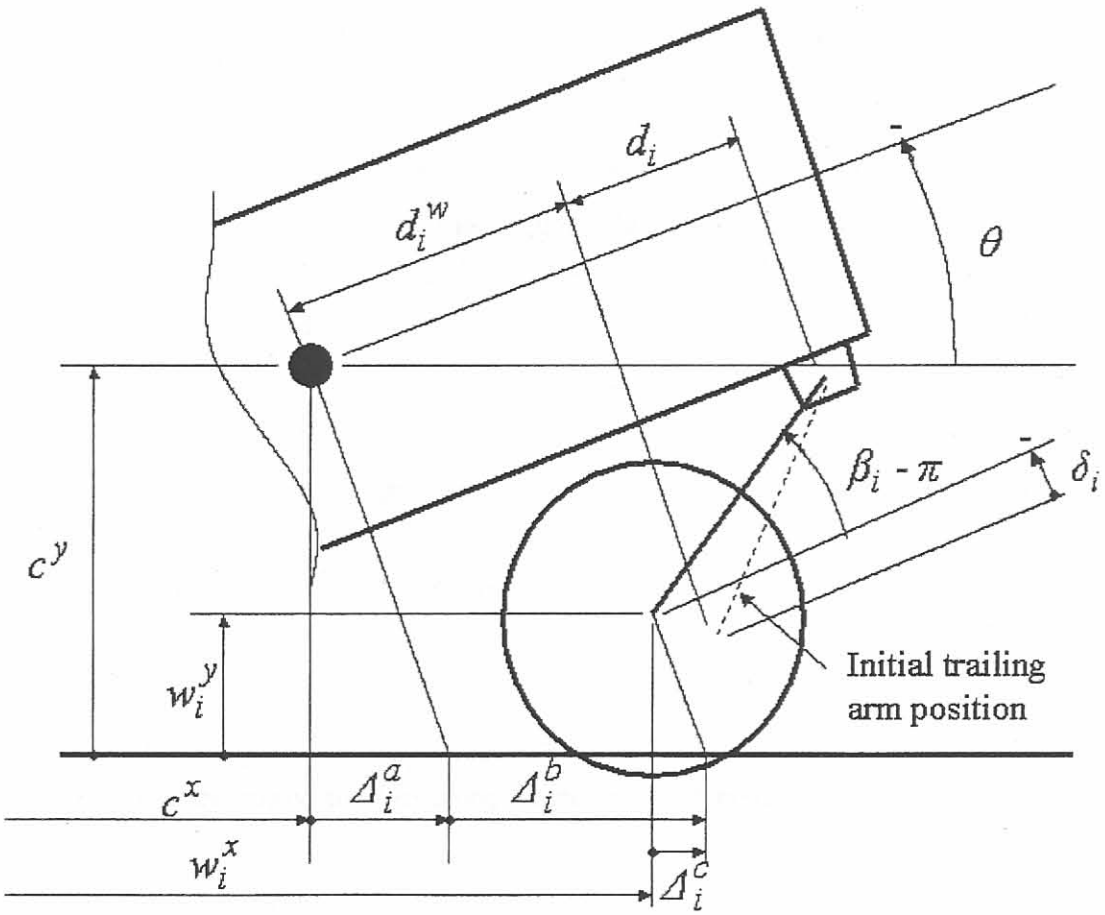

Figure 2.5: Schematic of a part of the vehicle model showing the parameters used to determine the tyre forces

The position coordinates relative to the reference point 0,0 shown in figure 2.1, of the centre of gravity of the vehicle are given by:

$$c^y = h + q_1 \tag{2.7}$$

$$c^x = vt - L \tag{2.8}$$

The pitch angle of the vehicle is given by the second degree of freedom:

$$\theta = q_2 \tag{2.9}$$

The longitudinal distance d_i^w between the wheel centre of axle i and the centre of gravity, for the initial prescribed position, is given by

for the front axle, *(i = 1)*: $d_1^w = L$ (2.10)

for the second axle, *(i = 2)*: $d_2^w = L - a_1$ (2.11)

for the third axle, *(i = 3)*: $d_3^w = L - (a_1 + a_2)$ (2.12)

for the fourth axle, *(i = 4)*: $d_3^w = L - (a_1 + a_2 + a_3)$ (2.13)

The horisontal position, w_i^x of the wheel centre as measured from the reference point, and the total wheel force f_i^w, are obtained via the detailed argument below (up to eq. 2.28).

The vertical height of wheel centre *i*, $i = 1,2,3,4$, is given by:

$$w_i^y = q_{i+2} + r_i + \delta_i^t \tag{2.14}$$

(remember $\delta_i^t < 0$ for tyre compression)

The length of the equivalent trailing arm is given by:

$$t_i = \sqrt{e_i^2 + d_i^2} \tag{2.15}$$

and the angle β_i of the trailing arm (assuming a deflection δ_i of the equivalent suspension) by:

$$\beta_i = arcsin\left(\frac{-(e_i + \delta_i)}{t_i}\right) \tag{2.16}$$

Note that for a trailing arm suspension d_i is positive and therefore $90° < \beta_i < 270°$, and for leading arm suspension geometry d_i is negative and therefore $-90° < \beta_i < 90°$. The e_i is defined positive if the original wheel centre position is lower than the equivalent trailing arm instantaneous centre.

The respective lengths Δ_i^a, Δ_i^b and Δ_i^c indicated in figure 2.5 are given by:

$$\Delta_i^a = -c^y \tan\theta \tag{2.17}$$

$$\Delta_i^b = \frac{d_i^w + d_i + t_i \cos\beta_i}{\cos\theta} \tag{2.18}$$

$$\Delta_i^c = -w_i^y \tan\theta \tag{2.19}$$

and the distance, w_i^x, is therefore given by

$$w_i^x = c^x + \Delta_i^a + \Delta_i^b - \Delta_i^c \tag{2.20}$$

If the sector tyre model is used then, determine the radial tyre deflection δ_i^w at (w_i^x, w_i^y), the angle for the resultant tyre force φ_i and the tyre force factor Λ_i using the tyre sector model [3]. The tyre force factor Λ_i is a factor that takes the shape of the specific obstacle (that deflects the tyre) into consideration. The tyre stiffness is normally measured for deflection from a flat surface and in this instance $\Lambda_i = 1$. For other shapes of obstacles the factor Λ_i is determined by the ratio between the deflection area (in side view) for the specific obstacle, and that obtained for deflection from a flat surface. Normally in these instances $\Lambda_i < 1$.

If the point follower tyre model is used then, determine the height of the road profile h_i^r, at w_i^x using cubic spline interpolation of the prescribed road profile data. For this model:

$$\delta_i^w = q_{i+2} - h_i^r + \delta_i^t \tag{2.21}$$

$$\varphi_i = 0 \tag{2.22}$$

$$\Lambda_i = 1 \tag{2.23}$$

The wheel deflection is limited to negative values since the tyres can only experience compression, i.e.:

$$\text{If } \delta_i^w > 0 \text{ then set } \delta_i^w = 0 \tag{2.24}$$

The tyre deflection rates are estimated by backward finite differences:

$$\dot{\delta}_i^w = \frac{\delta_i^w(t) - \delta_i^w(t-\delta^t)}{\delta^t} \tag{2.25}$$

for i, $i = 1,2,3,4$, and where δ^t is a suitable small time step.

Once the tyre deflections $\delta_i^w, i = 1,2,3,4$ are known, the wheel forces F_i^{ws} can be calculated by using equations 2.1 to 2.6 together with the tyre stiffness/deflection parameters characterising the tyre stiffness. Once F_i^{ws} is known, the wheel force due to tyre stiffness can be determined using the prescribed input for the number of tyres per axle, n_i^w, and the tyre factor Λ_i, calculated by using the tyre sector model or the point follower model. The wheel force is then given by:

$$f_i^w = F_i^{ws} n_i^w \Lambda_i \tag{2.26}$$

Using the tyre deflection rate $\dot{\delta}_i^w$, the tyre damping force F_i^{wd} may be computed in a similar manner by using equations 2.1 to 2.6 and the prescribed tyre damping characterising parameters. The tyre damping force is then added to f_i^w above to give the total tyre force on the specific axle i:

$$f_i^w = f_i^w + F_i^{wd} n_i^w \Lambda_i \tag{2.27}$$

Limiting the tyre force to negative values, i.e. only compression allowed, the following rule is applied:

$$\text{If } f_i^w > 0 \text{ then set } f_i^w = 0 \tag{2.28}$$

2.1.1.2 The spring, damper and bump stop forces

For each axle, i, the suspension deflection of the equivalent suspension is given by (refer to figure 2.5 for a schematic and section A2 of Appendix A):

$$\delta_i = \frac{c^y - (d_i^w + d_i + t_i \cos\beta_i)\sin\theta - w_i^y}{\cos\theta} - (h - r_i - \delta_i^t) \tag{2.29}$$

and the deflection rate by direct differentiation with respect to time follows:

$$\dot{\delta}_i = \frac{\dot{q}_1}{\cos\theta} - (d_i^w + d_i + t_i \cos\beta_i)\dot{q}_2 - \frac{\dot{q}_{i+2}}{\cos\theta} \tag{2.30}$$

In the equivalent suspension approach used in this study the actual springs, dampers and bump stops are modelled by the equivalent suspension as shown in figure 2.2. Due to the geometrical position of the actual spring on axle i, a ratio between the deflection of the actual spring and the equivalent suspension deflection δ_i exists. This ratio is given by $\kappa_i^s, i = 1,2,3,4$. Similarly for each axle i, a ratio between the actual damper and bump stops deflection and the equivalent suspension deflection exists. These ratios are respectively denoted by κ_i^d and $\kappa_i^b, i = 1,2,3,4$.

The respective deflections may now be determined as follows. The deflection at the actual spring is given by:

$$\Delta_i^s = \delta_i \kappa_i^s + \delta_i^s \qquad (2.31)$$

where

κ_i^s = the ratio between the actual spring deflection and that for the equivalent suspension,

δ_i^s = the initial spring deflection,

and the deflection at the actual bump stop:

$$\Delta_i^b = \delta_i \kappa_i^b + \delta_i^b \qquad (2.32)$$

where

κ_i^b = the ratio between the actual bump stop deflection and that for the equivalent suspension,

δ_i^b = the initial bump stop deflection,

and the deflection rate at the actual damper:

$$\dot{\Delta}_i^d = \dot{\delta}_i \kappa_i^d \qquad (2.33)$$

where

κ_i^d = the ratio between the actual damper deflection rate and that for the equivalent suspension.

Using the spring deflection $\Delta_i^s, i = 1,2,3,4,$ the spring force F_i^s may be calculated using the spring stiffness versus deflection piece-wise data and equations 2.1 to 2.6. With the respective F_i^s known, the equivalent suspension force due to the spring force may be obtained:

$$f_i^s = F_i^s n_i^s \kappa_i^s \tag{2.34}$$

where

n_i^s = the number of springs on the axle.

Also at a deflection of Δ_i^b use the bump stop stiffness versus deflection piece-wise data and calculate the bump stop force F_i^b. Calculate the equivalent suspension force due to F_i^b:

$$f_i^b = F_i^b n_i^b \kappa_i^b \tag{2.35}$$

where

n_i^b = the number of bump stops on the axle.

Similarly, using the damping coefficient versus deflection rate piece-wise data, the damper force F_i^d may be determined at a specific deflection rate $\dot{\Delta}_i^d$. With F_i^d known, the equivalent suspension force for axle i may be calculated:

$$f_i^d = F_i^d n_i^d \kappa_i^d \tag{2.36}$$

where

n_i^d = the number of dampers on the axle.

2.1.1.3 Acceleration of the vehicle body

Once all the forces acting on the body are known the acceleration and pitch acceleration of the vehicle body can be computed.

From eq. 2.34 to 2.36 the total equivalent suspension force at each wheel i is given by:

$$f_i^e = f_i^s + f_i^d + f_i^b \tag{2.37}$$

Applying a force equilibrium in the direction of the equivalent trailing arm (see figure 2.6) the force f_i^a in each equivalent trailing arm is approximately given by (the effect of the acceleration of the axle in the direction of the trailing arm is neglected due to the fact that this acceleration will normally be small for $\beta_i \approx 180°$ and due to the fact that the mass of the axle m_{i+1} is very small compared to m_1):

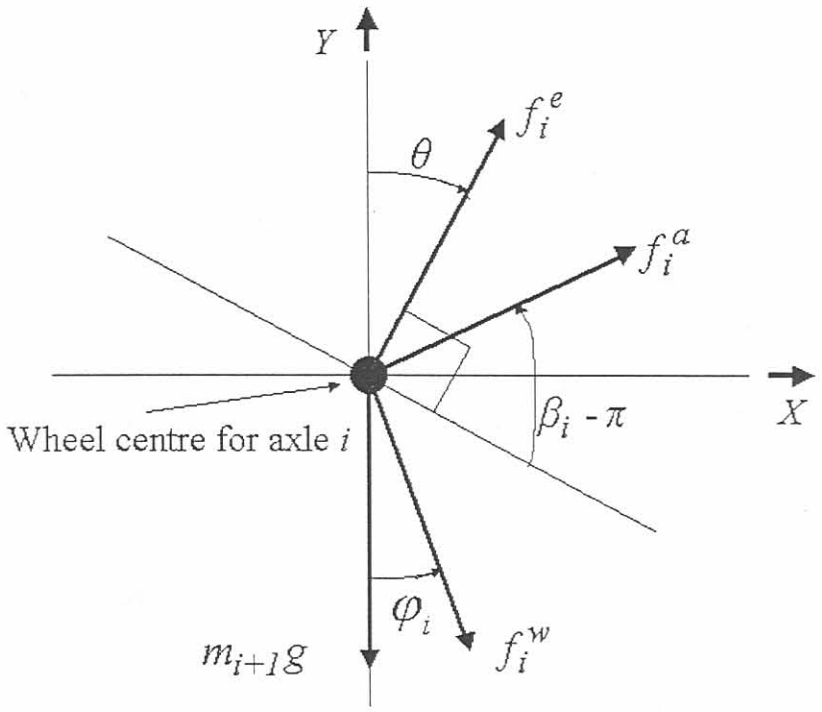

Figure 2.6: Schematic of forces acting at the wheel centre

$$f_i^a = -f_i^e \cos(\frac{3\pi}{2} - \beta_i) + f_i^w \cos(\frac{3\pi}{2} - \beta_i + \theta + \varphi_i) + m_{i+1} g \cos(\frac{3\pi}{2} - \beta_i + \theta) \qquad (2.38)$$

which simplifies to:

$$f_i^a = f_i^e \sin\beta_i + f_i^w \sin(\theta + \varphi_i - \beta_i) + m_{i+1} g \sin(\theta - \beta_i) \qquad (2.39)$$

The total sum of the components of the trailing arm forces in the direction of q_1 or Y in figure 2.7 is given by:

$$F^a = \sum_{i=1}^{4} f_i^a \cos(\frac{3\pi}{2} - \beta_i + \theta) = \sum_{i=1}^{4} f_i^a \sin(\theta - \beta_i) \qquad (2.40)$$

and the sum of the suspension forces:

$$F^s = \sum_{i=1}^{4} f_i^e \cos\theta \qquad (2.41)$$

The body acceleration is now given by:

$$\ddot{q}_1 = \frac{-m_1 g - F^a - F^s}{m_1} \qquad (2.42)$$

The moments acting on the vehicle body (refer to figures 2.3, 2.5 and 2.7 as well as the detailed derivation in section A3 of Appendix A) due to axle i is given by:

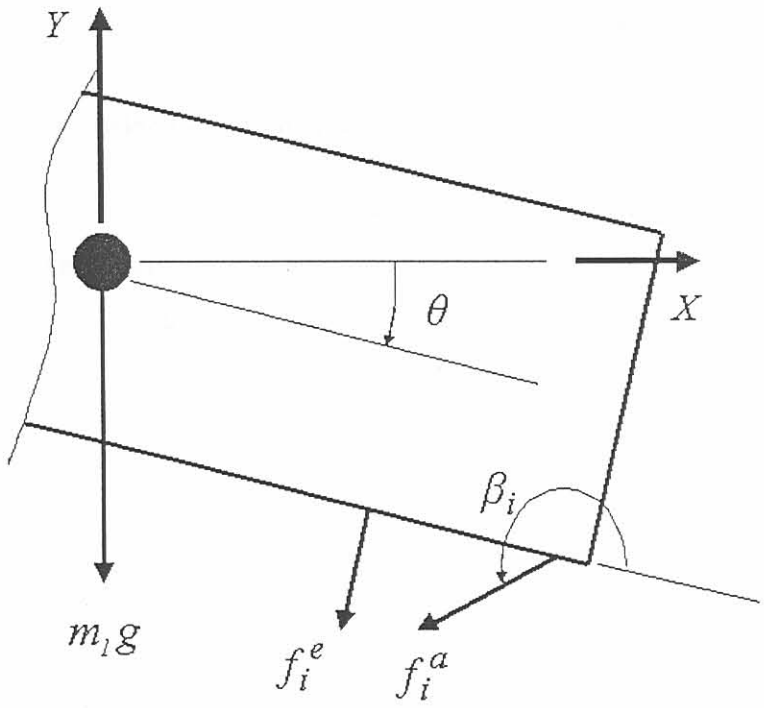

Figure 2.7: Schematic of forces acting on vehicle body

$$M_i = f_i^e (d_i^w + d_i + t_i \cos\beta_i) - f_i^a (d_i^w + d_i)\sin\beta_i - f_i^a (h - r_i - \delta_i^t - e_i)\cos\beta_i \qquad (2.43)$$

The pitch acceleration can be determined from:

$$\ddot{q}_2 = \frac{\sum_{i=1}^{4} M_i}{I} \qquad (2.44)$$

2.1.1.4 Axle accelerations

The accelerations of the different wheels (perpendicular to the equivalent trailing arm) can be shown (see section A4 of Appendix A) to be given by:

$$\ddot{q}_i^a = \frac{-f_i^e \cos\beta_i + m_{i+1} g \cos(\beta_i - \theta) + f_i^w \cos(\beta_i - \theta - \varphi_i)}{m_{i+1}} \qquad (2.45)$$

This acceleration can be transformed to the direction of the degrees of freedom for the axles as well as adding the acceleration of the equivalent trailing arm instantaneous centre to obtain the accelerations of the axle centres $i, i = 12,3,4$:

$$\ddot{q}_{i+2} = -\ddot{q}_i^a \cos(\beta_i - \theta) + \ddot{q}_1 - \ddot{q}_2[(d_i^w + d_i)\cos\theta - (h - r_i - \delta_i^t - e_i)\sin\theta] \qquad (2.46)$$

2.1.1.5 Solving for the velocities and displacements

Equations 2.42, 2.44 and 2.46 represent a system of six second order differential equations. Once the initial conditions, i.e. initial displacements and velocities $q_i(0)$ and $\dot{q}_i(0), i = 1,2,...,6$ at $t = 0$ are specified, they may be solved numerically to give the displacements and velocities at successive time instants t at intervals of δ^t. In this study a fourth order Runga Kutta method [56] is use to solved the equations and the solution is initiated from equilibrium such that $\dot{q}_i(0) = 0$ for all i.

2.1.2 Equilibrium

Before applying the procedure described in 2.1.1 for the solution of the vehicle dynamics, it is important to first determine the initial equilibrium configuration of the vehicle system from which the solution is to be started. To obtain equilibrium at $t = 0$, the following heuristic iterative process is proposed and applied:

1. Set $q_i = \dot{q}_i = 0, \ i = 1,2,...,6$ *(2.47)*
2. Determine the accelerations $(\ddot{q}_i, \ i = 1 \text{ to } 6)$ using equations 2.42, 2.44 and 2.46.
3. For $i = 1,2,4,5,6$:

$$\begin{aligned} &\text{If } \ddot{q}_i > 0.005 \text{ then set } q_i = q_i + \ddot{q}_i / 5000 \\ &\text{If } \ddot{q}_i < -0.005 \text{ then set } q_i = q_i + \ddot{q}_i / 1330 \end{aligned} \qquad (2.48)$$

4. And for $i = 2$:

$$\begin{aligned} &\text{If } \ddot{q}_i > 0.005 \text{ then } q_i = q_i + \ddot{q}_i / 10000 \\ &\text{If } \ddot{q}_i < -0.005 \text{ then } q_i = q_i + \ddot{q}_i / 1850 \end{aligned} \qquad (2.49)$$

(The values of 5000, 1330, 10000 and 1850 used in equations 2.48 and 2.49 were determined experimentally. The heuristic proved effective in obtaining equilibrium relatively quickly for most of the vehicle configurations tested.)

5. Determine the sum of the absolute values of the vertical accelerations:

$$T^q = |\ddot{q}_1| + |\ddot{q}_3| + |\ddot{q}_4| + |\ddot{q}_5| + |\ddot{q}_6| \qquad (2.50)$$

6. If $T^q < 0.005 + 0.005 * n_a$ *and* $|\ddot{q}_2| < 0.005$, where n_a is the number of axles, then equilibrium is assumed, otherwise, with the current displacements q_i again set $\dot{q}_i = 0, \ i = 1,2,...,6$ and go to step 2.

Of course, in the event of failure of the above iterative scheme to produce equilibrium, the computationally more expensive option remains to perform the simulation with $v = 0$ until equilibrium is obtained. Analysing the results of the simulation will yield the required initial spring, bump stop and tyre deflections.

2.2 Optimisation algorithm

Mathematical optimisation is the process of the formulation and then the solution of a constrained optimisation problem of the general mathematical form:

$$minimise_{\text{with respect to } x}\ f(\mathbf{x}),\ \mathbf{x} = (x_1, x_2, \ldots x_n) \in R^n \qquad (2.51)$$

subject to constraints

$$g_j(\mathbf{x}) <= 0,\ j = 1,2,\ldots m \qquad (2.52)$$

$$h_j(\mathbf{x}) = 0,\ j = 1,2,\ldots r < n \qquad (2.53)$$

where $f(\mathbf{x})$, $g_j(\mathbf{x})$ and $h_j(\mathbf{x})$ are scalar functions of $\mathbf{x}$ [53]. The variables $\mathbf{x}$ are called the design variables, $f(\mathbf{x})$ the objective function and $g_j(\mathbf{x})$ and $h_j(\mathbf{x})$ are respectively referred to as the inequality and equality constraint functions.

The formulation of the optimisation problem requires identifying the objective function, the variables and the constraints. This is done by means of a mathematical model of the system or process that is to be optimised. The construction of an appropriate model, in this case of a vehicle suspension system, is thus the first step in the optimisation process. If the model is too simplistic, it will not give useful insight into the practical problem, but if it is too complex it may become difficult to solve [66]. Once the formulation has been done an optimisation algorithm can be selected to find the solution. Usually the algorithm and model are sufficiently complicated that a computer is needed to implement the optimisation process. There is no universal optimisation algorithm. Rather, there are numerous algorithms, each of which is tailored to a particular type of optimisation problem.

Excellent texts on design optimisation exist, including in particular those of Arora [68], Haftka & Gürdal [69], Papalambros & Wilde [70] and Vanderplaats [71]. These works describe various classical and traditional optimisation algorithms that have been used with success in solving engineering optimisation problems. In this study, however, the relatively novel LFOPC algorithm of Snyman [53-55] is selected as the optimisation algorithm to be used. Section A5 of Appendix A gives a more detailed description of the LFOPC algorithm. The LFOPC algorithm has the following characteristics:

i. it uses only function gradient information,
ii. no explicit line searches are performed,
iii. it is extremely robust and handles steep valleys and discontinuities in functions and gradients with ease,

iv. the algorithm seeks relative low local minima and can thus be used as a basic component in a methodology for global optimisation,

v. it is not as efficient on smooth and near quadratic functions as classical methods, but

vi. it is particularly robust and reliable in dealing with the presence of numerical noise in the objective and constraint functions – this is expected to be the case in this study where the objective function is to be evaluated via numerical simulations.

For a complete description of the LFOPC mathematical code the reader is referred to [51, 53-55].

In using the LFOPC optimisation algorithm in conjunction with the vehicle simulation program for the optimisation of vehicle and/or suspension characteristics, the following demands are to be satisfied:

i. A baseline vehicle is to be modelled.

ii. The user should be able to select the required vehicle parameters to be optimised and couple them to design variables of the optimisation code. For a specific vehicle parameter selected the baseline design variable value is to be normalised to a value of 1, i.e. when the design variables are changed by the LFOPC algorithm then:

$$\textit{New vehicle parameter} = \textit{Baseline vehicle parameter} * \textit{design variable} \qquad (2.54)$$

iii. Constraints and general parameters for the optimisation process are to be prescribed.

iv. The user should be able to select / construct a specific suitable objective function to be minimised.

v. The vehicle dynamic simulation is to be performed for the specified set of vehicle parameters with the results of the simulation being stored.

vi. Using the saved simulation results the specific objective function is to be calculated.

vii. The LFOPC algorithm should be capable of communicating with the simulator so that the effect on the objective function, of small changes in the respective values of the design variables, can be determined. In particular this is necessary for the computation of approximations to the components of the gradient vector of the objective function through forward finite differences.

viii. Using the gradient vector the optimisation algorithm should compute a next set of design variables lying along a trajectory leading to the optimum design. Thus each new set of design variables represents the next step (iteration) along the optimisation path.

ix. At each iteration the whole process (step v to viii) is to be repeated until no further significant improvement in the objective function is obtained. The final set of design variables is taken as the optimum giving a corresponding optimum objective function value.

Etman [23] states that the coupling of a detailed and comprehensive multi-body code to a mathematical programming algorithm may be difficult to implement and can lead to high computational cost. In heeding this warning an attempt is made in this study to keep the vehicle

model as simple as possible. The dramatic increase in computer processing speed over the past few years has also made the development of a realistic suspension optimisation system, by means of which the above demands may be met, a more realistic proposition.

2.3 Summary

In this chapter the mathematical model for the two dimensional simulation of vehicle dynamics is described. The respective six piece-wise continuous linear approximations used to describe the non-linear suspension characteristics of the springs, dampers, bump stops and tyres to be used in the simulation, are also given. Basically the vehicle model consists of up to five solid bodies, one corresponding to the vehicle body and the others to up to four axles on the vehicle. Six degrees of freedom describe the motion of the system of bodies. The suspension is modelled by using an equivalent trailing arm approach. The governing equations of motion of the system are derived. Accelerations are determined once the forces acting on the bodies due to prescribed road input are calculated. Using a fourth order Runga Kutta numerical integration scheme the velocities and displacements of the bodies are computed. The importance of determining the equilibrium configuration of the vehicle before commencing the simulation is stressed. The actual method by means of which the required equilibrium configuration is determined through iteration is briefly described.

The coupling of the LFOPC optimisation algorithm to the vehicle dynamics model is also briefly discussed. Using the LFOPC algorithm a set of design variables, related to vehicle parameters, can be specified. The optimum set with respect to a user defined objective function may then be determined by LFOPC.

Although the literature overview warns of the difficulties associated with coupling a multi-body code directly to a mathematical optimisation algorithm, this approach is nevertheless taken in this study. Due to the fact that computer processing power and speed has recently increased dramatically such a task has become more realisable. Keeping the multi-body code as simple as possible and exploiting the robustness and effectiveness of the LFOPC algorithm, an attempt is now made to develop a practically useful suspension optimisation system.

CHAPTER 3:

SIMULATION PROGRAM

3. Simulation program

In chapter 1 the need for a two-dimensional vehicle simulation program was explained. Chapter 2 described the mathematical model for such a simulation program as well as the use of the LFOPC optimisation code, in conjunction with which the vehicle model is to be optimised with respect to certain vehicle parameters. In this chapter the simulation program Vehsim2d, that was developed to fulfil the first need, is described.

3.1 Introduction

A demonstration version of the program is included on compact disc in appendix B. The simulation program Vehsim2d is used to simulate two dimensional vehicle dynamics. The program is two-dimensional and can only simulate the pitch and bounce of the vehicle over symmetrical obstacles, i.e. the same route profile underneath the left and right wheels. The effect of different inputs under the left and right wheels as well as the effect of anti-roll bars cannot be simulated by Vehsim2d, and can only be done by using a three-dimensional vehicle dynamics program. It is proposed that Vehsim2d is to be used during the concept design phase and that a complete three-dimensional simulation be used during the detail design phase if necessary.

For Vehsim2d the individual suspension modules of a vehicle is broken up into a spring, damper, bump stop, suspension geometry and tyre characteristics. The suspension characteristic of a component is prescribed using a six piece-wise continuous linear representation of the stiffness versus deflection, or damping force versus deflection speed relationship. The wheels of the vehicle are modelled with a spring stiffness and damping which may both be non-linear. Two tyre models are also available; a point follower and a sector tyre model.

Coupled to Vehsim2d is the optimisation algorithm LFOPC. This algorithm can be used to optimise certain specified vehicle parameters or vehicle suspension characteristics, subject to certain constraints, through the minimisation of an appropriate objective function. The characteristics that need to be optimised as well as the objective function to be used can be prescribed by the user. The details of the optimisation module is described in the next chapter.

3.2 Vehsim2d simulation capabilities

Vehsim2d is a two-dimensional vehicle simulation program and can be used to simulate the vehicle dynamics of a vehicle over symmetrical obstacles. The motion of the vehicle is simulated by prescribing the vehicle geometry, unsprung mass and inertia, the mass of the different sprung components and the suspension characteristics. The characteristics of the suspension components and the tyres may be non-linear and are prescribed using a six piece-wise continuous linear

approximation for each component. The specific route profile and speed of the vehicle are also prescribed.

The dynamics of the vehicle over the specified route profile is solved during the simulations by the method detailed in chapter 2. The result of a simulation is stored and can then be analysed using a postprocessor. The postprocessor is also used to generate data for use in a coupled program, which is used to calculate ride comfort criteria for the simulation. An animation of the vehicle movement can also be done.

The constrained optimisation program LFOPC [51, 53-55] is also coupled to the program. This routine can be used to optimise user specified vehicle parameters or suspension characteristics through the minimisation of a user specified objective function. A typical example is the optimisation of the damper characteristics on specific axles in order to obtain the best ride comfort for the driver and rear passengers in the vehicle.

3.3 Program structure

Vehsim2d uses a graphical user interface (GUI) operating in a Microsoft Windows 95/98/2K/NT environment. It was developed using Microsoft Visual Basic 6.0 (Enterprise edition). Vehsim2d is divided into different functional subprograms that may be called by buttons on the main input screen of the program as shown in figure 3.1.

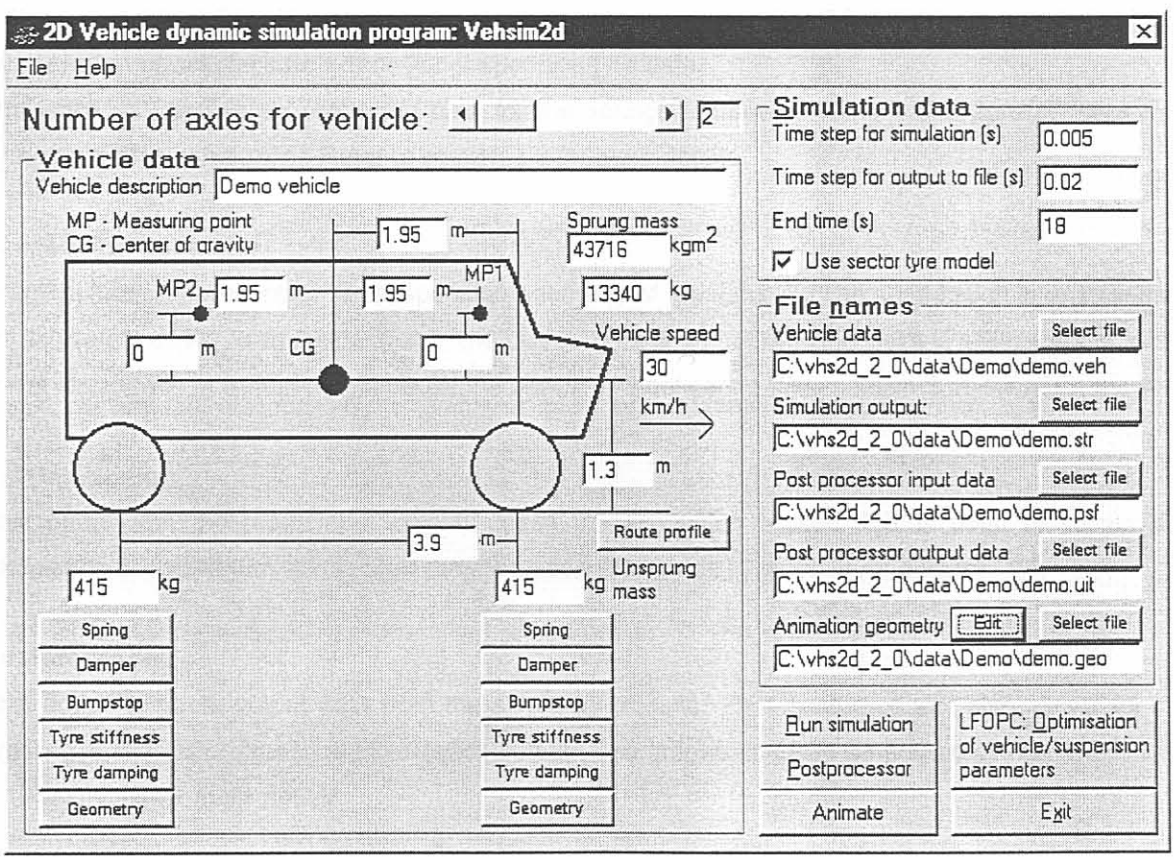

Figure 3.1: Vehsim2d – Main Input Screen

Main input screen

The main screen is used to provide vehicle information relating to mass, inertia and geometry, number of axles, points of interest (measuring points), suspension components, simulation input data and relevant file names for simulation input and results. The execution of the various tasks: simulation, postprocessing, suspension optimisation, editing of the animation geometry and performing animation, are also available through the options and buttons displayed on the main input screen. The pull-down menu is used to open and save the vehicle files and to provide access to the help files. See 3.6 for more detail on the main input screen.

A short discussion of the main features available through interaction with the main input screen now follows.

Animation geometry editor

This editor is used to edit or create the vehicle geometry required for the animation. Only the geometry of the vehicle hull is required. See section 3.7 for more details.

Two dimensional data editor (for route profile data)

This editor is used to prescribe the data for the route profile used in the simulation. Route profile data is given as a two-dimensional data array with data sets for the distance and height of the road profile. Section 3.8 gives more details.

Suspension characteristic editor (for suspension/tyre data)

This editor is used to prescribe the data for the springs, dampers, bump stops, tyre stiffness and damping for the simulation. Refer to section 3.9 for more details.

Suspension geometry

This input screen prescribes the suspension geometry of the vehicle. The suspension is analysed as an equivalent trailing arm suspension. The position of the virtual reaction point is prescribed in terms of the distance in front and height above the relevant wheel centre. See section 3.10 for more details.

Run simulation

This button (on the main input screen) loads the simulation screen that is used to initiate the calculation of equilibrium and to start the simulation. Section 3.11 gives more details.

Postprocessor

This option extracts output data from the simulation results. The postprocessor also allows for the drawing of graphs of prescribed simulation output. The graphs can also be printed. Refer to sections 3.12 and 3.13 for more details.

Animate

The animation feature may be used to get a subjective feel of the simulation being performed. See section 3.14 for more details.

LFOPC: Optimisation of vehicle/suspension parameters

This button enables the selection of the design variables and appropriate objective function to be used by the optimisation algorithm LFOPC. Paragraph 3.15 gives more detail on the optimisation.

3.4 Simulations

A vehicle is modeled by prescribing the general vehicle characteristics, i.e. unsprung mass, unsprung pitch inertia, position of centre of gravity, number of axles and axle placement. Data for the springs, dampers, bump stops, tyre stiffness, tyre damping and suspension geometry of the different axles are also prescribed. The route profile, vehicle speed and simulation time steps are prescribed. Once all the required data is available the simulation can be performed. The entire vehicle, suspension and simulation data are saved in a vehicle file (*.veh). The first step during simulations is to perform the equilibrium calculations by means of which the equilibrium position of the vehicle is determined. Once equilibrium is obtained, the simulation can be commenced. With the forces known the accelerations are available and by using a fourth order Runga-Kutta technique the velocity and displacements of the different components are calculated at prescribed time instants during the ride. All these results are saved in a simulation output (.str) file.

Once the simulation is completed, the postprocessor can be used to extract the required simulation results and to write these to a postprocessor output (*.out) file. The required selection for output from the postprocessor is saved in a postprocessor input file (*.psf). The output of the postprocessor can be graphed using the graph option. The postprocessor can also be used to generate a file for ride comfort analysis (*.rcd) that can be used in performing ride comfort analysis with a separate module. Other buttons available on the postprocessor screen can be used for initiating the calculation of the root mean square, minimum and maximum values (*.rms) and the calculation of a vibration dose value (*.vdv).

An animation of the simulation can be done using the animator. For this purpose a geometry file (*.geo) is required which prescribes the geometry of the vehicle body. This animation geometry file can be compiled using the available geometry editor.

Optimising the suspension requires the selection of design variables, connecting vehicle/suspension characteristics to the design variables and specifying the objective function to be used. The input for the optimising algorithm is saved in the lfopc.dat, lfopc_fun.dat and lfopc_par.dat files. Once these values are prescribed the optimisation can be performed. This will automatically perform a simulation of the vehicle, run the postprocessor, draw graphs of the objective functions, change the design

variables and the required vehicle characteristics and loop the simulation until the minimum objective function has been obtained within the constraints specified. Output for the optimisation process is written to the lfopc.out and lfopc.grf files.

3.5 Vehsim2d files

The program Vehsim2d uses default extensions to identify different files used during the simulations. The following tables give a summary of the files used.

Table 3.1: Vehsim2d files - Program files

File name	Extension	File type	Comments
Vehsim2d	.exe	Executable	The Vehsim2d executable file
Vehsim2d	.hlp	Help file	The Vehsim2d help file

Table 3.2: Vehsim2d files - Component, vehicle and output files

File name	Extension	File type	Comments
Vehicle	.veh	ASCII	Vehicle, suspension and simulation data
Vehicle	.str	Binary	Simulation output file
Vehicle	.out	ASCII	Output file for postprocessor
Vehicle	.psf	ASCII	Postprocessor input file
Vehicle	.geo	ASCII	Animation geometry data file
Vehicle	.rcd	ASCII	Output file for ride comfort analysis
Vehicle	.rms	ASCII	Output file for rms values
Vehicle	.vdv	ASCII	Output file for vdv values

***Note**: The name "Vehicle" shown above is used for demonstration purposes, the actual name is given by the user during creation of the files.*

Table 3.3: Optimisation files – Input and output files

File name	Extension	File type	Comments
Lfopc	.dat	ASCII	Input file with optimisation variables and constraints
Lfopc_fun	.dat	ASCII	Input file with objective function data
Lfopc_par	.dat	ASCII	Input file with general optimisation data
Parameters	.lst	ASCII	File with vehicle parameters available
Fun_parameters	.lst	ASCII	File with objective function parameters available
Lfopc	.out	ASCII	Output file for optimisation algorithm
Lfopc	.grf	ASCII	Detail output file for optimisation algorithm and input for optimisation graphs

***Note**: The file names shown above are fixed and will be overwritten each time input/output are changed.*

3.6 Main input screen

Via these sub frames the main input screen (see figure 3.1) is used to supply the following:

* vehicle data,
* simulation data, and
* file names.

This screen is also used for the following:

* Saving and opening of vehicle files: use the "File" menu item and click on "File Open" or "File Save".
* Exit the program: use the "File" menu and click on "Exit" or click the "Exit" button. The user will be prompted to save the vehicle file before closing the program.
* Obtaining help: click on the "Help" menu item.

***Note**: If calculation of equilibrium was performed with one of the options where the bump stop initial deflections were reset during equilibrium calculations then the calculated initial deflections for the springs will be saved in the vehicle when saving the vehicle file. For more details see Run simulation (Section 3.11)*

The respective sub frames introduced above are now individually dealt with below.

3.6.1 Vehicle data

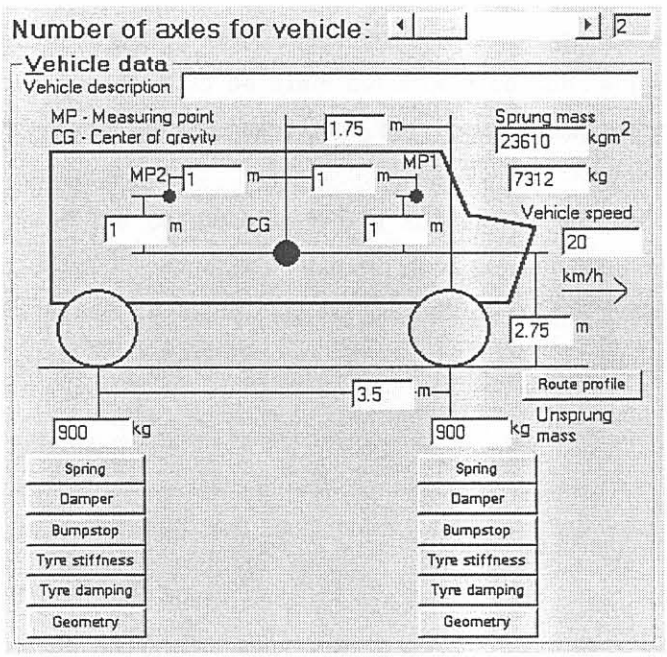

Figure 3.2: Main Input Screen - Vehicle data

Number of axles:

Select the number of axles for the vehicle using the provided scroll bar. The number of axles that can be selected range between two and four.

Enter the general vehicle data:

* Unsprung mass.
* Pitch inertia of unsprung mass about the centre of gravity (CG) of the unsprung mass.
* Position of the CG: the horizontal position is prescribed as the distance between the front axle and the CG and the vertical position (height) is defined from the road surface.
* Positions of two measuring points, points of interest or monitoring points. The accelerations, velocities and displacements of these two points and that of the CG will be computed during the simulation and saved as simulation time histories. The two special points are usually situated at the driver and at the rear passenger seats.
* Axle placements as indicated. The distances between the axle centres are prescribed.
* Vehicle speed in km/h.
* Vehicle description in alphanumeric characters.

Click on the provided buttons to input data for the following:

* General and two-dimensional data for the springs, dampers and bump stops.
* General and two-dimensional data for the tyres.
* Suspension geometry.
* Route profile.

***Note**: The initial conditions for the vehicle model are specified as close as possible to static equilibrium. For simulation purposes initial deflection for the springs, bump stops and tyres are prescribed. These values need not to be exact but should be sufficiently realistic to aid in the calculation of equilibrium. Before the simulation is run, the precise equilibrium position is calculated.*

***Warning**: Even if some of the components of the suspension are not used, data for those components must be specified. For example if no bump stops are simulated the bump stop data must contain a zero type characteristic, i.e. in this case the force will be 0 for all deflections.*

3.6.2 Simulation data

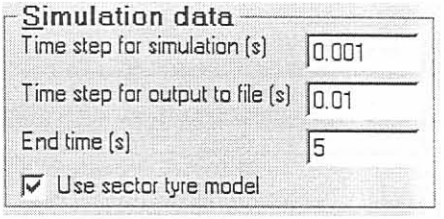

Figure 3.3: Main Input Screen - Simulation data

Enter the following:

* Time step for simulations: The time step for solving the equation of motion for velocities and displacements during simulation. A fourth order Runga-Kutta technique is used for the numerical integration. In general the time step should be as small as possible for accuracy but this will have a detrimental effect on the time required to perform the simulation. A general guideline, obtained through years of vehicle simulation experience, is to allow for eight simulation steps for a specific obstacle in the route profile. For example, if a simulation over a 200 mm half round discrete obstacle is done at 18 km/h, a time step for every 25 mm of vehicle longitudinal movement is required. At 18 km/h the vehicle travels at 5.0 m/s. For 25 mm of travel a time step of 0.025 / 5 = 0.005 s is required. For a "smoother" route profile a longer time step may be used.
* Time step for output to file: this is the time interval at which the simulation results are to be saved to the output file (*.str). A maximum of 3800 saving steps per file are allowed.
* End time: The end time for the simulation.

Options:

Two tyre models are available in the program: A point follower model in which the tyre deflection is calculated at a single point vertically below the tyre centre. This tyre model is appropriate for simulation over smooth profiles where the obstacle "radius" is larger than two times that of the tyre radius. The second and default model is a tyre sector model that is used for more severe obstacles that have radii smaller than two times the tyre radius. In this model the tyre is divided into 40 sectors and the deflection and force for each sector is calculated and combined to obtain the resultant tyre force. The sector tyre model requires a longer computational time so, if appropriate, rather select the point follower model for faster running simulations. The point follower model is used by de-selecting the tyre sector model in the option box provided.

***Note**: The selected tyre model is not saved with the vehicle file. Each time the program is started the tyre model will default to the sector model. Ensure that the required tyre model is selected before the simulation or optimisation is run.*

3.6.3 File names

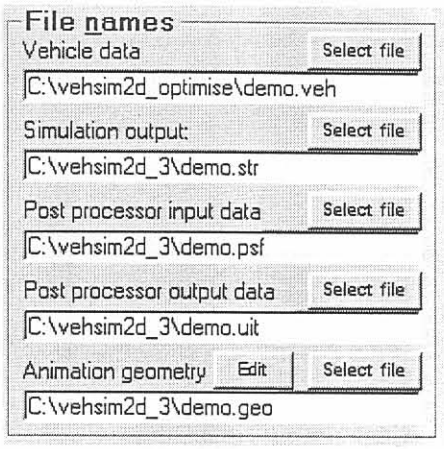

Figure 3.4: Main Input Screen - File names

This frame groups the main input file names for the simulation:

Vehicle data

The file name for the vehicle data (*.veh). Selecting this file does not open the specific file, it only indicates the vehicle file name for saving the vehicle data when using the "File", "File Save" pull-down menu item. Selecting a vehicle file will put default file names in the other file name text boxes if these were empty before selecting the vehicle file. To open a specific vehicle file, use the "File", "File Open" pull-down menu item.

Simulation output

The name for the simulation output file (*.str). This can be an existing or new file.

Postprocessor input data

The postprocessor input data file (*.psf). This file indicates the required values to be extracted from the simulation output file during use of the postprocessor. This can be an existing or new file.

Post processor input data

The name for the postprocessor output file (*.out). This file will be used for saving the output of the postprocessor. An existing or new file can be selected.

Animation geometry

The animation geometry data file (*.geo). This file prescribes the geometry of the vehicle as drawn for the animations. Use the "Edit" button to edit / create this file.

3.7 Animation geometry editor

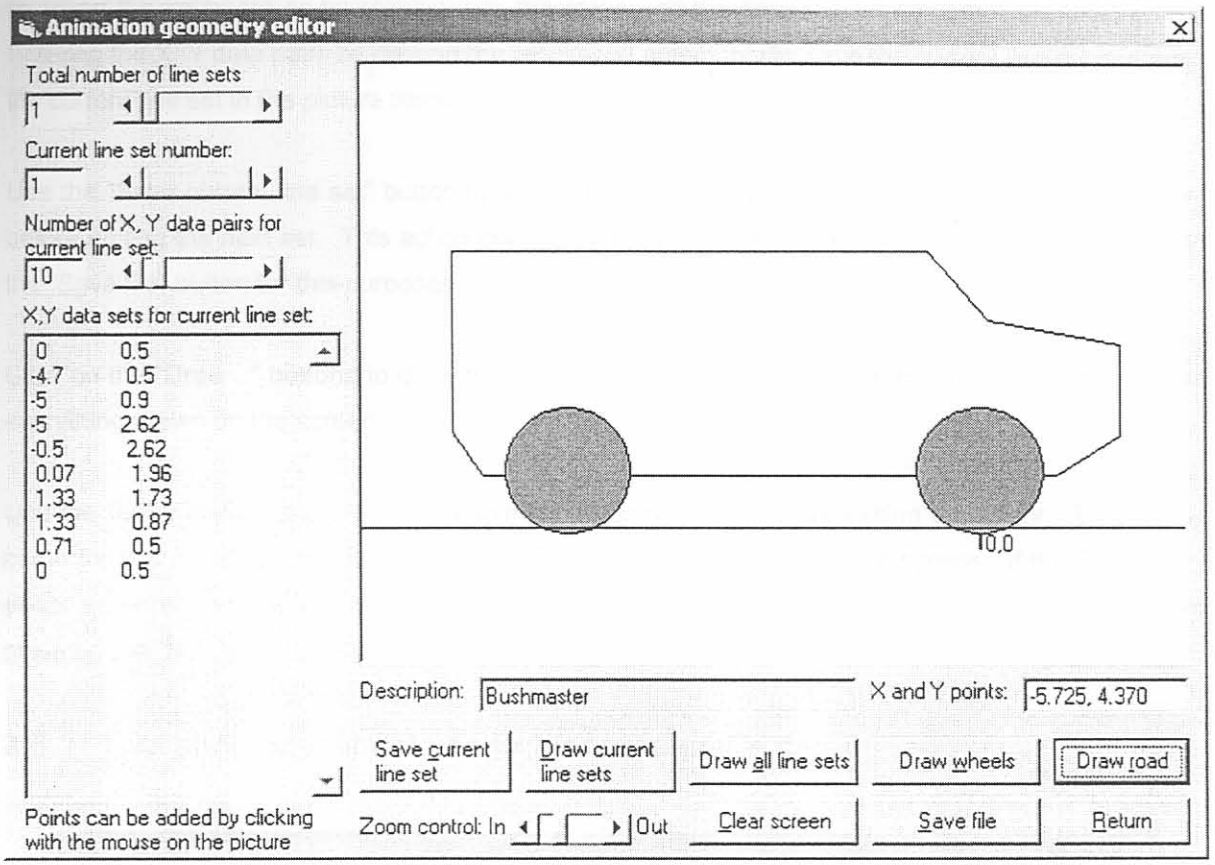

Figure 3.5: Animation geometry editor

The animation geometry editor is used to edit the prescribed geometry of the vehicle for the animation. In figure 3.5 the X,Y data pairs successively indicates the start and end co-ordinates of the lines, outlining the body of the vehicle. Point 0,0 is defined on the road surface below the front axle centre and the X-axis is horizontal and positive to the right. Y is the vertical axis and positive upwards.

The wheels of the vehicle are not prescribed in this file but are drawn by using the placement of the axles as prescribed on the Vehicle data frame on the main input screen. The tyre radii are as prescribed by using the "Tyre stiffness" or "Tyre damping" buttons.

Up to 20 line sets may be specified to represent the vehicle geometry. A line set is defined as a series of lines prescribed by X, Y data pairs. A line set is therefore a series of lines connecting the prescribed X, Y data pairs. Each line set can be defined by a minimum of 2 and a maximum of 100 X, Y data pairs.

Use the scroll bars to select the total number of line sets, the current line set in edit and the number of X, Y data pairs for the current line set. The X, Y data pairs are entered into the X, Y data set text box by using the keyboard or by clicking with the mouse on the required X, Y point in the picture box. Entering the X, Y data pairs by clicking the mouse will automatically save the current line set and draw the current line set in the picture frame.

Use the "Save current line set" button to save the X, Y data pairs for the specific line set in memory before editing the next set. This action does not save the line set in the animation geometry file, use the "Save file" button for this purposes.

Click on the "Draw .." buttons to draw the indicated entities. Use the "Clear screen" button to delete everything drawn on the screen.

Use the "Save file" button to save the animation geometry file before exiting the editor. The default name for this file is prescribed on the File names frame on the main input screen. If the file already exists a warning will be displayed before overwriting the file. A new file name can be selected by pressing the "No" button on the overwrite warning and selecting a new file on the File dialog box.

3.8 **Two dimensional data editor** (for route profile data)

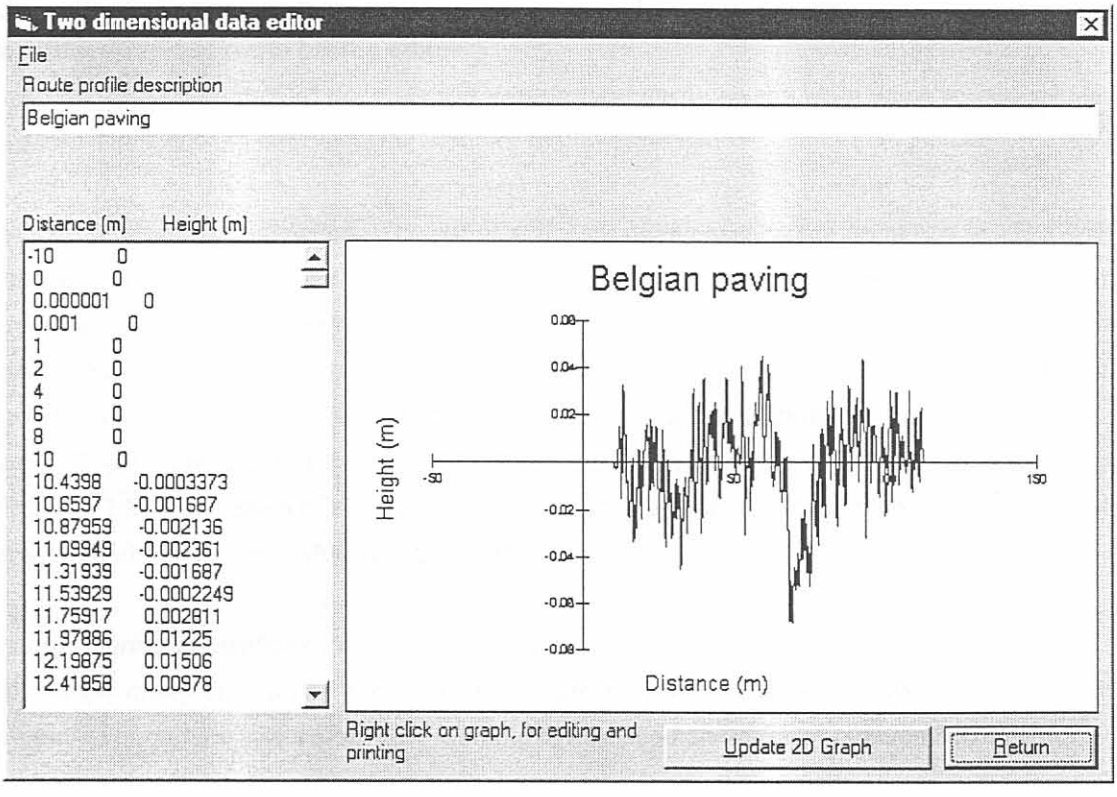

Figure 3.6: Two dimensional data editor for route profile data

This editor (as shown in figure 3.6) is used to edit the two dimensional data for the route profile.

General operation

The two dimensional data is entered in the text box displayed at the bottom left of the screen. Data is entered by specifying the X and Y values of successive points for the two-dimensional data pairs. X and Y values must be separated by one or more spaces or by a comma. Clicking the "Update 2D Data and graph" button will sort the data pairs in increasing X-values and display a graph. Identical X-values will be edited during this operation by adding a very small value to each identical X-value. The graph is drawn by cubic spline interpolation of the X, Y data set. For drastic changes in Y-values prescribe small X-value increments for accurate interpolation. A straight line is obtained by prescribing three data pairs. *A minimum of 3 data pairs and a maximum of 1000 data pairs are allowed.*

The two-dimensional data set can be saved to a file by using the "File", "Save data to a file" menu item on the pull-down menu. The "File", "Import data from a file" pull-down menu item can also be used to load previously saved data from an existing file. The file to be imported should be an ASCII text file with the X, Y data pairs in free format. *No default extensions are used for these files, the user can name these files using his own format for later identification.*

Right click on the graph to edit the graph to activate the Graph Control window in order to select the print option, change headings, etc. Detailed help on the Graph Control is available by clicking the "Help" button.

Detail description of route profile editor

Clicking on the "Route profile" button in the Vehicle data frame on the Main input screen will activate the editor. The following describes the input for the route profile:

Enter the route profile description. The set of X, Y data pairs describe the route profile. The point 0,0 is defined as a point at ground level underneath the front axle centre. The height of the front axle centre is equal to the tyre radius minus the tyre deflection plus the Y value. The X-value is the horizontal distance from 0 and positive in the direction of travel. The Y-data is positive for an increase in height. Remember to prescribe data points for the route profile underneath the vehicle at time = 0 s as well. Due to the fact that the point 0,0 is defined below the front axle the road below the other wheels will have a negative X-value. To aid the calculation of equilibrium prescribe a flat and horizontal road beneath the wheels at time = 0 s.

***Warning**: During simulations interpolation / extrapolation of the prescribed data is used. To avoid extrapolation make sure that the characteristics are prescribed for the complete range that will be experienced during the simulations. No warning is displayed should extrapolation be required.*

3.9 Suspension characteristics editor (for spring, damper, bump stop, tyre stiffness and tyre damping)

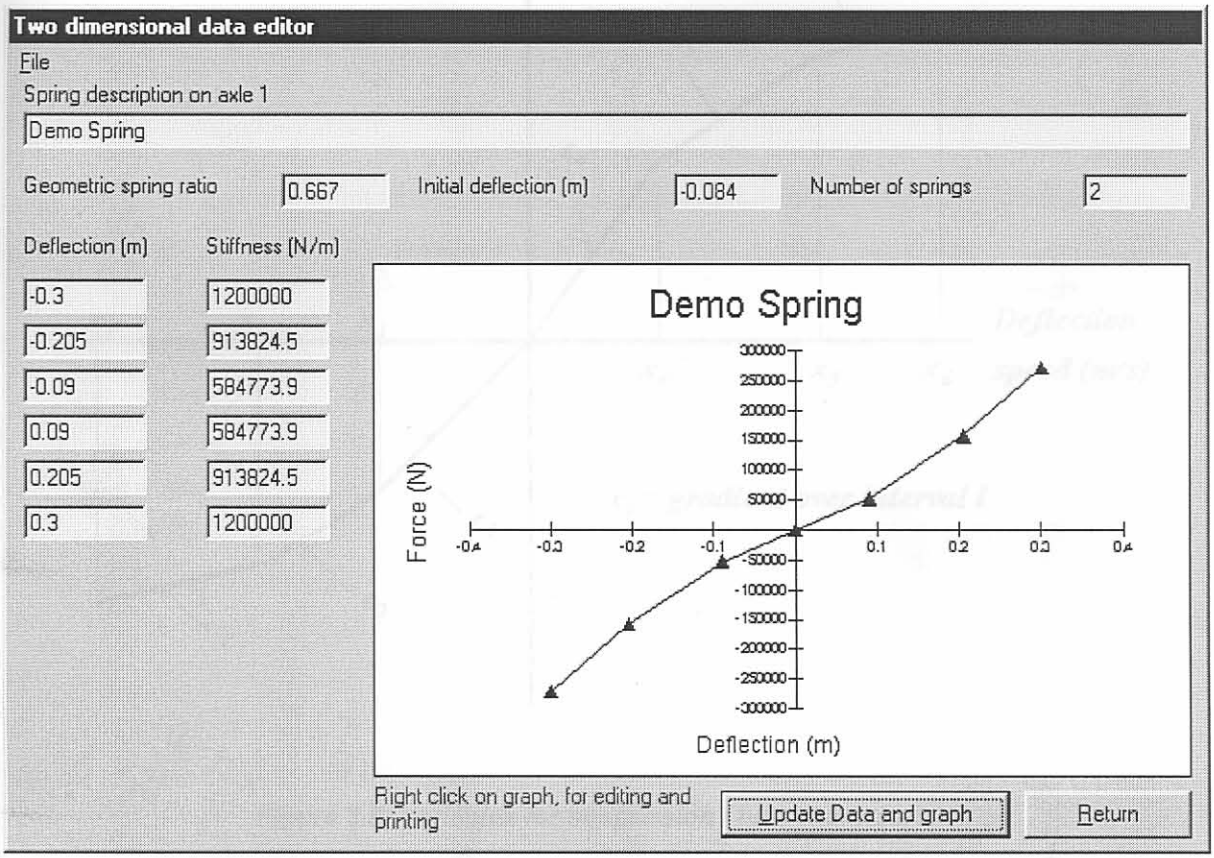

Figure 3.7: Two dimensional data editor (for suspension components)

This editor is used to edit the data for the suspension and tyre characteristics.

General operation

The suspension and tyre characteristics are prescribed using a six piece-wise continuous linear approximation as shown in figure 3.8 for a typical damper characteristic. Data is entered by entering the abscissas x_1 to x_6 as well as the corresponding slopes or gradients c_1 to c_6 in the text boxes supplied to the left of the graph as shown in figure 3.7. The x_1 to x_6 and c_1 to c_6 values are entered from top to bottom. Clicking the "Update 2D Data and graph" button will sort the data pairs in increasing X-values and display a graph as shown. Identical X-values will be edited during this operation by adding a very small value to each identical X-value. *All six points must be prescribed. Also note that the characteristic must pass through the origin (0,0) as indicated.* Refer to section 2.1 for more details regarding this six piece-wise continuous linear approximation.

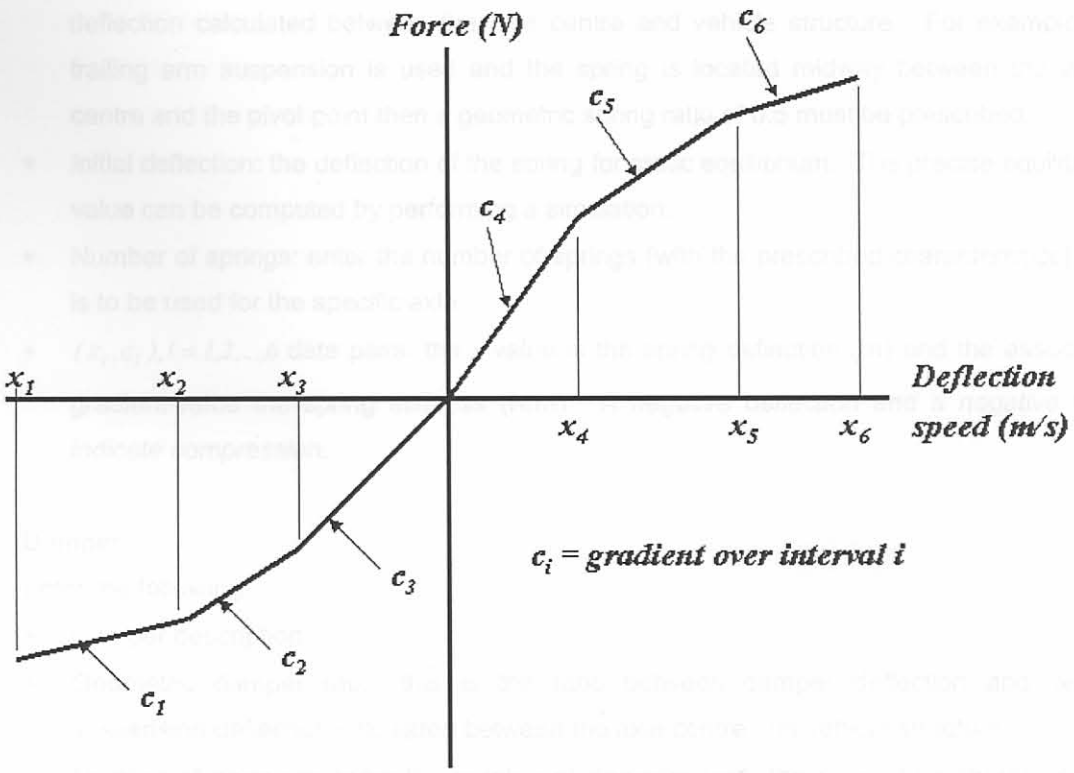

Figure 3.8: Variables for suspension / tyre characteristic

The data can be saved to a file by using the "File", "Save data to a file" menu item on the pull-down menu. The "File", "Import data from the file" pull-down menu item can also be used to load previously saved data from an existing file. The file to be imported should be an ASCII text file with the x_i, c_i data pairs in free format. *No default extensions is used for these files, the user can name these files using his own format for later identification.*

Right click on the graph to edit the graph to activate the Graph Control window in order to select the print option, change headings, etc. Detailed help on the Graph Control is available by clicking the "Help" button.

Detailed description of editor

Clicking on the different suspension and tyre buttons in the Vehicle data frame on the Main input screen will activate the editor. The input detail on the editor may change according to the specific button clicked. The following describe the input for the different buttons:

Spring

Enter the following:

* Spring description in alphanumeric characters.

* Geometric spring ratio: this is the ratio between spring deflection and vertical suspension deflection calculated between the axle centre and vehicle structure. For example if a trailing arm suspension is used and the spring is located midway between the wheel centre and the pivot point then a geometric spring ratio of 0.5 must be prescribed.
* Initial deflection: the deflection of the spring for static equilibrium. The precise equilibrium value can be computed by performing a simulation.
* Number of springs: enter the number of springs (with the prescribed characteristics), that is to be used for the specific axle.
* $(x_i, c_i), i = 1,2,...,6$ data pairs: the x-value is the spring deflection (m) and the associated gradient-value the spring stiffness (N/m). *A negative deflection and a negative force indicate compression.*

Damper

Enter the following:

* Damper description.
* Geometric damper ratio: this is the ratio between damper deflection and vertical suspension deflection calculated between the axle centre and vehicle structure.
* Number of dampers: enter the number of dampers (with the prescribed characteristics) that is to be used for the specific axle.
* $(x_i, c_i), i = 1,2,...,6$ data pairs: the x-value is the damper deflection rate (speed) (m/s) and the gradient-value the damper stiffness (damping coefficient) (Ns/m). *A negative speed and a negative force indicate compression.*

Bump stop

Enter the following:

* Bump stop description.
* Geometric bump stop ratio: this is the ratio between bump stop deflection and vertical suspension deflection calculated between the axle centre and vehicle structure.
* Initial deflection: the deflection of the bump stop for static equilibrium. The precise equilibrium value can be computed by performing a simulation. This value can be used to change the suspension travel without changing the bump data.
* Number of bump stops: enter the number of bump stops (with the prescribed characteristics) that is to be used for the specific axle.
* $(x_i, c_i), i = 1,2,...,6$ data pairs: the x-value is the bump stop deflection (m) and the gradient-value the bump stiffness (N/m). *A negative deflection and a negative force indicate compression.*

Tyre stiffness

Enter the following:

* Tyre description.
* Unloaded tyre radius: this value is used for animation and calculation of tyre deflection.
* Initial deflection: the deflection of the tyre for static equilibrium. The precise equilibrium value can be computed by performing a simulation.
* Number of tyres: enter the number of tyres (with the prescribed characteristics) that is to be used for the specific axle.
* $(x_i, c_i), i = 1,2,...,6$ data pairs: the x-value is the tyre deflection (m) and the gradient-value the tyre stiffness (N/m). *A negative deflection and a negative force indicate compression.* The deflection / force characteristic is that for deflection on a flat surface. The sector tyre model will estimate the deflection and force with for other types of obstacles.

Tyre damping

Enter the following:

* Tyre description.
* Unloaded tyre radius: this value is used for animation and calculating tyre deflection.
* Initial deflection: the deflection of the tyre for static equilibrium. The precise equilibrium value can be computed by performing a simulation.
* Number of tyres: enter the number of tyres (with the prescribed characteristics) that is to be used for the specific axle.
* $(x_i, c_i), i = 1,2,...,6$ data pairs: the x-value is the tyre deflection rate (speed) (m/s) and the gradient-value the tyre damping stiffness (coefficient) (Ns/m). *A negative deflection rate and a negative force indicate compression.* The deflection rate / force characteristic is that for deflection on a flat surface. The sector tyre model will estimate the deflection and force for other types of obstacles.

Warning:

During simulations interpolation / extrapolation of the prescribed data is performed. To limit extrapolation make sure that the characteristics are prescribed for the complete range that will be experienced during the simulations. No warning is displayed during extrapolation.

Even if some of the components on the suspension are not used, data for those components must be specified. For example, if no bump stops are to be simulated the bump stop data must contain a zero type characteristic, i.e. in this case the force will be 0 for all deflections.

3.10 Suspension geometry

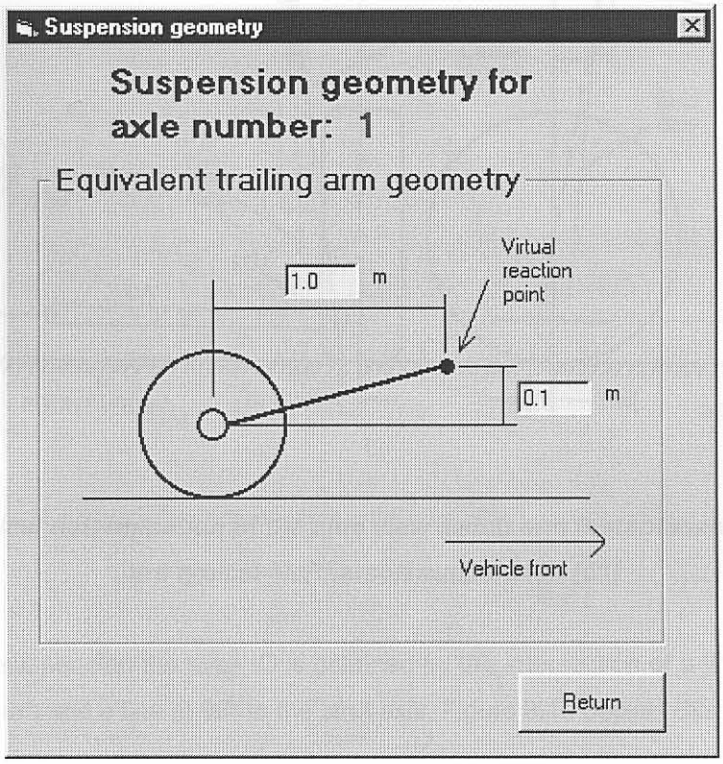

Figure 3.9: Input screen for the suspension geometry

The suspension is simulated by an equivalent trailing arm approximation (see section 2.1 for more details). For this purposes the virtual reacting point of an equivalent trailing arm is prescribed – see figure 3.9. Enter the relative co-ordinates (m) of this virtual reaction point in the appropriate text boxes. If an equivalent leading arm suspension is simulated, the horizontal distance must be entered as a negative value.

The virtual reaction point is also known as the side view swing arm instantaneous centre (svsa IC) [61]. Figures 3.10 to 3.13 show the determination of this point for some generally used suspension systems.

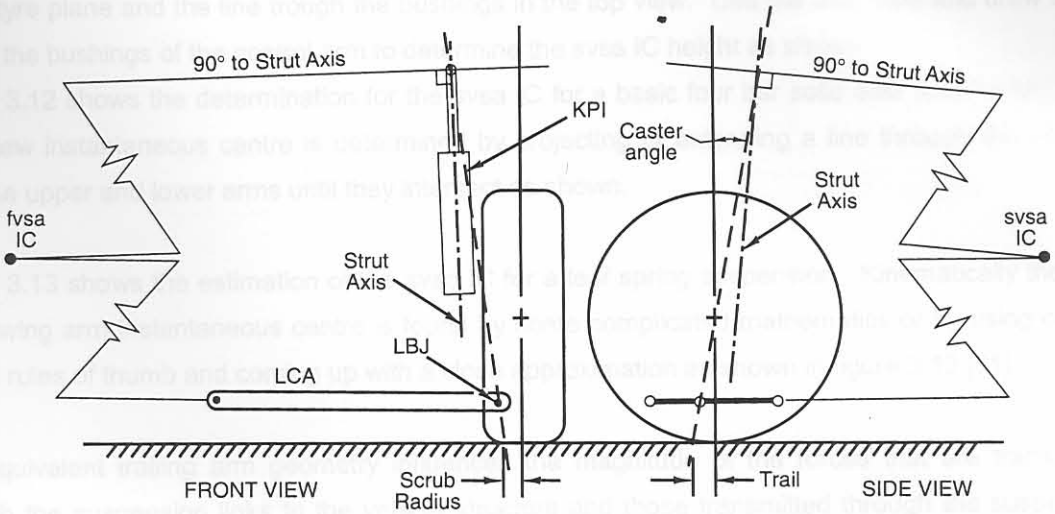

Figure 3.10: Graphical determination of the side view swing arm instantaneous centre (svsa IC) for a typical McPherson suspension [61]

For the McPherson suspension the svsa IC is obtained by the intersection of a line through the plane of the lower control arm and a line at 90° to the strut axis. Figure 3.10 depicts this construction.

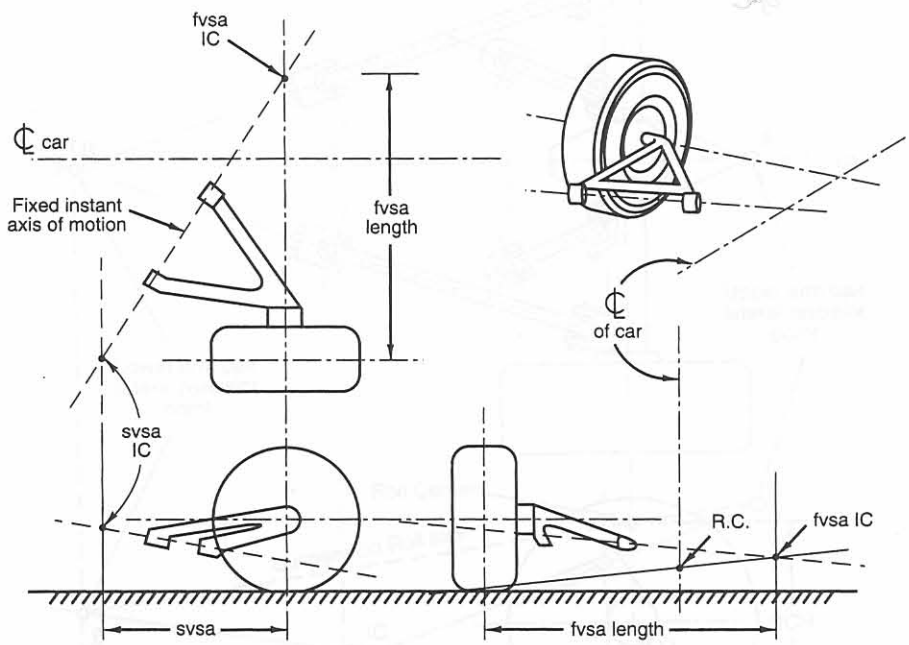

Figure 3.11: Graphical determination of the side view swing arm instantaneous centre (svsa IC) for a typical semi-trailing arm suspension [61]

The svsa IC for the semi-trailing arm is shown in figure 3.11. The svsa IC is determined by drawing a line through the swing arm bushings in a top view. The svsa length is determined by the intersection

of the tyre plane and the line trough the bushings in the top view. Use the side view and draw a line trough the bushings of the control arm to determine the svsa IC height as shown.
Figure 3.12 shows the determination for the svsa IC for a basic four bar solid axle suspension. The side view instantaneous centre is determined by projecting or extending a line through the ends of both the upper and lower arms until they intersect as shown.

Figure 3.13 shows the estimation of the svsa IC for a leaf spring suspension. Kinematically the side view swing arm instantaneous centre is found by some complicated mathematics or by using certain simple rules of thumb and coming up with a close approximation as shown in figure 3.13 [61].

The equivalent trailing arm geometry influences the magnitude of the forces that are transmitted through the suspension links to the vehicle structure and those transmitted through the suspension components (springs, dampers, etc) – refer to section 2.1 for more detail on the mathematical vehicle model. The geometry will also influence the accelerations that are experienced by the vehicle when hitting a severe obstacle such as a bump. For example, think of the difference between pulling and pushing a wheel burrow over an obstacle.

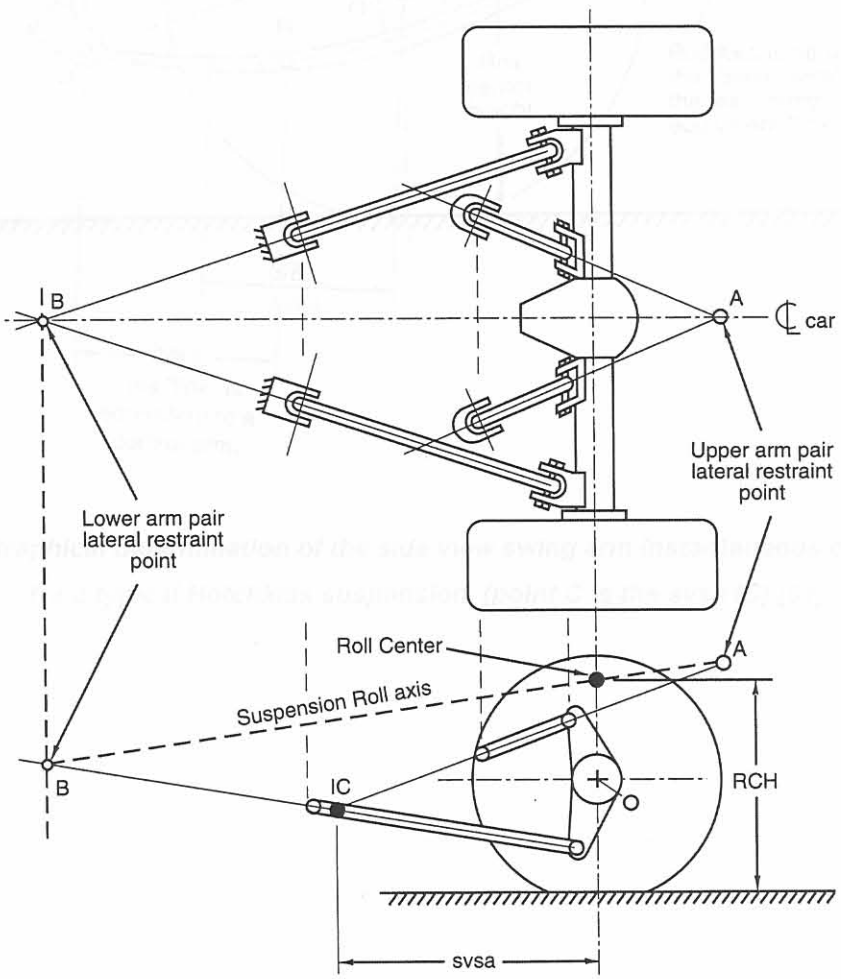

Figure 3.12: Graphical determination of the side view swing arm instantaneous centre (svsa IC) for a typical basic 4 bar suspension (point IC is the svsa IC) [61]

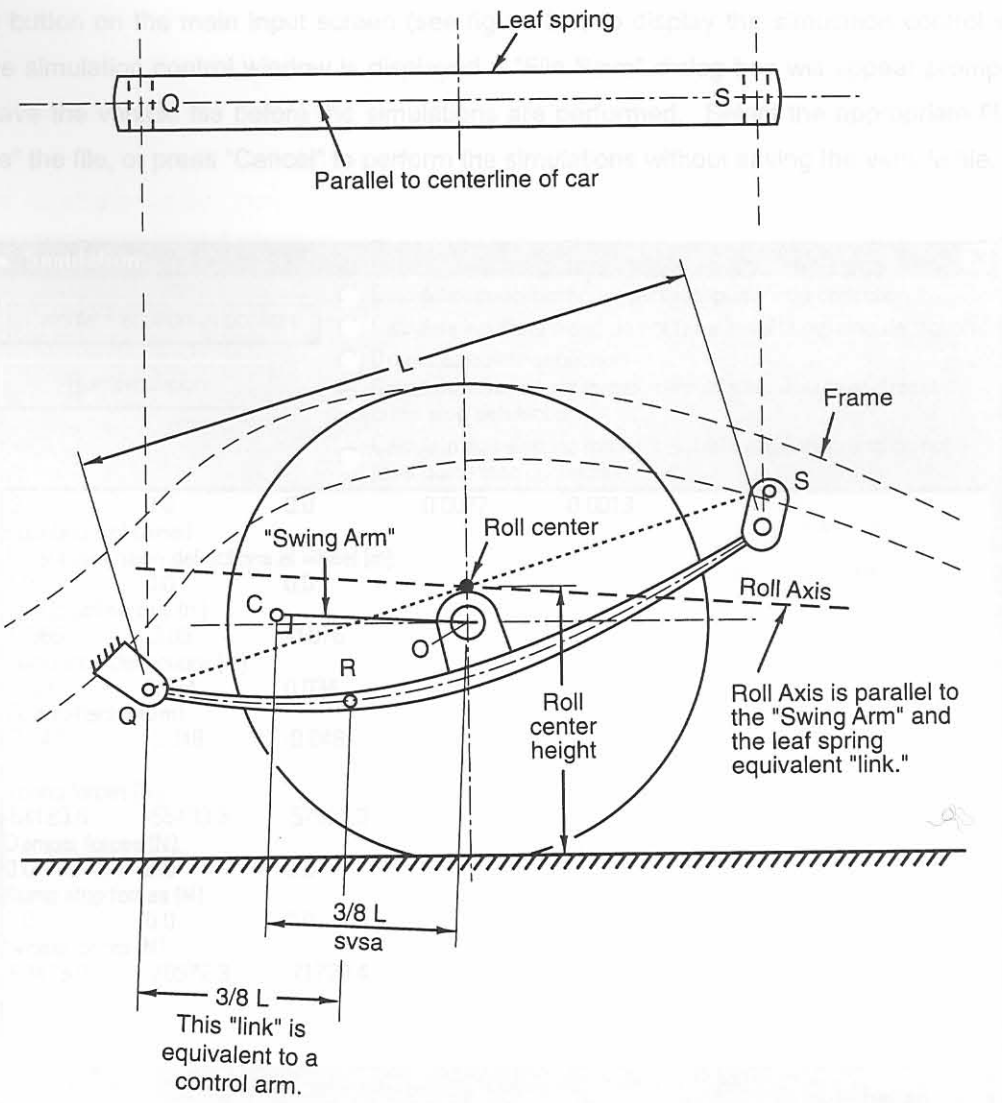

Figure 3.13: Graphical determination of the side view swing arm instantaneous centre (svsa IC) for a typical Hotchkiss suspension (point C is the svsa IC) [61]

3.11 Run simulation

Click this button on the main input screen (see figure 3.1) to display the simulation control window. Before the simulation control window is displayed a "File Save" dialog box will appear prompting the user to save the vehicle file before the simulations are performed. Select the appropriate file name and "Save" the file, or press "Cancel" to perform the simulations without saving the vehicle file.

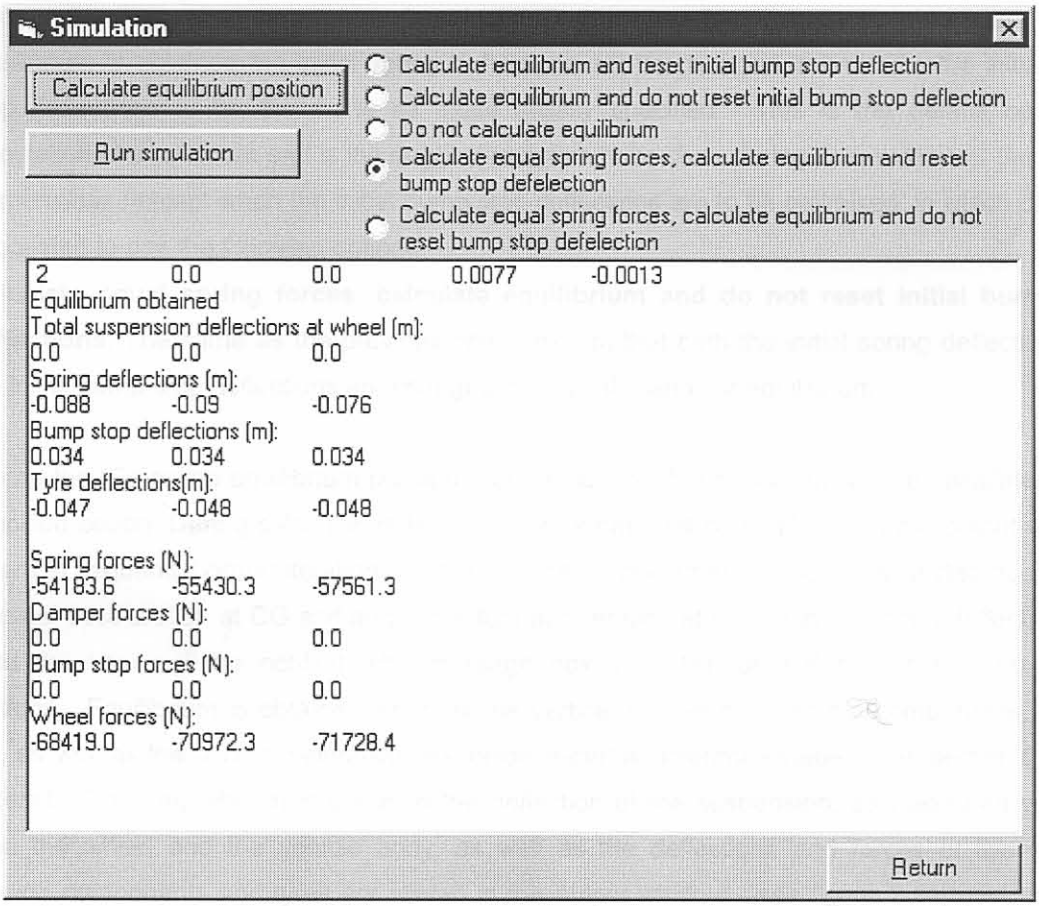

Figure 3.14(a): Simulation control

The first step is to calculate the equilibrium position. The following options for the calculation of equilibrium is available:

* **Calculate equilibrium and reset initial bump stop deflections**: This option will calculate equilibrium from the initial prescribed position (refer to section 2.1 for more detail) as specified in the vehicle file. Once equilibrium is obtained the initial spring deflections will be changed in order to keep the initial bump stop deflections the same as those initially specified – see section 3.9. This process will continue until the initial spring deflections are such that the initial bump stop deflections are the same as those initially specified. This option can be used where the exact bump stop deflection or bump stop clearance in static equilibrium is known.

* **Calculate equilibrium and do not reset initial bump stop deflections**: Equilibrium will be calculated from the initial prescribed position as specified in the vehicle file.
* **Do not calculate equilibrium**: No equilibrium position will be calculated and the simulation will start from the initial prescribed position as specified in the vehicle file.
* **Calculate equal spring forces, calculate equilibrium and reset initial bump stop deflection**: This option will start by calculating the initial spring deflections in order to obtain equal spring forces on all the axles. These equal forces are determined by the sprung weight and number of axles. Starting with the calculated spring deflections equilibrium will be calculated. Once equilibrium is obtained the initial spring deflections will be changed in order for the initial bump stop deflections to be the same as those initially specified. This is the default option for calculation of equilibrium and is the suggested option to be used during optimisation of the vehicle suspensions (except when the initial bump stop deflections are to be optimised, in which case it is suggested to use the following option).
* **Calculate equal spring forces, calculate equilibrium and do not reset initial bump stop deflections**: The same as the previous option except that both the initial spring deflections and the initial bump stop deflections are changed during calculation of equilibrium.

By clicking the "Calculate equilibrium position" button the equilibrium position will be calculated using the specified option. During calculations five columns of data will be displayed in the output window. These are in sequential order: iteration number, vertical displacement of CG, angular displacement of CG, vertical acceleration at CG and angular (pitch) acceleration at CG. If initial spring deflections are changed the user will be notified with message boxes. Click on OK to continue equilibrium calculations. Equilibrium is obtained when all the vertical accelerations of the components and the vehicle, as well as the pitch acceleration, are below a certain tolerance value – see section 2.1.2 for more detail. Once equilibrium is obtained the deflection of the suspension, as measured vertically between the wheel and the vehicle body, as well as the deflections and forces of the different suspension components and tyres are shown in the output window - see figure 3.14(b). Use these values to check that the vehicle is being simulated correctly by interpreting values for the suspension travel, static wheel loads, etc. The calculated equilibrium deflections can also be used to change the suspension component data for initial deflections closer to the required value to ensure that the vehicle is modelled close to static equilibrium – see section 3.9 for input of these initial values. When using one of the options where the initial spring deflections are changed during equilibrium calculations, saving the vehicle file will automatically store the new values to the vehicle file. ***It is necessary to perform the equilibrium calculation before each simulation run.***

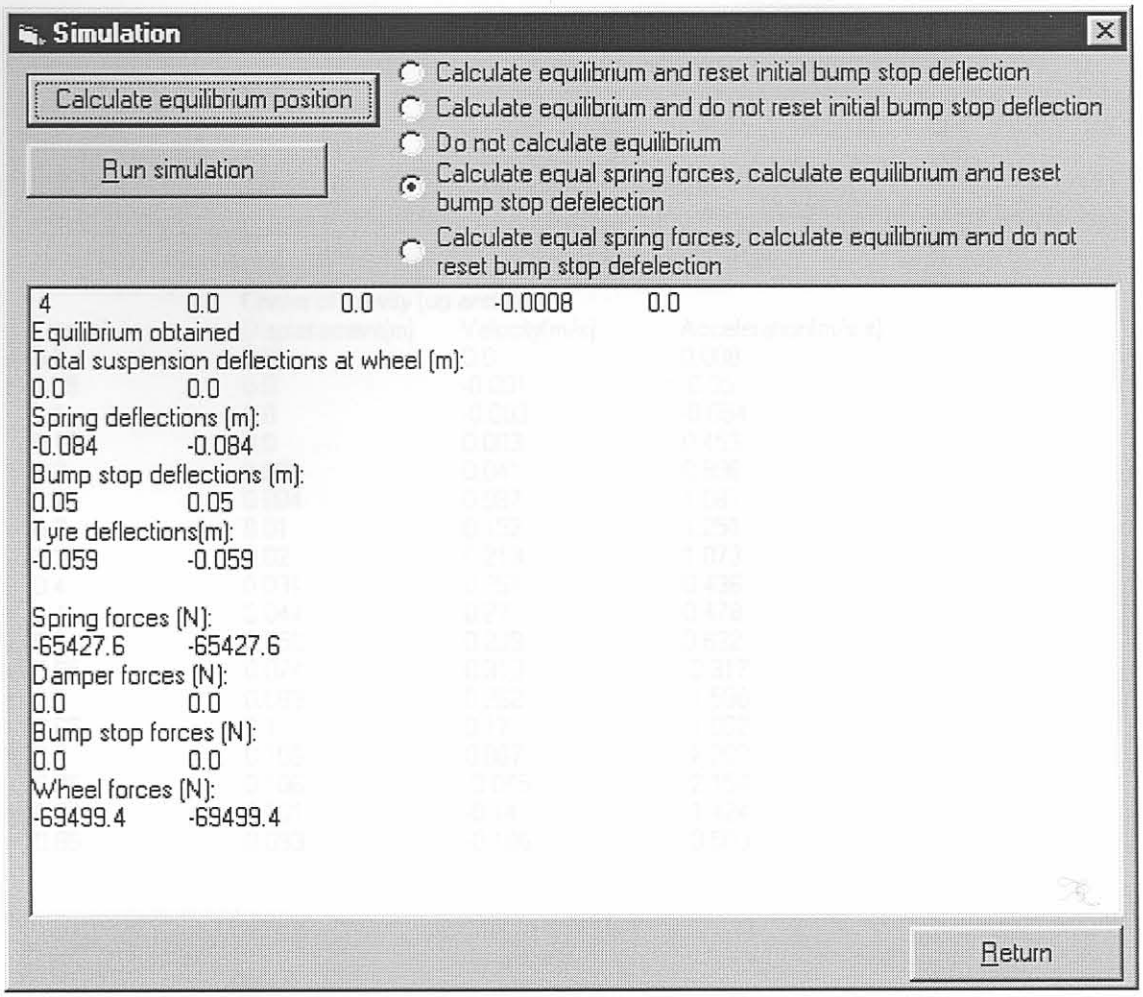

Figure 3.14(b): Equilibrium obtained

Click the "Run simulation" button to start the simulation. Simulation results for the movement of the centre of gravity at the specified output time intervals will be displayed on the screen – see figure 3.15. Once the simulation is started the "Stop" button will be available and can be used to stop the simulation prematurely. Results up to the time at which the simulation was stopped will be available in the output file (*.str). Alternatively, when the end time is reached, the simulation will stop and the "Return" button will be available.

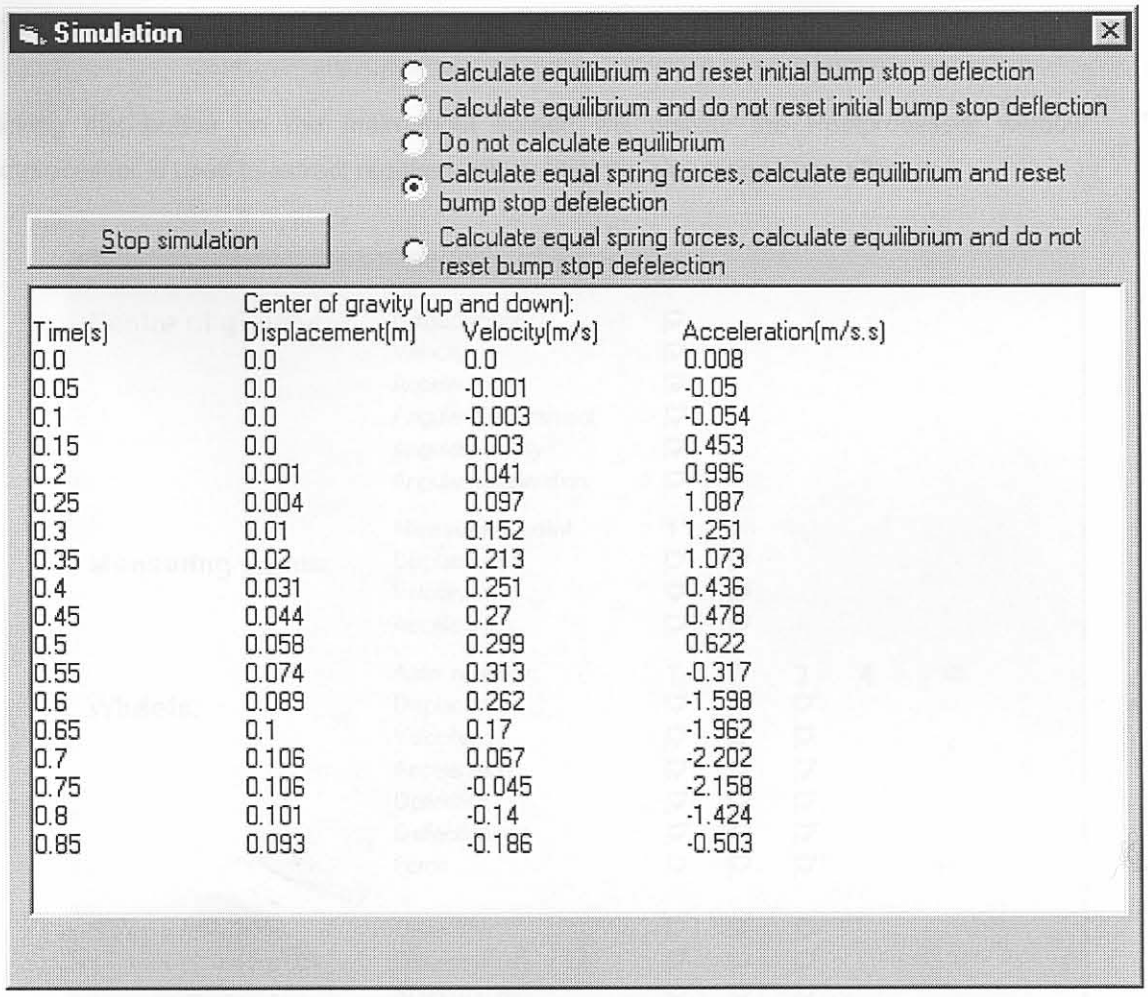

Figure 3.15: Performing simulations

3.12 Postprocessor

Clicking this button on the main input screen will display the Postprocessor window. The postprocessor is used to extract required values from the simulation output file.

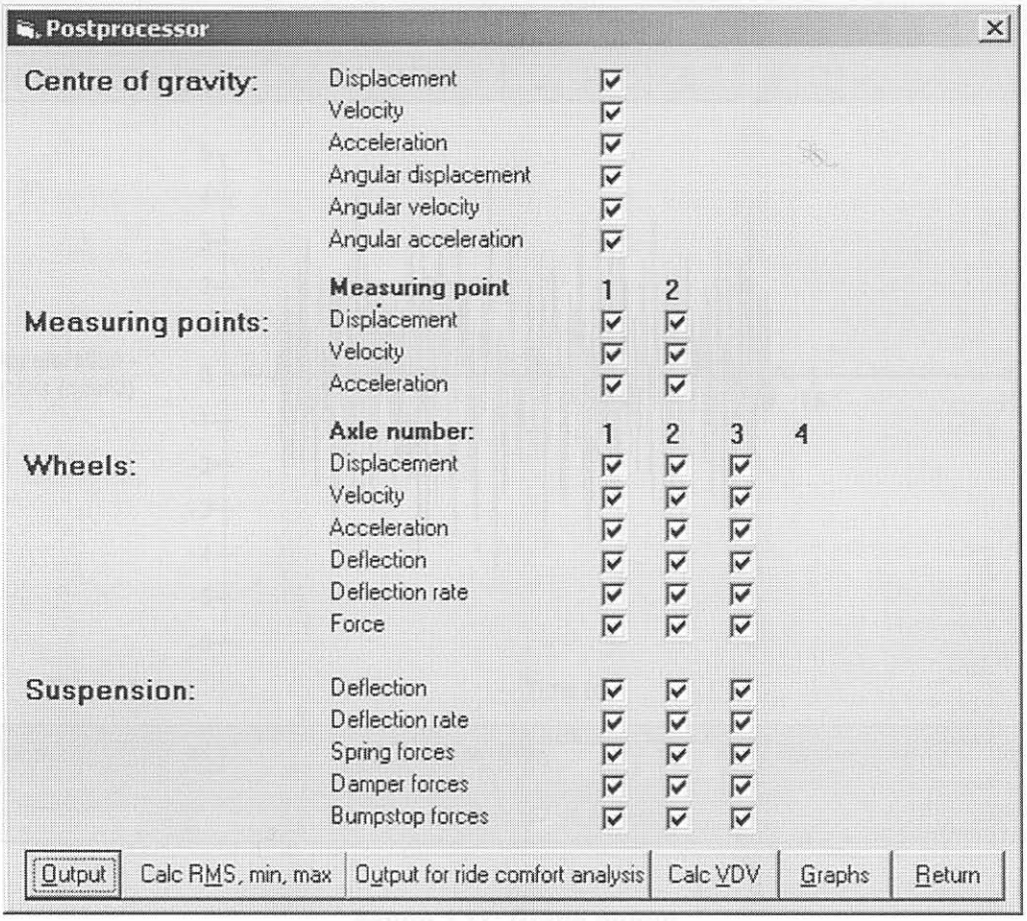

Figure 3.16 Postprocessor input

Select the required values for output by using the option boxes available. Selections as previously used and stored in the postprocessor file (*.psf) will be selected when the postprocessor is activated. The selection will automatically be saved to this file when the postprocessor is closed. The selection made here will not influence the output created during optimisation. In this instance all the available output will be written to the output files.

Click on the "Output" button to extract the required values. This will also save the extracted data to the postprocessor output file (*.out). Once these extractions are completed the "Graph", "Calc RMS,min,max", "Output for ride comfort analysis" and "Calc VDV" buttons will be available for the user.

The "Graphs" button is used to display graphs of the postprocessor output. Help on the graph is available by using the buttons at the top of the graph. These buttons can both be used to change the appearance of the graph and for printing the graph (use the "System" button for printing). For more details see section 3.13.

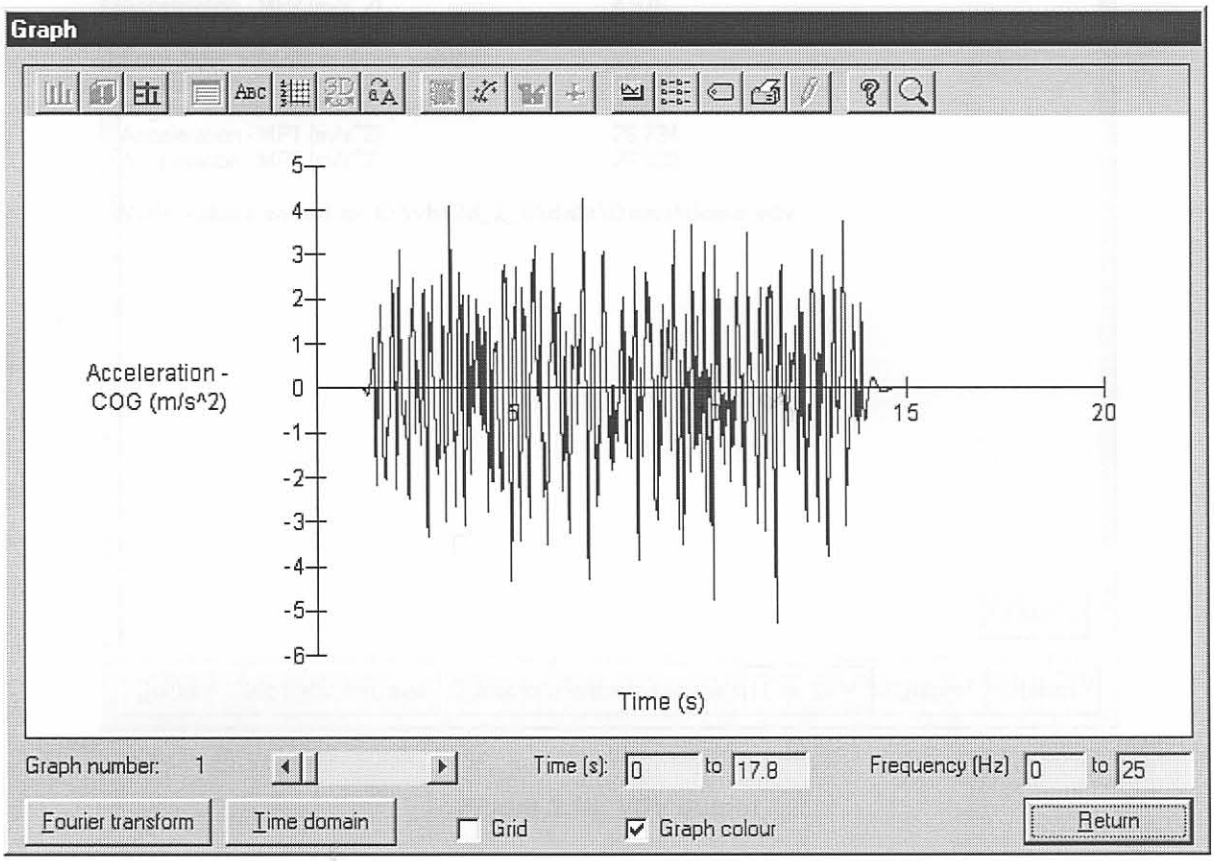

Figure 3.17: Graph output

The "Calc RMS, min, max" button is used to calculate these values for the selected output. The results are also stored in a file (*.rms).

Clicking the "Output for ride comfort analysis" button will create a file (*.rcd) for use with a separate module to calculate the ride comfort of the vehicle according to different criteria. This file contains column data for time, CG vertical acceleration, CG pitch acceleration, vertical acceleration at position MP1 (monitoring point 1) and vertical acceleration at position MP2 (monitoring point 2).

The "Calc VDV" button can be used to calculate the vibration dose values for the simulation performed – see figure 3.18 for an example of calculated VDV values. This calculation is not as comprehensive as that used by the separately available ride comfort analysis program and must only be use for estimation purposes or optimisation. Again it is emphasized that for more accurate values the separately available ride comfort program should be used.

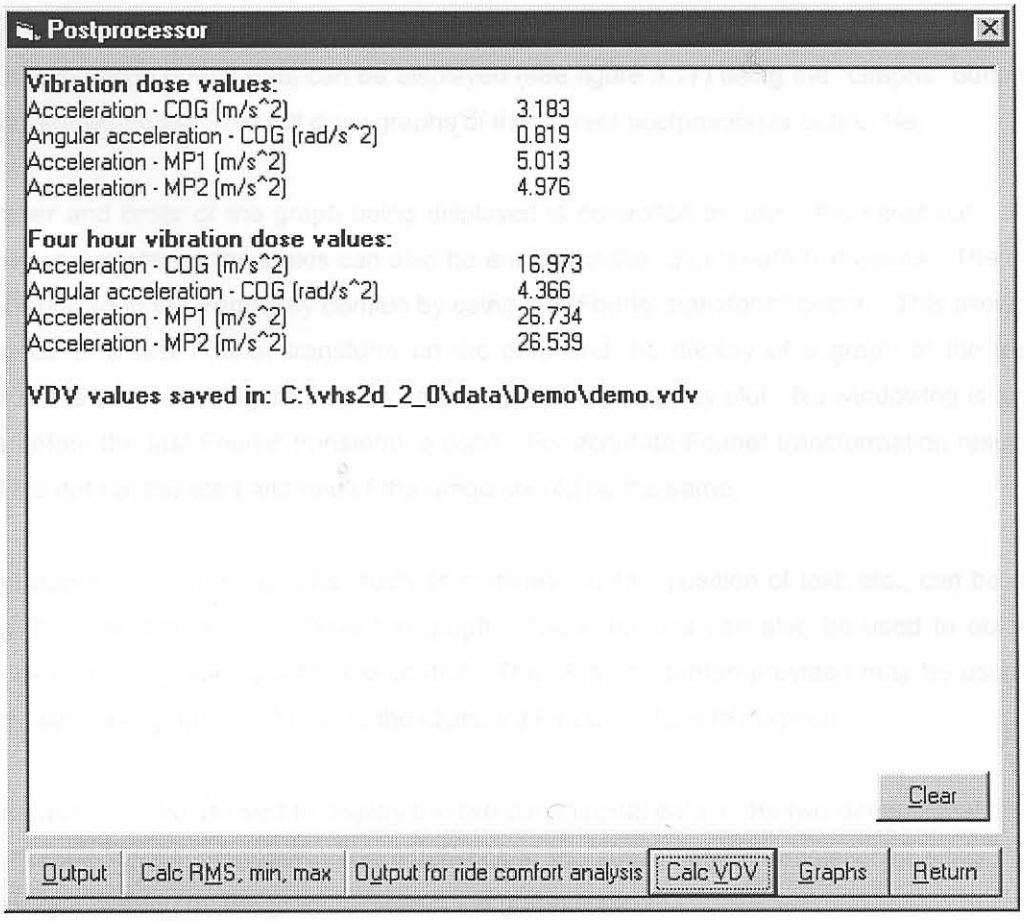

Figure 3.18: VDV output

Warning

If the postprocessor output file (.out) already exist when the postprocessor is activated the "Graphs" button will be available in the postprocessor window. If a new simulation was performed, first click on the "Output" button to update the postprocessor output file before using the "Graph" button*

3.13 Graphs

Graphs of simulation output data can be displayed (see figure 3.17) using the "Graphs" button on the postprocessor windows. This will draw graphs of the current postprocessor output file.

The number and order of the graph being displayed is controlled by using the scroll bar. Minimum and maximum values for the x-axis can also be entered in the appropriate text boxes. The data can also be displayed in the frequency domain by using the "Fourier transform" button. This allows for the performance of a fast Fourier transform on the data and the display of a graph of the frequency contents of the data – see figure 3.20 as an example of a frequency plot. No windowing is applied to the data before the fast Fourier transform is done. For accurate Fourier transformation results the y-value of the data at the start and end of the range should be the same.

Details in appearance of the graphs, such as gridlines, scales, position of text, etc., can be changed by using the available buttons above the graph. These buttons can also be used to obtain more detailed help on the graph options and control. The "System" button provided may be used to print the graph, save the graph to a file or to the clipboard for cut and paste purposes.

The same graph control is used to display the two-dimensional data in the two-dimensional data editor and the graphs for the suspension characteristics in the suspension characteristics editor. In these instances right clicking on the graph activates the graph control.

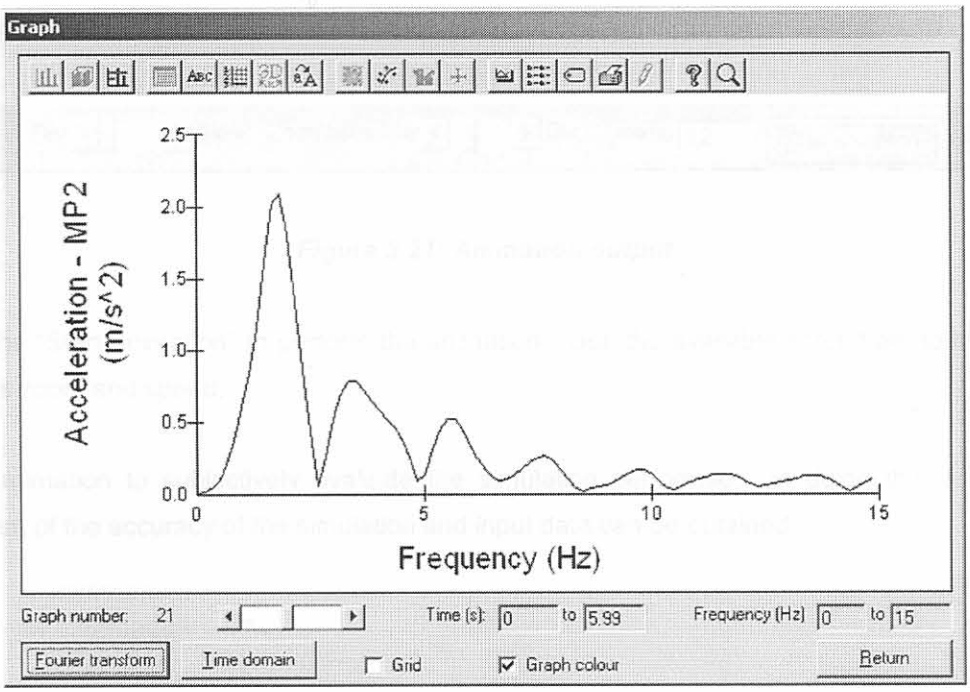

Figure 3.20: Graph output (frequency plot)

3.14 Animation

Use the "Animate" button on the main input screen (see figure 3.1) to perform animations of the simulation results. *Before animations can be performed the animation geometry must be created by clicking the "Edit" button on the File names frame on the main input screen to activate the animation geometry editor.* Figure 3.21 shows a snap shot of the animation at a particular instant in time.

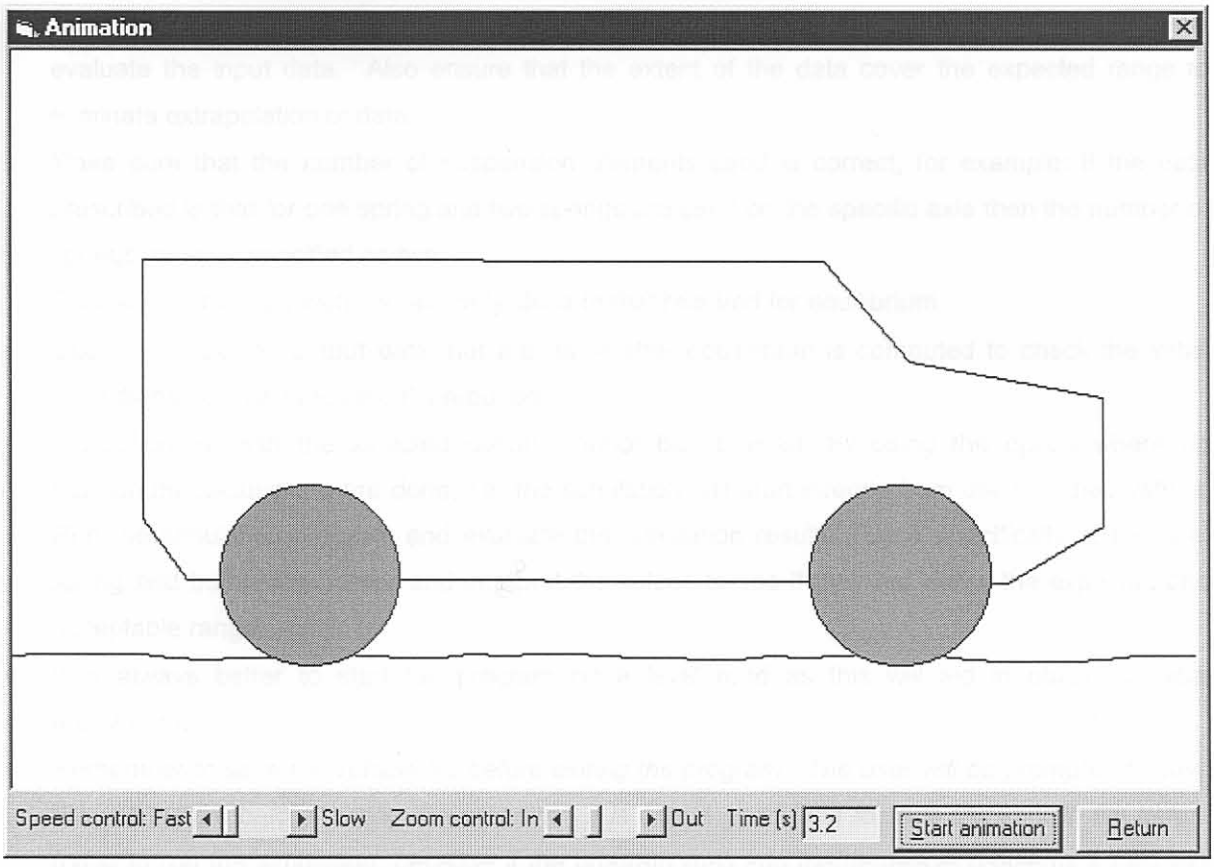

Figure 3.21: Animation output

Click on the "Start animation" to perform the animation. Use the available scroll bars to change the animations zoom and speed.

Use the animation to subjectively evaluate the simulation performed. In doing this a subjective assessment of the accuracy of the simulation and input data can be obtained.

3.15 Simulation hints

The critical steps in building the vehicle model are the following:

* Geometry: make sure that all the geometrical specifications of the vehicle, i.e. position of CG, placements of axles, etc. are supplied correctly (all units are in SI units, i.e. m, kg, kgm^2, etc.)
* Ensure that the suspension/tyre data is correct and that the sign convention is applied correctly. Negative for compression (jounce) and positive for rebound. Use the graph option to subjectively evaluate the input data. Also ensure that the extent of the data cover the expected range to eliminate extrapolation of data.
* Make sure that the number of suspension elements used is correct, for example: if the data prescribed is that for one spring and two springs are used on the specific axle then the number of springs must be specified as two.
* Choose the initial deflections relatively close to that required for equilibrium.
* Use the simulation output data that are given after equilibrium is computed to check the initial deflections. Correct the model if required.
* If equilibrium, with the selected option, cannot be obtained, try using the option where no equilibrium calculations are done, i.e. the simulation will start directly from the specified values. Run the simulation program and evaluate the simulation results. Look specifically at the tyre, spring and bump stop forces and interpret the values to see if they are within the expected and acceptable range.
* It is always better to start the program on a level road as this will aid in obtaining initial equilibrium.
* *Remember to save the vehicle file before exiting the program. The user will be prompted to save the vehicle file before exiting the program. It is also a good idea to save the vehicle file before trying to run the simulation, because if the program runs into mathematical problems it may exit due to a program error and the data will be lost.*

3.16 Example Simulation

An example simulation is installed in the /data/demo directory of the installation directory as part of the installation process. The vehicle file, demo.veh, in this directory is for an example vehicle. If the program was installed into a different drive or directory, ensure that all files are specified correctly in the "File names" frame group on the main input screen after opening the vehicle file. Use the "Select file" button to select the required files. The correct files are named DEMO.*

The demo files installed are for a typical four wheel vehicle as shown in figure 3.22:

Figure 3.22: Vehicle model for the example simulation

3.16.1 Running the example

Open the vehicle file DEMO.VEH using the "File", "File Open" menu item on the pull-down menu. Once the vehicle file is opened the main input screen will be similar to figure 3.23.

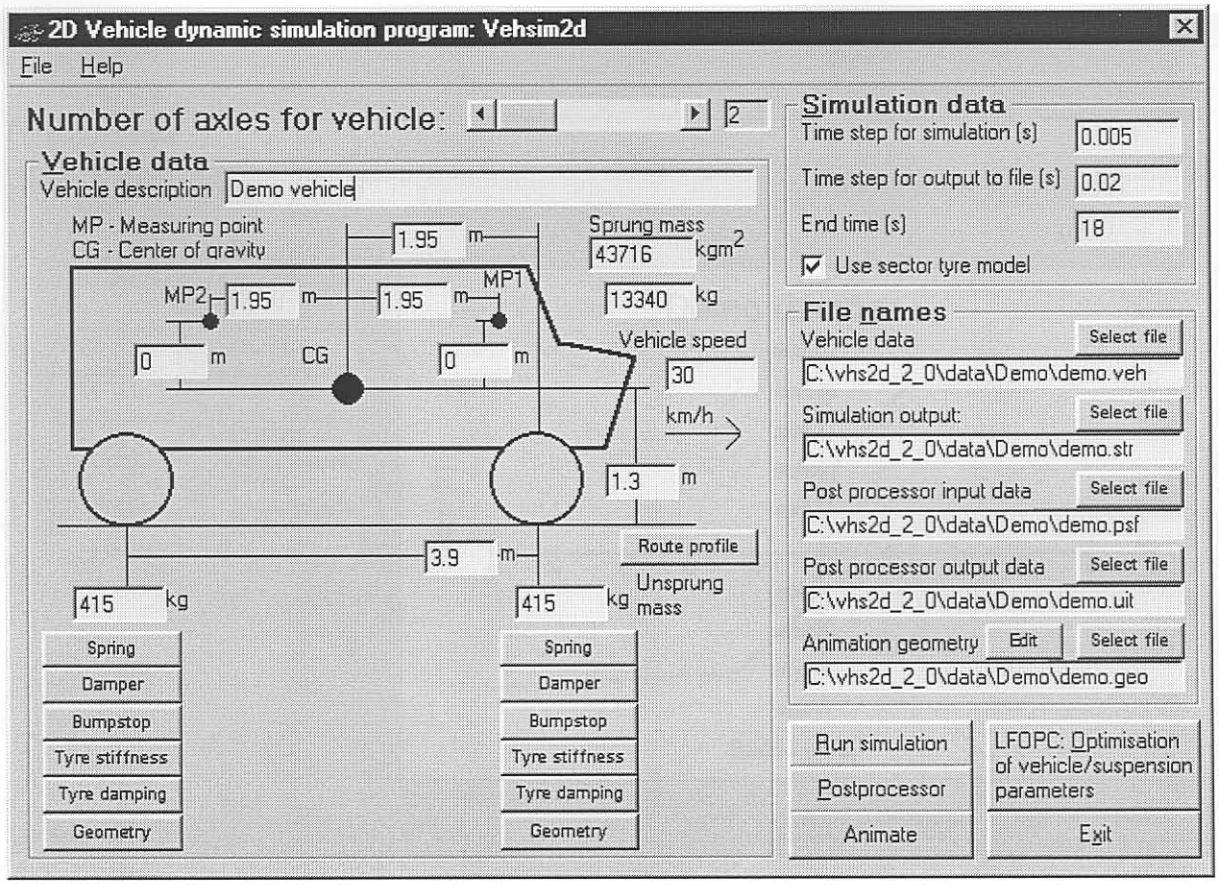

Figure 3.23: Vehicle data for demonstration vehicle

Ensure that the other file names for the simulation are specified correctly by looking at the File names frame on the main input screen. Select the correct files named demo.* by using the "Select file" buttons provided.

The buttons below the wheels can be used to inspect the data for the different components. For example, the spring characteristic for the front axle dampers, is as displayed in figure 3.24.

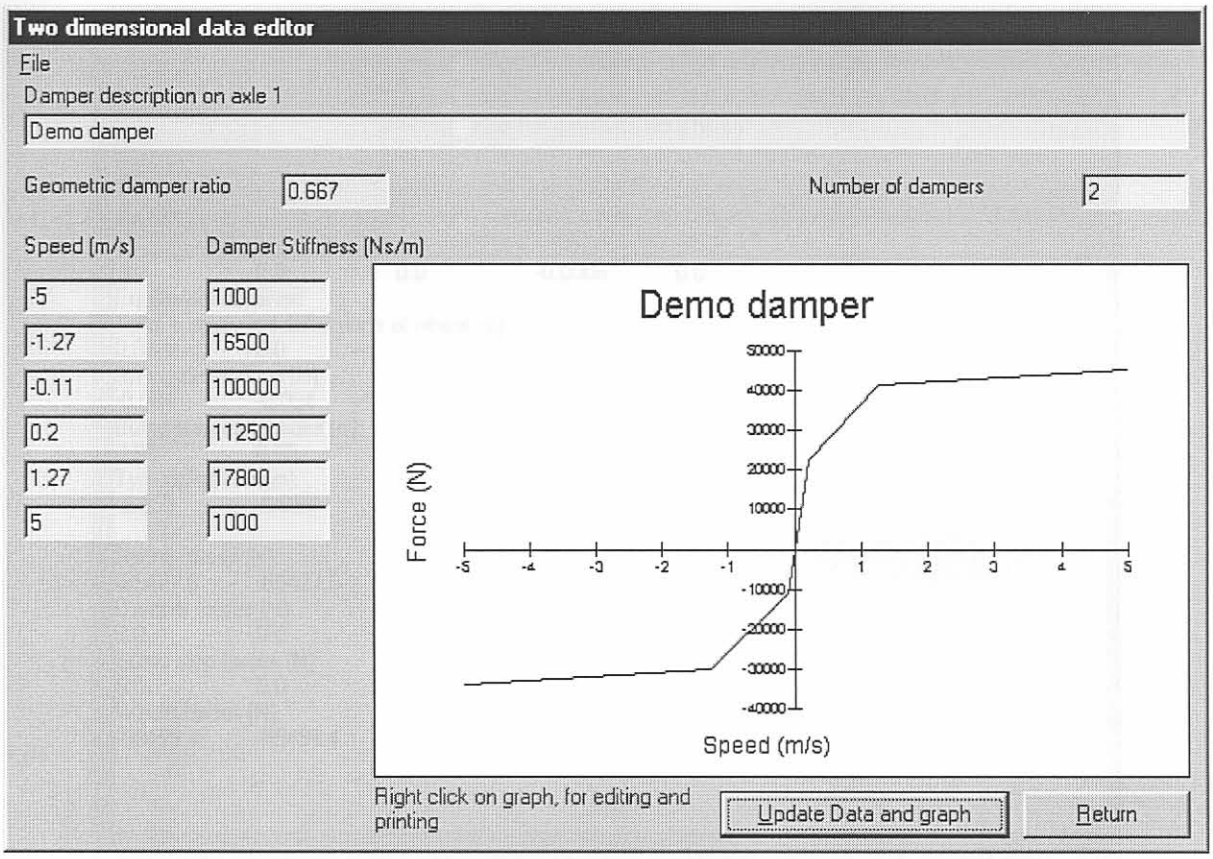

Figure 3.24: Damper data for demonstration vehicle

Use the "Update data and graph" button on the data editor to draw graphs of the characteristics.

Click on the "Run simulation" button to obtain the simulation control window. Click on the "Calculate equilibrium" button to calculate the static equilibrium for the vehicle. The results may be inspected in the window shown in figure 3.25.

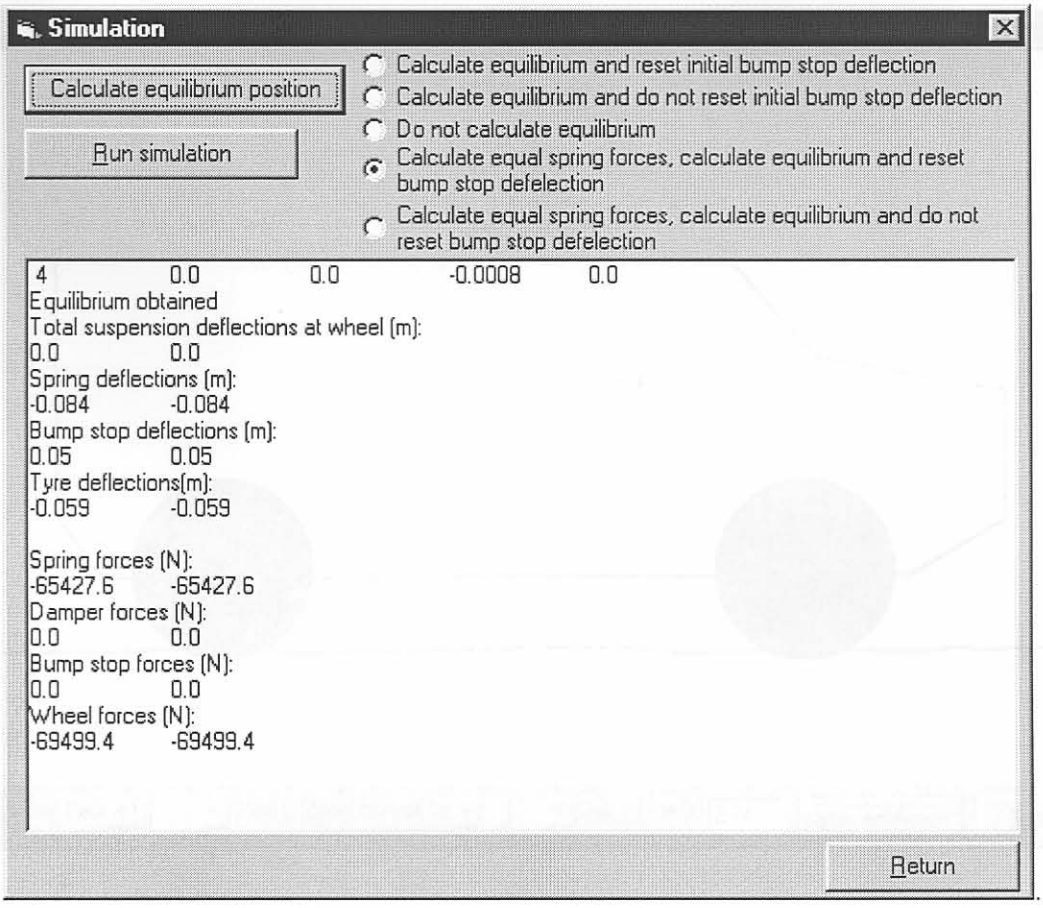

Figure 3.25: Equilibrium calculations for demonstration vehicle

Once equilibrium is obtained click on the "Run simulation" button to start the simulation. After completion of the simulation, click on the "Return" button to return to the main input screen.

Click on the "Animate" button to perform an animation of the simulation. Figure 3.26 shows a snapshot of the animation for a particular time step.

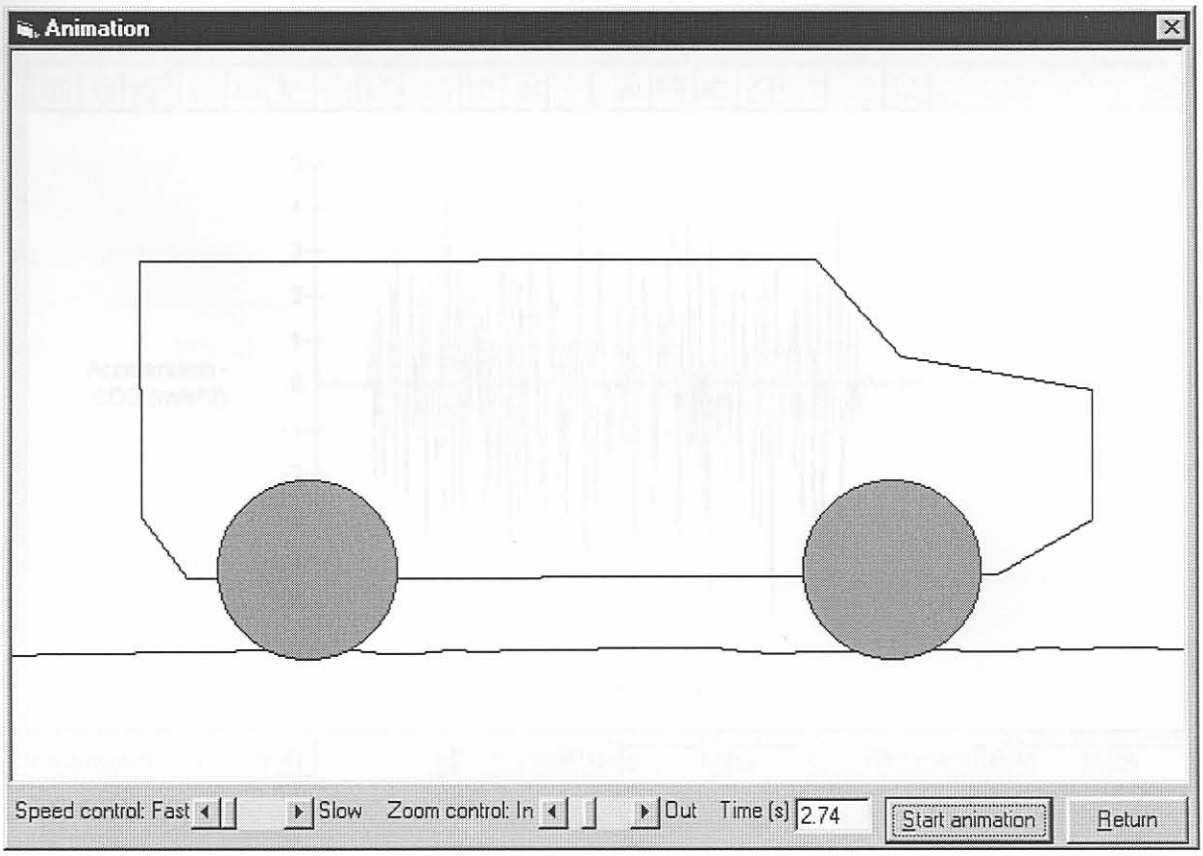

Figure 3.26: Animation snapshot of demonstration vehicle

On the main input screen click on the "Postprocessor" button to activate the postprocessor. Then select the required output options and click the "Output" button to extract the output. The "Graphs" button can now be used to graph the simulation results, as shown for the example in figure 3.27.

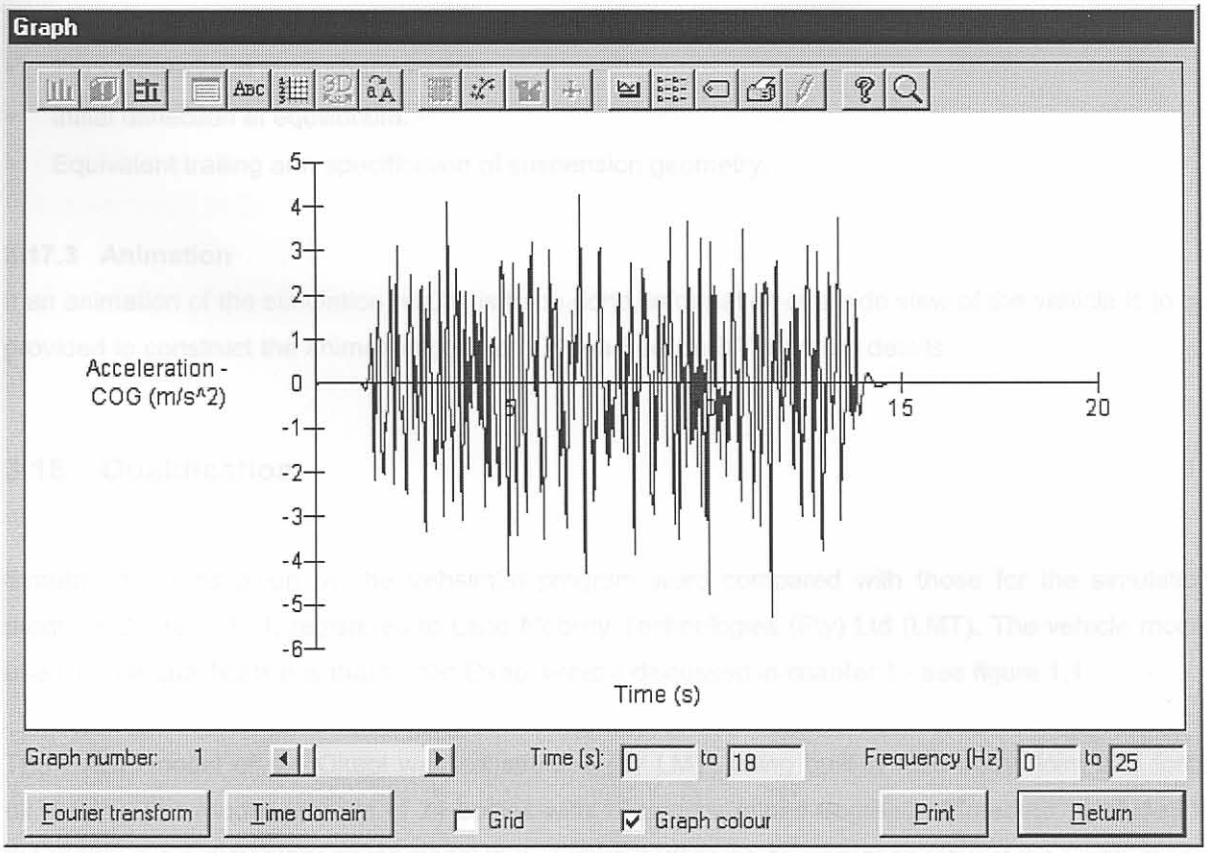

Figure 3.27: Simulation results for demonstration vehicle

Click on the graph number scroll bar to view the graphs for the other selected outputs. Use the icons on top of the graph to configure the graph display, etc.

On the postprocessor use the other buttons to analyse the results, etc.

For a more detailed description of the different options and windows, refer to the required sections in the help file.

3.17 Summary of input data required

3.17.1 Vehicle

* Number of axles.
* Position of Centre of gravity.
* Axle placement.
* Unsprung mass and unsprung pitch inertia.
* Placement of required measuring points.

3.17.2 Suspension data (for each suspension component)

* Two dimensional force characteristic.
* Initial deflection at equilibrium.
* Equivalent trailing arm specification of suspension geometry.

3.17.3 Animation

If an animation of the simulation results is to be done, information of a side view of the vehicle is to be provided to construct the animation geometry – see Section 3.7 for more details.

3.18 Qualification

Simulation results given by the Vehsim2d program were compared with those for the simulation program DADS v 9.51, registered to Land Mobility Technologies (Pty) Ltd (LMT). The vehicle model used for the qualification is that for the Okapi vehicle discussed in chapter 1 - see figure 1.1.

The DADS model of the Okapi was constructed (by LMT) using built-in rigid body, joint and force elements. The model consists of 24 bodies with 18 unconstrained degrees of freedom. Included in the model is a rudimentary driver model [62]. Figure 3.28 gives an animation view of the Okapi model in DADS.

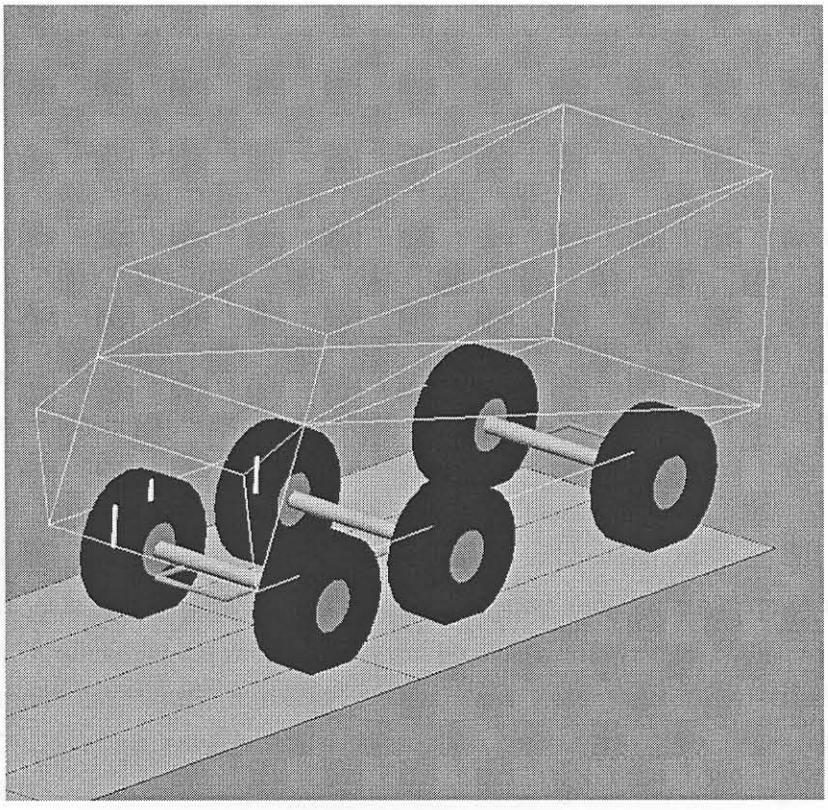

Figure 3.28: Animation view of Okapi model in DADS [62]

The vehicle model for the Okapi vehicle in Vehsim2d consists of four bodies and the suspension components. No anti-roll bars, as can be seen in figure 3.28 for the DADS model, can be simulated in Vehsim2d. Due to the fact that Vehsim2d is limited to two-dimensional simulation, qualification was performed over a symmetrical obstacle, namely a 200 mm half round bump. Figure 3.29 shows an animation frame of the Okapi model in Vehsim2d during the qualification run.

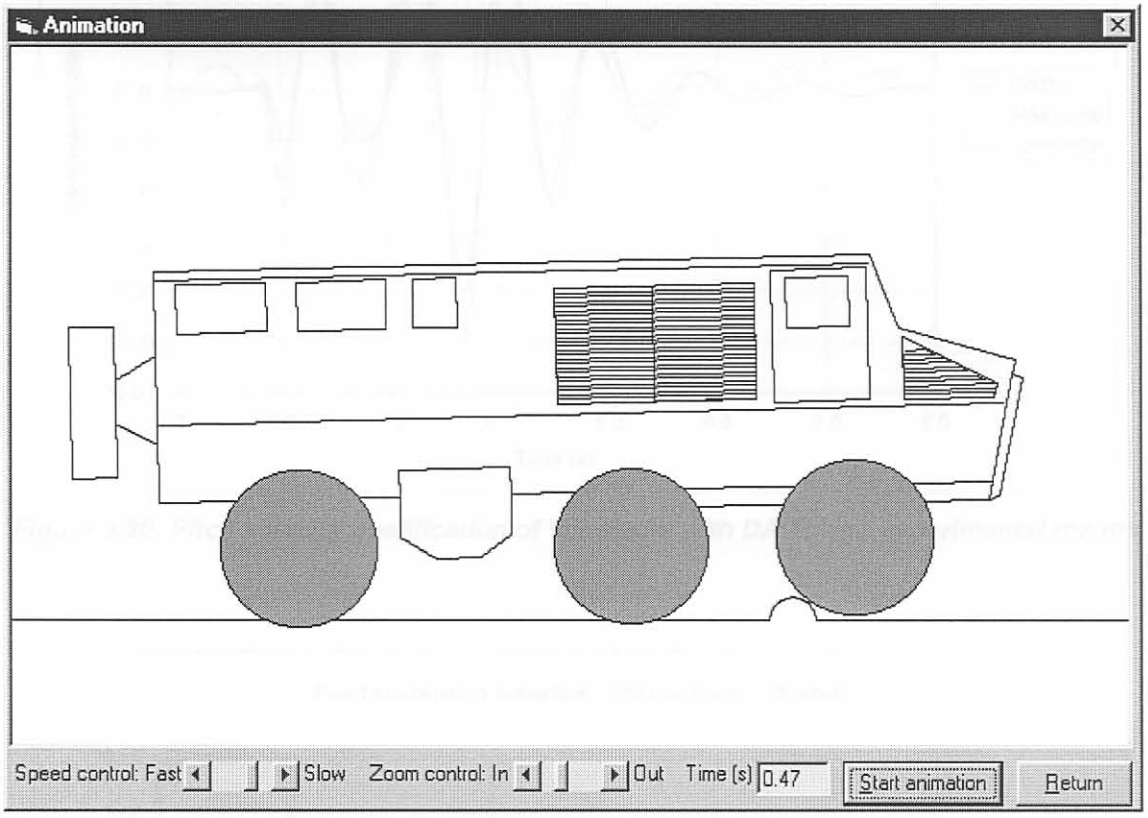

Figure 3.29: Animation view of Okapi model in Vehsim2d

Experimental measurements were done on the Okapi vehicle during actual crossing of the same 200 mm half round obstacle at the Gerotek vehicle testing track (http://www.gerotek.co.za/, Pretoria, South Africa). LVDT (displacement transducer) measurements were taken of the suspension deflections between front axle and the body, and between the second axle and the body. A gyroscope was also used in the vehicle body to measure the pitch velocity of the vehicle.

Figures 3.30 to 3.32 show comparisons of the simulation results of Vehsim2d and DADS with the experimentally measured values. Very good correlation is obtained between the measured and simulated results. It is also evident that the simulation models' motions are damped out quicker than is experimentally observed for the vehicle. This can be attributed, amongst others, to the fact that the suspension compliance (damper's rubber bushes) was not modelled. Modelling suspension compliance in DADS would have greatly increased the complexity of the simulation model, with a corresponding increase in the computational time, without significantly affecting the quality of the simulation [62].

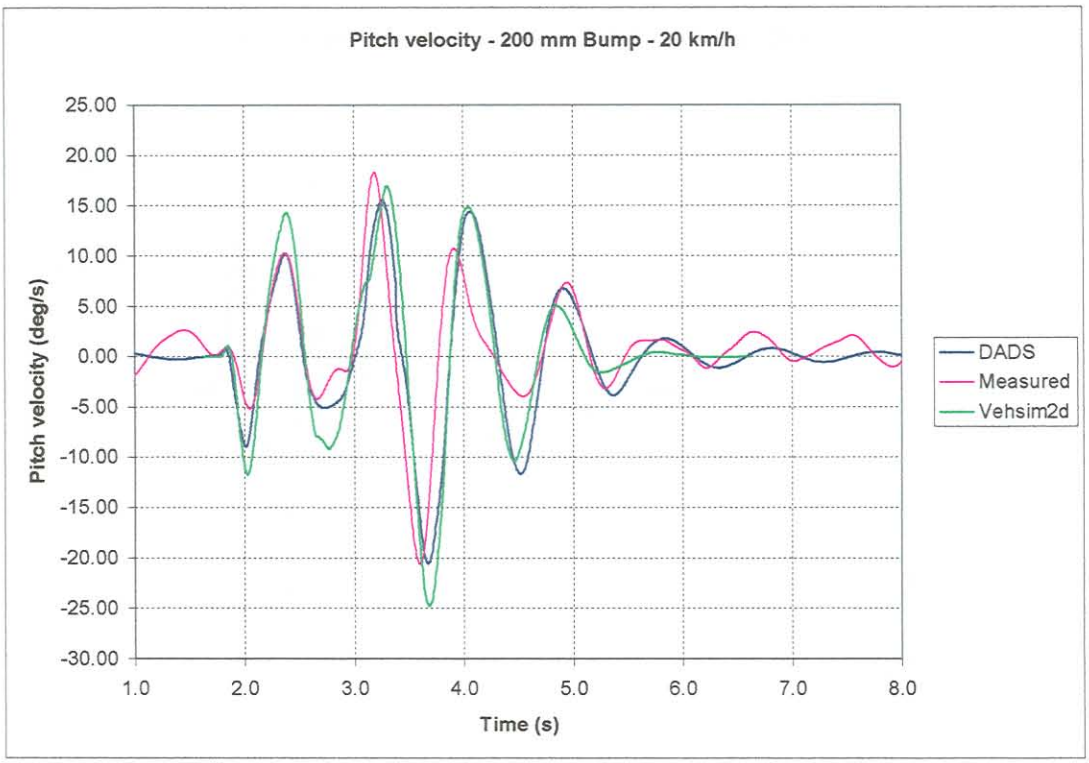

Figure 3.30: Pitch velocity qualification of Vehsim2d with DADS and experimental results.

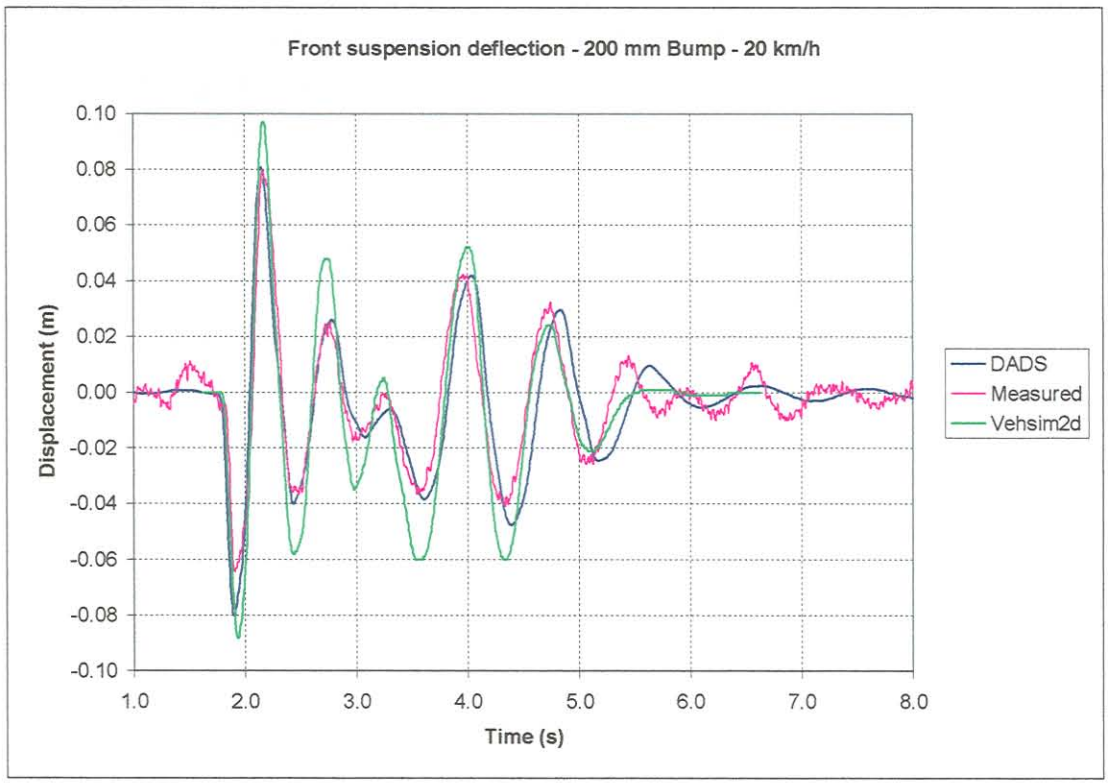

Figure 3.31: Front axle suspension deflection qualification of Vehsim2d with DADS and experimental results.

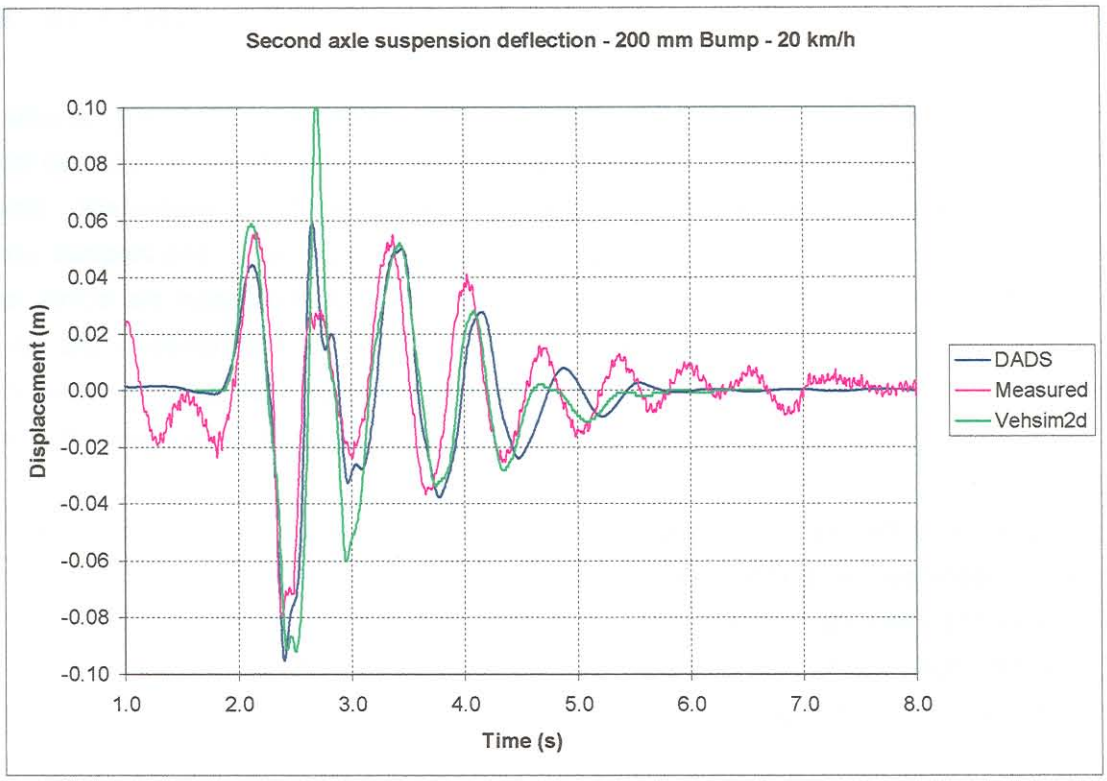

Figure 3.32: Second axle suspension deflection qualification of Vehsim2d with DADS and experimental results.

From the qualification results obtained it is concluded that the relative simple two-dimensional program Vehsim2d gives realistic results and is therefore a valid simulation program. This program may be used with confidence during vehicle concept design to model vehicle dynamics.

3.19 Summary

The program Vehsim2d was developed as a two-dimensional simulation program for analysis of vehicle dynamics during the concept design phase. The input for the program is kept as basic as possible. The suspension of the vehicle is modelled using an equivalent trailing arm approach and springs, dampers and bump stops are the basic of components of the suspension system. The tyres of the vehicle are modelled by both spring and damping characteristics. Two tyre models, a point follower and a sector tyre model are available. The suspension and tyre characteristics are prescribed by using six piece-wise continuous linear approximations, each using twelve parameters to describe the normally non-linear characteristics.

To qualify the simulation program Vehsim2d, both the simulation program DADS and experimental measurements were used. For qualification purposes the Okapi vehicle, as described in chapter 1, was actually driven over a 200 mm half round bump at a speed of 20 km/h and experimental measurements were made. The motion for the same route was simulated using both Vehsim2d and DADS. Comparison between simulated and measured data showed good correlation. From this qualification it was concluded that the simulation program Vehsim2d gives realistic results and can be successfully used as a simulation program during vehicle concept design.

CHAPTER 4:

OPTIMISATION MODULE

4. OPTIMISATION MODULE

This chapter describes the optimisation module that is coupled to the simulation program Vehsim2d described in the previous chapter. In particular a general description of the optimisation algorithm will be given, the input to the program will be described and finally an example of an optimisation exercise will be presented.

4.1 Optimisation of vehicle / suspension parameters

Use the "LFOPC: Optimisation of vehicle/suspension parameters" button on the main input screen (see figure 3.1) to display the LFOPC optimisation input screen as shown in figure 4.1. The LFOPC algorithm is an extremely robust gradient based optimisation method for constrained optimisation.

When clicking the "LFOPC: Optimisation of vehicle/suspension parameters" button the user will be prompted to save the vehicle file. Save the vehicle if the data have not been saved previously or was changed before clicking the button. The data as saved in the vehicle file will be used as baseline and optimisation will be done starting with the saved vehicle and suspension characteristics.

4.1.1 General description

For a more detailed description of the LFOPC algorithm the user is refer to section 2.2 and section A.5 of Appendix A.

Optimisation takes place with reference to a well-defined objective function. The objective function is prescribed by using certain objective criteria, for example the vibration dose values. The purpose of the optimisation is to minimise the objective function through a systematic variation of the design variables. The user specifies the appropriate objective function that must be minimised during the optimisation.

The optimisation starts by computing the objective function value for the starting values of the design variables (the base line values). The next step is to calculate the influence of each design variable on the objective function. This is done by changing each design variable separately by a small specified value, performing the simulation and calculating the new corresponding objective function value. This allows for the computation of an approximation to each component of the gradient vector of the objective function through forward finite differences. This gradient is used by the optimisation algorithm in computing the next set of design variables, which represents a step (iteration) in the direction of the optimum set. This iterative procedure is continued until no further improvement in the objective function is possible and convergence is obtained. The set of design variables at convergence corresponds to the optimum design for the specific objective function. Note that,

because of the use of finite differences for computing the gradients, one iteration of the optimisation process corresponds to $n + 1$ simulations, where n is the number of design variables.

4.1.2 LFOPC Main Input

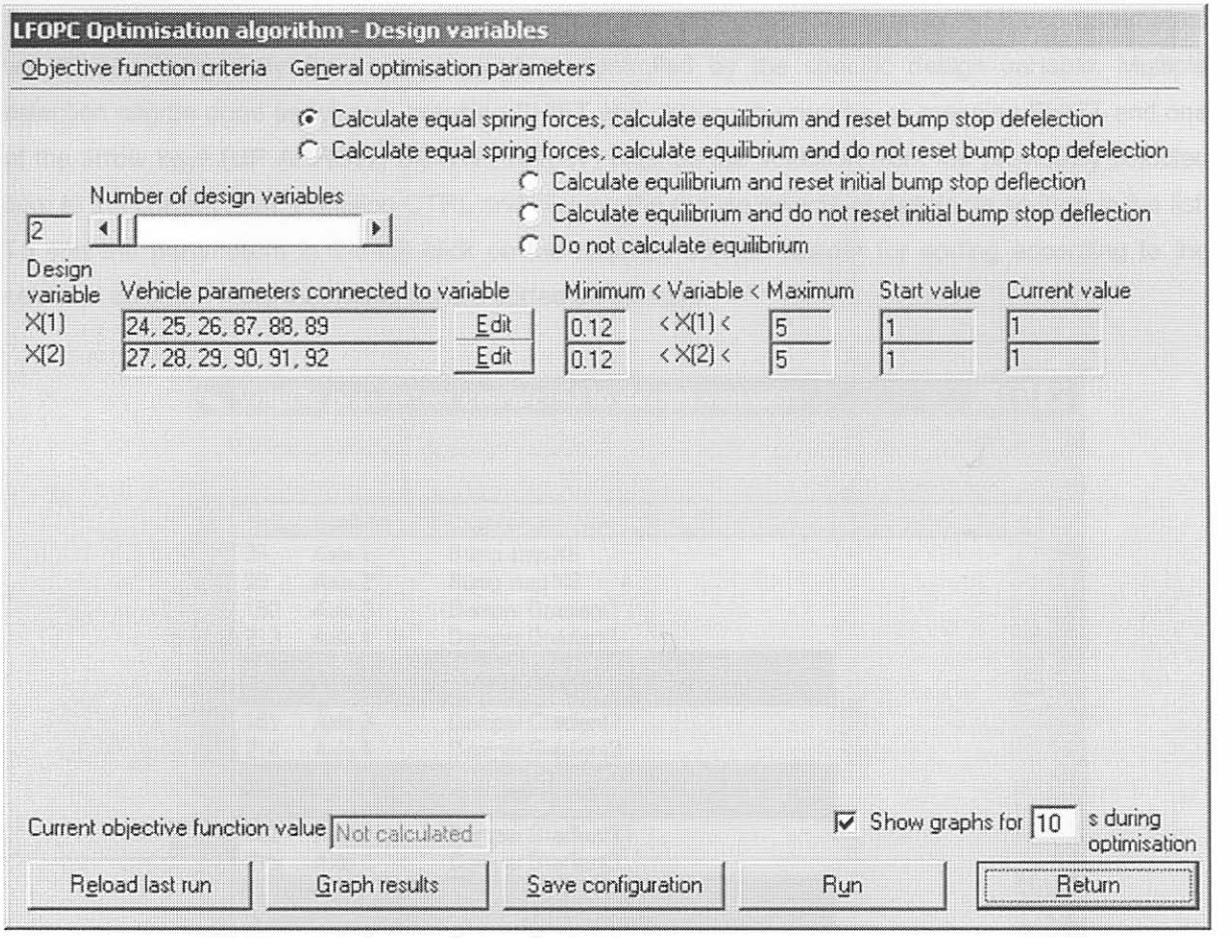

Figure 4.1: LFOPC Main input

Select the required option for calculation of equilibrium on the options available on the input window (figure 4.1) – see section 3.11 for a detailed description on the options available.

The following input are prescribed on the main LFOPC window:

Number of design variables

Prescribe the number of design variables ($X(i)$'s) that will be used by using the scroll bar. Possible values are between 1 and 255.

For each design variable ($X(i)$) supply the following:

Vehicle parameters connected to variable

Use the "Edit" button supplied to select the required parameters from the available list that will be displayed once the "Edit" button is clicked. See figure 4.2 for a description of the vehicle parameters that may be assigned to the design variables shown in figure 4.1. Clicking on the required parameter in the parameter list makes the selection. *More than one vehicle/suspension parameter can be assigned to the same design variable X(i).* If more than one parameter is selected these parameters will all be changed by the same amount as controlled by the specific design variable. Multiple selection can be done as follows: pressing SHIFT and clicking the mouse, or pressing SHIFT and one of the arrow keys (UP ARROW, DOWN ARROW) extends the selection from the previously selected item to the current item. Pressing CTRL and clicking the mouse selects or deselects an item in the list. To sort the parameters in the list click on the required column header for sorting according to the selected column. Note that numbers are sorted as strings.

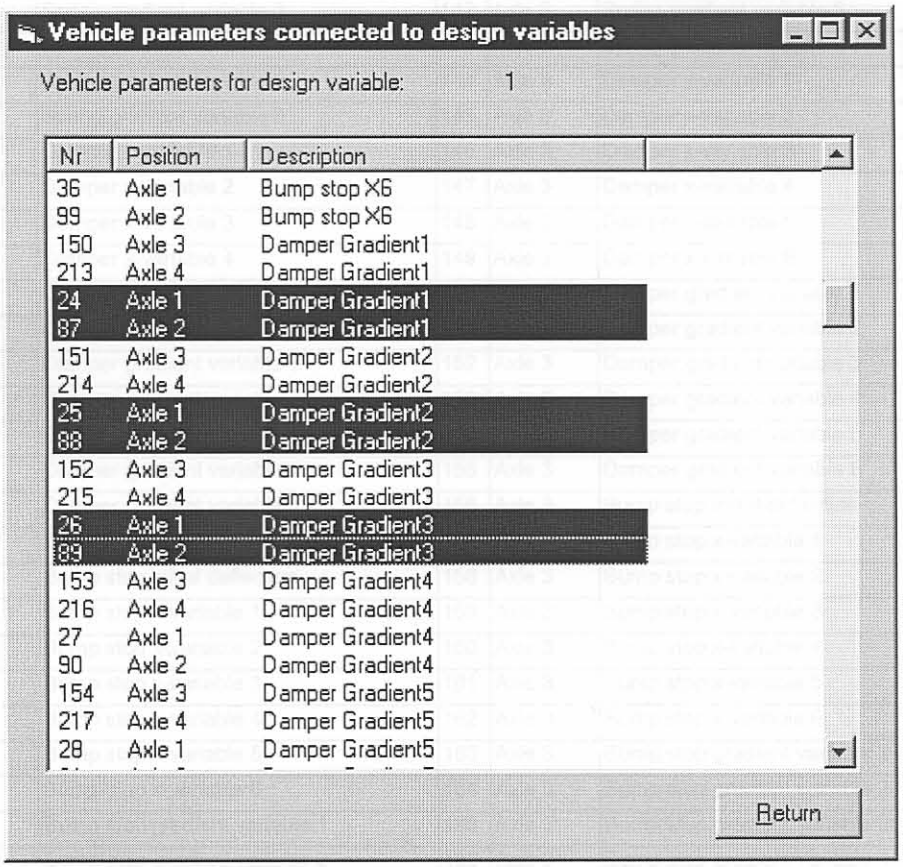

Figure 4.2: Selection of vehicle parameters

Table 4.1 lists all the possible vehicle / suspension parameters that can be linked to the design variables.

Table 4.1: Vehicle / suspension parameters available for linking to design variables

Nr	Position	Vehicle / suspension parameter	Nr	Position	Vehicle / suspension parameter
1	Vehicle	Mass	129	Axle 2	Tyre damping gradient variable 6
2	Vehicle	Pitch inertia	130	Axle 3	Unsprung mass
3	Vehicle	Position of cg behind front axle centre	131	Axle 3	Distance between axle 2 and axle 3
4	Vehicle	Height of cg above ground	132	Axle 3	Spring x-variable 1
5	Axle 1	Unsprung mass	133	Axle 3	Spring x-variable 2
6	Axle 1	Spring x-variable 1	134	Axle 3	Spring x-variable 3
7	Axle 1	Spring x-variable 2	135	Axle 3	Spring x-variable 4
8	Axle 1	Spring x-variable 3	136	Axle 3	Spring x-variable 5
9	Axle 1	Spring x-variable 4	137	Axle 3	Spring x-variable 6
10	Axle 1	Spring x-variable 5	138	Axle 3	Spring gradient variable 1
11	Axle 1	Spring x-variable 6	139	Axle 3	Spring gradient variable 2
12	Axle 1	Spring gradient variable 1	140	Axle 3	Spring gradient variable 3
13	Axle 1	Spring gradient variable 2	141	Axle 3	Spring gradient variable 4
14	Axle 1	Spring gradient variable 3	142	Axle 3	Spring gradient variable 5
15	Axle 1	Spring gradient variable 4	143	Axle 3	Spring gradient variable 6
16	Axle 1	Spring gradient variable 5	144	Axle 3	Damper x-variable 1
17	Axle 1	Spring gradient variable 6	145	Axle 3	Damper x-variable 2
18	Axle 1	Damper x-variable 1	146	Axle 3	Damper x-variable 3
19	Axle 1	Damper x-variable 2	147	Axle 3	Damper x-variable 4
20	Axle 1	Damper x-variable 3	148	Axle 3	Damper x-variable 5
21	Axle 1	Damper x-variable 4	149	Axle 3	Damper x-variable 6
22	Axle 1	Damper x-variable 5	150	Axle 3	Damper gradient variable 1
23	Axle 1	Damper x-variable 6	151	Axle 3	Damper gradient variable 2
24	Axle 1	Damper gradient variable 1	152	Axle 3	Damper gradient variable 3
25	Axle 1	Damper gradient variable 2	153	Axle 3	Damper gradient variable 4
26	Axle 1	Damper gradient variable 3	154	Axle 3	Damper gradient variable 5
27	Axle 1	Damper gradient variable 4	155	Axle 3	Damper gradient variable 6
28	Axle 1	Damper gradient variable 5	156	Axle 3	Bump stop initial deflection
29	Axle 1	Damper gradient variable 6	157	Axle 3	Bump stop x-variable 1
30	Axle 1	Bump stop initial deflection	158	Axle 3	Bump stop x-variable 2
31	Axle 1	Bump stop x-variable 1	159	Axle 3	Bump stop x-variable 3
32	Axle 1	Bump stop x-variable 2	160	Axle 3	Bump stop x-variable 4
33	Axle 1	Bump stop x-variable 3	161	Axle 3	Bump stop x-variable 5
34	Axle 1	Bump stop x-variable 4	162	Axle 3	Bump stop x-variable 6
35	Axle 1	Bump stop x-variable 5	163	Axle 3	Bump stop gradient variable 1
36	Axle 1	Bump stop x-variable 6	164	Axle 3	Bump stop gradient variable 2
37	Axle 1	Bump stop gradient variable 1	165	Axle 3	Bump stop gradient variable 3
38	Axle 1	Bump stop gradient variable 2	166	Axle 3	Bump stop gradient variable 4
39	Axle 1	Bump stop gradient variable 3	167	Axle 3	Bump stop gradient variable 5
40	Axle 1	Bump stop gradient variable 4	168	Axle 3	Bump stop gradient variable 6
41	Axle 1	Bump stop gradient variable 5	169	Axle 3	Tyre stiffness x-variable 1
42	Axle 1	Bump stop gradient variable 6	170	Axle 3	Tyre stiffness x-variable 2
43	Axle 1	Tyre stiffness x-variable 1	171	Axle 3	Tyre stiffness x-variable 3
44	Axle 1	Tyre stiffness x-variable 2	172	Axle 3	Tyre stiffness x-variable 4
45	Axle 1	Tyre stiffness x-variable 3	173	Axle 3	Tyre stiffness x-variable 5
46	Axle 1	Tyre stiffness x-variable 4	174	Axle 3	Tyre stiffness x-variable 6
47	Axle 1	Tyre stiffness x-variable 5	175	Axle 3	Tyre stiffness gradient variable 1
48	Axle 1	Tyre stiffness x-variable 6	176	Axle 3	Tyre stiffness gradient variable 2

49	Axle 1	Tyre stiffness gradient variable 1	177	Axle 3	Tyre stiffness gradient variable 3
50	Axle 1	Tyre stiffness gradient variable 2	178	Axle 3	Tyre stiffness gradient variable 4
51	Axle 1	Tyre stiffness gradient variable 3	179	Axle 3	Tyre stiffness gradient variable 5
52	Axle 1	Tyre stiffness gradient variable 4	180	Axle 3	Tyre stiffness gradient variable 6
53	Axle 1	Tyre stiffness gradient variable 5	181	Axle 3	Tyre damping x-variable 1
54	Axle 1	Tyre stiffness gradient variable 6	182	Axle 3	Tyre damping x-variable 2
55	Axle 1	Tyre damping x-variable 1	183	Axle 3	Tyre damping x-variable 3
56	Axle 1	Tyre damping x-variable 2	184	Axle 3	Tyre damping x-variable 4
57	Axle 1	Tyre damping x-variable 3	185	Axle 3	Tyre damping x-variable 5
58	Axle 1	Tyre damping x-variable 4	186	Axle 3	Tyre damping x-variable 6
59	Axle 1	Tyre damping x-variable 5	187	Axle 3	Tyre damping gradient variable 1
60	Axle 1	Tyre damping x-variable 6	188	Axle 3	Tyre damping gradient variable 2
61	Axle 1	Tyre damping gradient variable 1	189	Axle 3	Tyre damping gradient variable 3
62	Axle 1	Tyre damping gradient variable 2	190	Axle 3	Tyre damping gradient variable 4
63	Axle 1	Tyre damping gradient variable 3	191	Axle 3	Tyre damping gradient variable 5
64	Axle 1	Tyre damping gradient variable 4	192	Axle 3	Tyre damping gradient variable 6
65	Axle 1	Tyre damping gradient variable 5	193	Axle 4	Unsprung mass
66	Axle 1	Tyre damping gradient variable 6	194	Axle 4	Distance between axle 3 and axle 4
67	Axle 2	Unsprung mass	195	Axle 4	Spring x-variable 1
68	Axle 2	Distance between axle 1 and axle 2	196	Axle 4	Spring x-variable 2
69	Axle 2	Spring x-variable 1	197	Axle 4	Spring x-variable 3
70	Axle 2	Spring x-variable 2	198	Axle 4	Spring x-variable 4
71	Axle 2	Spring x-variable 3	199	Axle 4	Spring x-variable 5
72	Axle 2	Spring x-variable 4	200	Axle 4	Spring x-variable 6
73	Axle 2	Spring x-variable 5	201	Axle 4	Spring gradient variable 1
74	Axle 2	Spring x-variable 6	202	Axle 4	Spring gradient variable 2
75	Axle 2	Spring gradient variable 1	203	Axle 4	Spring gradient variable 3
76	Axle 2	Spring gradient variable 2	204	Axle 4	Spring gradient variable 4
77	Axle 2	Spring gradient variable 3	205	Axle 4	Spring gradient variable 5
78	Axle 2	Spring gradient variable 4	206	Axle 4	Spring gradient variable 6
79	Axle 2	Spring gradient variable 5	207	Axle 4	Damper x-variable 1
80	Axle 2	Spring gradient variable 6	208	Axle 4	Damper x-variable 2
81	Axle 2	Damper x-variable 1	209	Axle 4	Damper x-variable 3
82	Axle 2	Damper x-variable 2	210	Axle 4	Damper x-variable 4
83	Axle 2	Damper x-variable 3	211	Axle 4	Damper x-variable 5
84	Axle 2	Damper x-variable 4	212	Axle 4	Damper x-variable 6
85	Axle 2	Damper x-variable 5	213	Axle 4	Damper gradient variable 1
86	Axle 2	Damper x-variable 6	214	Axle 4	Damper gradient variable 2
87	Axle 2	Damper gradient variable 1	215	Axle 4	Damper gradient variable 3
88	Axle 2	Damper gradient variable 2	216	Axle 4	Damper gradient variable 4
89	Axle 2	Damper gradient variable 3	217	Axle 4	Damper gradient variable 5
90	Axle 2	Damper gradient variable 4	218	Axle 4	Damper gradient variable 6
91	Axle 2	Damper gradient variable 5	219	Axle 4	Bump stop initial deflection
92	Axle 2	Damper gradient variable 6	220	Axle 4	Bump stop x-variable 1
93	Axle 2	Bump stop initial deflection	221	Axle 4	Bump stop x-variable 2
94	Axle 2	Bump stop x-variable 1	222	Axle 4	Bump stop x-variable 3
95	Axle 2	Bump stop x-variable 2	223	Axle 4	Bump stop x-variable 4
96	Axle 2	Bump stop x-variable 3	224	Axle 4	Bump stop x-variable 5
97	Axle 2	Bump stop x-variable 4	225	Axle 4	Bump stop x-variable 6
98	Axle 2	Bump stop x-variable 5	226	Axle 4	Bump stop gradient variable 1
99	Axle 2	Bump stop x-variable 6	227	Axle 4	Bump stop gradient variable 2
100	Axle 2	Bump stop gradient variable 1	228	Axle 4	Bump stop gradient variable 3

101	Axle 2	Bump stop gradient variable 2	229	Axle 4	Bump stop gradient variable 4
102	Axle 2	Bump stop gradient variable 3	230	Axle 4	Bump stop gradient variable 5
103	Axle 2	Bump stop gradient variable 4	231	Axle 4	Bump stop gradient variable 6
104	Axle 2	Bump stop gradient variable 5	232	Axle 4	Tyre stiffness x-variable 1
105	Axle 2	Bump stop gradient variable 6	233	Axle 4	Tyre stiffness x-variable 2
106	Axle 2	Tyre stiffness x-variable 1	234	Axle 4	Tyre stiffness x-variable 3
107	Axle 2	Tyre stiffness x-variable 2	235	Axle 4	Tyre stiffness x-variable 4
108	Axle 2	Tyre stiffness x-variable 3	236	Axle 4	Tyre stiffness x-variable 5
109	Axle 2	Tyre stiffness x-variable 4	237	Axle 4	Tyre stiffness x-variable 6
110	Axle 2	Tyre stiffness x-variable 5	238	Axle 4	Tyre stiffness gradient variable 1
111	Axle 2	Tyre stiffness x-variable 6	239	Axle 4	Tyre stiffness gradient variable 2
112	Axle 2	Tyre stiffness gradient variable 1	240	Axle 4	Tyre stiffness gradient variable 3
113	Axle 2	Tyre stiffness gradient variable 2	241	Axle 4	Tyre stiffness gradient variable 4
114	Axle 2	Tyre stiffness gradient variable 3	242	Axle 4	Tyre stiffness gradient variable 5
115	Axle 2	Tyre stiffness gradient variable 4	243	Axle 4	Tyre stiffness gradient variable 6
116	Axle 2	Tyre stiffness gradient variable 5	244	Axle 4	Tyre damping x-variable 1
117	Axle 2	Tyre stiffness gradient variable 6	245	Axle 4	Tyre damping x-variable 2
118	Axle 2	Tyre damping x-variable 1	246	Axle 4	Tyre damping x-variable 3
119	Axle 2	Tyre damping x-variable 2	247	Axle 4	Tyre damping x-variable 4
120	Axle 2	Tyre damping x-variable 3	248	Axle 4	Tyre damping x-variable 5
121	Axle 2	Tyre damping x-variable 4	249	Axle 4	Tyre damping x-variable 6
122	Axle 2	Tyre damping x-variable 5	250	Axle 4	Tyre damping gradient variable 1
123	Axle 2	Tyre damping x-variable 6	251	Axle 4	Tyre damping gradient variable 2
124	Axle 2	Tyre damping gradient variable 1	252	Axle 4	Tyre damping gradient variable 3
125	Axle 2	Tyre damping gradient variable 2	253	Axle 4	Tyre damping gradient variable 4
126	Axle 2	Tyre damping gradient variable 3	254	Axle 4	Tyre damping gradient variable 5
127	Axle 2	Tyre damping gradient variable 4	255	Axle 4	Tyre damping gradient variable 6
128	Axle 2	Tyre damping gradient variable 5			

Constraints:

Prescribe the **minimum, maximum and starting value** for each design variable *X(i)*. Normally the minimum value should be a small positive number. Negative values for the minimum, maximum and starting value are not allowed. The smallest minimum value must also be larger than *2 times the prescribed Delta X(i)* for numerical differentiation – see section 4.1.4. This last requirement is to enable the calculation of forward differences for the gradient of the objective function and to assure that, for example, a negative spring stiffness does not occur during the simulations.

At the top of the LFOPC main input screen (figure 4.1) two menu items are available:

* "Objective function criteria": click to edit the selection of the required objective function criteria. See Section 4.1.3 for more detail.
* "General optimisation parameters": click to edit general optimisation parameters, for example the convergence criteria, step sizes, etc. Section 4.1.4 gives more detail.

The following buttons are also available on this screen and are used as follows:

Reload last run

This button is used to reload the last optimisation run. This will only load the last values of all the design variables (*X(i)*'s) and can be used if there was an abnormal program abortion or power failure during the optimisation process. This button must be used with care due to the fact that all other optimisation internal parameters are lost and that the whole optimisation process will have to be restarted from new starting values. Do not try to perform optimisations by stopping the optimisation process, reloading the last run and restarting the optimisation. This will lead to unnecessary long optimisations. Once the optimisation process is started try to complete the whole process before stopping the program.

Graph results

Use this button to draw graphs of the last optimisation run. Two graphs will be shown – see figure 4.3 for a typical output. The top graph indicates the convergence history of the objective function value, as well as those for the different objective criteria (*F(i)*'s) used in evaluating the overall objective function value. The bottom graph indicates the convergence histories of all the design variables (*X(i)*'s) during the optimisation process.

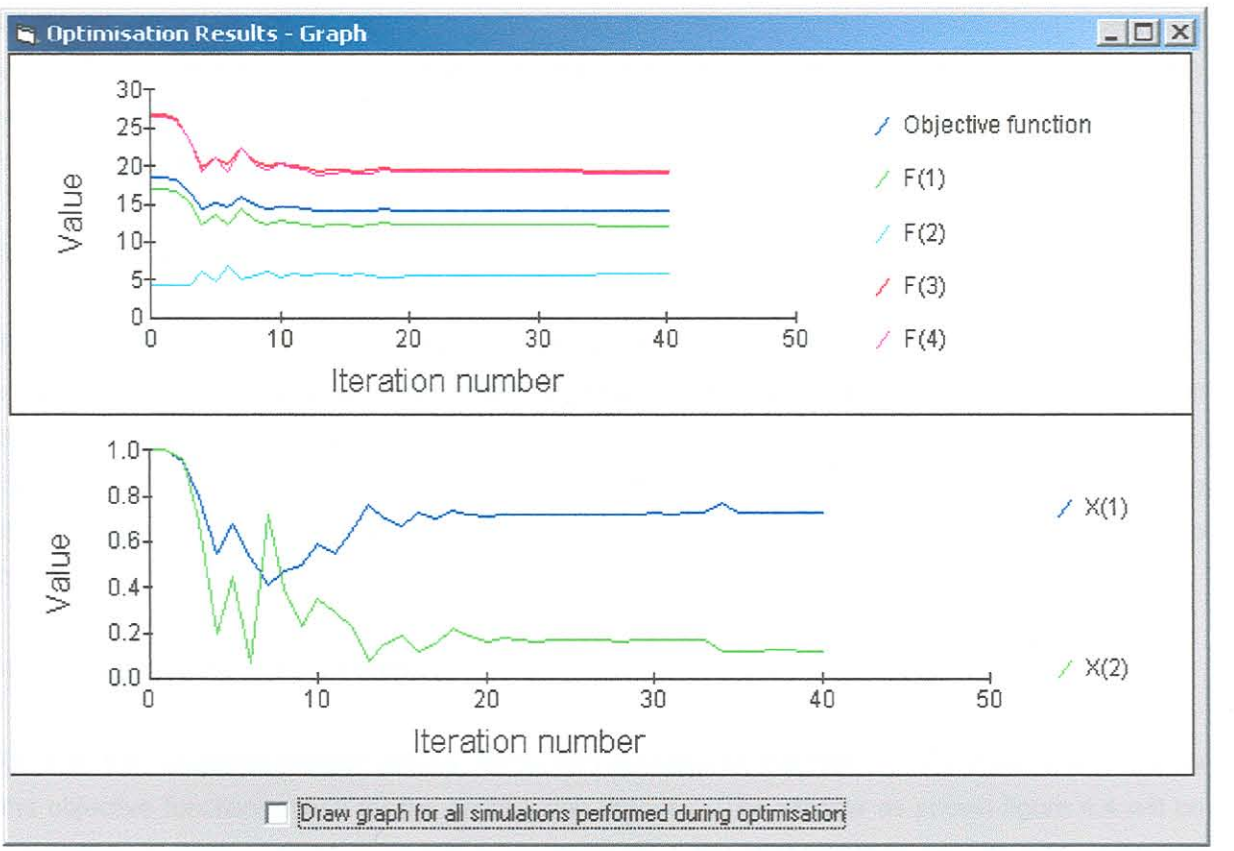

Figure 4.3: Graphs of convergence histories of the objective function and design variables during optimisation

The option exists to not only display the values of the functions and variables after each optimisation step (iteration), but also after each simulation (number of design variables + 1 simulation per step) required to compute the finite difference approximation to the gradient of the objective function – see option shown in figure 4.3. Right click on the graphs to start the Graph control dialog to edit the graph titles, printing, etc.

Run

Click the "Run" button to start the optimisation process. This will load the vehicle parameters, change the required vehicle/suspension parameters according to the *X(i)*'s, calculate equilibrium, perform the simulation, run the postprocessor, calculate root mean square, min and max values as well as the vibration dose values. If selected (see figure 4.1) graphs as described above (see figure 4.3) will be shown for a certain time period. The optimisation algorithm analyse the objective function value and if required adjusts the design variables and repeats the process. This loop will continue until a minimum objective function value with associated optimum design variable values (*X(i)*'s), within the prescribed bounds have been obtained.

Once the optimisation process is started all buttons and windows will be unavailable for user input and the process will automatically run through the prescribed loop. To quit the optimisation process wait until the simulation window appears and use the "Stop simulation" button to stop the process. This will end the optimisation process with resulting exit from the program. To restart the program, start the Vehsim2d program and load the required vehicle file.

Save configuration – see Section 4.1.5 for more detail.

Return – Click to exit the LFOPC input screen. When exiting the Vehsim2d program from the main screen after an optimisation was performed, do not save the vehicle using the same file name as that for the baseline vehicle that was initially selected for optimisation. The reason is that during the optimisation some of the vehicle or suspension parameters may have been changed, and by saving this under the same file name as for the baseline vehicle may overwrite these characteristics and the baseline data may be lost.

4.1.3 Objective function criteria

Click on the "Objective function criteria" menu item available on the main LFOPC window to prescribe the objective function criteria for the optimisation process. The window as shown figure 4.4 will be displayed.

Select and prescribe the objective function *F* using the input available. The objective function can be linked to a number of objective criteria (*F(i)*'s). A prescribed weight may be assigned to each criterion. Use the scroll bar to select the number of *F(i)*'s. For each *F(i)* select the objective criteria to

be used by clicking the "Edit" button which will display a list - see figure 4.5, of all the objective criteria available for each *F(i)*. Select the required criteria, *multiple selection is allowed*. Select the "Use abs" option if the absolute values of the selected objective criteria are to be used.

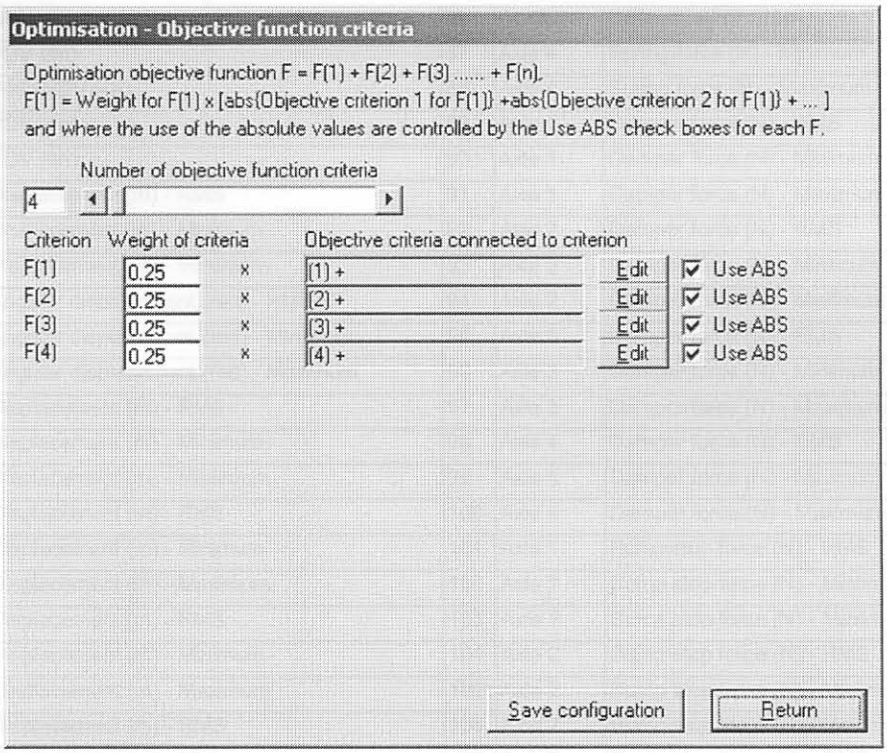

Figure 4.4: Objective function input

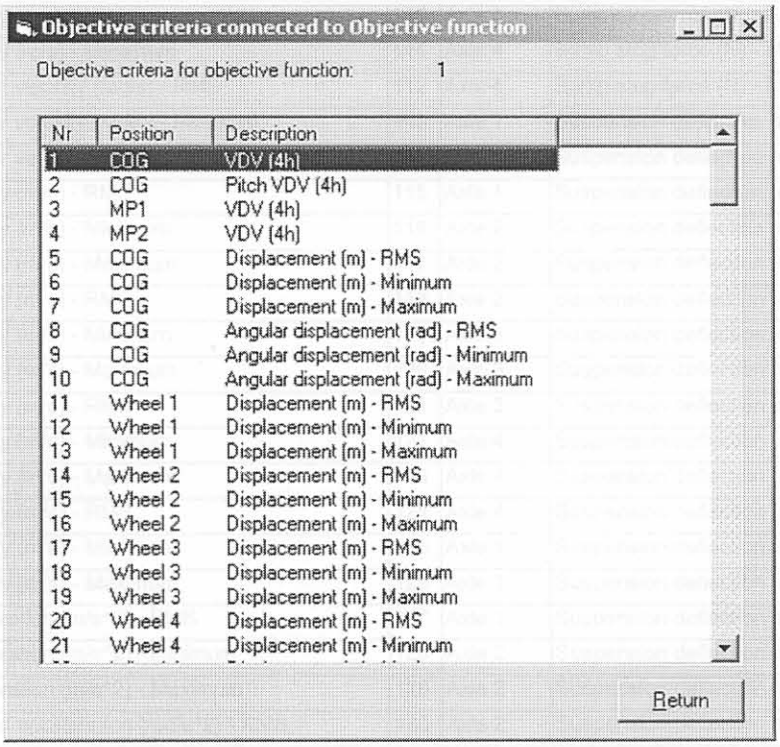

Figure 4.5: Selection of the objective criteria

Table 4.2 lists the possible objective criteria available for linking to the objective function.

Table 4.3: Possible objective criteria available for linking to the objective function.

Nr	Position	Objective criterion	Nr	Position	Objective criterion
1	COG	VDV (4h)	87	Axle 4	Spring force (N) - Minimum
2	COG	Pitch VDV (4h)	88	Axle 4	Spring force (N) - Maximum
3	MP1	VDV (4h)	89	Axle 1	Damper force (N) - RMS
4	MP2	VDV (4h)	90	Axle 1	Damper force (N) - Minimum
5	COG	Displacement (m) - RMS	91	Axle 1	Damper force (N) - Maximum
6	COG	Displacement (m) - Minimum	92	Axle 2	Damper force (N) - RMS
7	COG	Displacement (m) - Maximum	93	Axle 2	Damper force (N) - Minimum
8	COG	Angular displacement (rad) - RMS	94	Axle 2	Damper force (N) - Maximum
9	COG	Angular displacement (rad) - Minimum	95	Axle 3	Damper force (N) - RMS
10	COG	Angular displacement (rad) - Maximum	96	Axle 3	Damper force (N) - Minimum
11	Wheel 1	Displacement (m) - RMS	97	Axle 3	Damper force (N) - Maximum
12	Wheel 1	Displacement (m) - Minimum	98	Axle 4	Damper force (N) - RMS
13	Wheel 1	Displacement (m) - Maximum	99	Axle 4	Damper force (N) - Minimum
14	Wheel 2	Displacement (m) - RMS	100	Axle 4	Damper force (N) - Maximum
15	Wheel 2	Displacement (m) - Minimum	101	Axle 1	Bump stop force (N) - RMS
16	Wheel 2	Displacement (m) - Maximum	102	Axle 1	Bump stop force (N) - Minimum
17	Wheel 3	Displacement (m) - RMS	103	Axle 1	Bump stop force (N) - Maximum
18	Wheel 3	Displacement (m) - Minimum	104	Axle 2	Bump stop force (N) - RMS
19	Wheel 3	Displacement (m) - Maximum	105	Axle 2	Bump stop force (N) - Minimum
20	Wheel 4	Displacement (m) - RMS	106	Axle 2	Bump stop force (N) - Maximum
21	Wheel 4	Displacement (m) - Minimum	107	Axle 3	Bump stop force (N) - RMS
22	Wheel 4	Displacement (m) - Maximum	108	Axle 3	Bump stop force (N) - Minimum
23	COG	Velocity (m/s) - RMS	109	Axle 3	Bump stop force (N) - Maximum
24	COG	Velocity (m/s) - Minimum	110	Axle 4	Bump stop force (N) - RMS
25	COG	Velocity (m/s) - Maximum	111	Axle 4	Bump stop force (N) - Minimum
26	COG	Angular velocity (rad/s) - RMS	112	Axle 4	Bump stop force (N) - Maximum
27	COG	Angular velocity (rad/s) - Minimum	113	Axle 1	Suspension deflection (m) - RMS
28	COG	Angular velocity (rad/s) - Maximum	114	Axle 1	Suspension deflection (m) - Minimum
29	Wheel 1	Velocity (m/s) - RMS	115	Axle 1	Suspension deflection (m) - Maximum
30	Wheel 1	Velocity (m/s) - Minimum	116	Axle 2	Suspension deflection (m) - RMS
31	Wheel 1	Velocity (m/s) - Maximum	117	Axle 2	Suspension deflection (m) - Minimum
32	Wheel 2	Velocity (m/s) - RMS	118	Axle 2	Suspension deflection (m) - Maximum
33	Wheel 2	Velocity (m/s) - Minimum	119	Axle 3	Suspension deflection (m) - RMS
34	Wheel 2	Velocity (m/s) - Maximum	120	Axle 3	Suspension deflection (m) - Minimum
35	Wheel 3	Velocity (m/s) - RMS	121	Axle 3	Suspension deflection (m) - Maximum
36	Wheel 3	Velocity (m/s) - Minimum	122	Axle 4	Suspension deflection (m) - RMS
37	Wheel 3	Velocity (m/s) - Maximum	123	Axle 4	Suspension deflection (m) - Minimum
38	Wheel 4	Velocity (m/s) - RMS	124	Axle 4	Suspension deflection (m) - Maximum
39	Wheel 4	Velocity (m/s) - Minimum	125	Axle 1	Suspension deflection rate (m/s) - RMS
40	Wheel 4	Velocity (m/s) - Maximum	126	Axle 1	Suspension deflection rate (m/s) - Minimum
41	COG	Acceleration (m/s^2) - RMS	127	Axle 1	Suspension deflection rate (m/s) - Maximum
42	COG	Acceleration (m/s^2) - Minimum	128	Axle 2	Suspension deflection rate (m/s) - RMS
43	COG	Acceleration (m/s^2) - Maximum	129	Axle 2	Suspension deflection rate (m/s) - Minimum
44	COG	Angular acceleration (rad/s^2) - RMS	130	Axle 2	Suspension deflection rate (m/s) - Maximum
45	COG	Angular acceleration (rad/s^2) - Minimum	131	Axle 3	Suspension deflection rate (m/s) - RMS
46	COG	Angular acceleration (rad/s^2) - Maximum	132	Axle 3	Suspension deflection rate (m/s) - Minimum

47	Wheel 1	Acceleration (m/s^2) - RMS	133	Axle 3	Suspension deflection rate (m/s) - Maximum
48	Wheel 1	Acceleration (m/s^2) - Minimum	134	Axle 4	Suspension deflection rate (m/s) - RMS
49	Wheel 1	Acceleration (m/s^2) - Maximum	135	Axle 4	Suspension deflection rate (m/s) - Minimum
50	Wheel 2	Acceleration (m/s^2) - RMS	136	Axle 4	Suspension deflection rate (m/s) - Maximum
51	Wheel 2	Acceleration (m/s^2) - Minimum	137	Wheel 1	Tyre deflection (m) - RMS
52	Wheel 2	Acceleration (m/s^2) - Maximum	138	Wheel 1	Tyre deflection (m) - Minimum
53	Wheel 3	Acceleration (m/s^2) - RMS	139	Wheel 1	Tyre deflection (m) - Maximum
54	Wheel 3	Acceleration (m/s^2) - Minimum	140	Wheel 2	Tyre deflection (m) - RMS
55	Wheel 3	Acceleration (m/s^2) - Maximum	141	Wheel 2	Tyre deflection (m) - Minimum
56	Wheel 4	Acceleration (m/s^2) - RMS	142	Wheel 2	Tyre deflection (m) - Maximum
57	Wheel 4	Acceleration (m/s^2) - Minimum	143	Wheel 3	Tyre deflection (m) - RMS
58	Wheel 4	Acceleration (m/s^2) - Maximum	144	Wheel 3	Tyre deflection (m) - Minimum
59	MP1	Displacement (m) - RMS	145	Wheel 3	Tyre deflection (m) - Maximum
60	MP1	Displacement (m) - Minimum	146	Wheel 4	Tyre deflection (m) - RMS
61	MP1	Displacement (m) - Maximum	147	Wheel 4	Tyre deflection (m) - Minimum
62	MP2	Displacement (m) - RMS	148	Wheel 4	Tyre deflection (m) - Maximum
63	MP2	Displacement (m) - Minimum	149	Wheel 1	Tyre deflection rate (m/s) - RMS
64	MP2	Displacement (m) - Maximum	150	Wheel 1	Tyre deflection rate (m/s) - Minimum
65	MP1	Velocity (m/s) - RMS	151	Wheel 1	Tyre deflection rate (m/s) - Maximum
66	MP1	Velocity (m/s) - Minimum	152	Wheel 2	Tyre deflection rate (m/s) - RMS
67	MP1	Velocity (m/s) - Maximum	153	Wheel 2	Tyre deflection rate (m/s) - Minimum
68	MP2	Velocity (m/s) - RMS	154	Wheel 2	Tyre deflection rate (m/s) - Maximum
69	MP2	Velocity (m/s) - Minimum	155	Wheel 3	Tyre deflection rate (m/s) - RMS
70	MP2	Velocity (m/s) - Maximum	156	Wheel 3	Tyre deflection rate (m/s) - Minimum
71	MP1	Acceleration (m/s^2) - RMS	157	Wheel 3	Tyre deflection rate (m/s) - Maximum
72	MP1	Acceleration (m/s^2) - Minimum	158	Wheel 4	Tyre deflection rate (m/s) - RMS
73	MP1	Acceleration (m/s^2) - Maximum	159	Wheel 4	Tyre deflection rate (m/s) - Minimum
74	MP2	Acceleration (m/s^2) - RMS	160	Wheel 4	Tyre deflection rate (m/s) - Maximum
75	MP2	Acceleration (m/s^2) - Minimum	161	Wheel 1	Wheel force (N) - RMS
76	MP2	Acceleration (m/s^2) - Maximum	162	Wheel 1	Wheel force (N) - Minimum
77	Axle 1	Spring force (N) - RMS	163	Wheel 1	Wheel force (N) - Maximum
78	Axle 1	Spring force (N) - Minimum	164	Wheel 2	Wheel force (N) - RMS
79	Axle 1	Spring force (N) - Maximum	165	Wheel 2	Wheel force (N) - Minimum
80	Axle 2	Spring force (N) - RMS	166	Wheel 2	Wheel force (N) - Maximum
81	Axle 2	Spring force (N) - Minimum	167	Wheel 3	Wheel force (N) - RMS
82	Axle 2	Spring force (N) - Maximum	168	Wheel 3	Wheel force (N) - Minimum
83	Axle 3	Spring force (N) - RMS	169	Wheel 3	Wheel force (N) - Maximum
84	Axle 3	Spring force (N) - Minimum	170	Wheel 4	Wheel force (N) - RMS
85	Axle 3	Spring force (N) - Maximum	171	Wheel 4	Wheel force (N) - Minimum
86	Axle 4	Spring force (N) - RMS	172	Wheel 4	Wheel force (N) - Maximum

Prescribing an appropriate optimisation objective function is a very important step in the optimisation process and much thought should be given in selecting the correct criteria and weight.

4.1.4 General optimisation parameters

This menu item will display an input window for input of general optimisation parameters, as shown in figure 4.6, used during the optimisation process. Normally the default values should be sufficient but the user can explicitly change the setting should the user have other requirements.

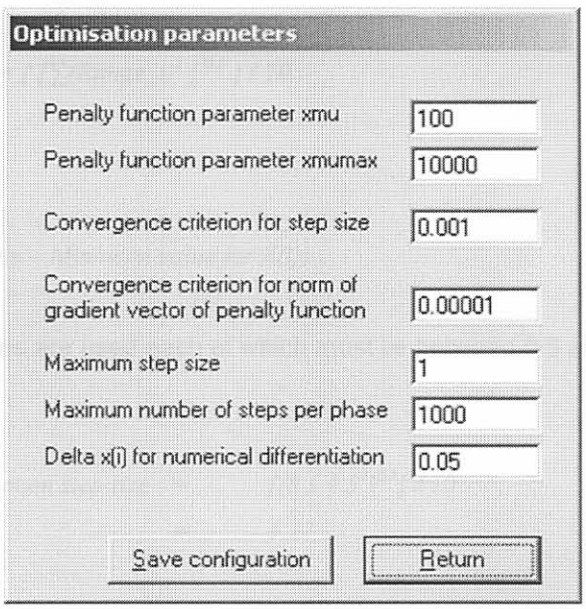

Figure 4.6: General optimising parameters

The following parameters inherent to the optimisation algorithm LFOPC may be changed:

* For higher accuracy, at the expense of economy, the value of the penalty function parameter *xmumax* may be increased. On the other hand, for greater economy at the expense of accuracy, both *xmumax* and *xmu* may be lowered in the same proportion. This may be necessary if the objective function is relatively "flat".
* The optimisation is terminated when either of the convergence criteria becomes active, that is when:

Step size = The norm of the change of the design variables vector < Convergence criterion for step size.

or

The norm of the gradient of the penalty function < Convergence criterion for the norm of the gradient of penalty function.

* For simulations with a low number of design variables the value for the Convergence criterion for step size may be decreased, e.g. 10^{-5}. For a high number of optimising variables the value may be increased e.g. 10^{-3}. The smaller this value is the more accurate the final result will be, but at the expense of a larger number of simulations being performed. Too large values for the convergence tolerances may lead to premature termination of the optimisation process.
* The maximum step size must be of the same order of magnitude as the "diameter of the region of interest", i.e.

$$Maximum\ step\ size = \{ [\sum (Range\_i)^2]^{0.5} \} / 10$$

where:

$$Range\_i = (Maximum - Minimum\ value\ for\ X(i))$$

e.g. if 8 design variables are used each of which must lie between 0.5 and 5 then:

$$Range\ i = 4.5$$

$$Recommended\ maximum\ step\ size = [(8 \times 4.5^2)^{0.5}] / 10$$

$$= 1.27$$

* Maximum number of steps per phase may be increased if the optimum values have not been determined within the prescribed number of iterations.
* The delta *X(i)* for numerical differentiation is the value with which each design variable (*X(i)*) is to be increased in turn to determine the influence of the specific *X(i)* on the objective function, i.e., to determine the *i-th* component of the gradient vector. A typically large value of 0.05 is used if numerical noise is expected to be relatively dominant. In such a case the delta *X(i)* should be larger than the wavelength of the noise. If, however, the *X(i)*'s have a strong influence on the value of the objective function and the effect on the objective function of numerical noise is negligible or small, then the value of delta *X(i)* may be decreased to give more accurate derivatives.

Arbitrary changes to the optimisation parameter values are not recommended as such changes may require a more in-depth knowledge of the optimisation algorithm.

4.1.5 Saving configurations

On each of the input screens click the "Save configuration" button to save the input to the files. No selection of file names are allowed and the following files are used for saving the configurations:

LFOPC.DAT – Input for the main LFOPC window, i.e. selection of design variables, etc.
LFOPC_FUN.DAT – Input for the objective function criteria
LFOPC_PAR.DAT – Input for general optimisation parameters

These files are saved in the application directory (i.e. the directory in which the Vehsim2d.exe file is located). Each time the "Save configuration" buttons are used or the LFOPC main window is exited, these configuration files are overwritten with the latest selected values. Backup copies of these files can be used for later reference or to save specific configurations.

4.1.6 Optimisation output

During the optimisation process the following output is created:

LFOPC.OUT

This ASCII file is a summary if the output of the simulation process. Use a program for instance Notepad to view the contents of the file. Typical contents of this file are as shown below:

START OF PHASE : 0
STEP = 0. GRADIENT NORM = 4.921E+00
OBJECTIVE FUNCTION VALUE : F = 18.60096
X-values:
1 1
STEP = 1. GRADIENT NORM = 5.335E+00
X-values:
0.9487166 0.9140347
STEP = 2. GRADIENT NORM = 5.571E+00
X-values:
0.795211 0.6356146
STEP = 3. GRADIENT NORM = 3.490E+00
X-values:
0.5509056 0.1464902
|
|
STEP = 35. GRADIENT NORM = 3.022E-03
OBJECTIVE FUNCTION VALUE : F = 14.22362
FINAL X-VALUES FOR CURRENT PHASE FOLLOW
X-values:
0.6646426 0.196326

START OF PHASE : 1
STEP = 35. GRADIENT NORM = 3.759E+00
OBJECTIVE FUNCTION VALUE : F = 14.22362
X-values:
0.6646426 0.196326
STEP = 36. GRADIENT NORM = 2.795E+00
X-values:
0.6646426 0.2014112
|
|
STEP = 62. GRADIENT NORM = 3.783E+00
OBJECTIVE FUNCTION VALUE : F = 14.23207
FINAL X-VALUES FOR CURRENT PHASE FOLLOW
X-values:
0.6637446 0.1998436

START OF PHASE : 2
STEP = 62. GRADIENT NORM = 1.183E+01

OBJECTIVE FUNCTION VALUE : F = 14.23207
X-values:
0.6637446 0.1998436
STEP = 63. GRADIENT NORM = 6.629E+01
X-values:
0.6637446 0.2008745
|
|
STEP = 77. GRADIENT NORM = 4.623E+01
OBJECTIVE FUNCTION VALUE : F = 14.23098
FINAL X-VALUES FOR CURRENT PHASE FOLLOW
X-values:
0.6637446 0.1993886
FINAL INEQUALITY CONSTRAINTS FUNCTION VALUES:
C(1)= -4.336256
C(2)= -0.4637446
C(3)= -4.800611
C(4)= 6.114393E-04

The optimisation process is performed in three phases (See section A.5 of Appendix A). During phase 0 the optimisation is performed with a moderate penalty parameter (xmu) for violation of the specified minimum or maximum design variable bounds (constraints). Each step involves the calculation of the gradient and a new set of *X(i)* values, i.e. for each step the simulation is performed *(Number of design variables + 1)* times. Once the convergence criteria are satisfied the final values of the *X(i)*'s are printed as well as the final objective function value for phase 0. If at the end of phase 0 any of the constraints are violated the process continues to phase 1 where a more severe penalty parameter (xmumax) is applied. At the end of phase 1 the active constraints are actually identified and in phase 2 a final trajectory is followed from the solution point of phase 1 to the nearest point in the subspace of points satisfying the active constraints.

LFOPC.GRF

This is a detail output ASCII file for each simulation during the process. A typical example of such a file is shown underneath:

18.60096
4
0.25 16.9257 0.25 4.354053 0.25 26.65999 0.25 26.46409
2
1 1
18.72701
4
0.25 17.05221 0.25 4.342792 0.25 26.84885 0.25 26.6642
2
1.05 1
18.81226
4

```
0.25    17.1101    0.25    4.397651    0.25    26.98139    0.25    26.75989
2
1.05    1
|
|
4
0.25    12.5919    0.25    5.419183    0.25    19.84062    0.25    19.62821
2
0.6637446    0.2493886
14.23098
4
0.25    12.35225    0.25    5.646798    0.25    19.61322    0.25    19.31164
2
0.6637446    0.1993886
```

The format for this file is:

Objective function value F
Number of F(i)'s
Weight for F(1) *Value for F(1)* *Weight for F(2)* *Value for F(2) .....*
Number of X(i)'s
Value for X(1) *Value for X(2) .....*

The above values are written for each simulation performed during the optimisation process including those required for the finite difference calculations.

This is the file used for graphing the optimisation results but can also be used to obtain more detail regarding the progress of the optimisation process.

Optimise_vehicle.veh

Each time the vehicle/suspension simulation parameters are changed through their coupling to the design variables, a vehicle file optimise_vehicle.veh is written. This file can be used to perform simulations with the optimised vehicle or to inspect the characteristics of the suspension and vehicle once the optimisation process is completed. Open this file as for any other vehicle file under vehsim2d.exe.

4.1.7 General optimisation considerations

Computational effort during optimisation can be excessive. Due to this fact the following should be kept in mind during the planning of the operation strategy and the selection of optimisation settings:

* Keep the number of design variables as small as possible. If possible couple more than one parameter to the same design variable. For instance if the vehicle uses the same dampers on the front and rear axles, then link them to the same design variables.
* Use the appropriate tyre model for the type of route profile being considered. Using the sector model on relative smooth surfaces will increase the computational time without improving simulation accuracy.
* When optimising the x-values (see figure 3.8) for springs, dampers, etc., consider the fact that the array of x-values for the component must remain in the sequence from small to large after adjustment of the design variables. For example if the first x-value for the damper is –5 m/s and the second value –1 m/s and the minimum and maximum value for the design variables are 0.2 and 2 then a situation may exist where the first x-value becomes –1 m/s and the second value –2 m/s. This is not allowed and will lead to inaccurate simulation results and may even cause abortion of the program. The required sequence is not enforced in the program and it is up to the user to ensure that the constraints are specified correctly.
* Ensure that the simulation time is long enough so that the complete required route profile (which will normally end with a flat road surface) is covered, and that the vehicle movement is damped out before the simulation end time, i.e. the accelerations used for calculating the VDV must all start at a value of 0 and end at a value of 0. This must be true for all the spring and damper characteristics that may be used during the optimisation process. This will improve the accuracy of the vibration dose values calculated, as no windowing is performed during the fast Fourier transform calculations during which the acceleration signals are weighed according to the required weighting functions. If the accelerations do not start and end at the same value it will lead to inaccuracy in calculating the Fast Fourier transform of the signals.
* Keep the specified minimum and maximum bounds within reasonable and practically possible limits.
* Use the correct and appropriate equilibrium calculation option – see section 3.11 for more details.
* Only one instance of the optimisation process or Vehsim2d.exe may be executed at a particular time. For example, under the Windows operating system which will allow multiple instances of the program to run, only one of the instances may be executed at a particular time. This is required to ensure that no file sharing violations occur and because multiple instances may read or write to the same file.
* The biggest problem that remains with this type of local optimisation process is the problem of finding a local minimum rather than the global minimum when starting from a given starting point. This situation is depicted for starting point 1, for the one-dimensional case in figure 4.7. One way of making sure that the lowest minimum obtained is likely to be the global minimum is to repeat

the optimisation, but starting from another starting point in the variable range, i.e., also starting from point 2. In extreme circumstances multiple starting points may be used in order to increase the probability of obtaining the global optimum.

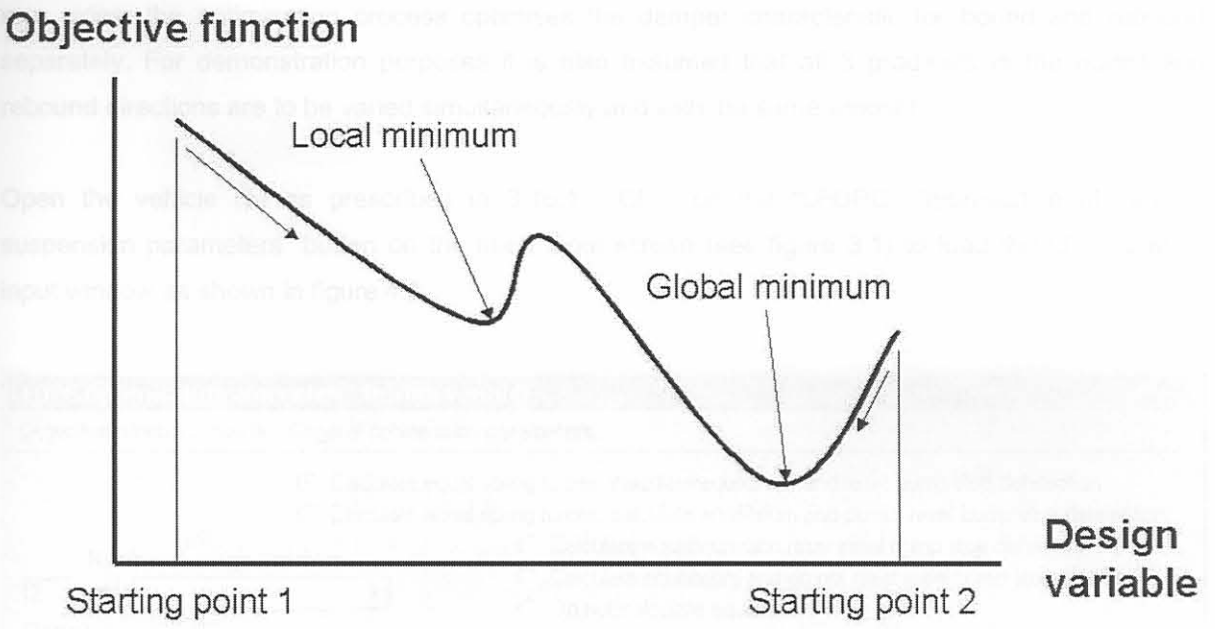

Figure 4.7: Schematic illustration of local and global minima

4.2 Optimisation example

The optimisation example described is that for the demo vehicle (see section 3.16) over a Belgian paving route profile at 30 km/h. Assuming that the same dampers are to be used on the front and rear axles, the optimisation process optimises the damper characteristic for bound and rebound separately. For demonstration purposes it is also assumed that all 3 gradients in the bound and rebound directions are to be varied simultaneously and with the same amount.

Open the vehicle file as prescribed in 3.16.1. Click on the "LFOPC: Optimisation of vehicle/ suspension parameters" button on the main input screen (see figure 3.1) to load the LFOPC Main input window as shown in figure 4.8.

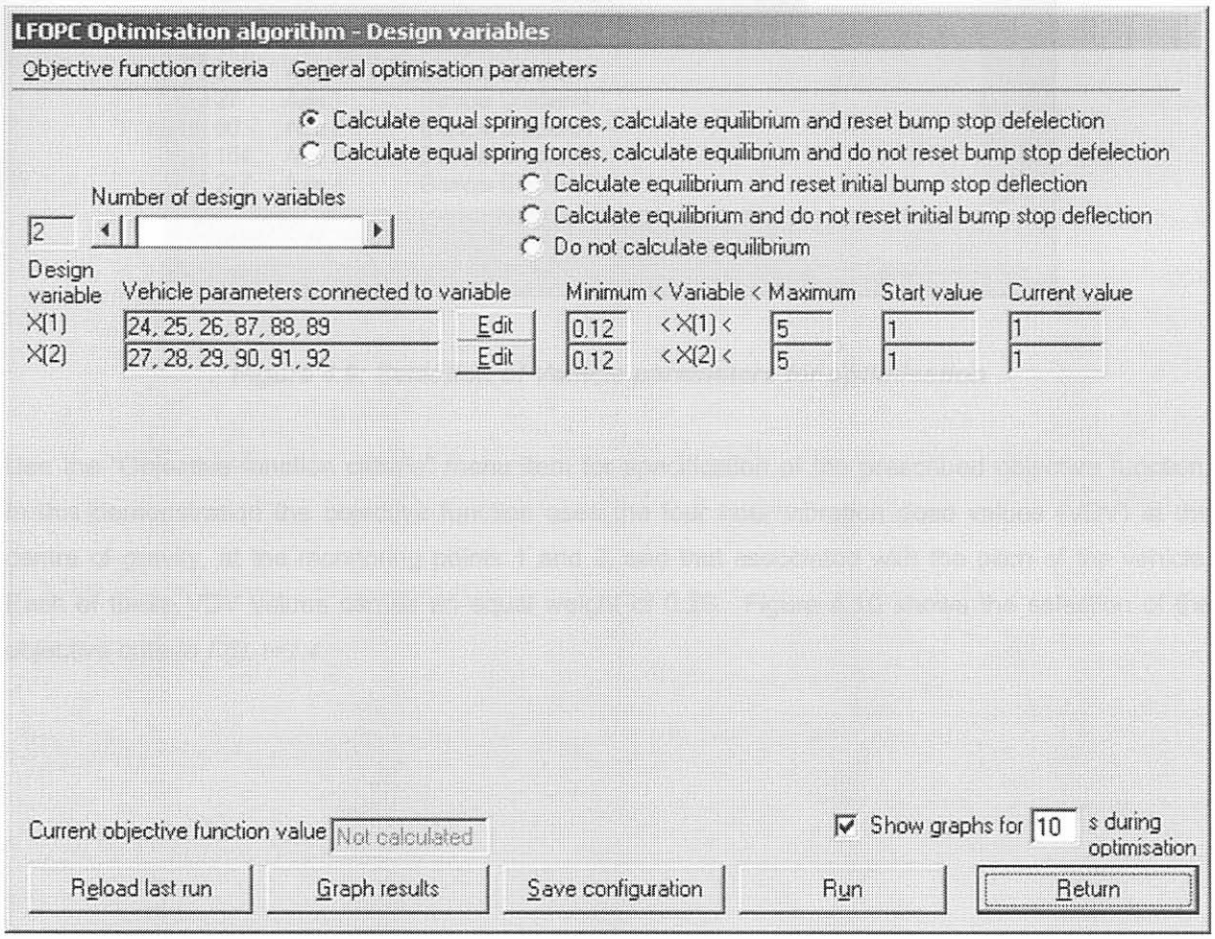

Figure 4.8: Optimisation input

In this example it is assumed that the design variables can lie between 0.12 and 5 (i.e. the characteristics linked to the design variable can change between 12% and 500% of that for the baseline vehicle) and will start from 1 (i.e. the baseline). Check the prescribed input for the design parameters by clicking on the "Edit" button. For example, the design parameters linked to variable *X(1)* are as shown in figure 4.9.

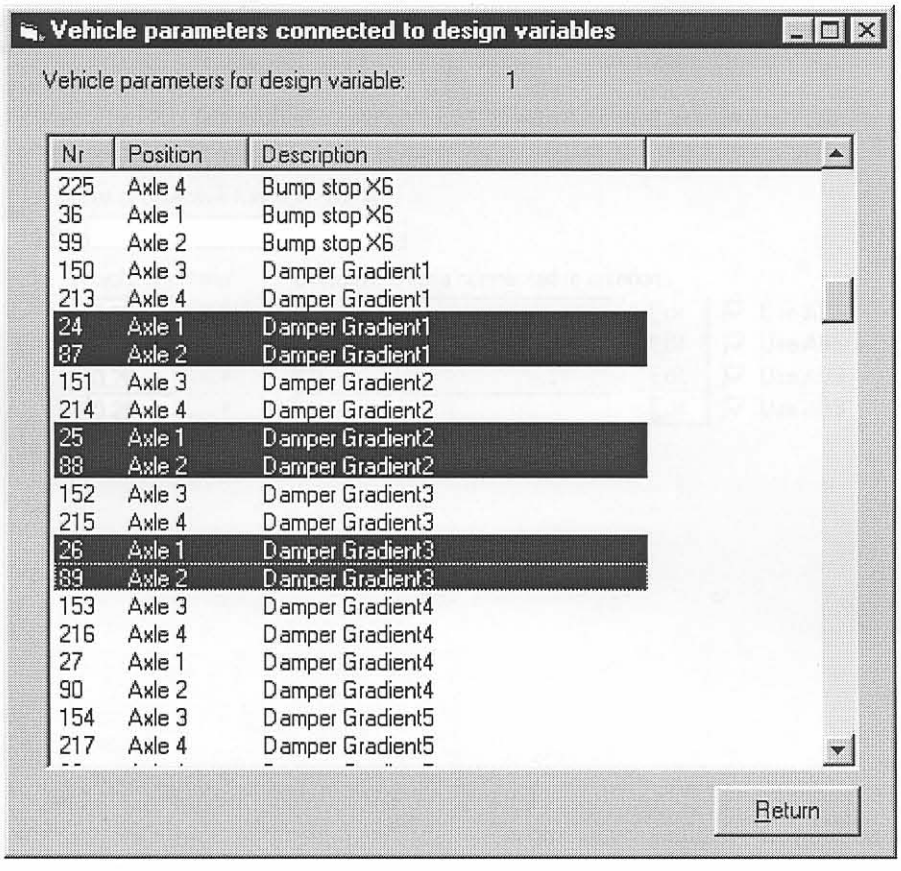

Figure 4.9: Selection of Vehicle parameters for optimisation

Use the "Objective function criteria" menu item for specification of the prescribed objective function. In this demonstration the objective function uses the four hour vibration dose values (VDV) at the centre of gravity, at the monitoring points 1 and 2, and that associated with the pitch of the vehicle. Each of these VDV values carries an equal weight of 0.25. Figure 4.10 shows the selection of the objective criteria $F(i),\ i=1,4$.

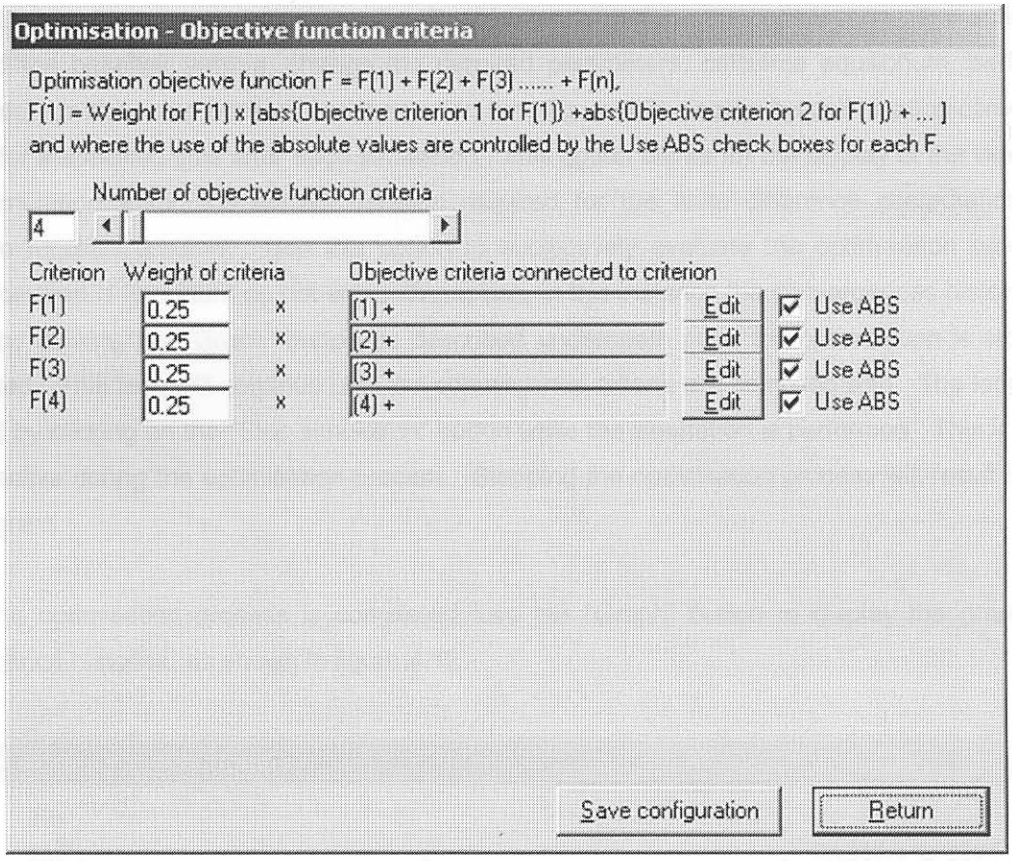

Figure 4.10: Objective function input

The general optimisation parameters are prescribed by using the "General optimisation parameters" menu item on the LFOPC Main input window. The general parameters selected here are as shown in figure 4.11.

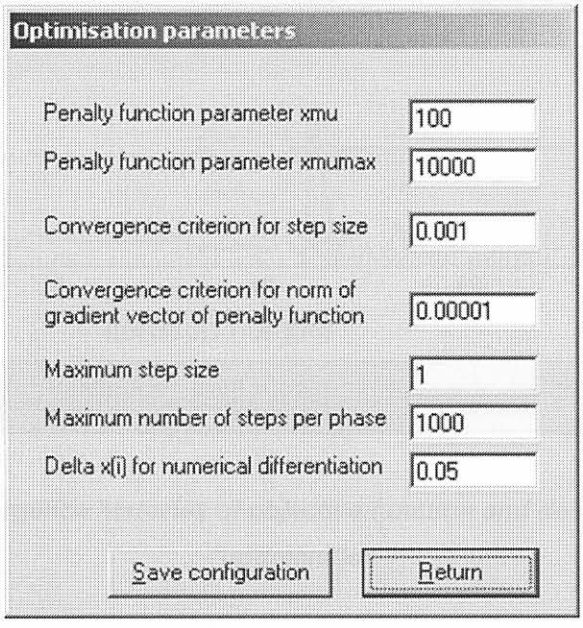

Figure 4.11: General parameters for optimisation algorithm

On the LFOPC Main input window use the "Run" button to perform the optimisation. The optimisation will load the baseline vehicle, change the required parameters, calculate equilibrium, perform the simulation, run the postprocessor and if selected (see figure 4.8) display the optimisation convergence graphs for a specified time after each simulation. This option allows for the display of the values after each simulation within the current iteration required for the finite difference computation of the objective function gradient. Use this option to subjectively evaluate the optimisation process. If simulation time is important do not select this option, in this instance the convergences history can be shown by clicking the "Graph" button as described underneath once the optimisation is stopped or completed. This loop will continue until the convergence criteria are complied with. The loop can be stopped by clicking on the "Stop simulation" button while the simulation is performed. This is the only button active during the optimisation process. Stopping the optimisation process will result in exiting the program.

Once the optimisation process is completed, use the "Graph" button to display the graph of the convergence histories, as shown in figure 4.12.

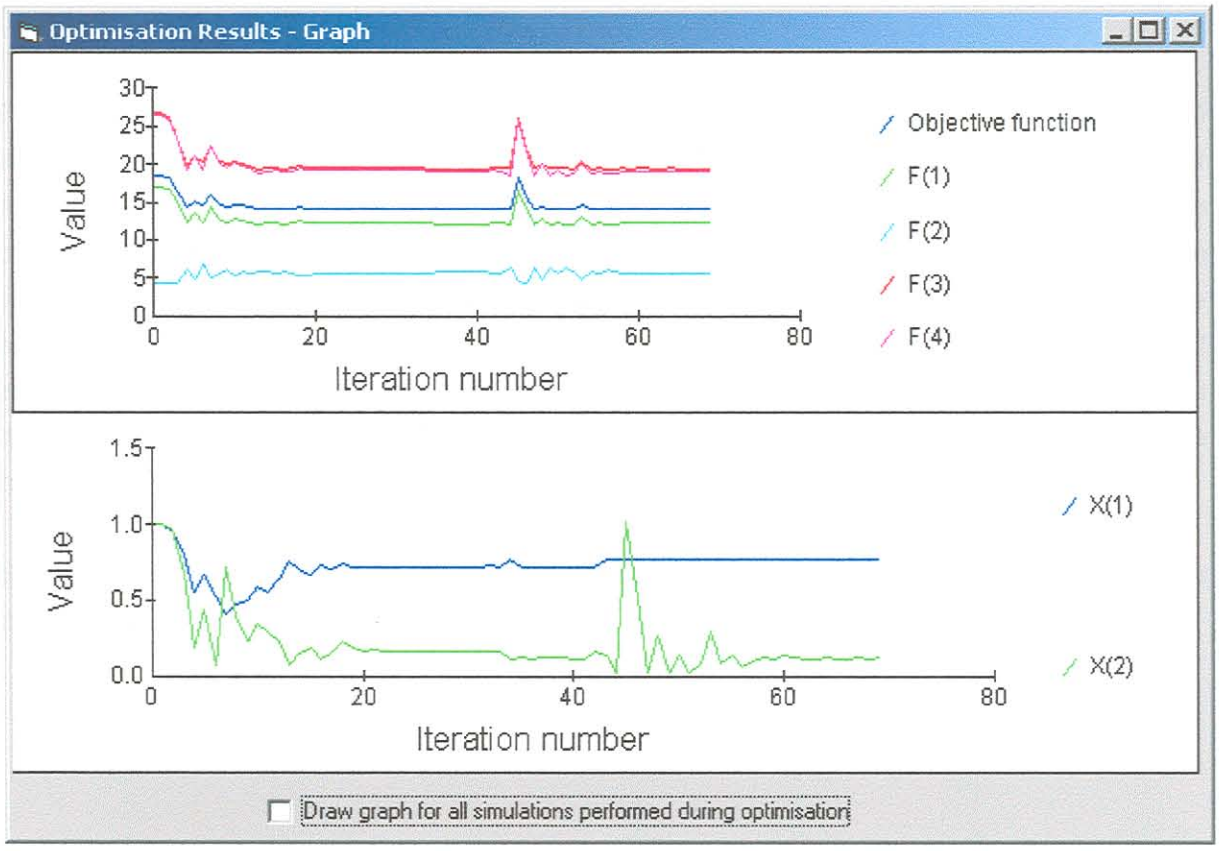

Figure 4.12: Convergence histories of objective function and design variables during optimisation

In figure 4.12 the objective function value and that for the individual objective criteria used are shown on the top graph. The bottom graph displays the values for design variables *X(1)* and *X(2)*. From the

convergence history, as shown in figure 4.12, the reduction in the objective function value from a starting value of 18.60 (for the baseline vehicle) to a minimum value of 14.07 (for the optimum configuration) can be seen. Thus a reduction of 24.4 % in the objective function value is obtained. The corresponding optimum design variable values obtained are $X(1)$ = 0.726 and $X(2)$ = 0.12. This means that the damper characteristic in the bump direction must be decreased to 0.726 of its baseline value and that in rebound to 0.12 of its baseline value to obtain the best ride comfort according to the specified objective function computed over the Belgian paving at 30 km/h.

At first glance it appears from the graphs shown in figure 4.12 that convergence has already been obtained at iteration number 22. Closer inspection of the design variables in this region, however, reveals that the value for $X(2)$ is slightly lower than the minimum constraint value of 0.12 and, because of the relative tight tolerances set, the algorithm continues to iterate. At approximately iteration number 45, phase 2 (see section A.5 of Appendix A) of the LFOPC algorithm is entered and a trajectory is initiated to a point on the nearest active constraint. Due to the flat gradient of the objective function in this region, big steps are initially taken for the design variable $X(2)$ but the algorithm recovers quickly and it finally converges to an optimum that exactly satisfies the constraints (see discussions in section 4.1.4 and 4.1.6).

For convergence to within the tolerances set a total number of 70 iteration steps, equivalent to, 210 simulations, were performed during the optimisation. On a Pentium III, 800 MHz personal computer the optimisation took 18 minutes. It can clearly be seen from figure 4.12, that an acceptable accurate optimum solution is already achieved during phase 1 after about 22 iterations (66 simulations), which requires only about 5.65 minutes computational time! Thus for this case looser tolerances could have been set. Allowance is also made for the user to interactively terminate the iteration process if effective convergence has obviously been reached. The tyre model used during the optimisation was the point follower model. Using the sector tyre model approximately doubles the simulation time required.

Selecting the "Optimise_vehicle.veh" file, the damper characteristic for the optimised damper is displayed as shown in figure 4.13.

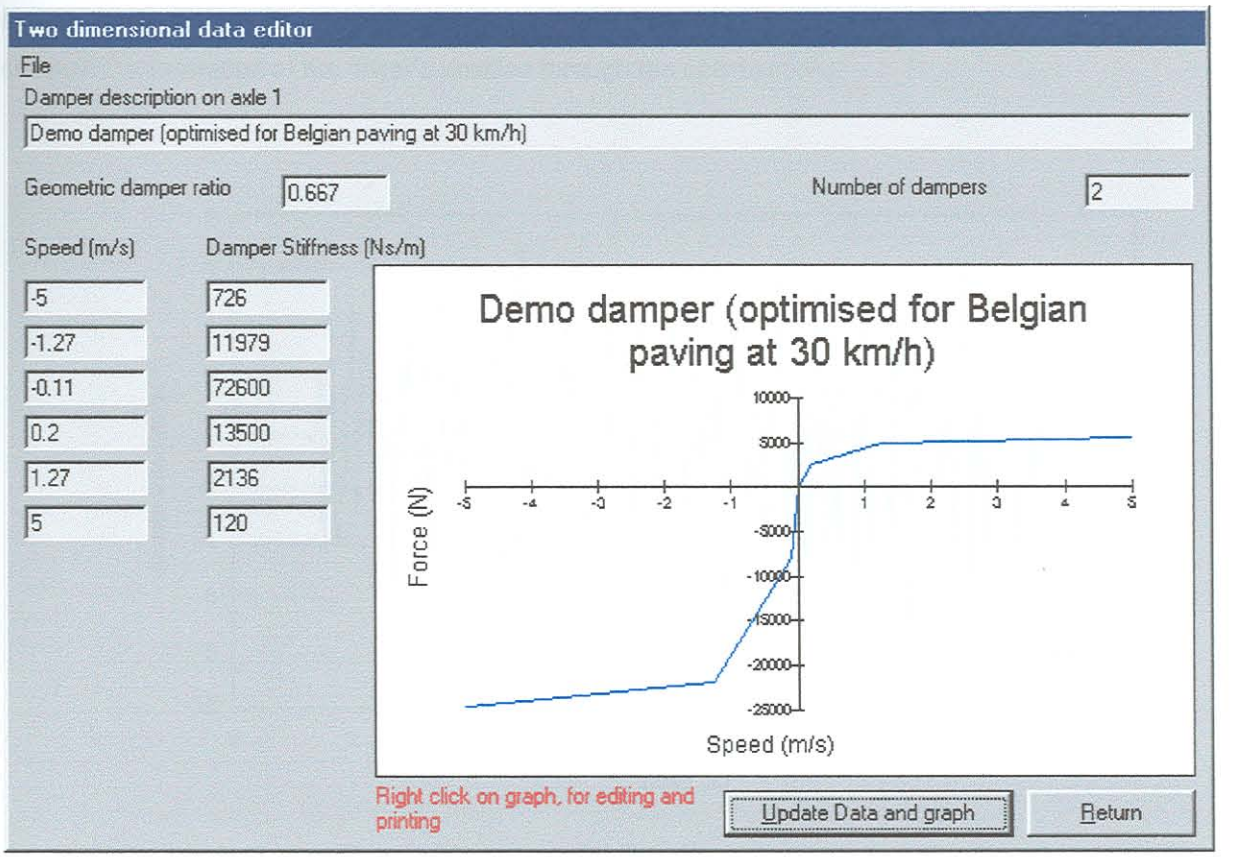

Figure 4.13: Optimised damper

Figure 4.14 shows a comparison between the baseline (see also figure 3.23) and optimum damper characteristics.

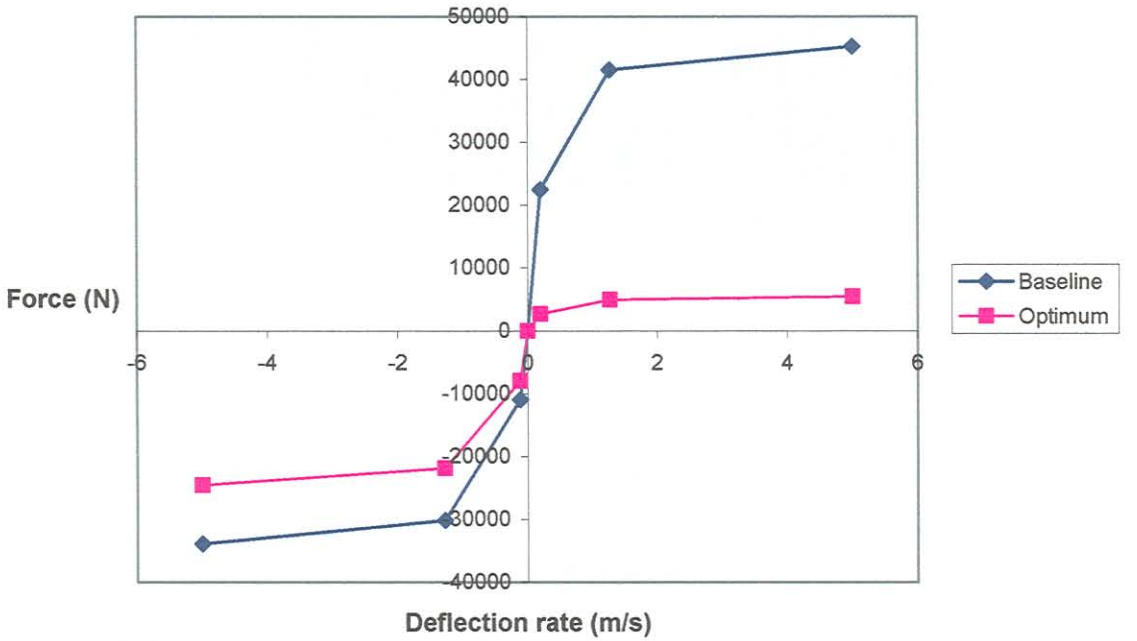

Figure 4.14: Comparison between baseline and optimised damper

Comparing figure 4.15(b) with 4.15(a) indicates the reduction obtained over the whole route, in the simulated acceleration at the driver's position through the optimisation.

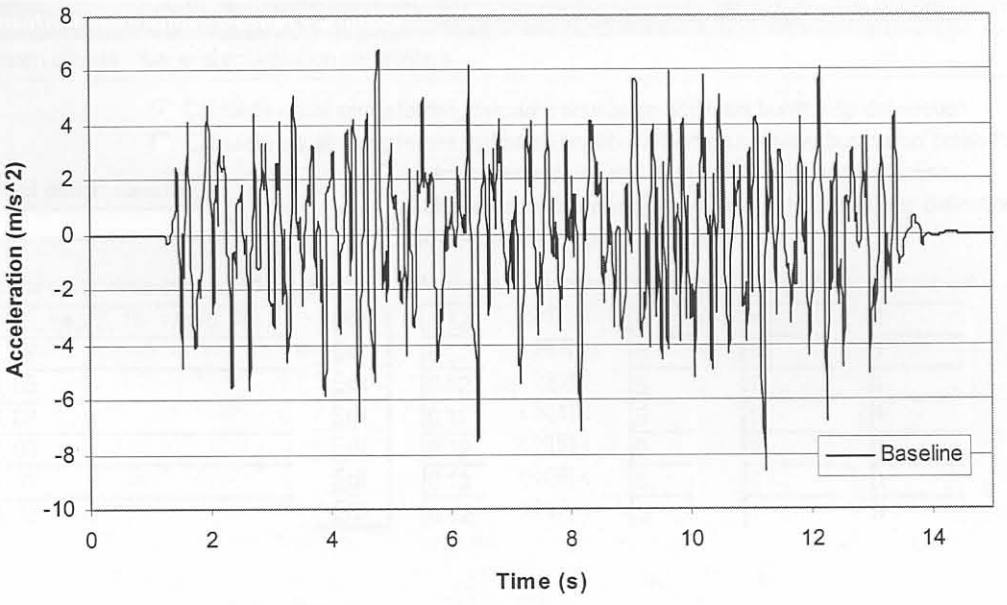

(a) Baseline

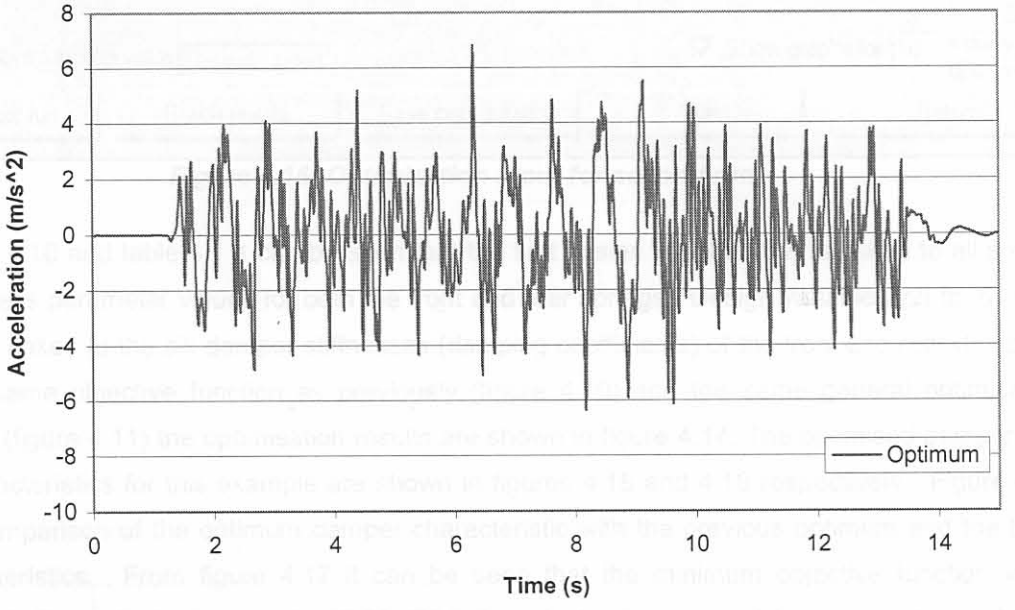

(b) Optimum

Figure 4.15: Comparison between simulated driver's position vertical acceleration for the baseline and the optimised damper

For the example described above only two design variables were used. To investigate if a further reduction in the objective function can be obtained, an optimisation was run with 7 design variables. The selection of the 7 design variables is shown in figure 4.16.

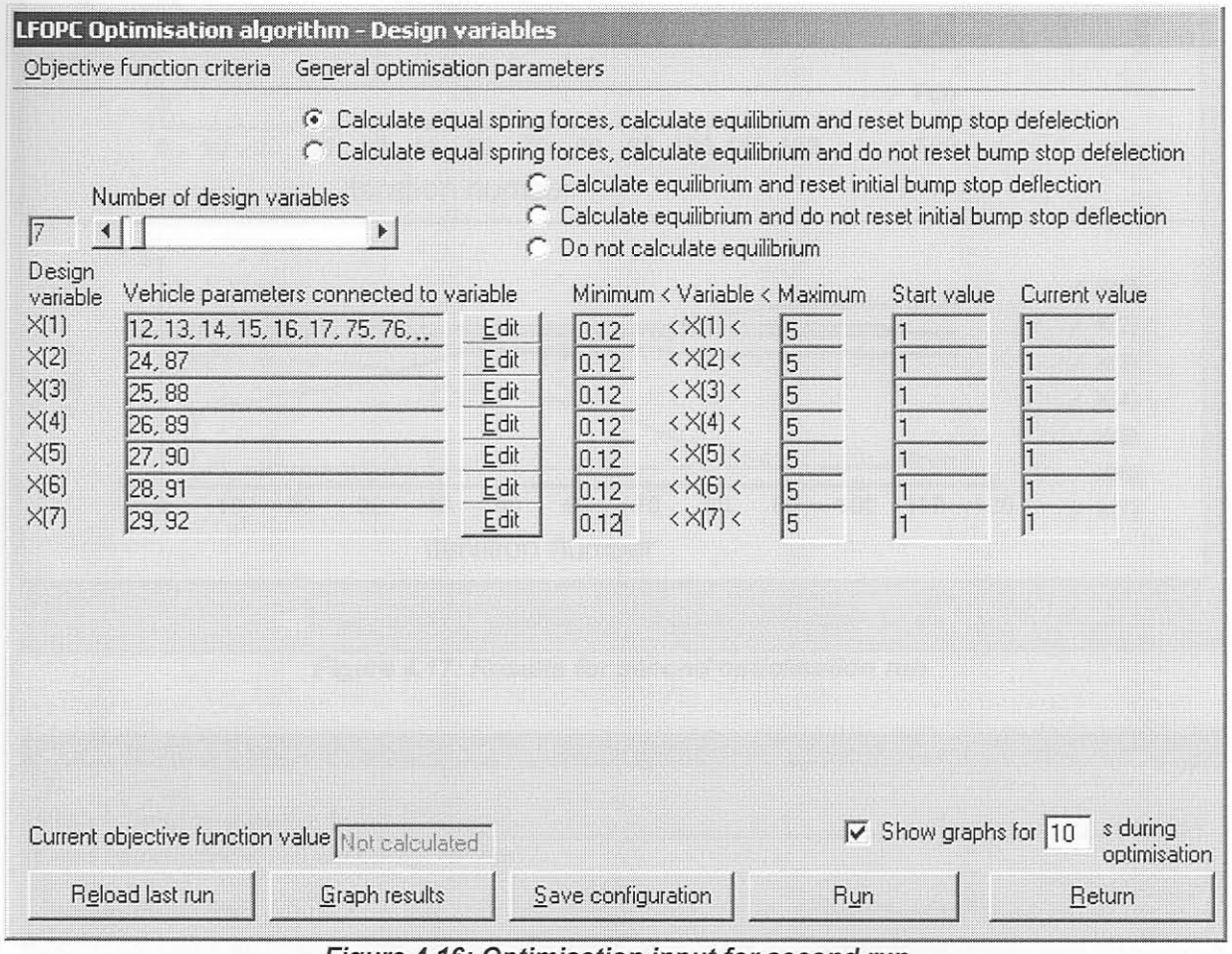

Figure 4.16: Optimisation input for second run

From figure 4.16 and table 4.1 it can be seen that the first design variable *X(1)* is linked to all six the spring stiffness parameter values for both the front and rear springs. Design variable *X(2)* to *X(7)* are respectively linked to the six damper stiffnesses (damping coefficients) of the front and rear dampers. Using the same objective function as previously (figure 4.10) and the same general optimisation parameters (figure 4.11) the optimisation results are shown in figure 4.17. The optimised damper and spring characteristics for this example are shown in figures 4.18 and 4.19 respectively. Figure 4.20 shows a comparison of the optimum damper characteristic with the previous optimum and the base line characteristics. From figure 4.17 it can be seen that the minimum objective function value obtained with this optimisation run is 13.85 (25.5 % reduction) compared to the baseline value of 18.60 and the previous optimum of 14.07 (24.4%) reduction. Thus in this case, increasing the number of variables results in only a marginal improvement in the optimum objective function value. The converged optimum values for *X(1)* to *X(7)*, as shown in figure 4.17, are respectively: 0.865, 0.995, 0.129, 1.179, 0.121, 0.121 and 1.00. From these values it is clear that the spring stiffness for the optimum configuration must be reduced to 86.5% of that for the baseline vehicle.

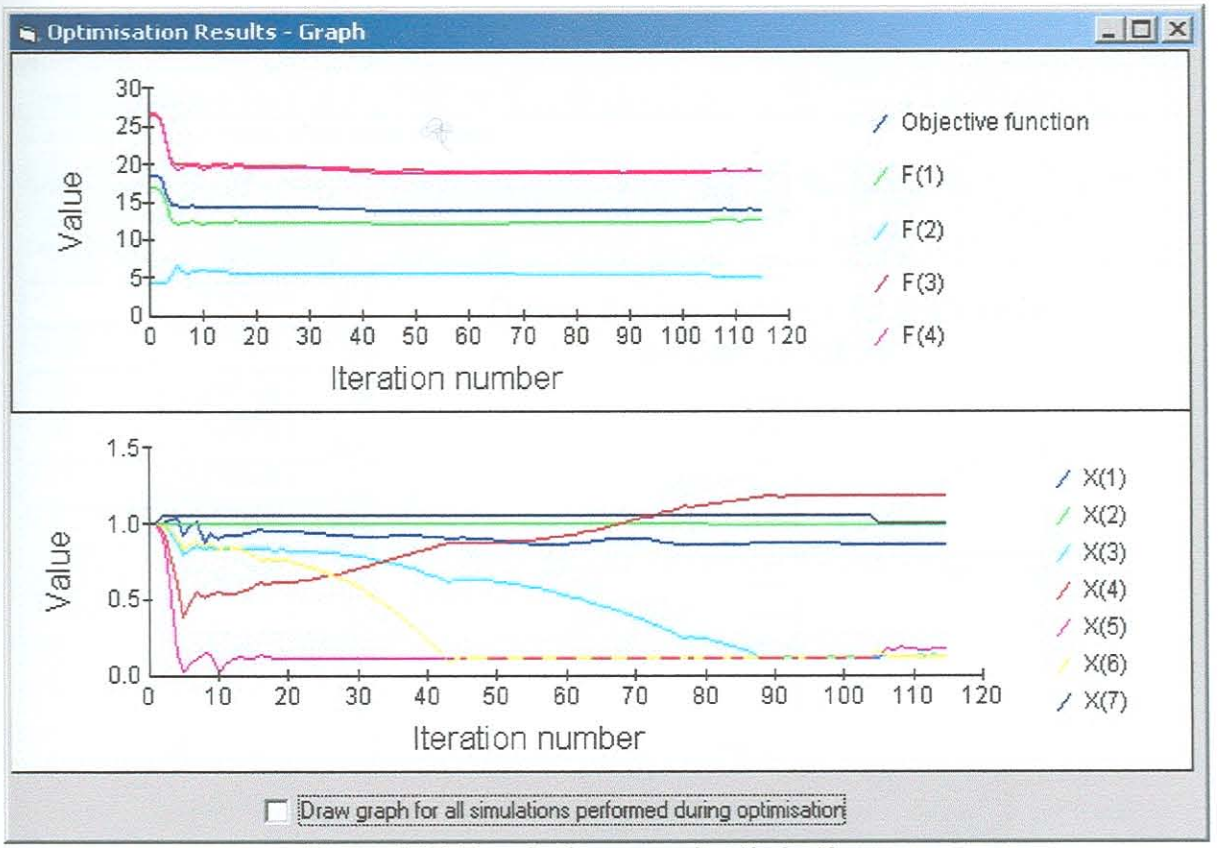

Figure 4.17: Results for second optimisation run

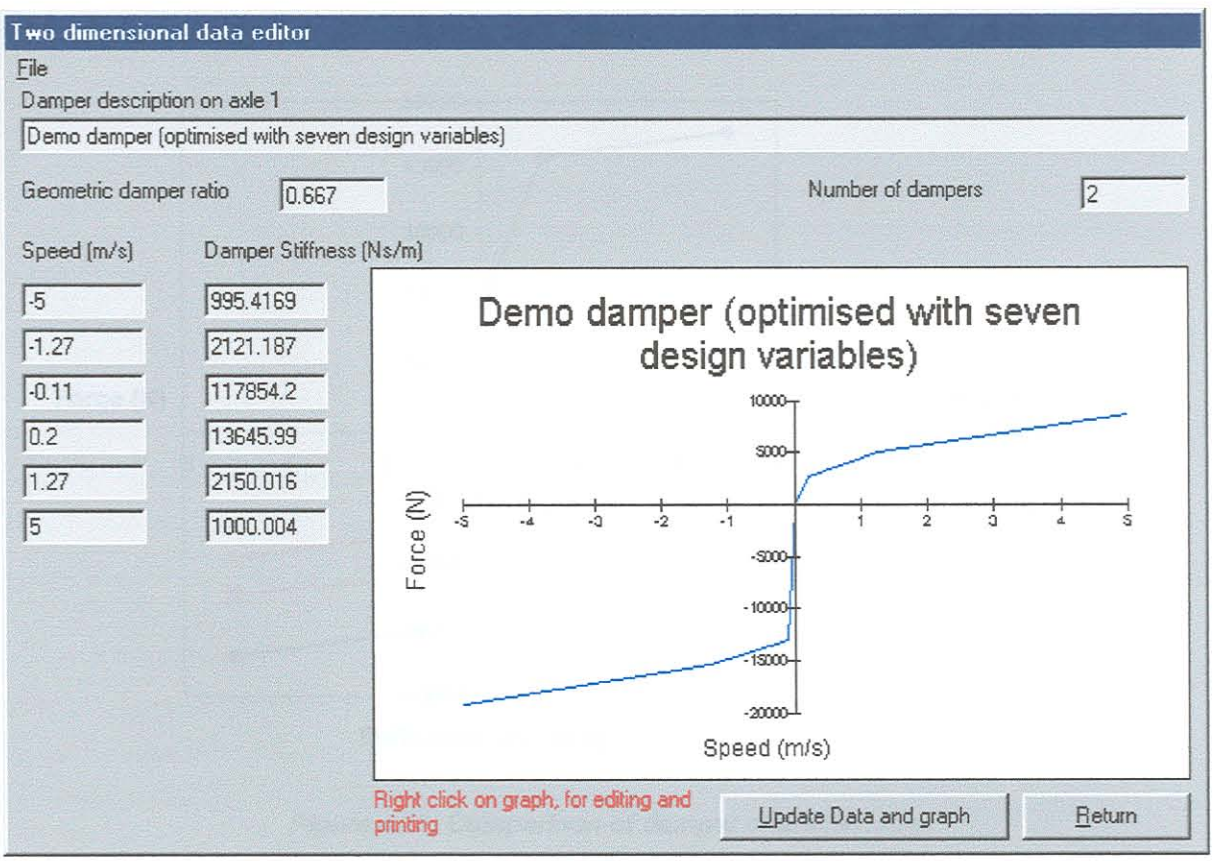

Figure 4.18: Optimised damper from second run

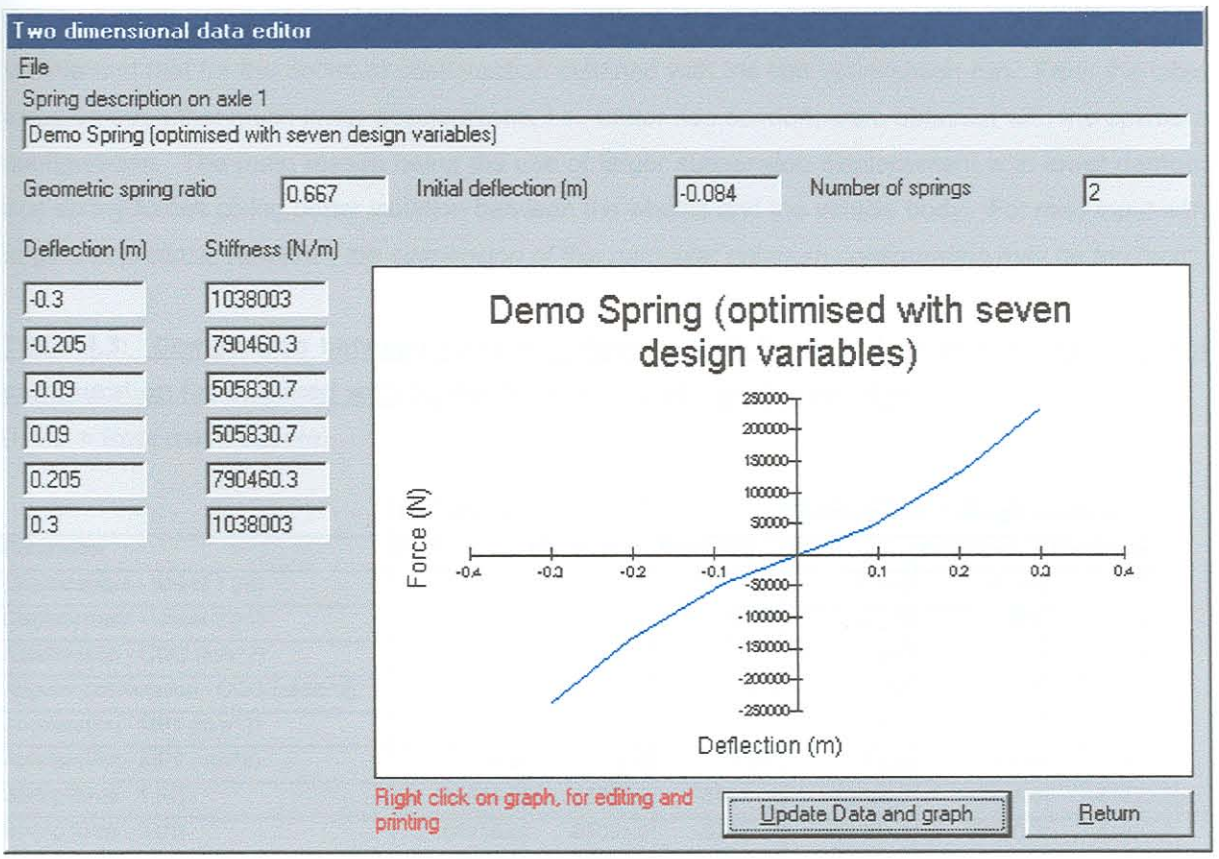

Figure 4.19: Optimised spring from second run

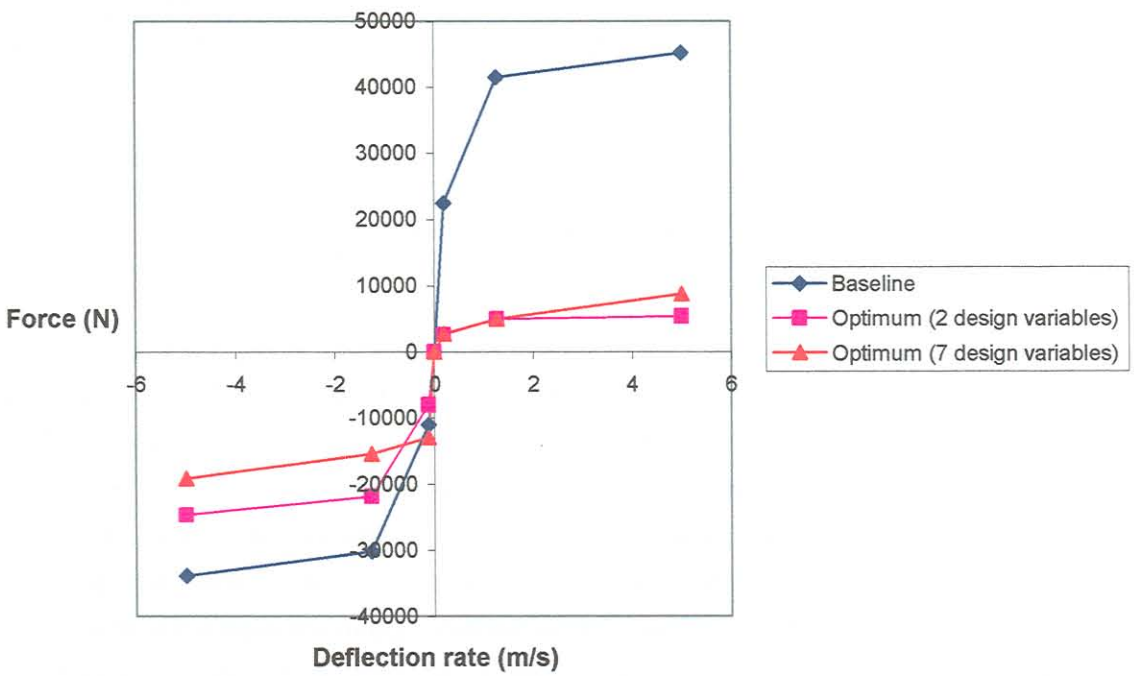

Figure 4.20: Comparison of damper characteristics

Table 4.3 shows a comparison for several objective criteria between the values for the baseline vehicle and that for the optimum configuration obtained with the last optimisation run. From the table it can be seen that much lower accelerations, i.e., better ride comfort, were obtained with the optimum configuration. The main reason being the use of larger suspension displacement with lower damper and spring forces giving better isolation between the wheels and the vehicle body. *For road input with larger fluctuations, however, the suspension of this particular optimum configuration may be too "soft".*

Table 4.3: Comparison between objective criteria values for base line vehicle and optimum configuration (as obtained with optimisation with seven design variables)

(RMS = Root mean square)

	Baseline vehicle			Optimum with 7 design variables		
Parameter	RMS	Minimum	Maximum	RMS	Minimum	Maximum
Displacement - wheel 1 (m)	0.016	-0.072	0.040	0.015	-0.066	0.039
Displacement - wheel 2 (m)	0.015	-0.072	0.040	0.015	-0.065	0.040
Acceleration - COG (m/s^2)	1.132	-4.507	2.874	0.800	-2.512	2.630
Angular acceleration - COG (rad/s^2)	0.755	-2.252	2.416	0.555	-1.914	1.705
Acceleration - MP1 (m/s^2)	1.854	-7.574	5.771	1.370	-4.628	4.474
Acceleration - MP2 (m/s^2)	1.858	-6.939	5.841	1.320	-4.149	4.141
Spring force - 1 (N)	66875.0	-86019.6	-50941.1	62026.3	-78845.9	-41430.0
Spring force - 2 (N)	66716.0	-85001.0	-52583.7	61854.1	-77760.3	-41637.9
Damper force - 1 (N)	10670.7	-22931.0	37783.2	7837.2	-19183.9	5072.5
Damper force - 2 (N)	10511.5	-24280.8	37377.7	7806.2	-19115.6	4932.4
Bump stop force - 1 (N)	0.000	0.000	0.000	0.000	0.000	0.000
Bump stop force - 2 (N)	0.000	0.000	0.000	0.000	0.000	0.000
Suspension deflection - 1 (m)	0.008	-0.029	0.028	0.015	-0.019	0.050
Suspension deflection - 2 (m)	0.008	-0.027	0.025	0.014	-0.018	0.049
Suspension deflection rate - 1 (m/s)	0.146	-0.727	0.790	0.215	-1.166	1.048
Suspension deflection rate - 2 (m/s)	0.142	-0.819	0.765	0.207	-1.130	0.975
Tyre deflection - 1 (m)	0.060	-0.085	-0.018	0.060	-0.087	-0.038
Tyre deflection - 2 (m)	0.060	-0.087	-0.018	0.060	-0.088	-0.036
Wheel force - 1 (N)	70493.2	-104290.4	-24405.2	70055.0	-94395.9	-46850.4
Wheel force - 2 (N)	70320.7	-101295.6	-23763.1	69883.6	-93166.1	-47088.5

For full convergence to the strict convergence tolerances set, the optimisation with the seven design variables required 115 iterations corresponding to 920 simulation runs (compared to the previous 210). The computational time was 79 minutes (compared to 18 minutes previously) on the same computer. For this particular example the use of more than the two design variables to optimise the suspension is probably not justified. This conclusion is, however, not generally true. One reason for the small improvement obtained in this case for the complete damper optimisation, is that the range of damper speeds of the base line design obtained on the specific road input, was already relatively low as can be seen from figure 4.21. It is again apparent from figure 4.17 that, if looser tolerances are set for convergence, an effective optimum objective function value may be achieved in a quarter of the time required for full convergence. Of course the user may interactively, by inspection of the displayed convergence graphs, terminate the optimisation process at any point if sufficient reduction in objective function has been achieved.

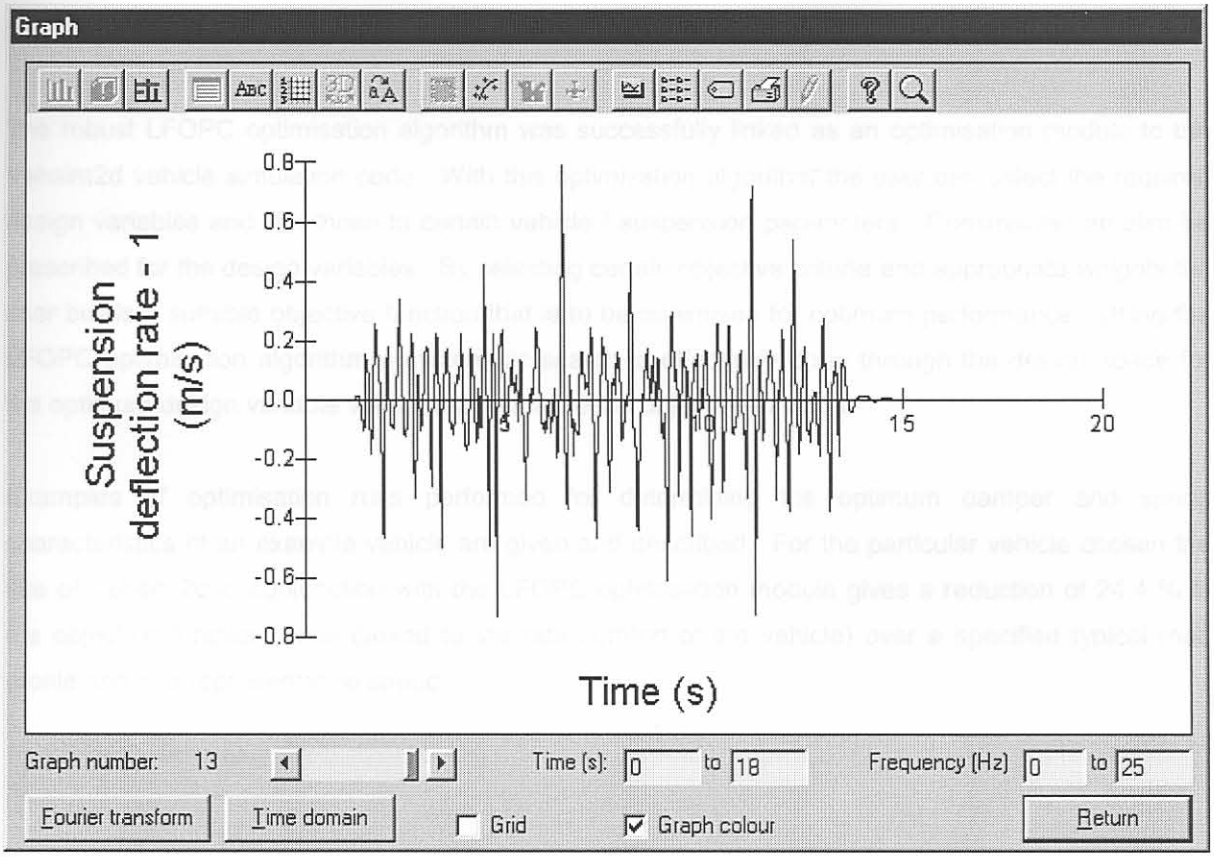

Figure 4.21: Damper speeds obtained (for the base line damper) during the simulation

4.3 Summary

The robust LFOPC optimisation algorithm was successfully linked as an optimisation module to the Vehsim2d vehicle simulation code. With this optimisation algorithm the user can select the required design variables and link these to certain vehicle / suspension parameters. Constraints can also be prescribed for the design variables. By selecting certain objective criteria and appropriate weights the user builds a suitable objective function that is to be minimised for optimum performance. Using the LFOPC optimisation algorithm a systematic search is effectively done through the design space for the optimum design variable values that minimise the objective function.

Examples of optimisation runs performed for determining the optimum damper and spring characteristics of an example vehicle are given and described. For the particular vehicle chosen the use of Vehsim2d in conjunction with the LFOPC optimisation module gives a reduction of 24.4 % in the objective function value (linked to the ride comfort of the vehicle) over a specified typical road profile and at a representative speed.

CHAPTER 5:

CASE STUDY

5. Case study

The problems experienced on the suspension of the Okapi vehicle (see figures 1.1 and 5.1) were described in section 1.1. This vehicle had gone through a series of design changes to improve mobility, fatigue life of the axles, and other general features of the vehicle [1, 2, 63, 64]. In spite of these improvements certain suspension failures remained and it was decided to perform a suspension optimisation on the vehicle using the simulation program Vehsim2d coupled to the LFOPC optimisation module.

Figure 5.1: Okapi vehicle as used in this case study

5.1 Introduction

The purpose of this case study is to **find the optimum damper characteristic for the Okapi vehicle** using the suspension optimisation system developed in chapters 3 and 4. Section 5.2 describes the Okapi vehicle model developed for use in this case study. Section 5.3 describes the route profiles used and in section 5.4 the implementation of the optimisation process and the results obtained from the optimisation are presented. In section 5.5 suggestions arising from the optimisation study are made regarding specific damper characteristics.

5.2 Vehicle model

The vehicle model for the Okapi was based on data received from Reumech Ermetek [63] and Vickers OMC [64].

5.2.1 Vehicle geometry

Figure 5.2 shows the vehicle geometry, mass and inertia characteristics prescribed.

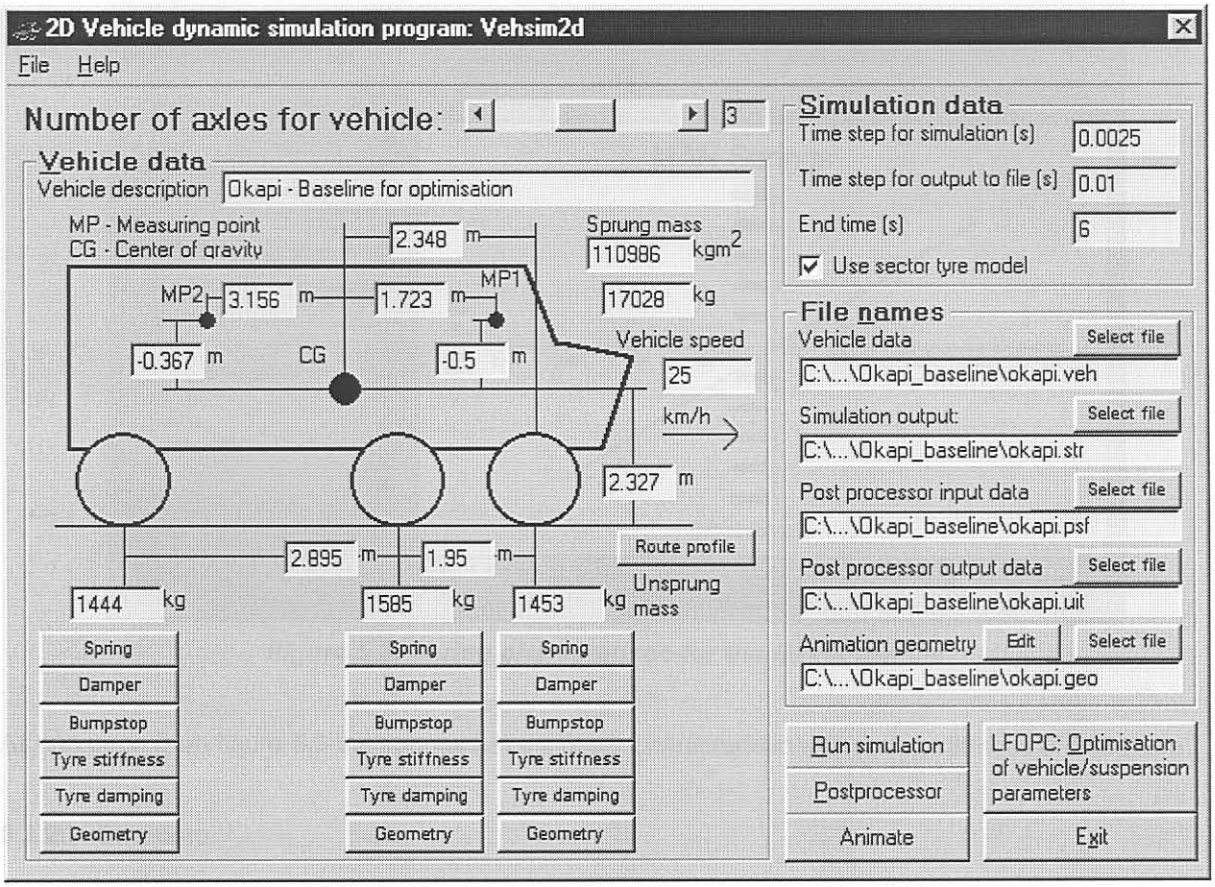

Figure 5.2: Simulation input for the Okapi vehicle

5.2.2 Suspension characteristics

The suspension characteristics are prescribed using a six piece-wise continuous linear approximation (see section 2.1 and figure 2.4 for more details).

5.2.2.1 Spring

Figure 5.3 shows the characteristic for the springs used on the Okapi vehicle. During the latest upgrade of the vehicle parabolic leaf springs, used by the truck manufacturer MAN on their new generation trucks, were fitted because they give minimum interleaf friction. This results in improved ride comfort and is an upgrade to the latest technology [64].

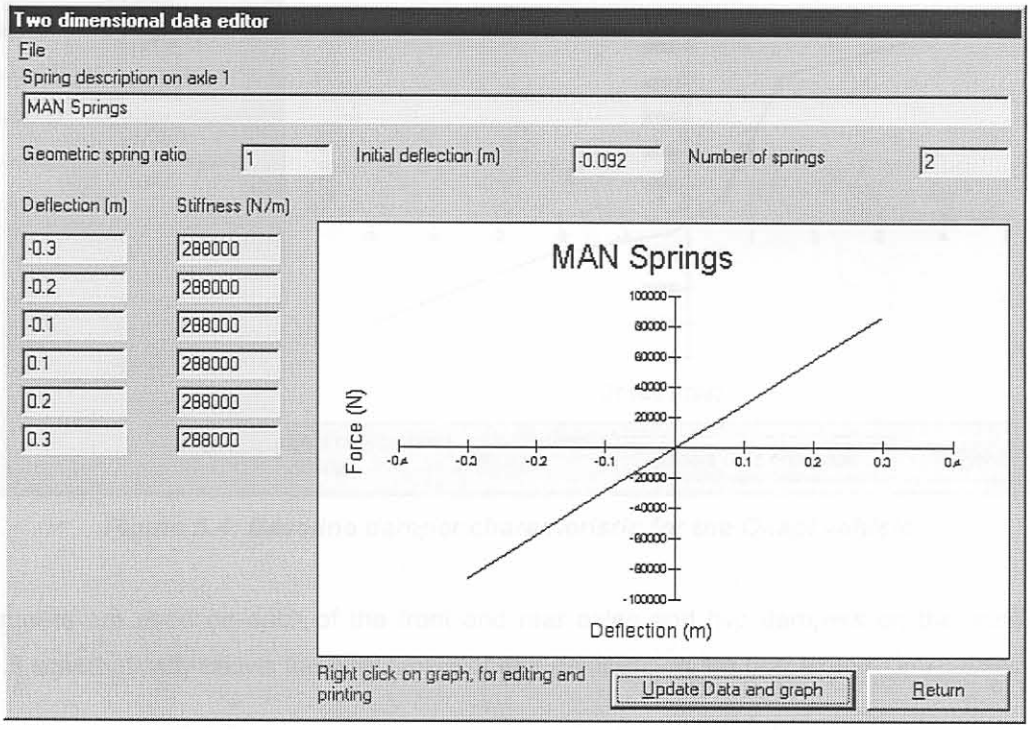

Figure 5.3: Spring characteristic for the Okapi vehicle

As can seen from figure 5.3 the springs have a linear characteristic with spring stiffness of 288 kN/m.

5.2.2.2 Dampers

The characteristics for the dampers were retrieved from the DADS model dated 24 July 1999 [63], and are shown in figure 5.4. The data for the dampers as used in the DADS model [63] were experimentally determined by testing the actual dampers as fitted on the Okapi [64]. A typical damper is referred to as Damper_new in figure 5.4 due to the fact that it is representative of the new dampers fitted to the vehicle during the 1999 upgrade project [64].

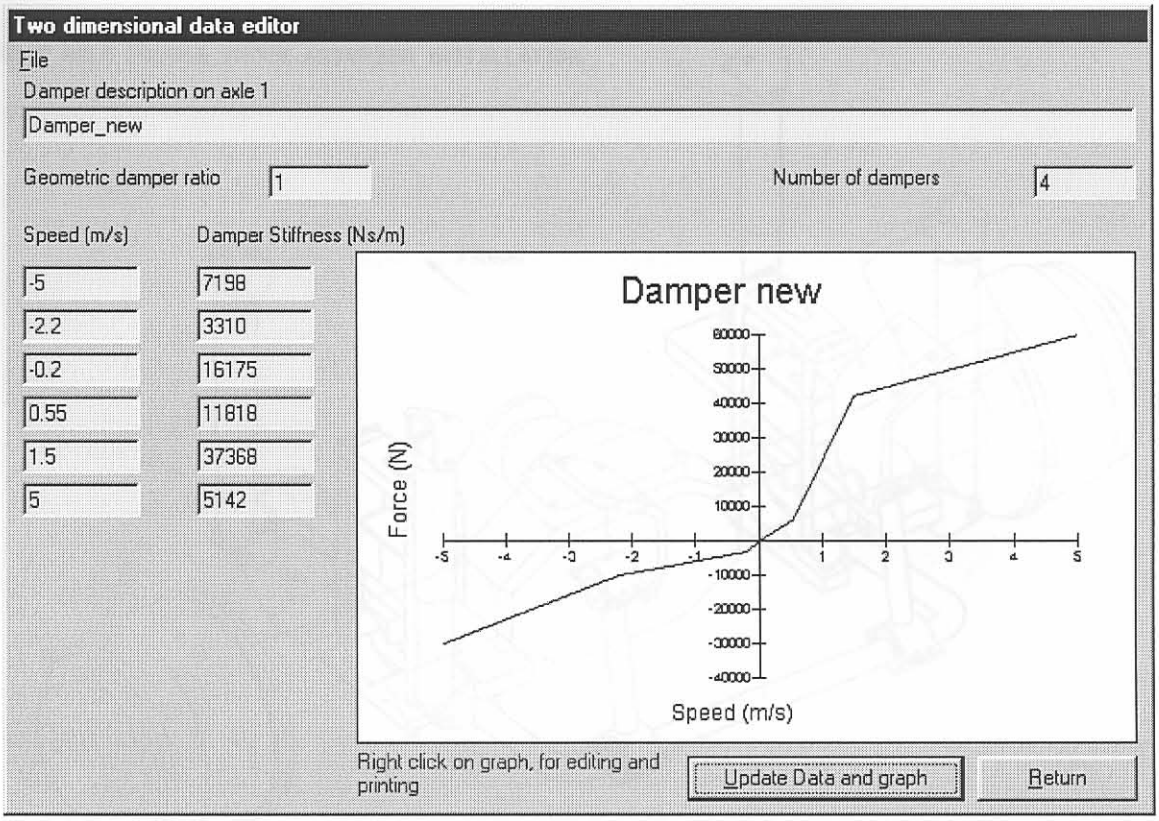

Figure 5.4: Baseline damper characteristic for the Okapi vehicle

Four dampers are used on each of the front and rear axles and two dampers on the middle axle. Figure 5.5 schematically shows the attachment of four dampers on the rear axle.

Figure 5.6 compares the damper characteristic of the damper shown in figure 5.4 (Damper_new, now referred to as that of Vehsim2d) with that actually measured for two other similarly sized dampers, namely the Samil and Gabriel dampers. As can be seen from figure 5.6 the damper characteristic used for the damper of the Okapi vehicle (Vehsim2d) is similar to that obtained experimentally for the Samil damper, except in the high rebound deflections region where the damping force are smaller than that for the Samil damper. Uncertainties, however, exist in the measurements of the high rebound damping forces for the Samil and Gabriel dampers.

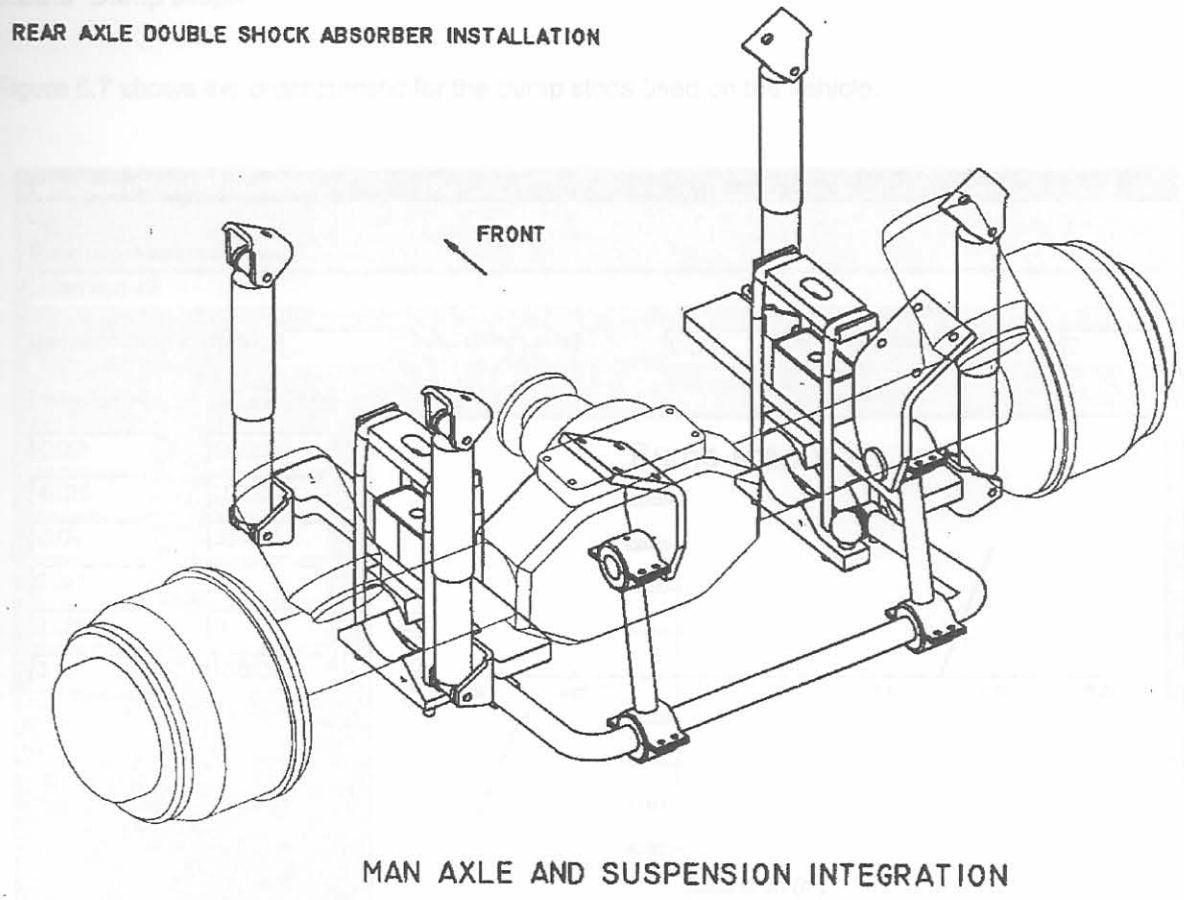

Figure 5.5: Drawing of the Okapi rear suspension showing the use of four dampers

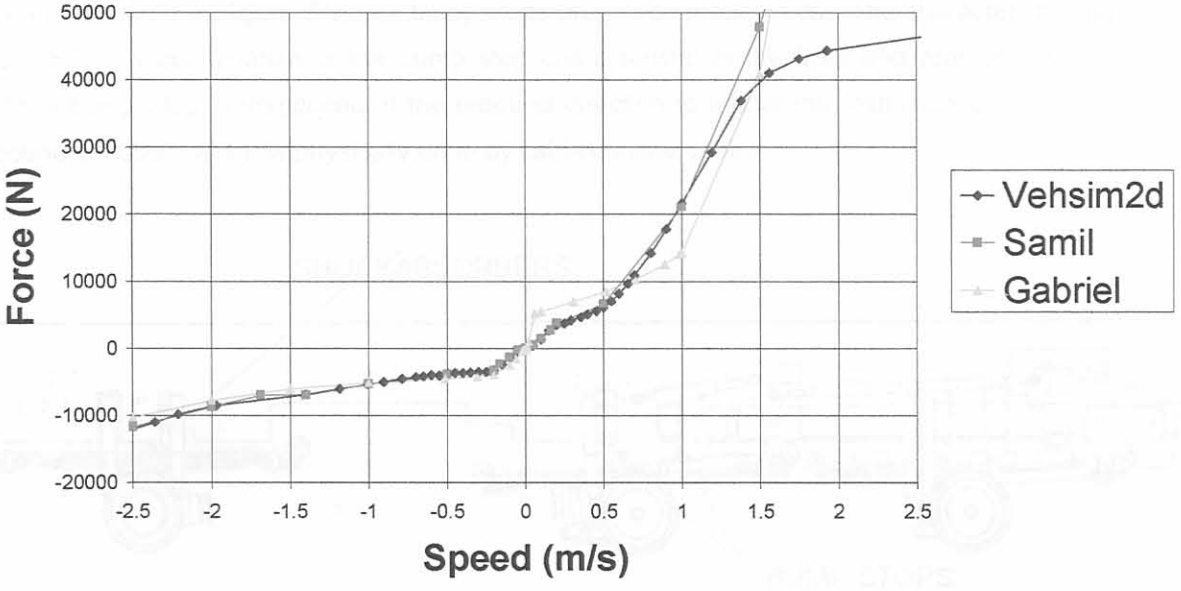

Figure 5.6: Comparison of damper characteristics for the Okapi vehicle (Vehsim2d) compared to similar dampers (Samil and Gabriel)

5.2.2.3 Bump stops

Figure 5.7 shows the characteristic for the bump stops used on the vehicle.

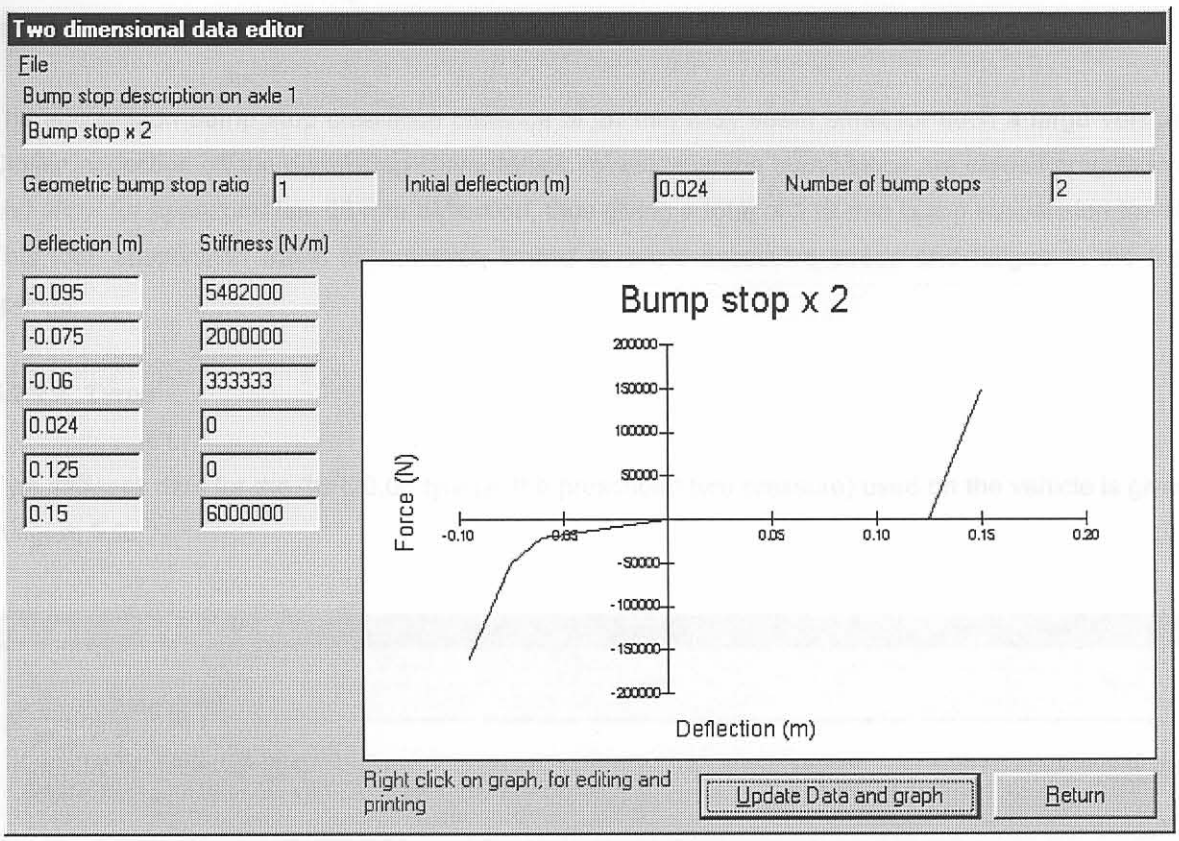

Figure 5.7: Bump stop characteristic for the Okapi vehicle

As can be seen from figure 5.8, four bump stops are used on each axle. The characteristic shown in figure 5.7 is a combination of the bump stop characteristic at the front and rear of the axle. An artificial bump stop is introduced in the rebound direction to model the restriction of the axle in the rebound direction, which is physically done by cables on the vehicle.

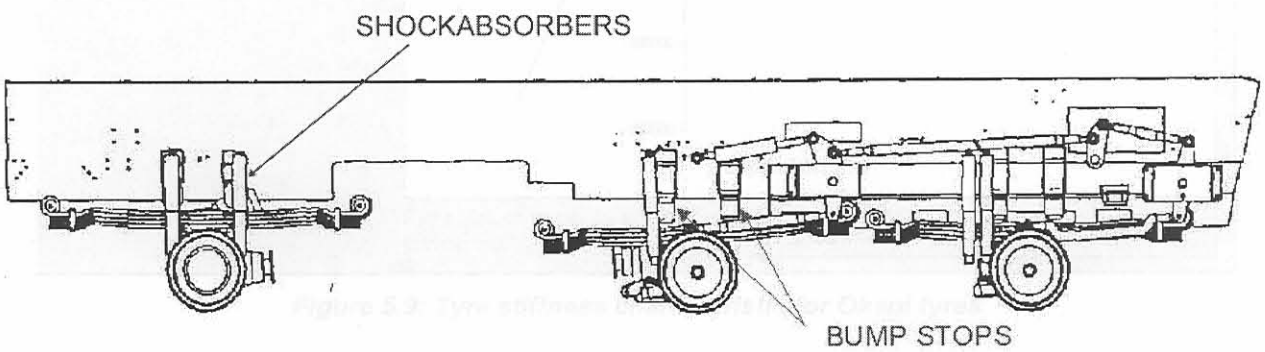

Figure 5.8: Bump stops used on the Okapi vehicle

The bump stops used are placed in such a manner that a suspension travel in the bump direction of 24 mm is available before the leaf spring makes contact with the bump stops. From figure 5.7 it can be seen that this suspension travel is taken into consideration by prescribing an initial deflection of 0.024 m. From this initial point 101 mm travel is allowed in the rebound direction before the cables limit the rebound travel of the suspension.

The suspension bump stop clearance distance of 24 mm may seem small for such a large vehicle. Closer inspection off the bump stop characteristic reveals that the bump stops are indeed progressive and allow for approximately 95 mm deflection, thus giving a total of 119 mm bump suspension travel. This total suspension travel is, however, limited to avoid excessive stress and fatigue in the leaf springs.

5.2.2.4 Tyres

Tyre stiffness data for the 16R20.00 tyre (at the prescribed tyre pressure) used on the vehicle is given in figure 5.9.

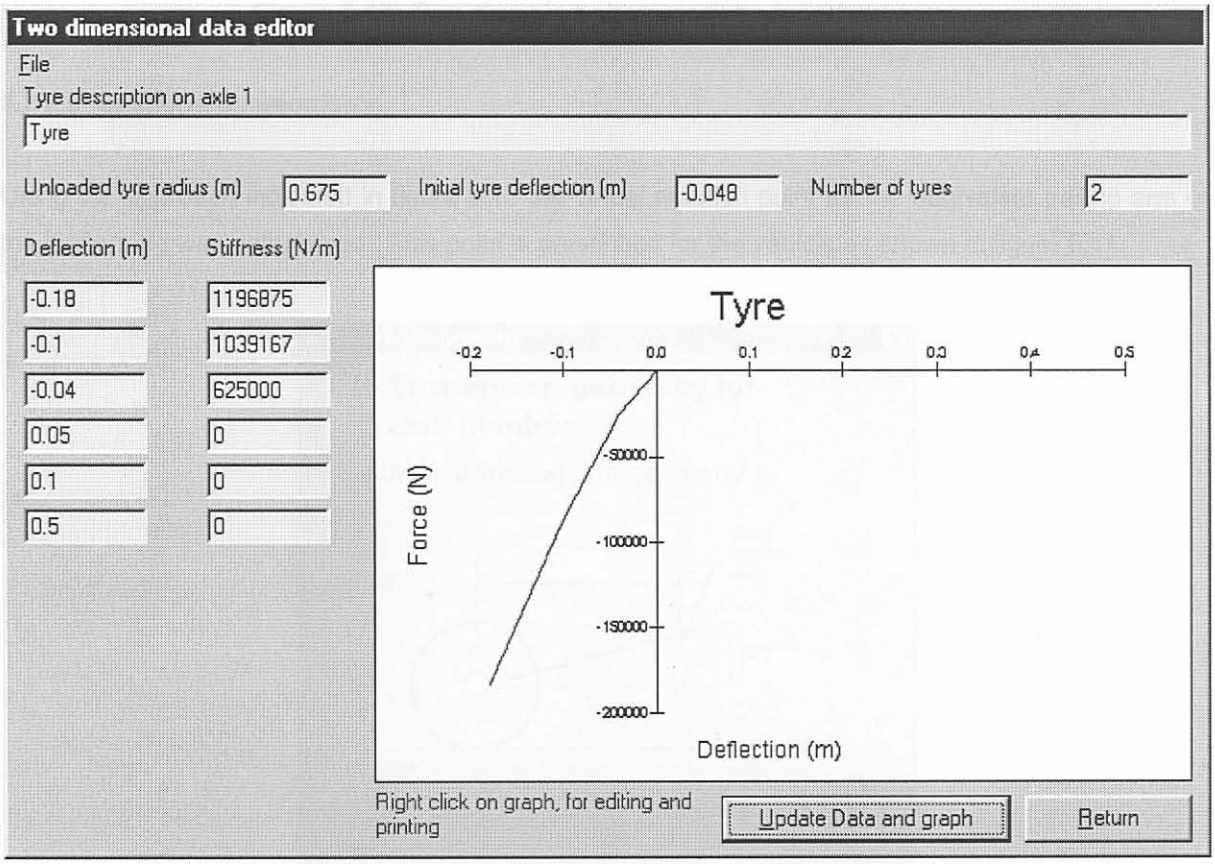

Figure 5.9: Tyre stiffness characteristic for Okapi tyres

The damping characteristic of the tyre is given in figure 5.10

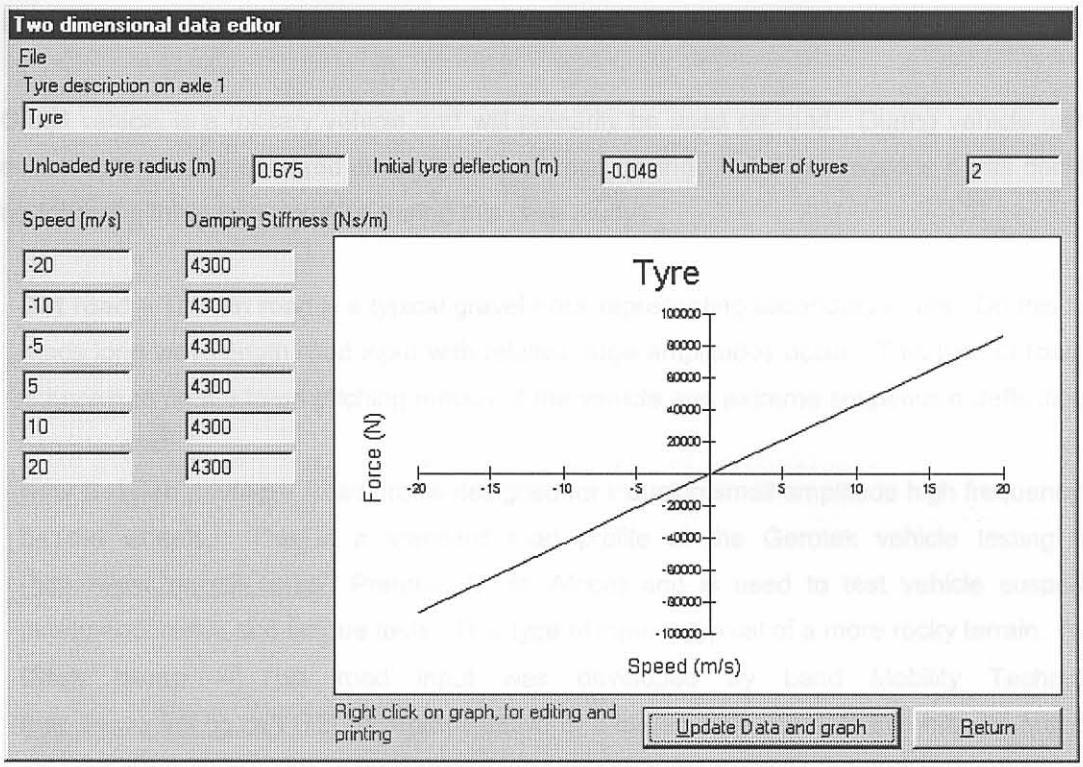

Figure 5.10: Tyre damping characteristic for Okapi tyres

5.2.2.5 Suspension geometry

Using the approach indicated in figure 3.13 the virtual reaction point for the equivalent trailing arm of the leaf spring was determined. This point is prescribed for the vehicle as shown in figure 5.11.

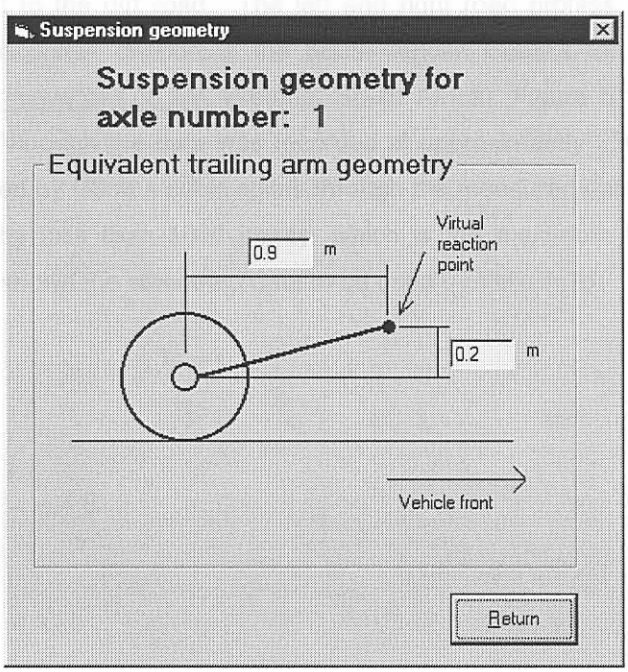

Figure 5.11: Virtual reaction point for Okapi vehicle

5.3 Route profiles

The Okapi vehicle is a military vehicle and will primarily be used off-road. During vehicle tests the suspension failures also occurred during typical off-road driving. For these reasons it was decided to use the following three route profiles during this case study:

* **Dirt road** – The dirt road is a typical gravel track representing secondary roads. On this type of roads long wavelength road input with relative large amplitudes occur. This type of road input is known to create large pitching motion of the vehicle and extreme suspension deflections are experienced.
* **New Belgian paving –** Road profile designed for inducing small amplitude high frequency input on the wheels. This is a standard road profile at the Gerotek vehicle testing facility (http://www.gerotek.co.za/, Pretoria, South Africa) and is used to test vehicle suspensions during endurance and fatigue tests. This type of input is typical of a more rocky terrain.
* **Ditch bump –** This road input was developed by Land Mobility Technologies (http://www.lmt.co.za/) [72] as representative of a large single obstacle that may be met during off-road movement. This is representative of crossing, for example, a fallen tree during off-road movement.

5.3.1 Dirt road

The dirt road data used here were obtained as the mean of the left and right profiles of the gravel track at Gerotek. The data is for a 2.2 km section of the road in an anti clockwise direction starting from the workshop next to the dirt road. The left and right road profiles were measured using a profilometer of the Transportek division of the South African Council for Scientific and Industrial Research (CSIR), (http://www.csir.co.za/, Pretoria, South Africa). Figure 5.12 shows the measured data for the dirt road. Although the data was recorded at approximately 250 mm intervals, the data used here were smoothed by fitting a cubic spline through the measured data to enable the 2.2 km of data to be prescribed by less than 1000 points, which is the maximum that can be handled by Vehsim2d. Figure 5.13 shows the smoothed data to be used by Vehsim2d.

Figure 5.12: Dirt road profile as measured with profilometer

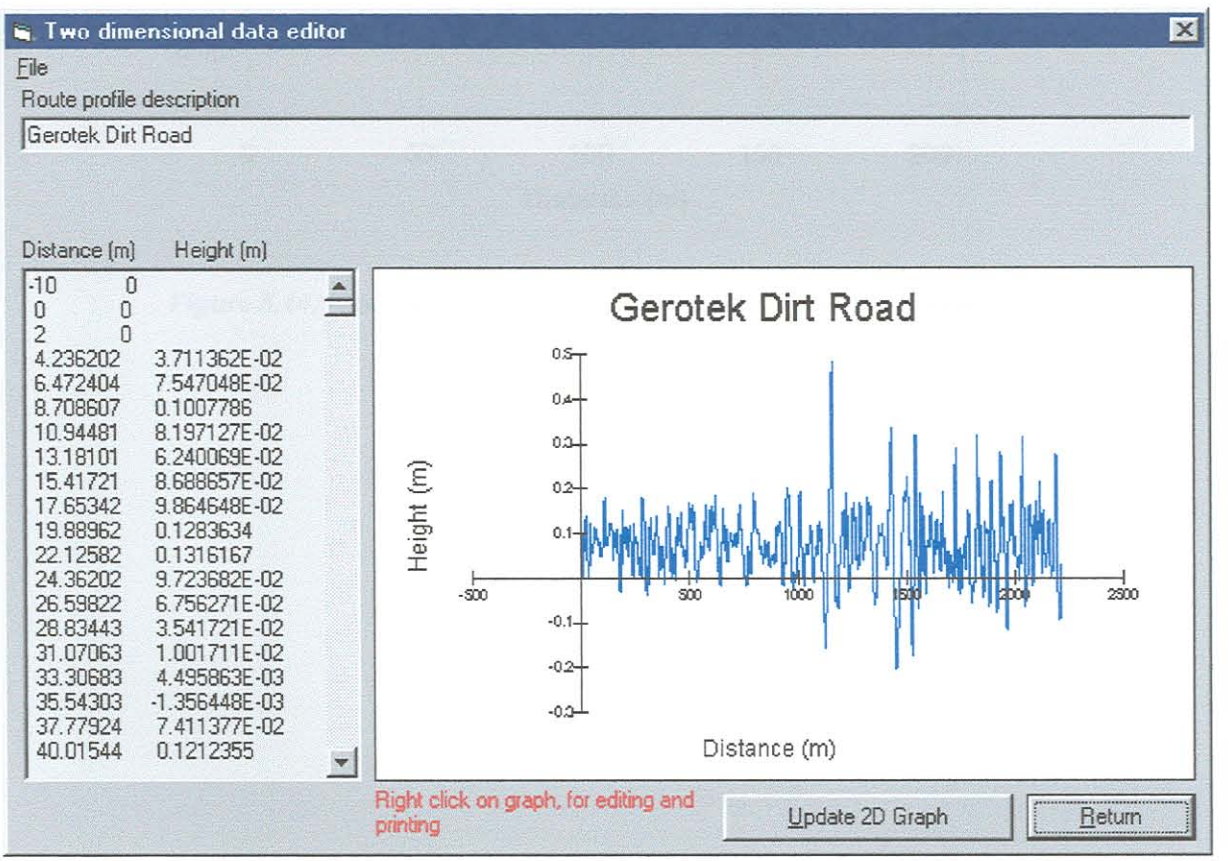

Figure 5.13: Dirt road profile as prescribed for Vehsim2d

5.3.2 New Belgian paving

Data for the new Belgian paving were also obtained using the CSIR profilometer. The data used in the simulation were obtained by combining the east to west data with west to east data as measured on the new Belgian paving to obtain approximately 200 m of route profile. Figure 5.14 shows the measured data and figure 5.15 the data prescribed for Vehsim2d.

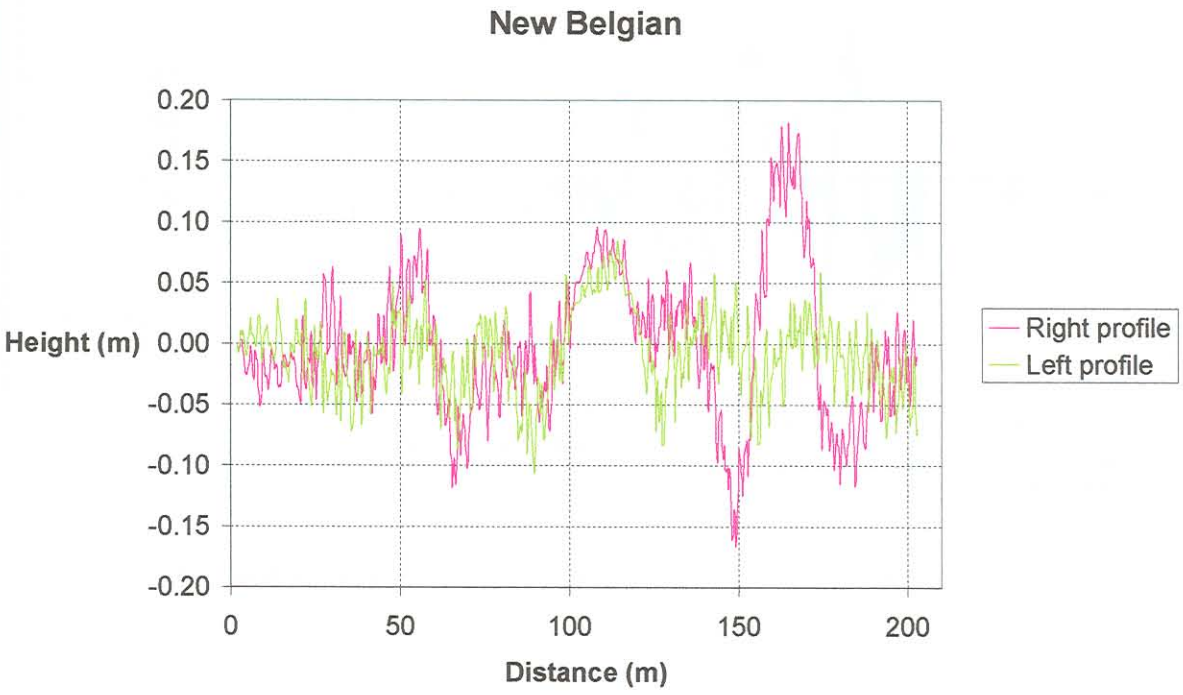

Figure 5.14: New Belgian road profile as measured with profilometer

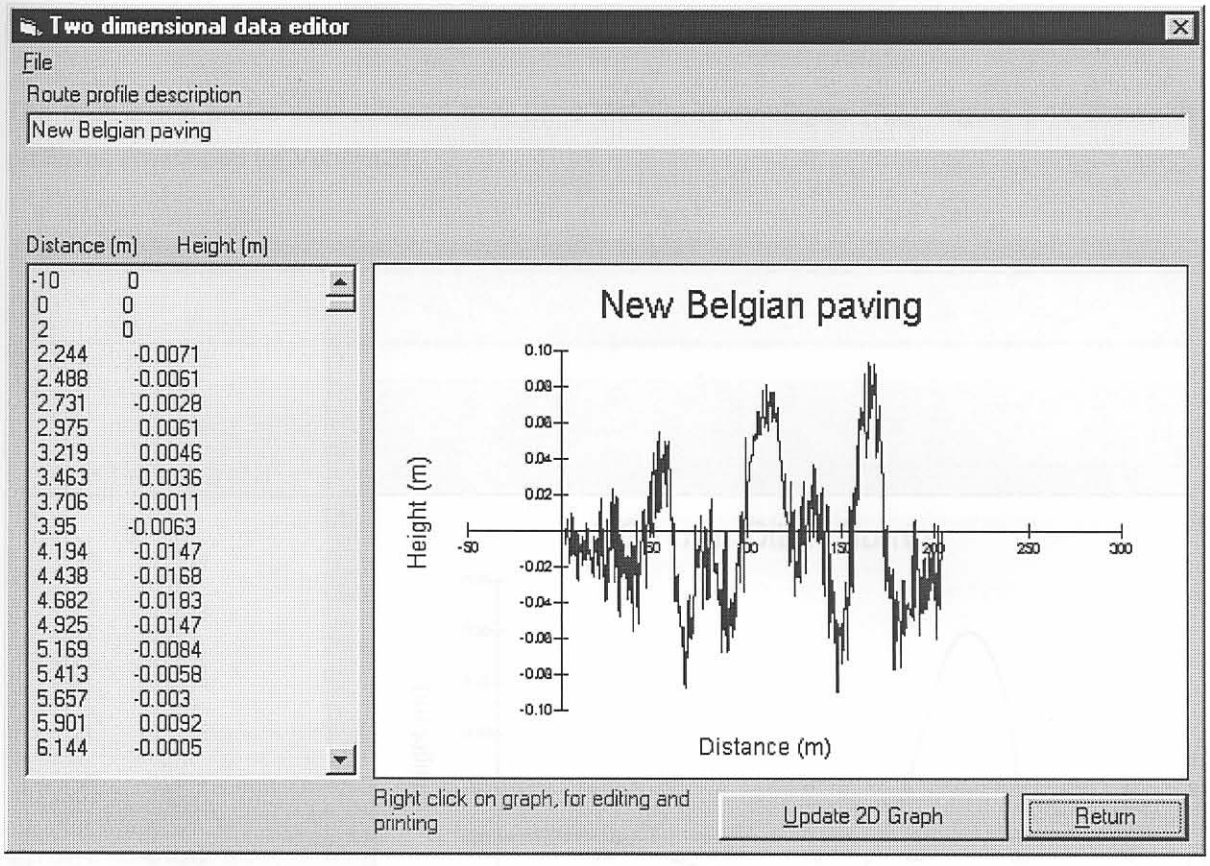

Figure 5.15: New Belgian road profile as prescribed for Vehsim2d

5.3.3 Ditch bump

The ditch bump profile was obtained from Land Mobility Technologies [72]. Figure 5.16 shows the profile as prescribed for Vehsim2d.

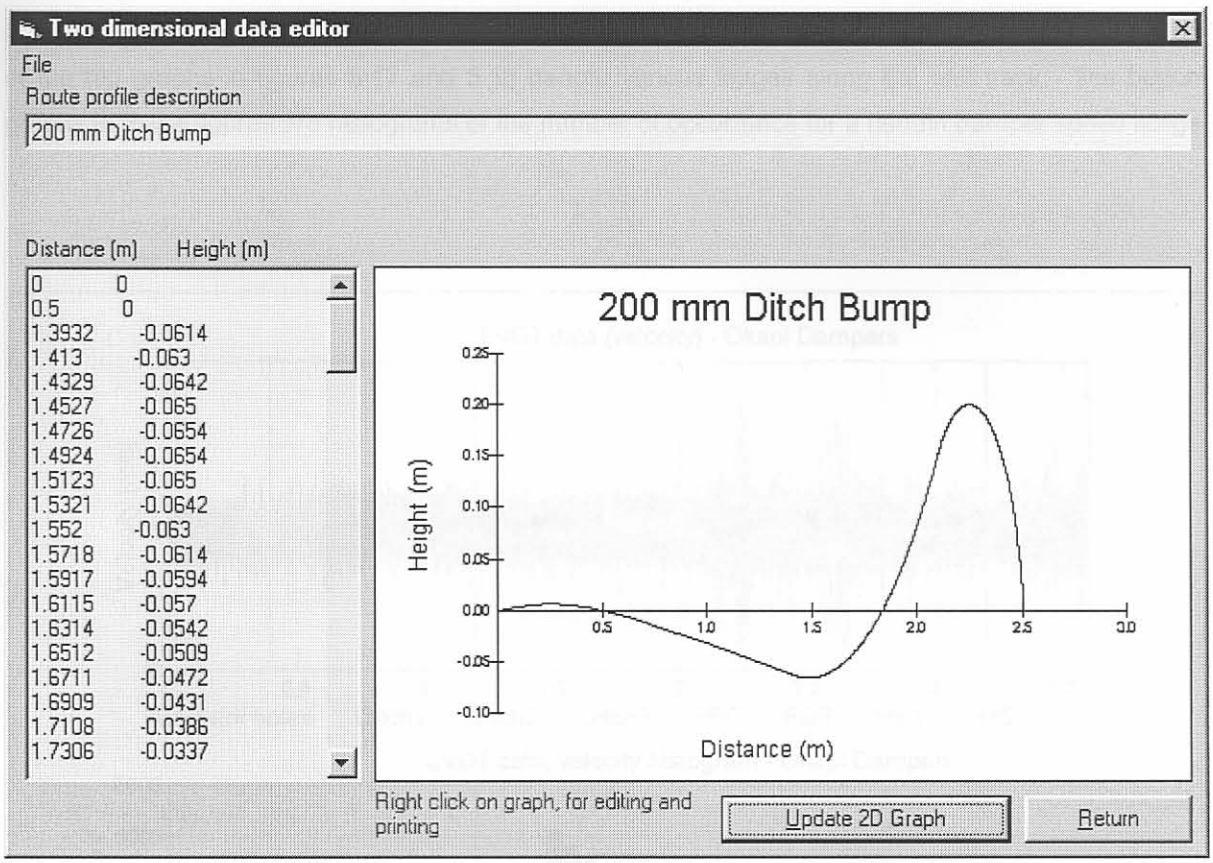

Figure 5.16: Ditch bump road profile as prescribed for Vehsim2d

5.4 Optimisation input

Inspection of the experimental data, in figures 5.17 and 5.18, for the Okapi vehicle driven over a certain test track, shows that damper deflection rates obtained were typically below 1.5 m/s. Figure 5.17 shows test data for the Okapi vehicle fitted with Okapi (Gabriel as shown in figure 5.6) dampers. Figure 5.18 displays the data for the Okapi fitted with Samil dampers. The annotations at the bottom of the top graphs in figures 5.17 and 5.18 denote various stages along the test track. The bottom graphs in these figures are histograms of the number of occurrence for a certain damper speed range.

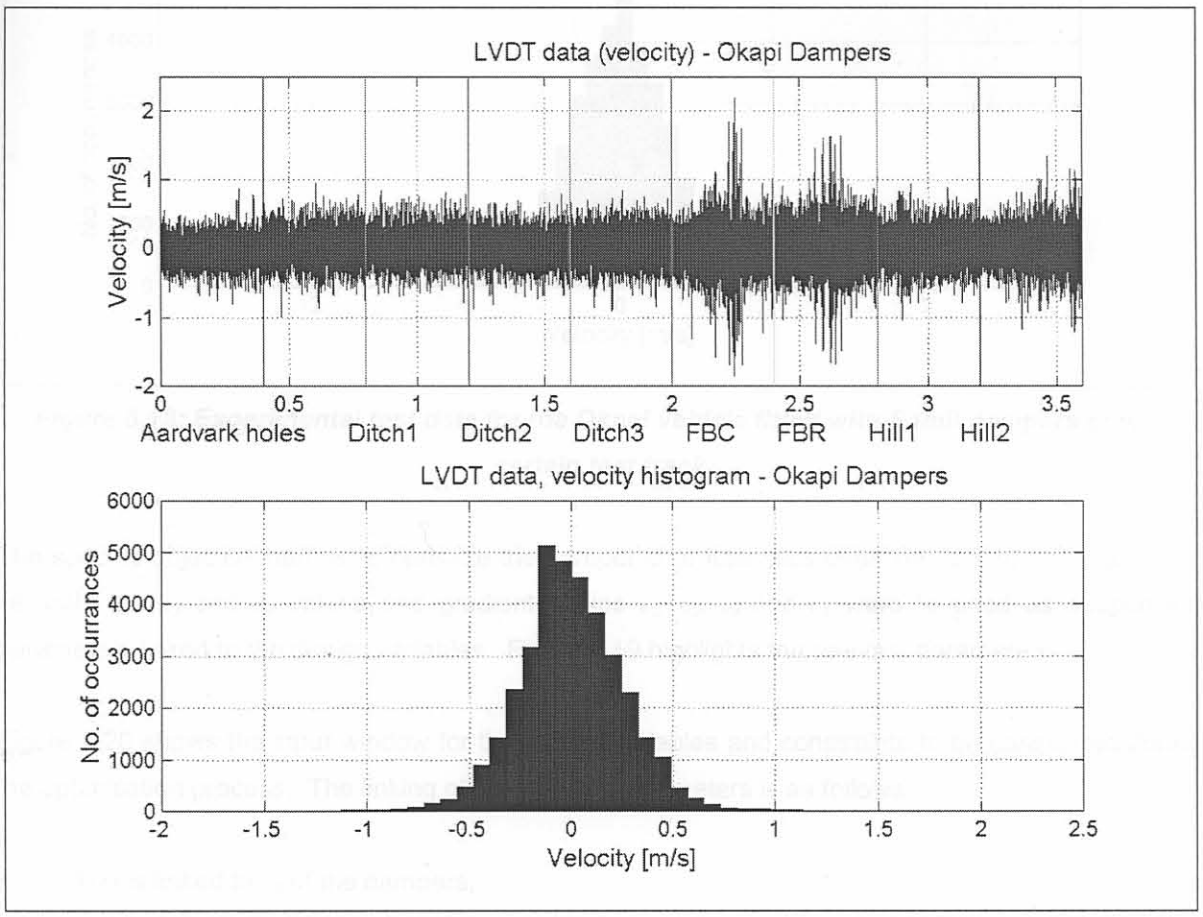

Figure 5.17: Experimental test data for the Okapi vehicle fitted with Okapi (Gabriel dampers) over a certain test track

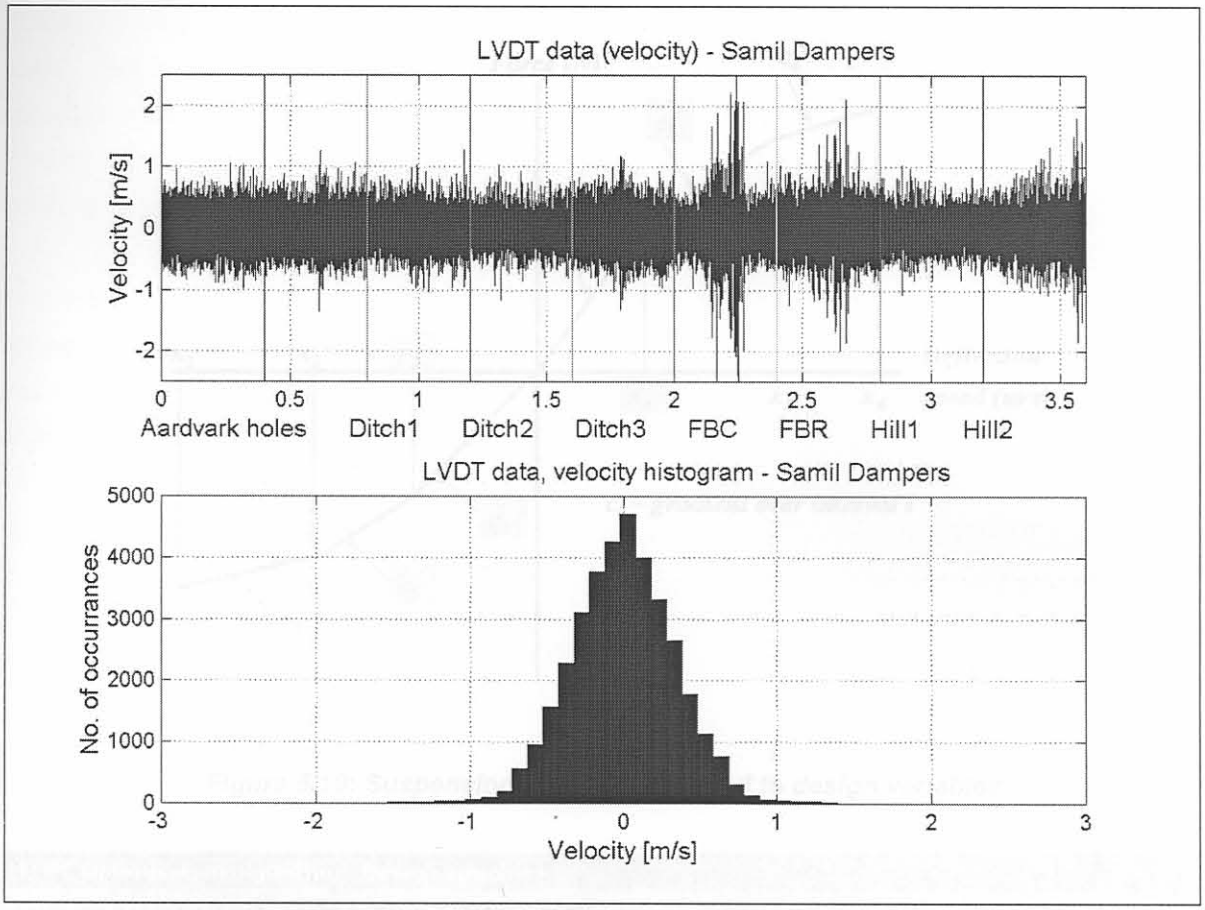

Figure 5.18: Experimental test data for the Okapi vehicle fitted with Samil dampers over a certain test track

The specific objective here is to optimise the damper characteristics over the –2.5 to 2.5 m/s range, i.e. only the x_3 and x_4 values and gradient values c_2, c_3, c_4 and c_5 were to used as suspension parameters linked to the design variables. Figure 5.19 highlights the relevant parameters.

Figure 5.20 shows the input window for the design variables and constraints to be considered during the optimisation process. The linking of variables to parameters is as follows:

* *X(1)* is linked to x_3 of the dampers,
* *X(2)* is linked to x_4 of the dampers,
* *X(3)* is linked to c_2 of the dampers,
* *X(4)* is linked to c_3 of the dampers,
* *X(5)* is linked to c_4 of the dampers and
* *X(6)* is linked to c_5 of the dampers.

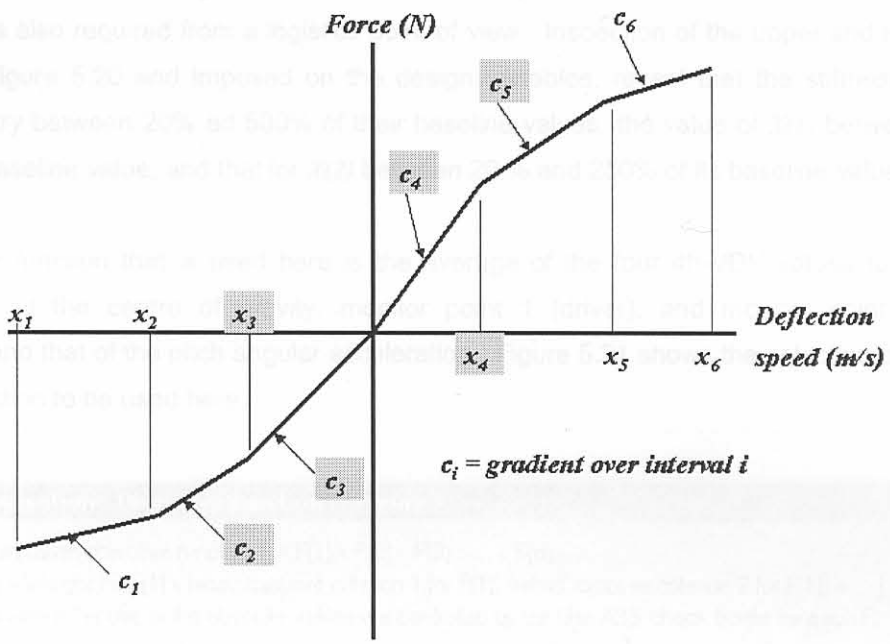

Figure 5.19: Suspension parameters linked to design variables

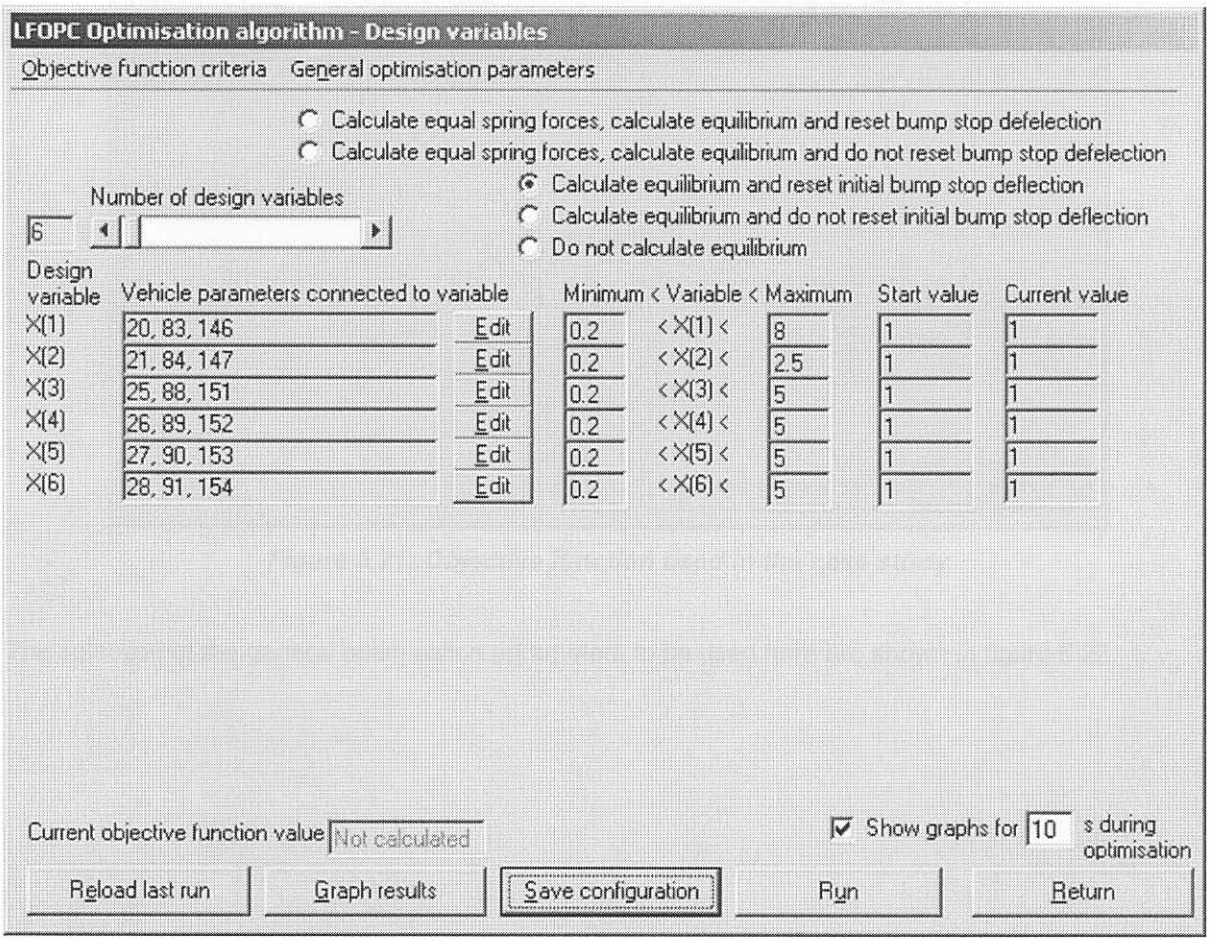

Figure 5.20: Design variable input for case study

According to this selection of parameters the same dampers are used on the front, middle and rear axles. This is also required from a logistics point of view. Inspection of the upper and lower bounds specified in figure 5.20 and imposed on the design variables, reveal that the stiffness values are allowed to vary between 20% ad 500% of their baseline values, the value of $X(1)$ between 20% and 800% of its baseline value, and that for $X(2)$ between 20 % and 250% of its baseline value.

The objective function that is used here is the average of the four 4h-VDV values for the vertical accelerations at the centre of gravity, monitor point 1 (driver), and monitor point 2 (left rear passenger), and that of the pitch angular acceleration. Figure 5.21 shows the selection of the specific objective function to be used here.

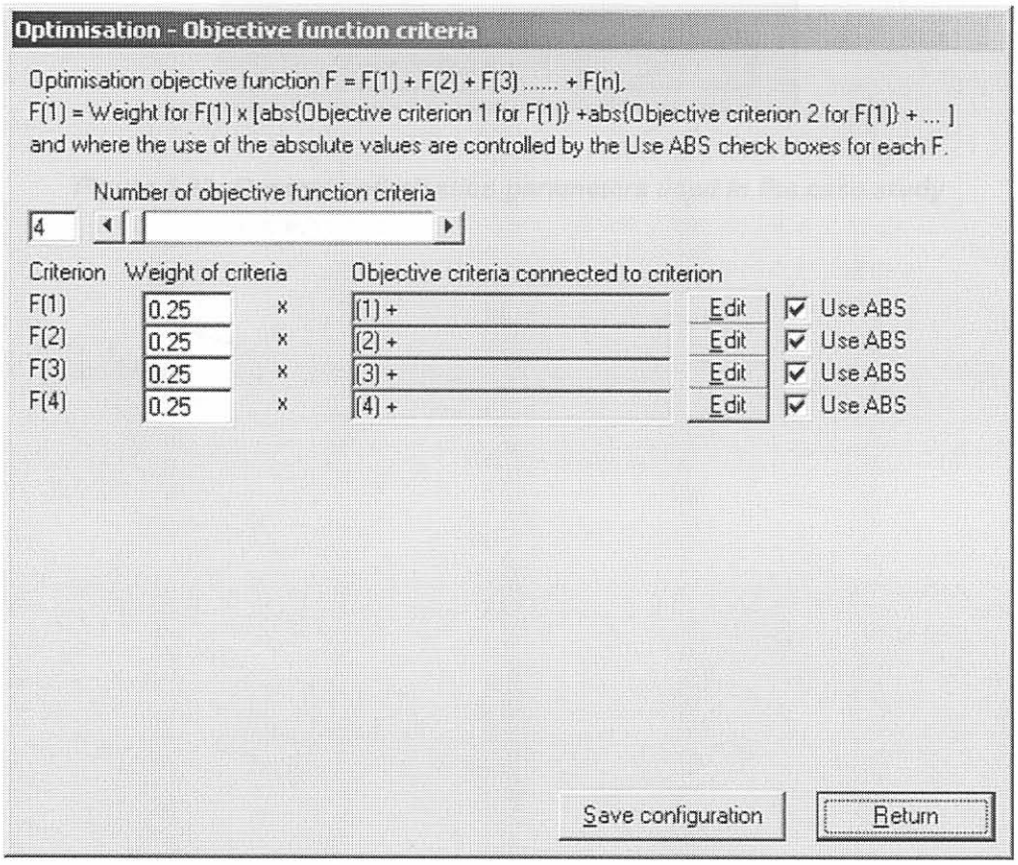

Figure 5.21: Objective function used in the case study

The selection of the general optimisation parameters to be used here are shown in figure 5.22.

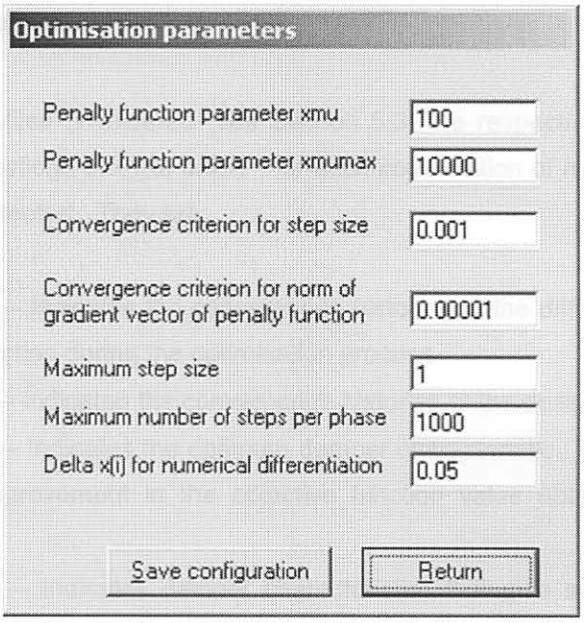

Figure 5.22: General optimisation parameters used in the case study

5.5 Optimisation results

For each of the route profiles considered (see Section 5.3) the respective optimisation results are displayed graphically in sections 5.5.1 to 5.5.7. For each combination of route profile and speed four graphical displays are presented. They are:

* Graphical display 1 – Indicates the convergence histories of the different objective criteria and overall objective function during the optimisation process.
* Graphical display 2 – Indicated the convergence histories of the design variables.
* Graphical display 3 – Indicates the optimum damper characteristic. The % value in the legend indicates the % improvement in the objective function value obtained with respect to the baseline value.
* Graphical display 4 – Indicates damper characteristics that give an objective function value within 5% of that of the optimum configuration.

A discussion of the results for the different optimisation runs is presented in section 5.5.8.

5.5.1 Dirt road 40 km/h

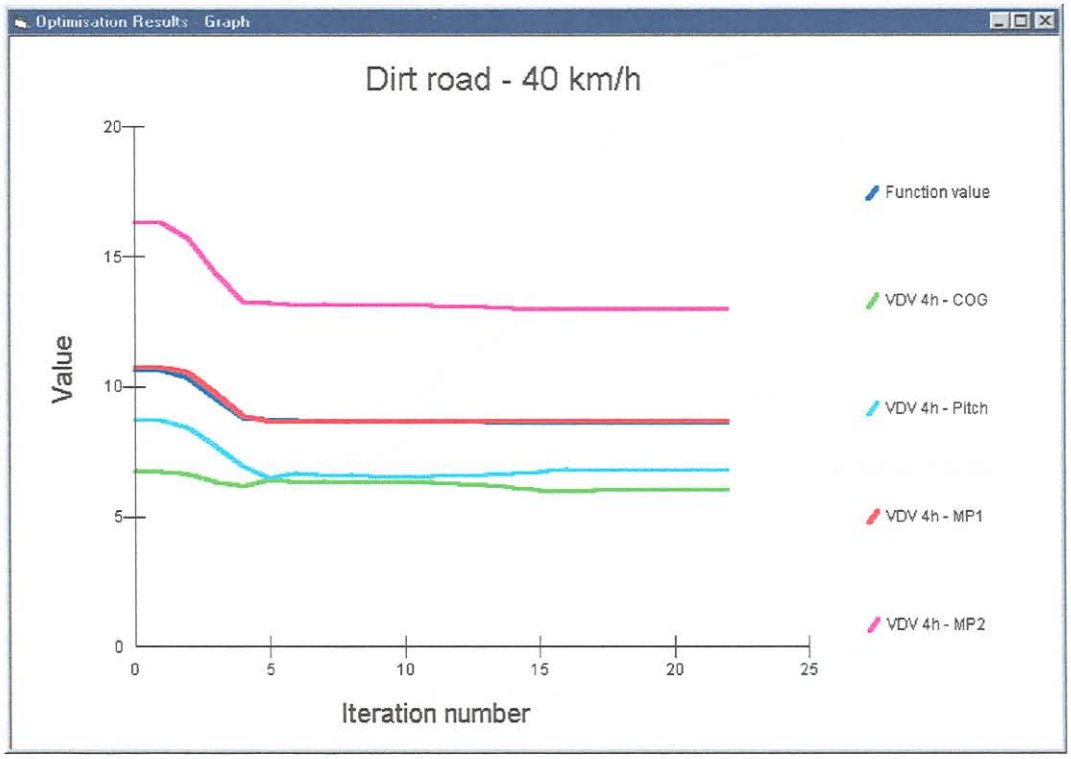

Figure 5.23: Objective function

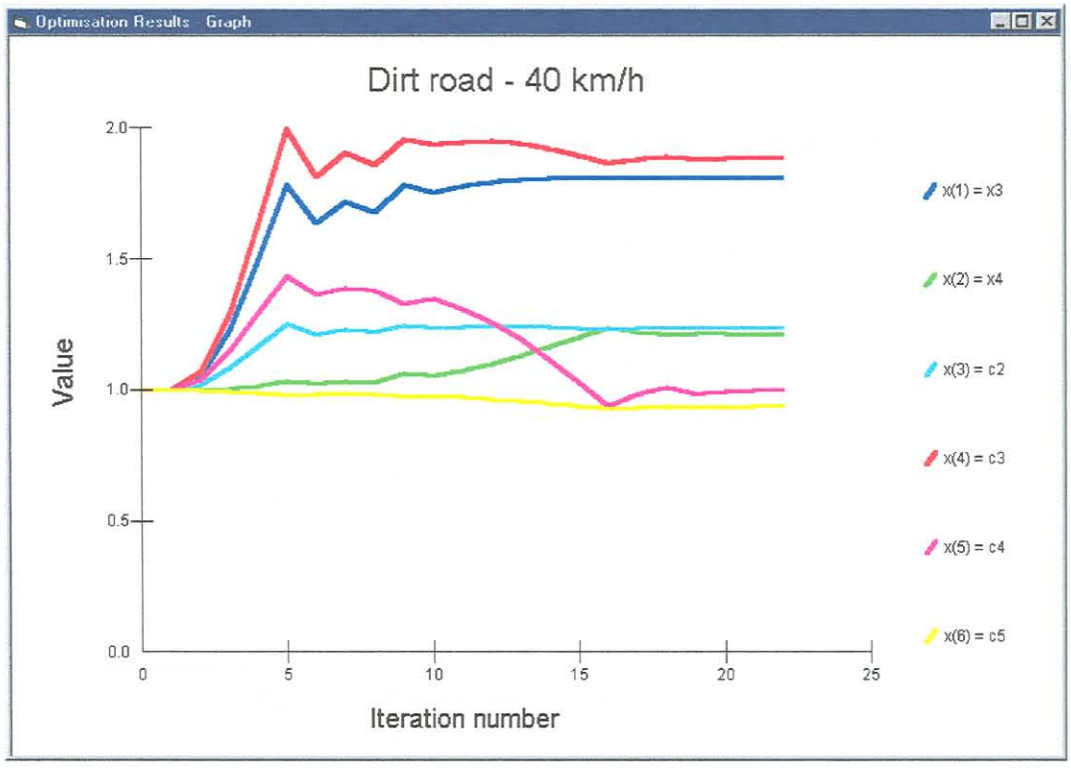

Figure 5.24: Design variables

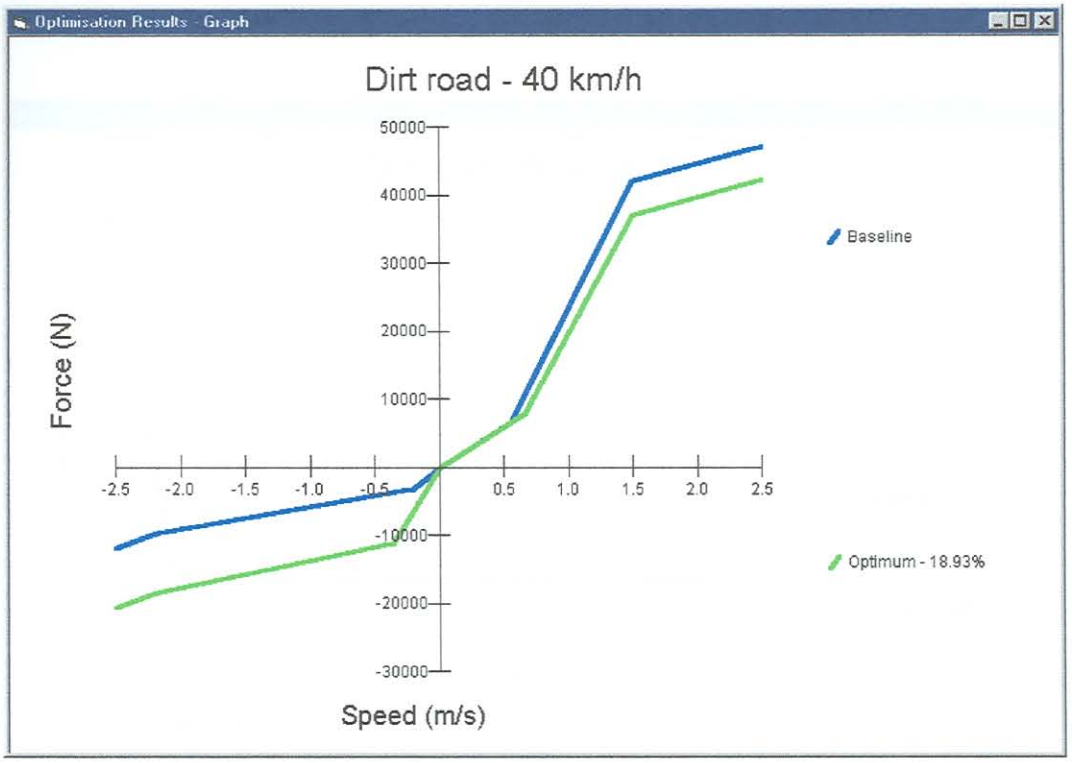

Figure 5.25: Optimum damper characteristics

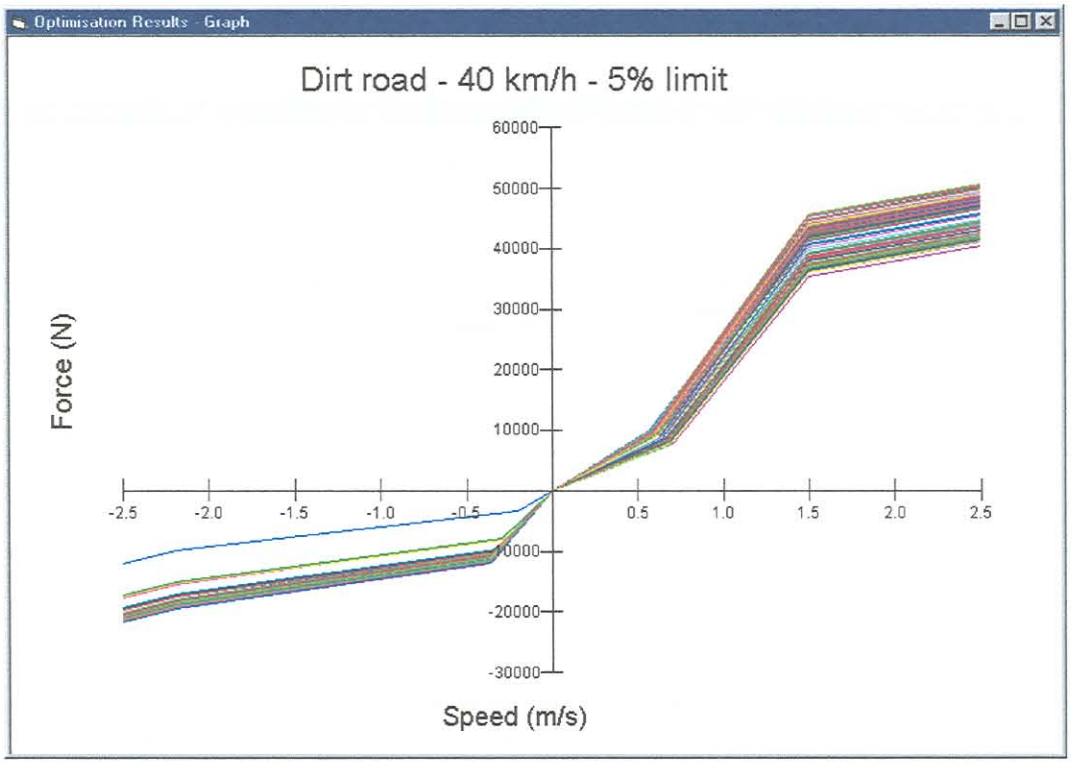

Figure 5.26: 5% Limit damper characteristics

5.5.2 Dirt road 60 km/h

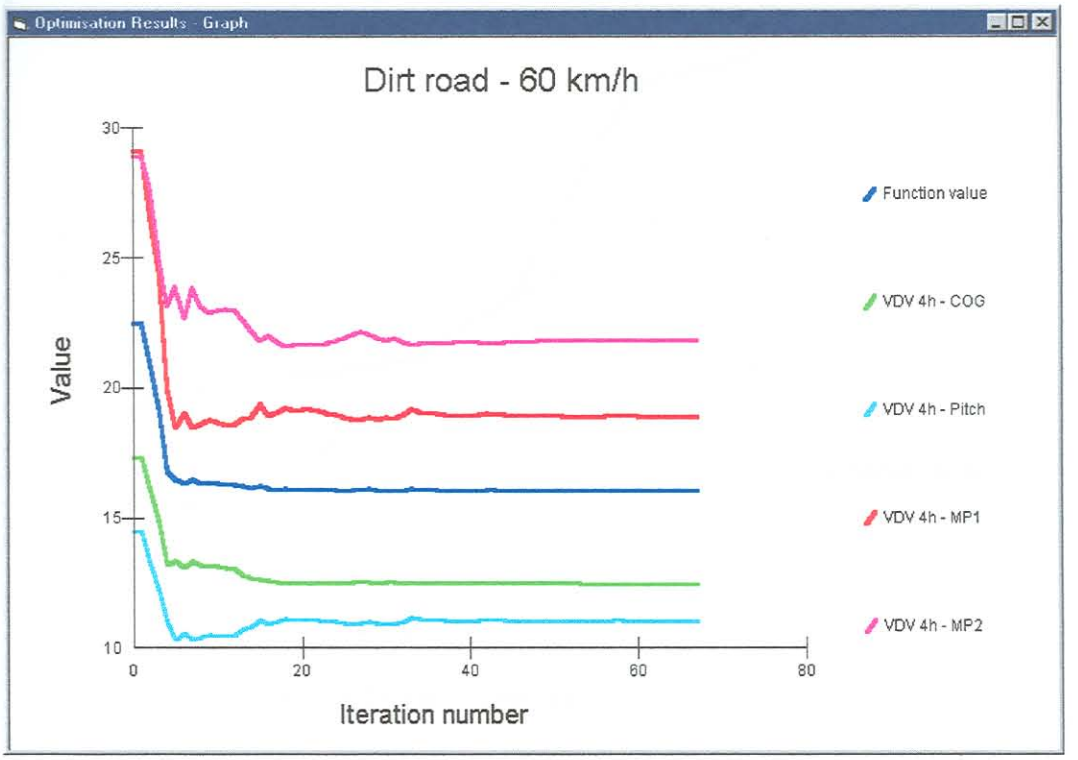

Figure 5.27: Objective function

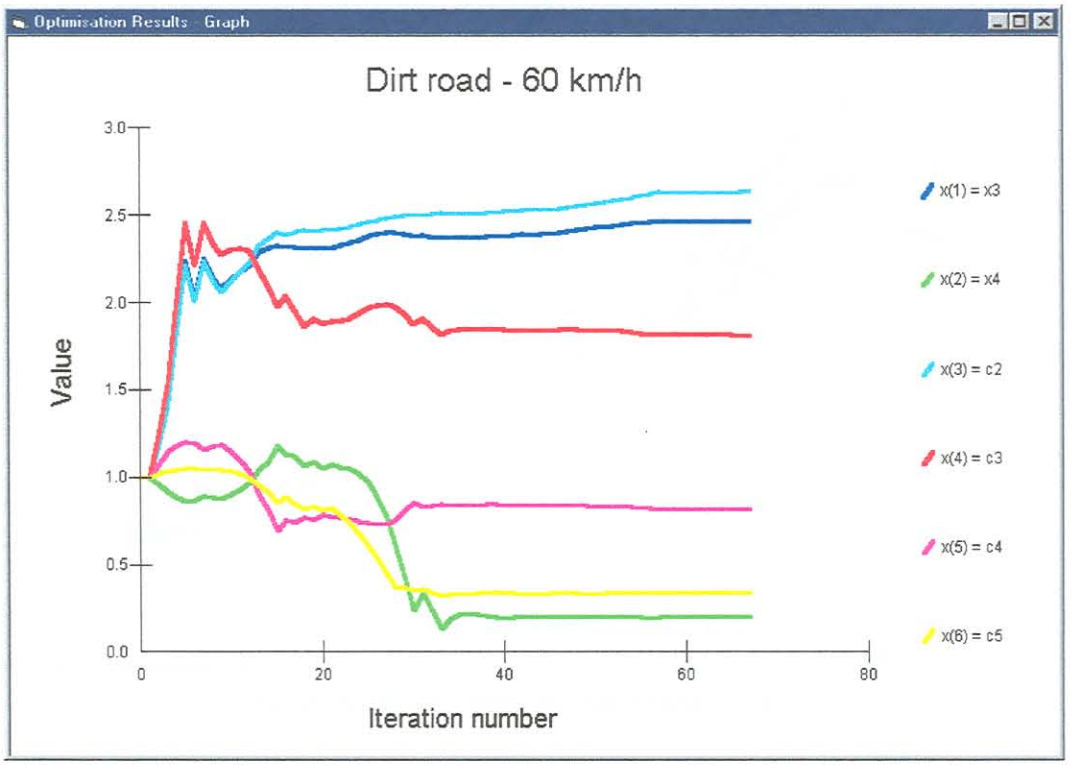

Figure 5.28: Design variables

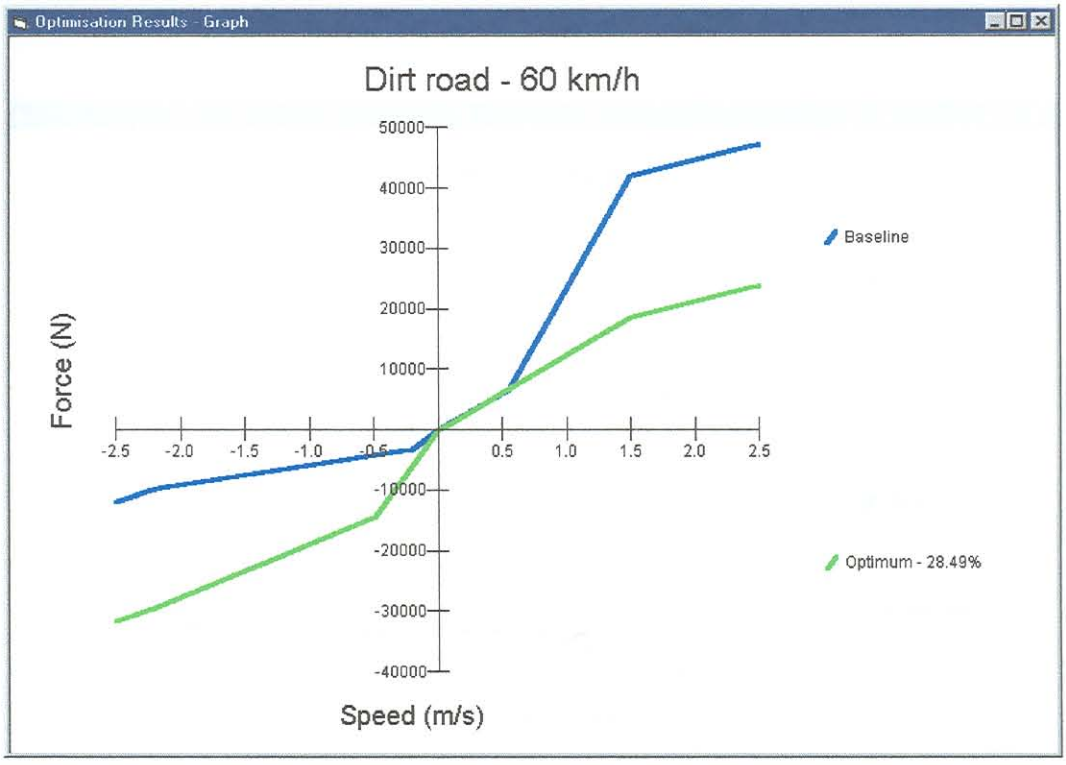

Figure 5.29: Optimum damper characteristics

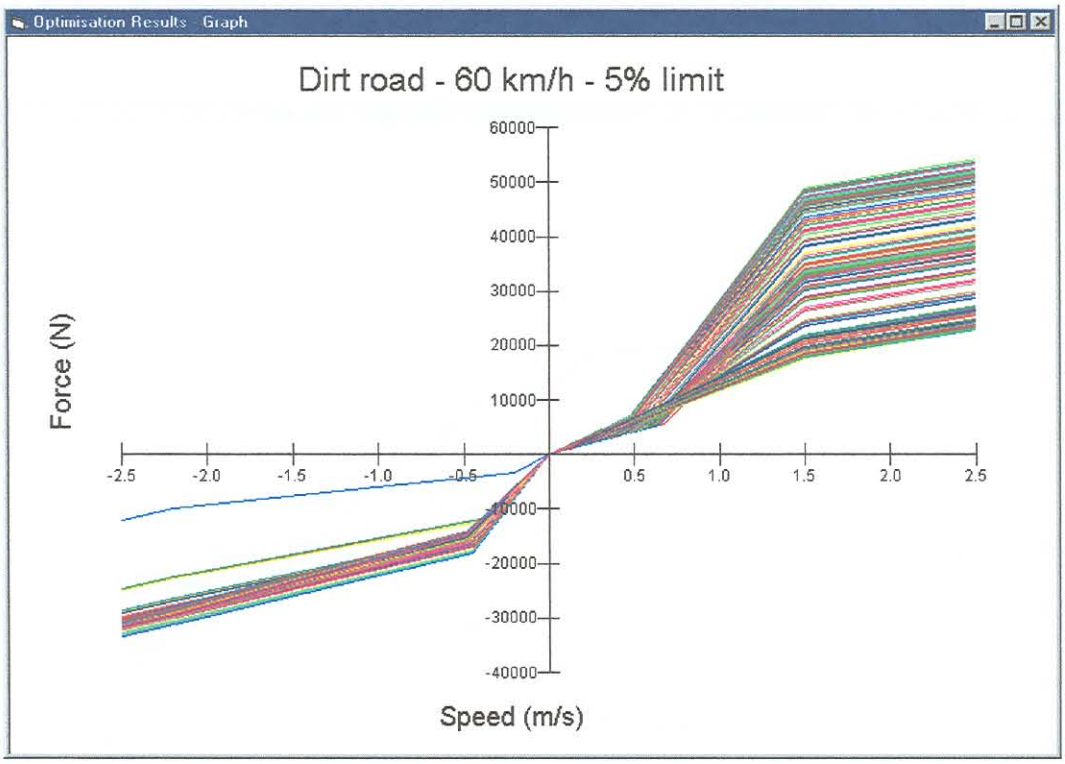

Figure 5.30: 5% Limit damper characteristics

5.5.3 Dirt road 70 km/h

Figure 5.31: Objective function

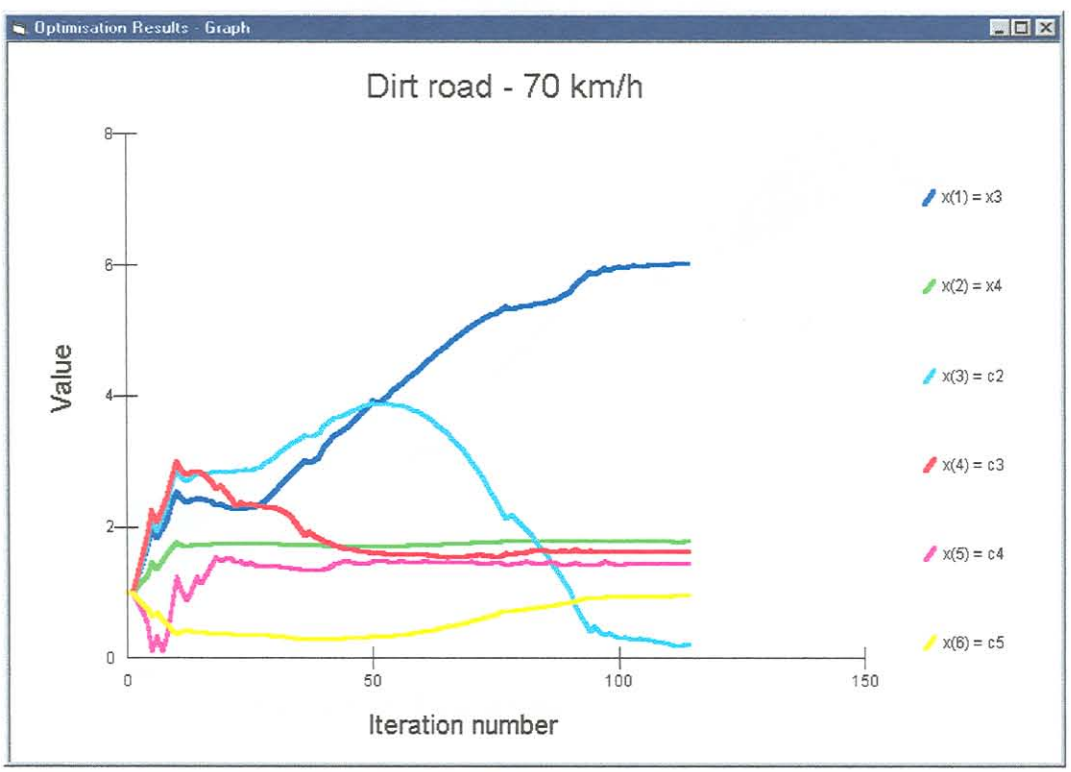

Figure 5.32: Design variables

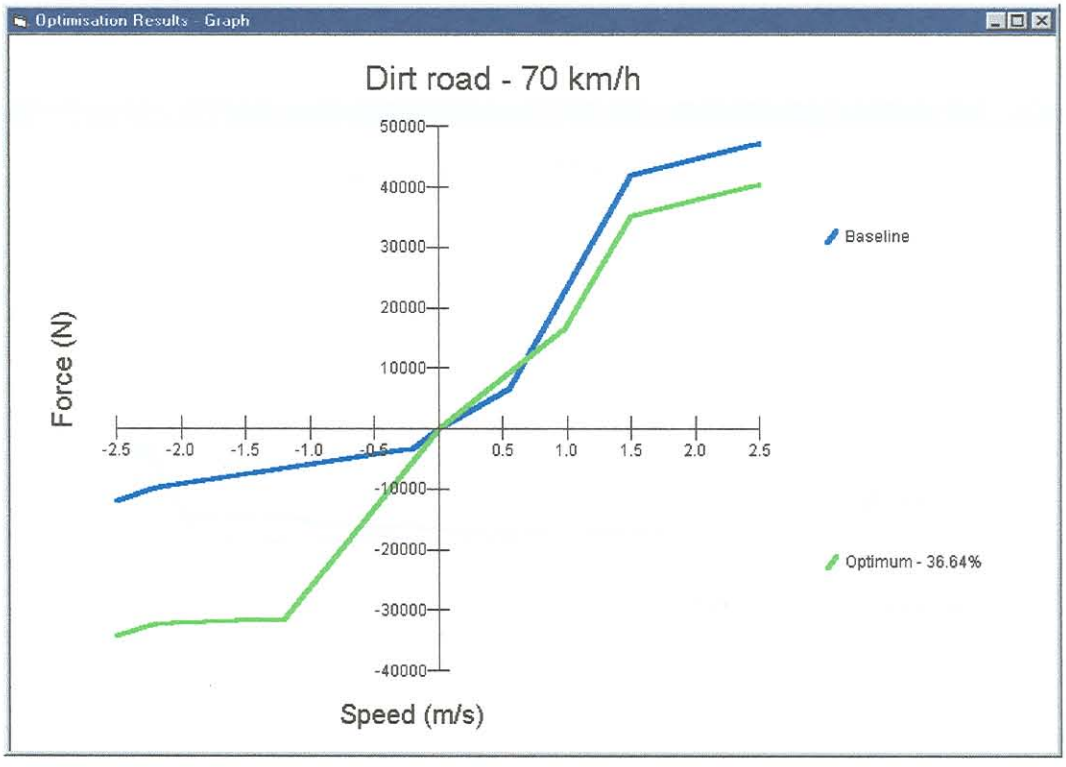

Figure 5.33: Optimum damper characteristics

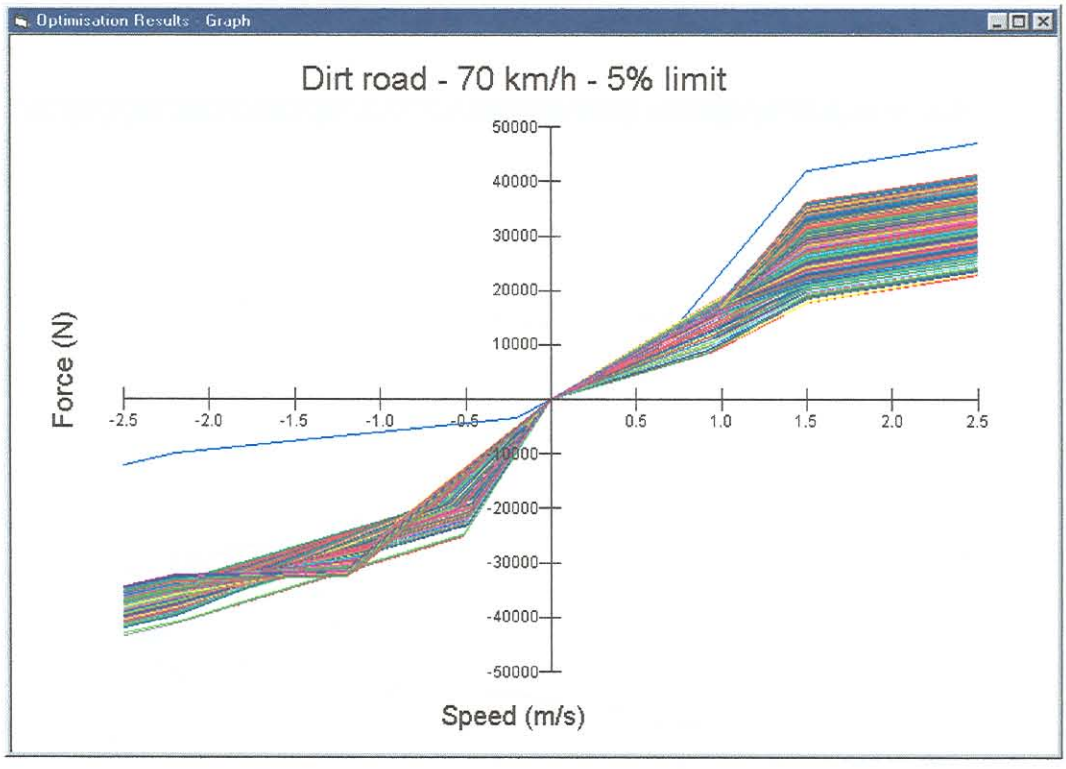

Figure 5.34: 5% Limit damper characteristics

5.5.4 Ditch bump 20 km/h

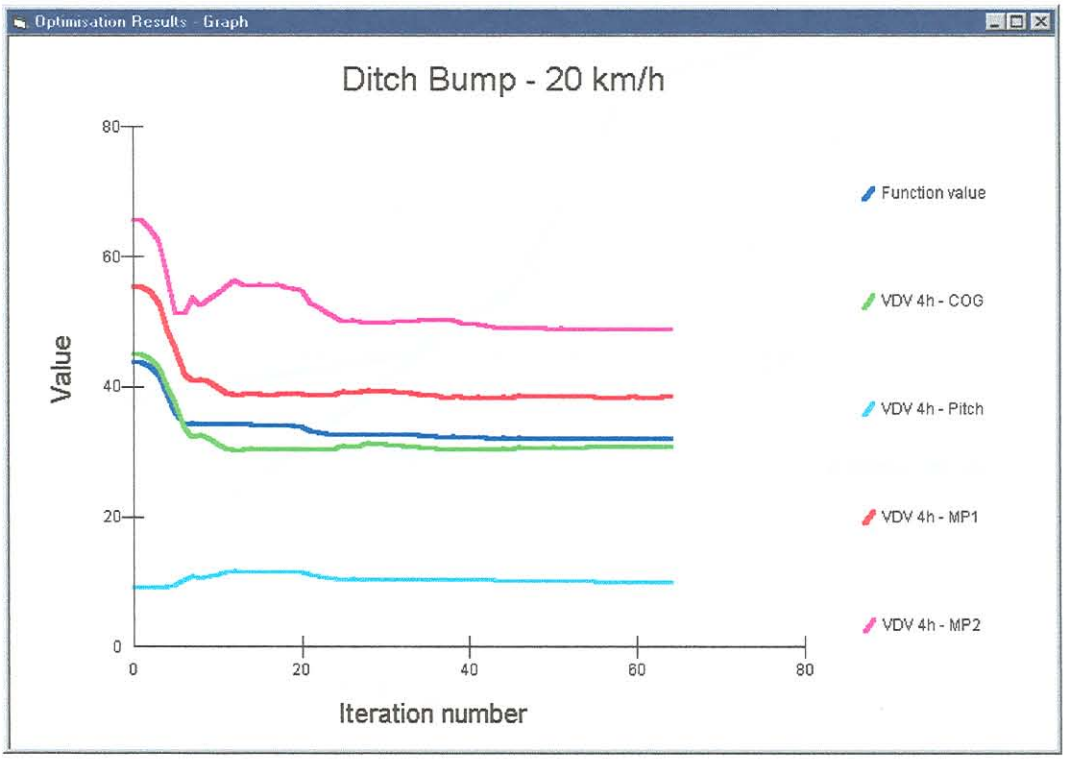

Figure 5.35: Objective function

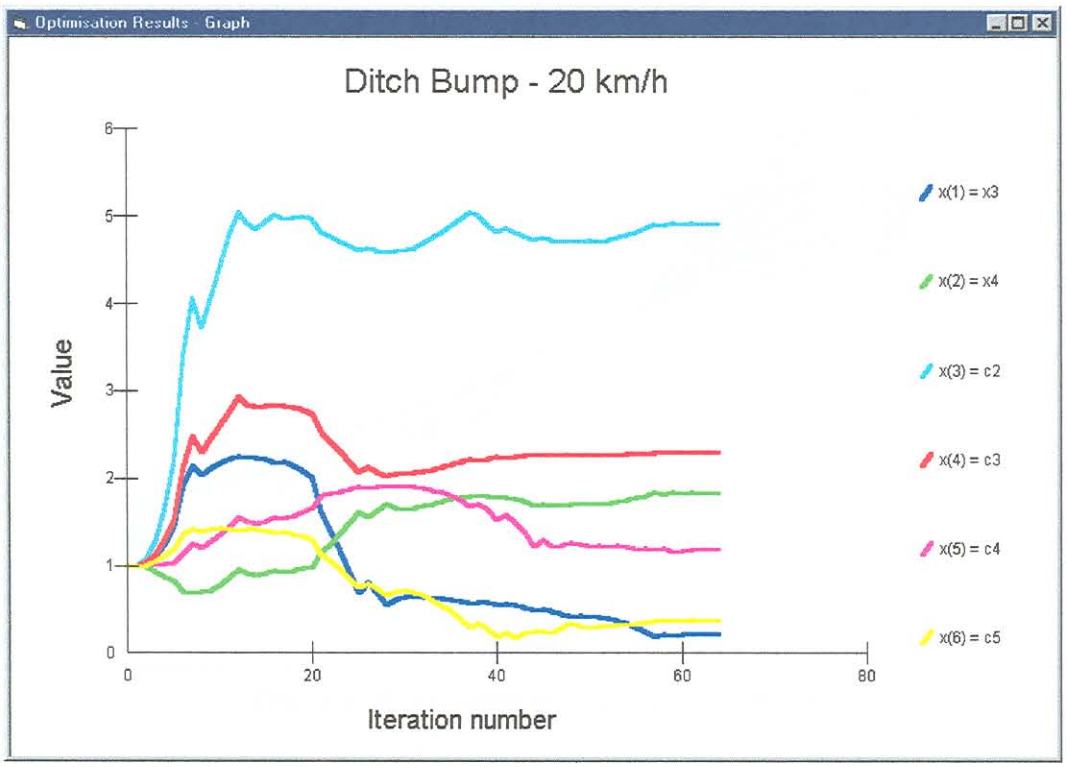

Figure 5.36: Design variables

Figure 5.37: Optimum damper characteristics

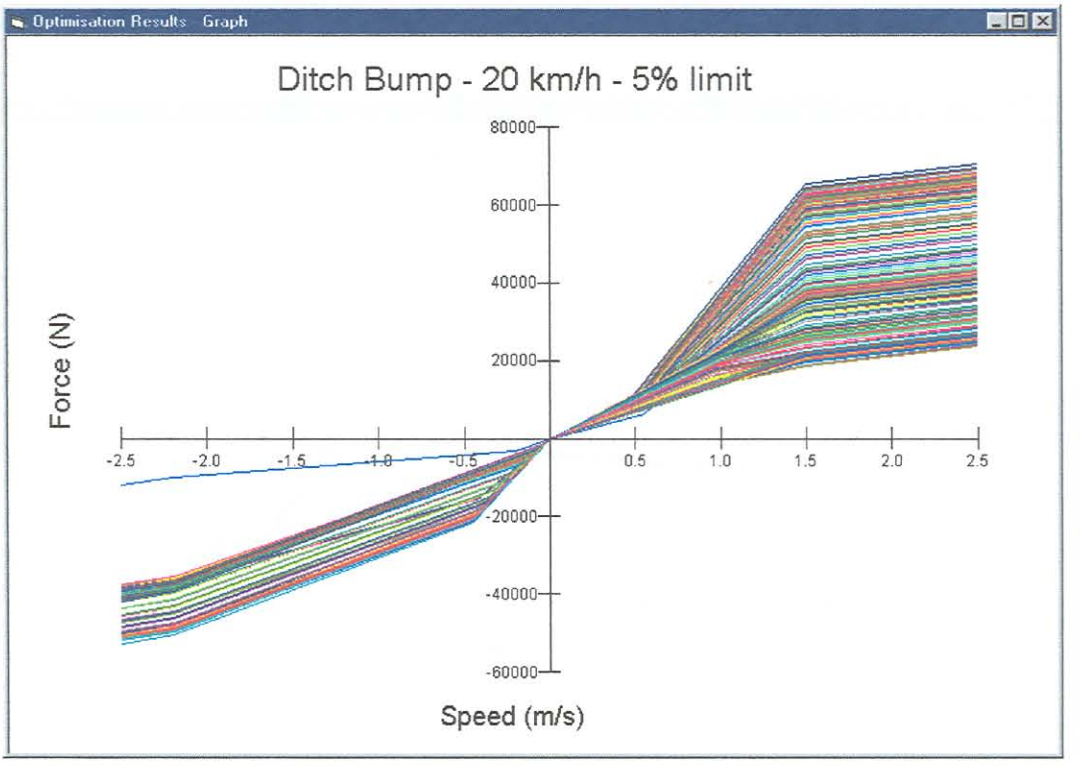

Figure 5.38: 5% Limit damper characteristics

5.5.5 Ditch bump – 30 km/h

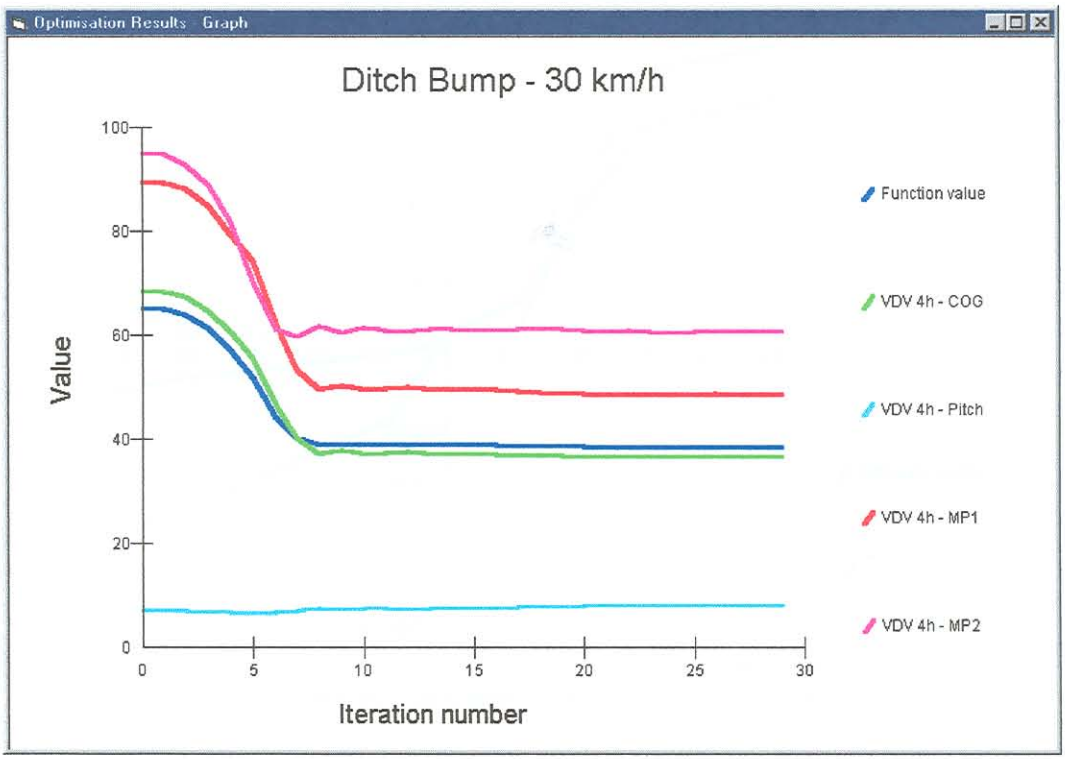

Figure 5.39: Objective function

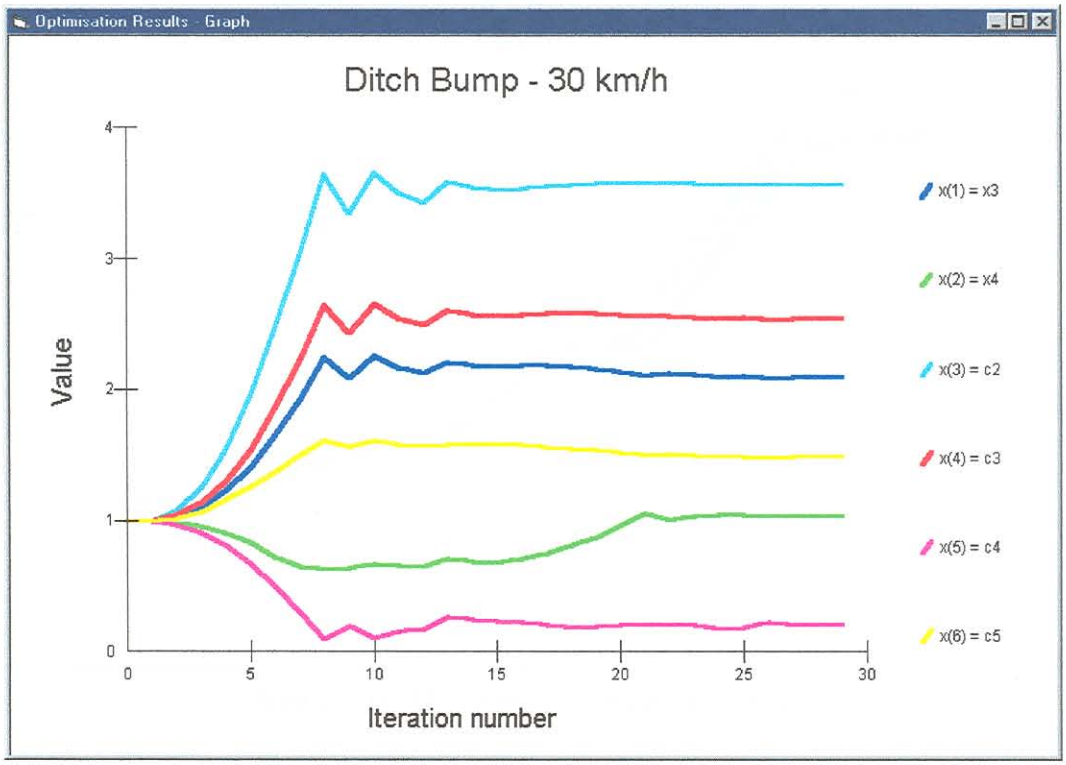

Figure 5.40: Design variables

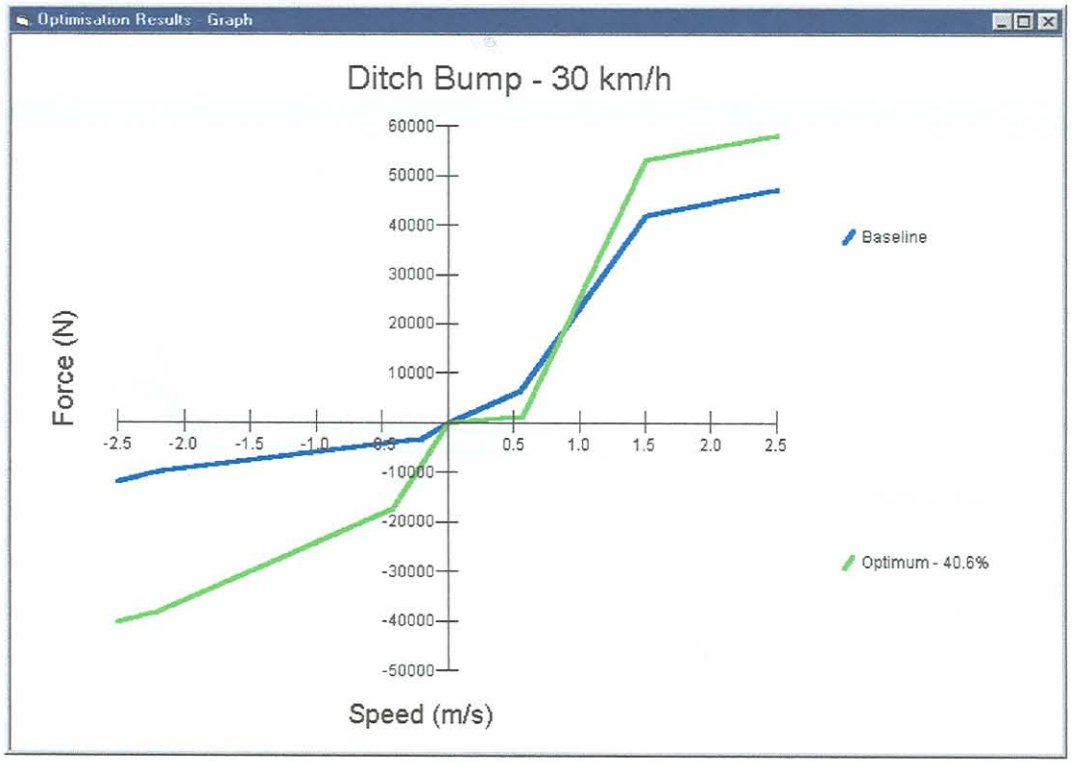

Figure 5.41: Optimum damper characteristics

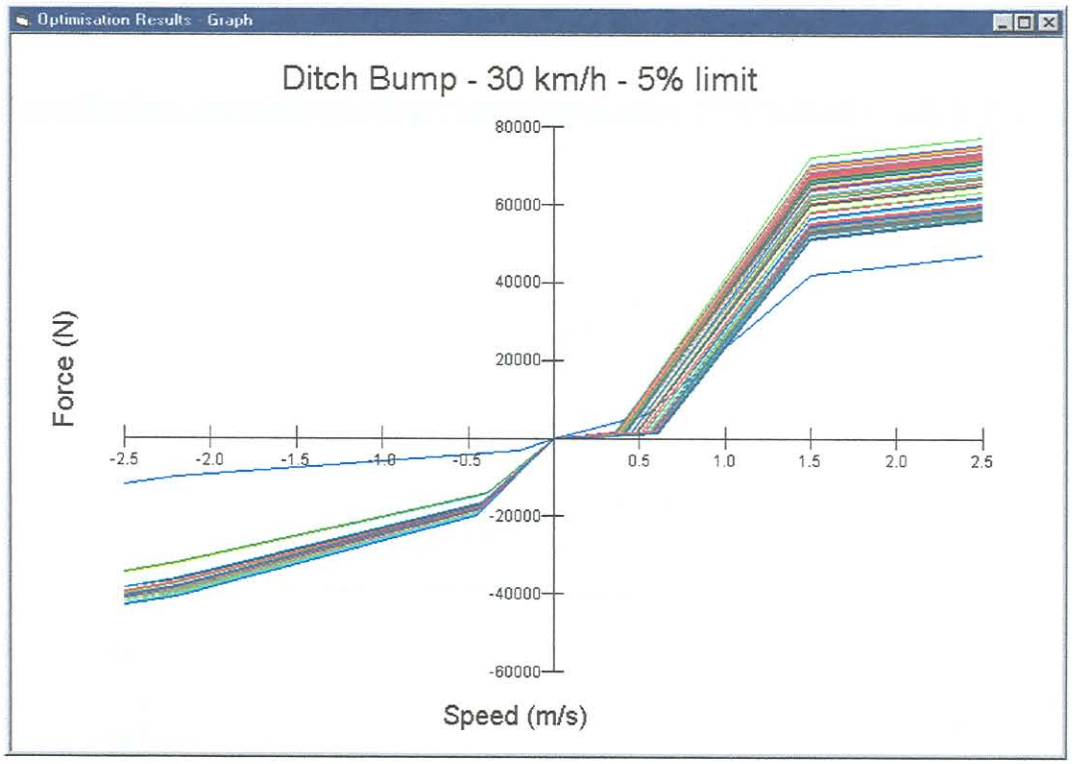

Figure 5.42: 5% Limit damper characteristics

5.5.6 New Belgian 30 km/h

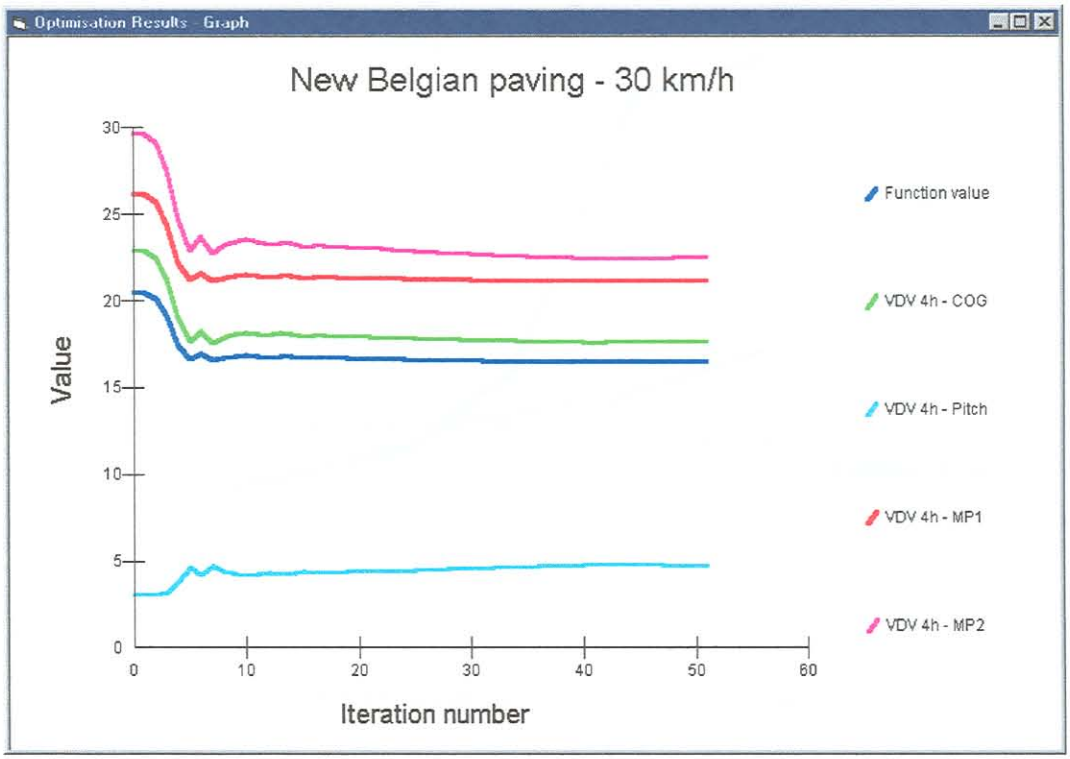

Figure 5.43: Objective function

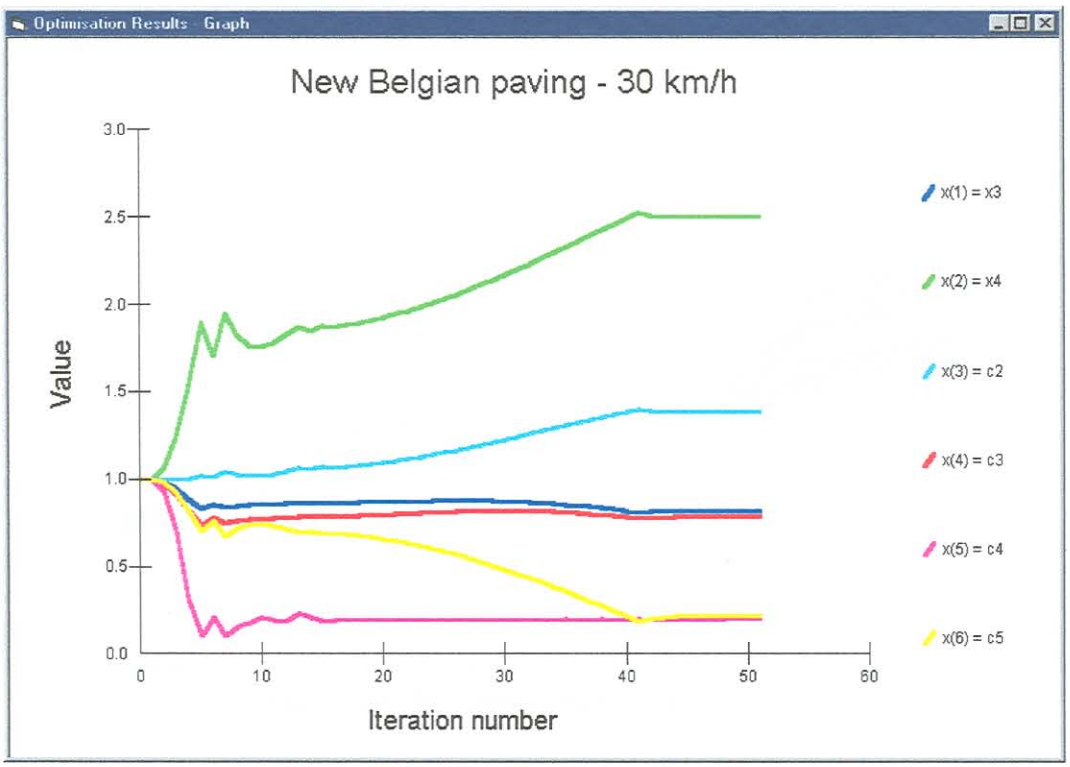

Figure 5.44: Design variables

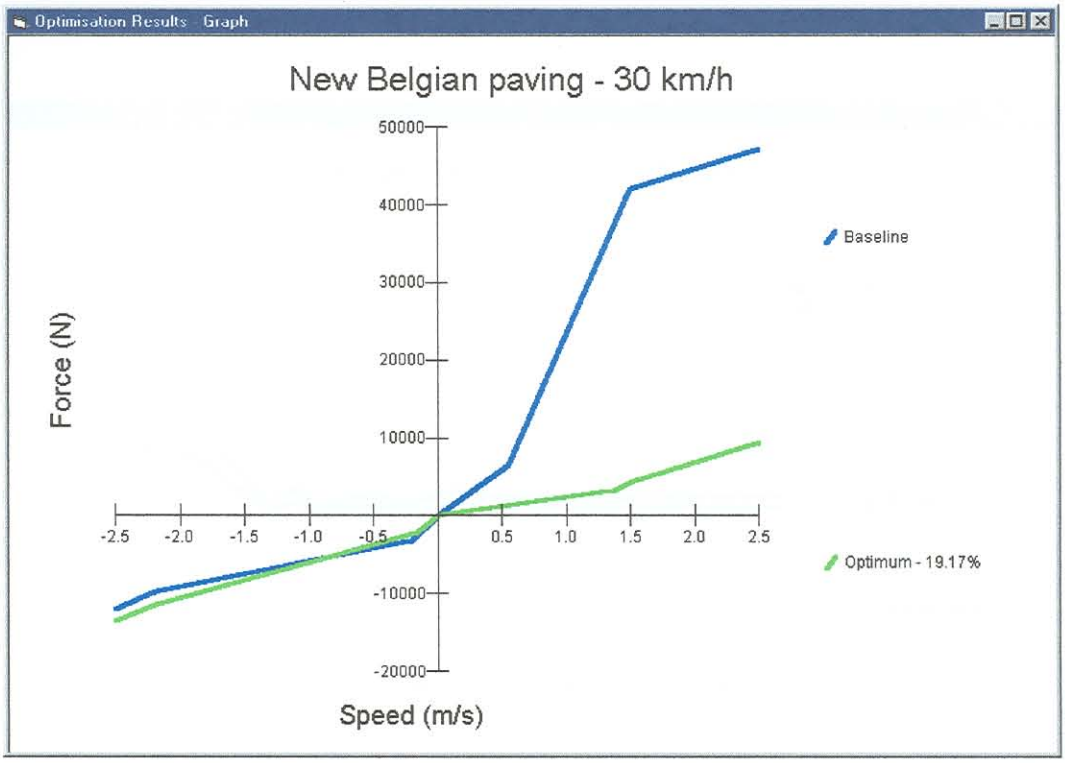

Figure 5.45: Optimum damper characteristics

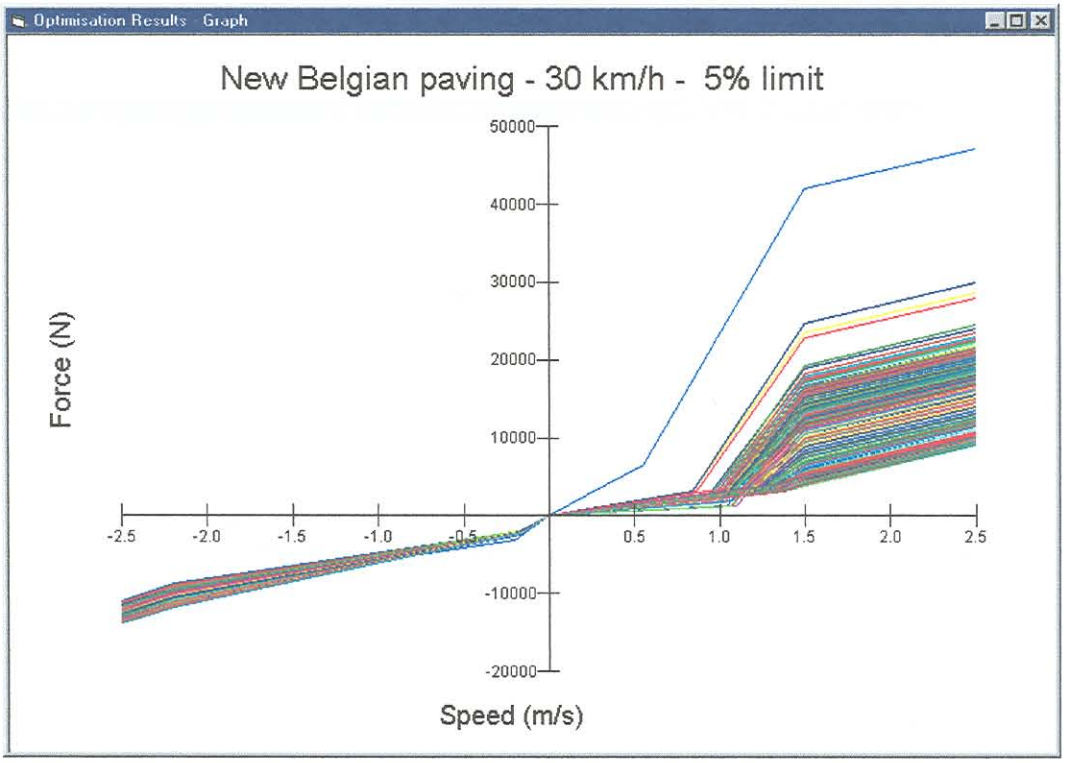

Figure 5.46: 5% Limit damper characteristics

5.5.7 New Belgian 40 km/h

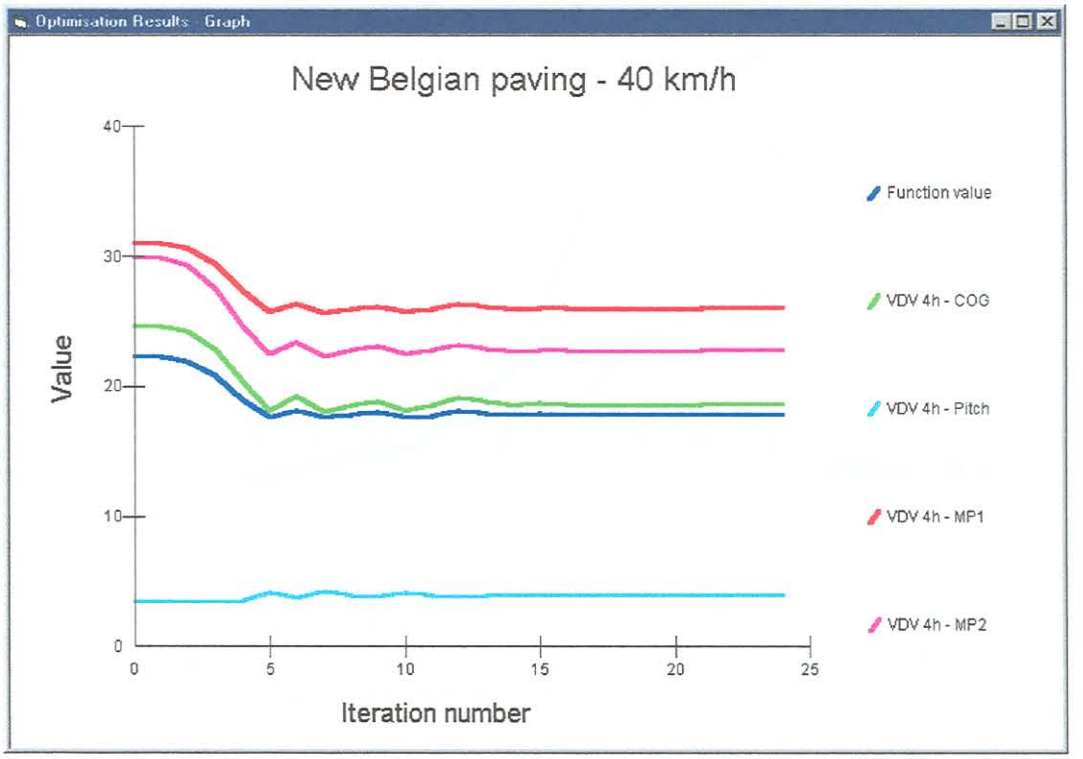

Figure 5.47: Objective function

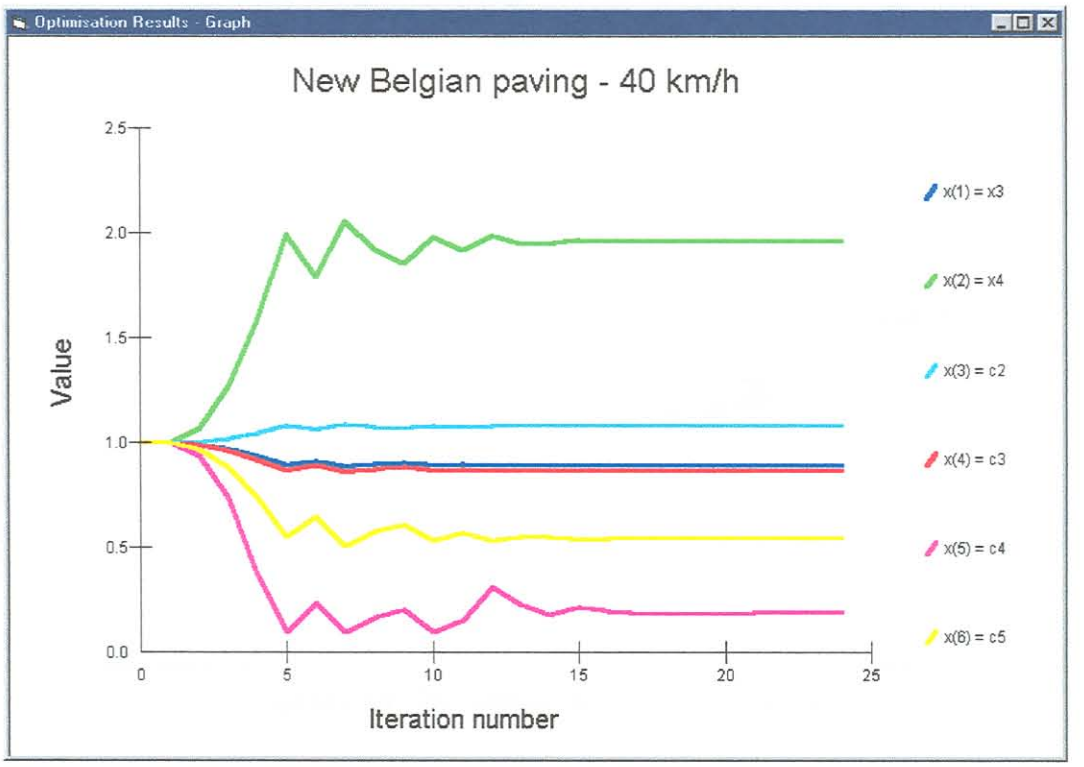

Figure 5.48: Design variables

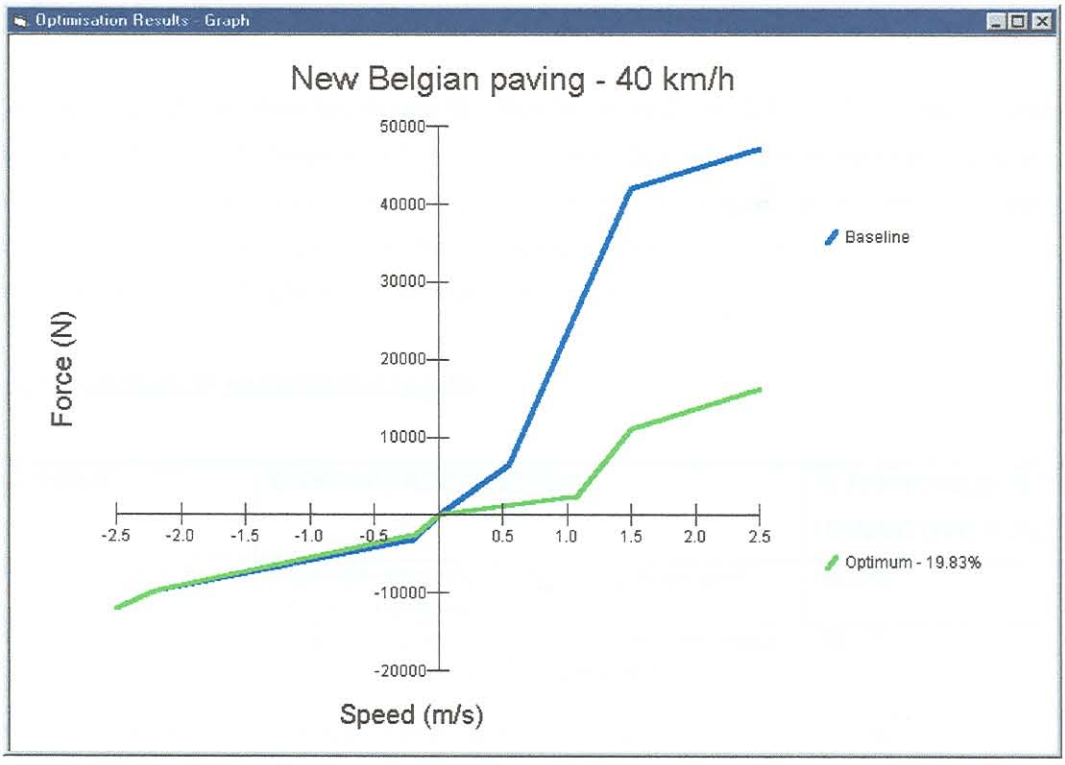

Figure 5.49: Optimum damper characteristics

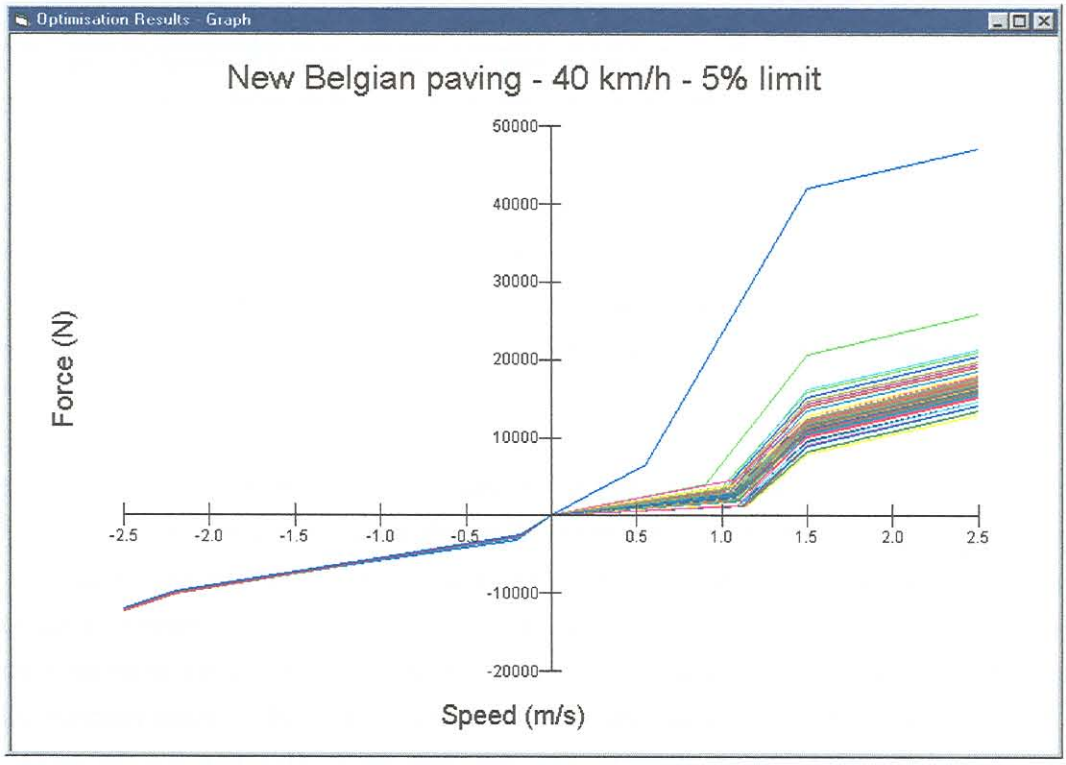

Figure 5.50: 5% Limit damper characteristics

5.5.8 Discussion of optimisation results

The main features of the optimisation results, depicted in sections, 5.5.1 to 5.5.7 are summarised in table 5.1. Reductions of between 40.6% and 18.9% are obtained in the respective objective function values for the different ride conditions. Critical requirements in damping are evident from the 5% limit graphs that indicate narrow bands in the damping region within which it is imperative that the characteristic fall in order to obtain appreciable improvement.

Table 5.1: Summary of optimisation results

ROAD INPUT	DAMPING REQUIREMENT	% IMPROVEMENT IN OBJECTIVE FUNCTION
Dirt road – 40 km/h	Increase damping for bump (critical) and rebound damping	18.9%
Dirt road – 60 km/h	Increase bump damping (critical), decrease rebound damping. Rebound damping not critical	28.5%
Dirt road – 70 km/h	Increase bump damping (critical)	36.5%
Ditch Bump – 20 km/h	Increase bump damping (critical)	26.7%
Ditch Bump – 30 km/h	Bump damping must be increased (critical)	40.6%
New Belgian – 30 km/h	Decrease rebound damping (critical)	19.2%
New Belgian – 40 km/h	Decrease rebound damping (critical)	19.8%

From table 5.1 it can be seen that on the average the damping in the bump direction must be increased and the damping in the rebound direction must decreased for improvement in the objective function. For every combination of speed and road input a different optimum damper characteristic is obtained. The specific mobility requirements for the vehicle will finally determine the suitable damper characteristics to be used.

Interesting results are obtained for the dirt road profile at 70 km/h (see section 5.5.3). Inspection of the behaviour of objective function value (figure 5.31) indicates that an optimum solution is effectively found after approximately 40 simulations, after which the objective function value remains more of less constant. Inspection of figure 5.32, however, shows that after simulation 40 there are large changes in some of the design variables ($X(1)$ and $X(3)$), although this only marginally improves the objective function value. This indicates that for this particular profile and speed, there are many combinations of $X(1)$ and $X(3)$ values that yield near optimum objective function values. Similar tendencies are also observed for some of the other profile and speed combinations.

5.6 Damper characteristics suggested by optimisation results

The optimum design variable values for the different road profiles and speeds are summarised in table 5.2.

Table 5.2: Summary of design variables for the damper characteristics.

Terrain & Speed	X(1)	X(2)	X(3)	X(4)	X(5)	X(6)
Dirt road 40 km/h	1.81	1.21	1.24	1.89	1.00	0.94
Dirt road 60 km/h	2.46	0.20	2.69	1.81	0.82	0.34
Dirt road 70 km/h	6.02	1.78	0.21	1.62	1.44	0.96
Ditch bump 20 km/h	0.21	1.83	4.91	2.30	1.19	0.38
Ditch bump 30 km/h	2.10	1.04	3.57	2.55	0.20	1.49
New Belgian 30 km/h	0.82	2.50	1.39	0.78	0.20	0.21
New Belgian 40 km/h	0.90	1.96	1.08	0.87	0.20	0.55
Average	*2.04*	*1.50*	*2.15*	*1.69*	*0.72*	*0.69*

In general greater damper stiffness is required for the bump direction and lower stiffness in the rebound direction. The above average values and other subjective considerations suggest the four sets of damper characteristics listed in table 5.3 for further investigation.

Table 5.3: Suggested damper characteristics

Damper configuration	x_3	x_4	c_2	c_3	c_4	c_5
Baseline	-0.20	0.55	3310.00	16175.00	11818.00	37368.00
Baseline x Average	-0.41	0.83	7130.29	27312.51	8508.96	25926.06
Suggestion 1	-0.40	0.83	7130.00	27310.00	8500.00	25900.00
Suggestion 2	-0.20	0.55	3310.00	16175.00	8500.00	25900.00
Suggestion 3	-0.40	0.55	7130.00	27310.00	11818.00	37368.00
Suggestion 4	-0.50	0.80	6000.00	40000.00	6250.00	20600.00

The damper characteristics suggested and that of the baseline are shown in figure 5.51.

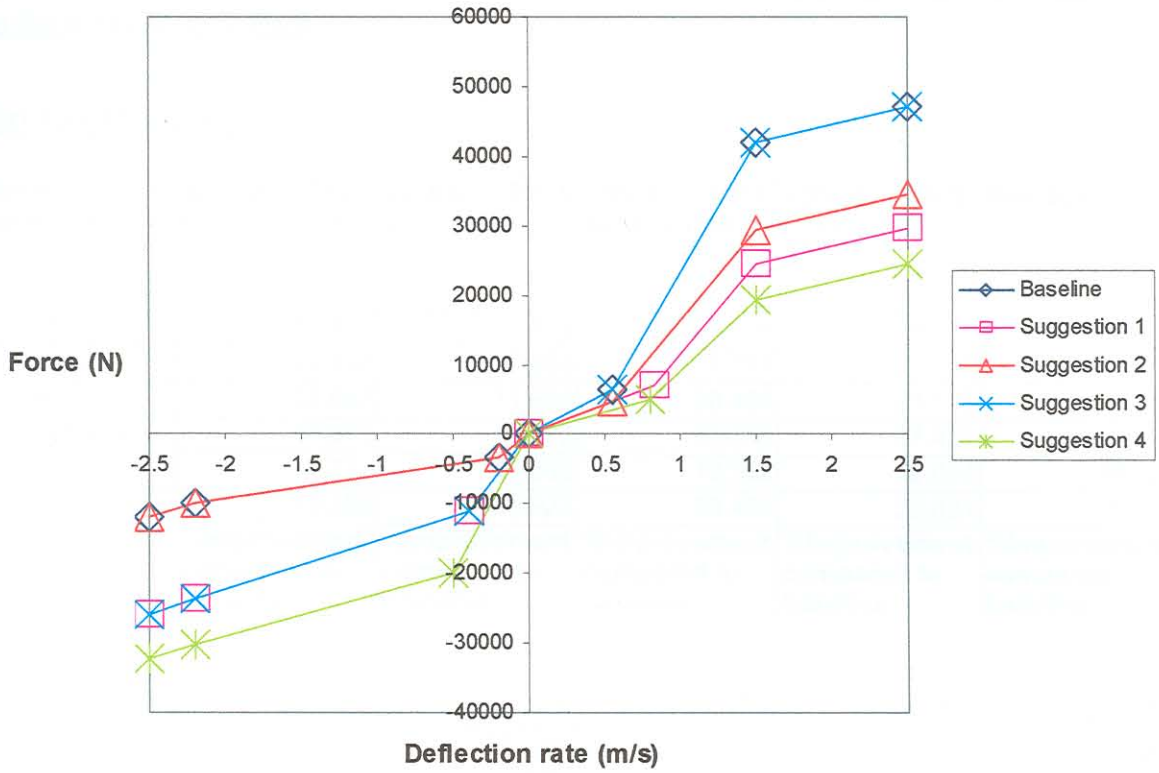

Figure 5.51: Comparison of suggested dampers with baseline damper characteristic

Suggestion 1 effectively uses the rounded-off average values as shown in table 5.2 and 5.3. Damper suggestions 2, 3 are used to investigate the influence of respectively lowering the rebound stiffness and increasing the bump stiffness separately. The damper characteristic of suggestion 4 is obtained through subjective inspection and evaluation of the optimum damper graphs (given in section 5.5).

Simulations with the above suggested damper configurations were performed for the new Belgian @ 40 km/h, dirt road @ 60 km/h, and for the ditch bump @ 30 km/h route profile–speed combinations. Tables 5.4 to 5.6 below show the influence of these choices of characteristics on the VDV 4h values.

Table 5.4: Comparison of VDV(4h) values for the different suggested damper configurations on the dirt road at 60 km/h

Dirt road 60 km/h

Damper configuration	VDV(4h) - CG Acceleration	VDV(4h) - Pitch acceleration	VDV(4h) - MP1 Acceleration	VDV(4h) - MP2 Acceleration	Average
Baseline	17.312	14.454	29.104	28.912	22.446
Optimum	12.498	10.985	18.817	21.919	16.055
Suggestion 1	12.647	11.991	20.484	21.145	16.567
Suggestion 2	17.373	15.472	30.228	27.451	22.631
Suggestion 3	12.774	11.363	19.952	22.014	16.526
Suggestion 4	13.362	10.923	20.426	22.821	16.883
	%Improvement compared to baseline	%Improvement compared to baseline	%Improvement compared to baseline	%Improvement compared to baseline	%Improvement compared to baseline
Optimum	27.81%	24.00%	35.35%	24.19%	28.47%
Suggestion 1	26.95%	17.04%	29.62%	26.86%	26.19%
Suggestion 2	-0.35%	-7.04%	-3.86%	5.05%	-0.83%
Suggestion 3	26.21%	21.39%	31.45%	23.86%	26.37%
Suggestion 4	22.82%	24.43%	29.82%	21.07%	24.78%

Table 5.5: Comparison of VDV(4h) values for the different suggested damper configurations on the ditch bump at 30 km/h

Ditch Bump 30 km/h

Damper configuration	VDV(4h) - CG Acceleration	VDV(4h) - Pitch acceleration	VDV(4h) - MP1 Acceleration	VDV(4h) - MP2 Acceleration	Average
Baseline	68.517	7.217	89.463	95.088	65.071
Optimum	36.758	8.247	48.79	60.819	38.654
Suggestion 1	48.242	7.419	64.521	66.232	46.604
Suggestion 2	68.173	8.192	88.577	98.695	65.909
Suggestion 3	50.265	6.866	66.345	64.747	47.056
Suggestion 4	40.957	7.861	54.867	58.99	40.669
	%Improvement compared to baseline	%Improvement compared to baseline	%Improvement compared to baseline	%Improvement compared to baseline	%Improvement compared to baseline
Optimum	46.35%	-14.27%	45.46%	36.04%	40.60%
Suggestion 1	29.59%	-2.80%	27.88%	30.35%	28.38%
Suggestion 2	0.50%	-13.51%	0.99%	-3.79%	-1.29%
Suggestion 3	26.64%	4.86%	25.84%	31.91%	27.69%
Suggestion 4	40.22%	-8.92%	38.67%	37.96%	37.50%

Table 5.6: Comparison of VDV(4h) values for the different suggested damper configurations on the new Belgian paving at 40 km/h

New Belgian 40 km/h

Damper configuration	VDV(4h) - CG Acceleration	VDV(4h) - Pitch acceleration	VDV(4h) - MP1 Acceleration	VDV(4h) - MP2 Acceleration	Average
Baseline	24.678	3.516	31.035	29.901	22.283
Optimum	18.634	4.019	26.013	22.787	17.863
Suggestion 1	26.842	3.392	31.873	33.924	24.008
Suggestion 2	22.41	3.492	28.967	26.906	20.444
Suggestion 3	28.171	3.178	33.106	35.659	25.029
Suggestion 4	30.602	3.869	35.247	39.102	27.205
	%Improvement compared to baseline	%Improvement compared to baseline	%Improvement compared to baseline	%Improvement compared to baseline	%Improvement compared to baseline
Optimum	24.49%	-14.31%	16.18%	23.79%	19.83%
Suggestion 1	-8.77%	3.53%	-2.70%	-13.45%	-7.74%
Suggestion 2	9.19%	0.68%	6.66%	10.02%	8.25%
Suggestion 3	-14.15%	9.61%	-6.67%	-19.26%	-12.32%
Suggestion 4	-24.01%	-10.04%	-13.57%	-30.77%	-22.09%

The results from tables 5.4 to 5.6 are graphically summarised in figure 5.52.

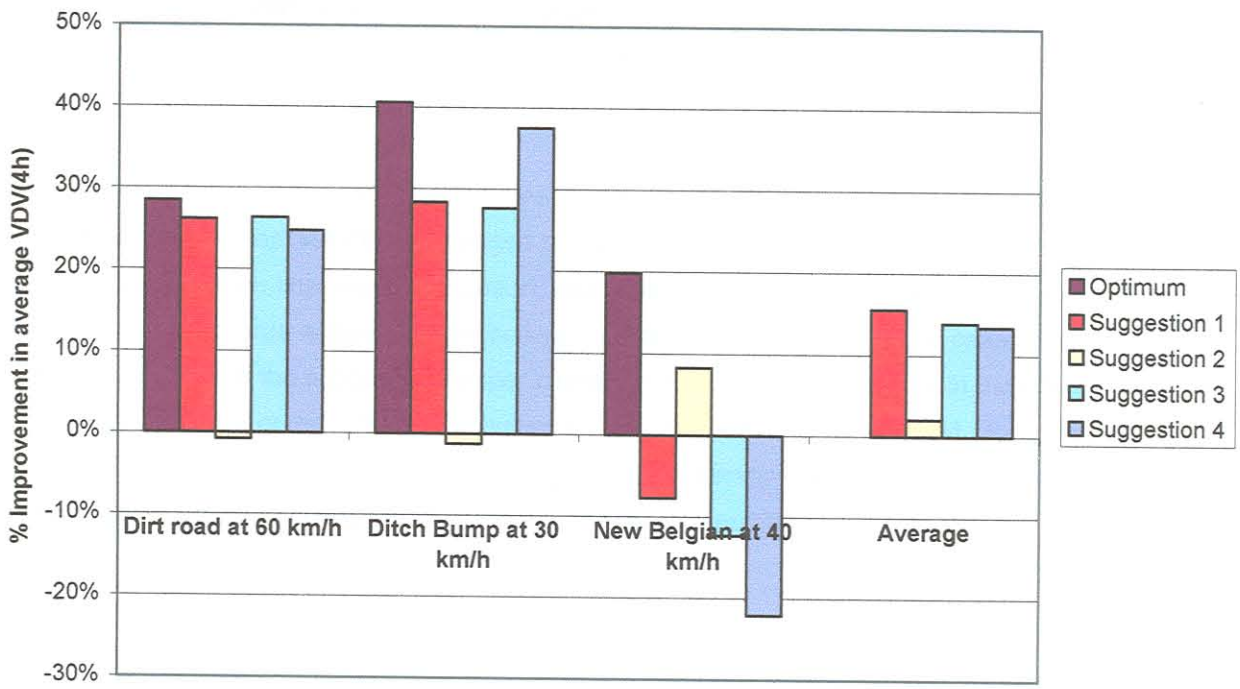

Figure 5.52: Average % improvement in VDV(4h) values for different suggested damper configurations at different road-speed combinations

From the results listed in tables 5.4 to 5.6 and depicted in figure 5.52 the following conclusions are evident:

i. Decreasing only the rebound stiffness (suggestion 2) improves the ride comfort over the new Belgian paving but increases the VDV values over the dirt road and the ditch bump.
ii. Increasing only the bump stiffness (suggestion 3) improves the ride comfort over the dirt road and the ditch bump but gives worse ride comfort over the new Belgian paving.
iii. Increasing the bump stiffness and decreasing the rebound stiffness (suggestions 1 and 4) improves the ride comfort over the dirt road and the ditch bump, but gives worse ride comfort over the new Belgian paving.
iv. The damper configuration of suggestion 1 gives overall the highest % improvement in the average of the VDV values over the three road inputs.

From these results it can be deduced that, in general, an increase in the damper bump stiffness decreases the severity with which the bump stops are "hit" during large suspension deflection in the bump direction, as is usually experienced on the dirt road and when encountering ditch bump profiles. Decreasing the rebound stiffness also aids in "resetting" the suspension travel after bump movement of the suspension. On the new Belgian paving smaller amplitudes of suspension deflection are experienced and therefore lower damping will improve the ride comfort in this instance.

Preliminary discussion with Gabriel [73] revealed that it is possible to increase the bump stiffness of the damper to the value specified in suggestion 1, but not as much as that specified by suggestion 4. Decreasing the rebound stiffness to the levels of suggestion 2 or 4 are also possible.

For overall better ride comfort, and lower forces in the suspension, it is suggested that the damper characteristic for the Okapi vehicle be changed to that given in suggestion 1 - see figure 5.51. With this damper configuration improved ride comfort, and lower suspension forces will be experienced on road profiles inducing large suspension deflections. A concession is made in the case of roads with smooth surfaces, where the suggested damper characteristic will give a decrease in the ride comfort. Due to the fact that the primary mobility requirement for the Okapi vehicle is good off-road mobility, this concession can be afforded. For the vehicle under consideration here it is much more important to improve the ride comfort during off-road conditions than on smoother road surfaces.

5.7 Qualification

Using DADS, and the vehicle model for the Okapi vehicle as described in section 3.19, simulations were performed for the vehicle fitted with three different dampers. Here assistance was received from LMT [62]. The dampers used are a Gabriel damper, a Samil damper, and the damper suggested here by the Vehsim2d optimisation study, i.e., that of suggestion 1. The respective damper characteristics are shown in figure 5.53.

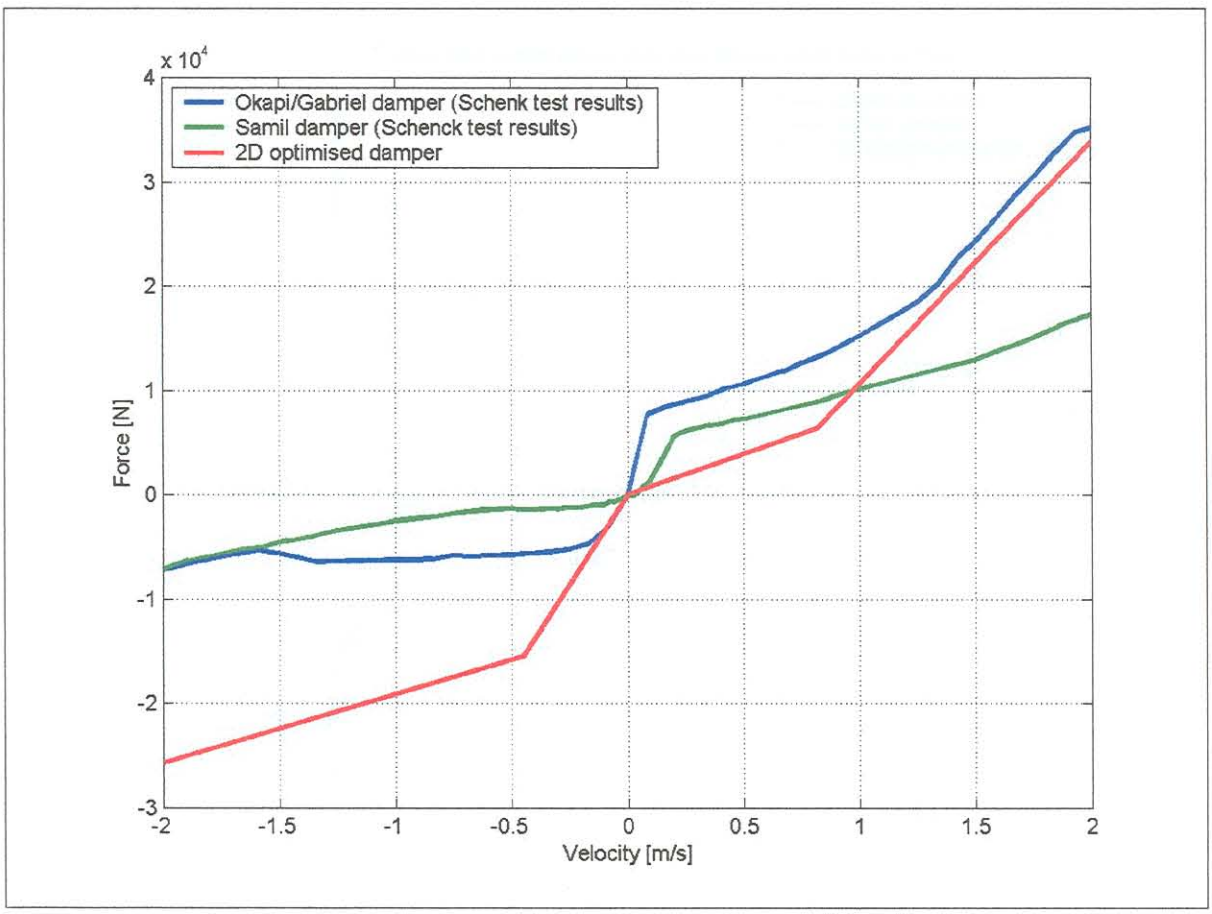

Figure 5.53: Damper characteristics used in the DADS qualification

5.7.1 Ditch bump simulations

DADS simulation results over the ditch bump at 40 km/h are depicted in figures 5.54 and 5.55. From these results it can be seen that that the 2D Optimised damper produces much lower accelerations at the driver seat (figure 5.54) and for the front axle (figure 5.55). For this damper the pitch velocity magnitudes are also lower than for the other dampers, while the variation of the left front wheel force is of the same magnitude.

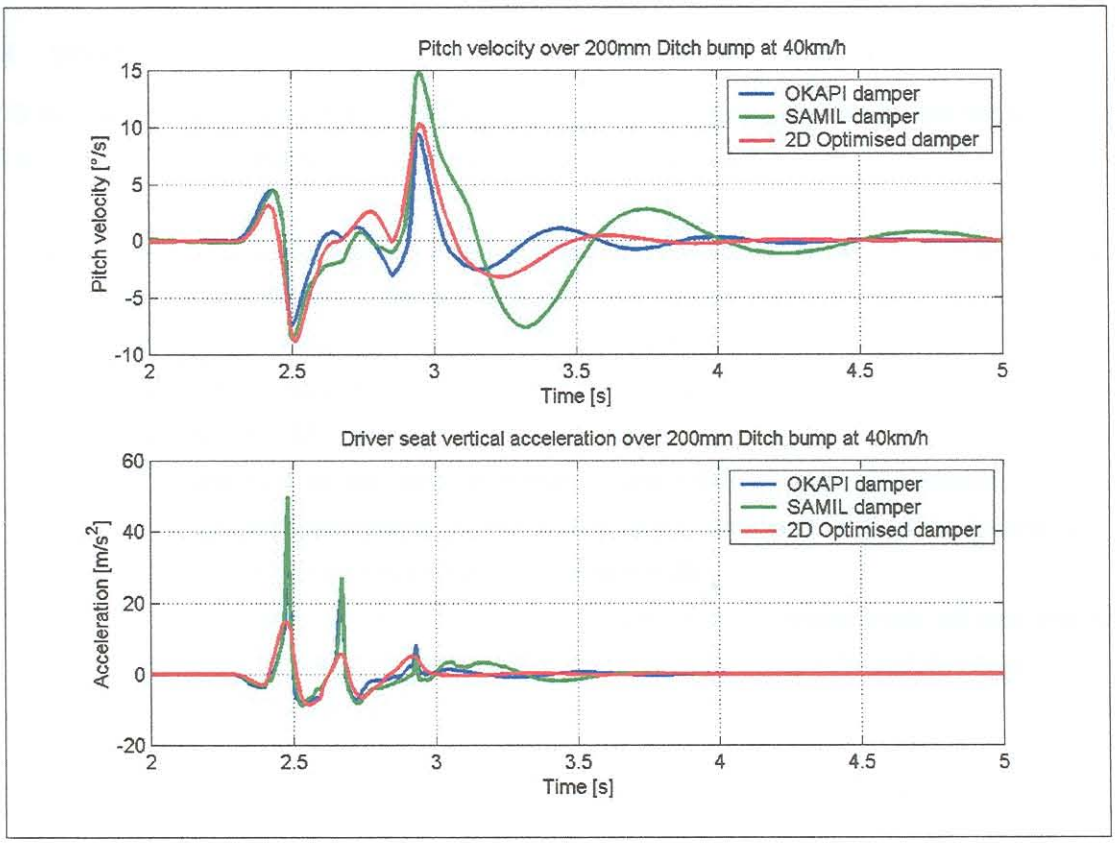

Figure 5.54: DADS simulation results for ditch bump at 40 km/h

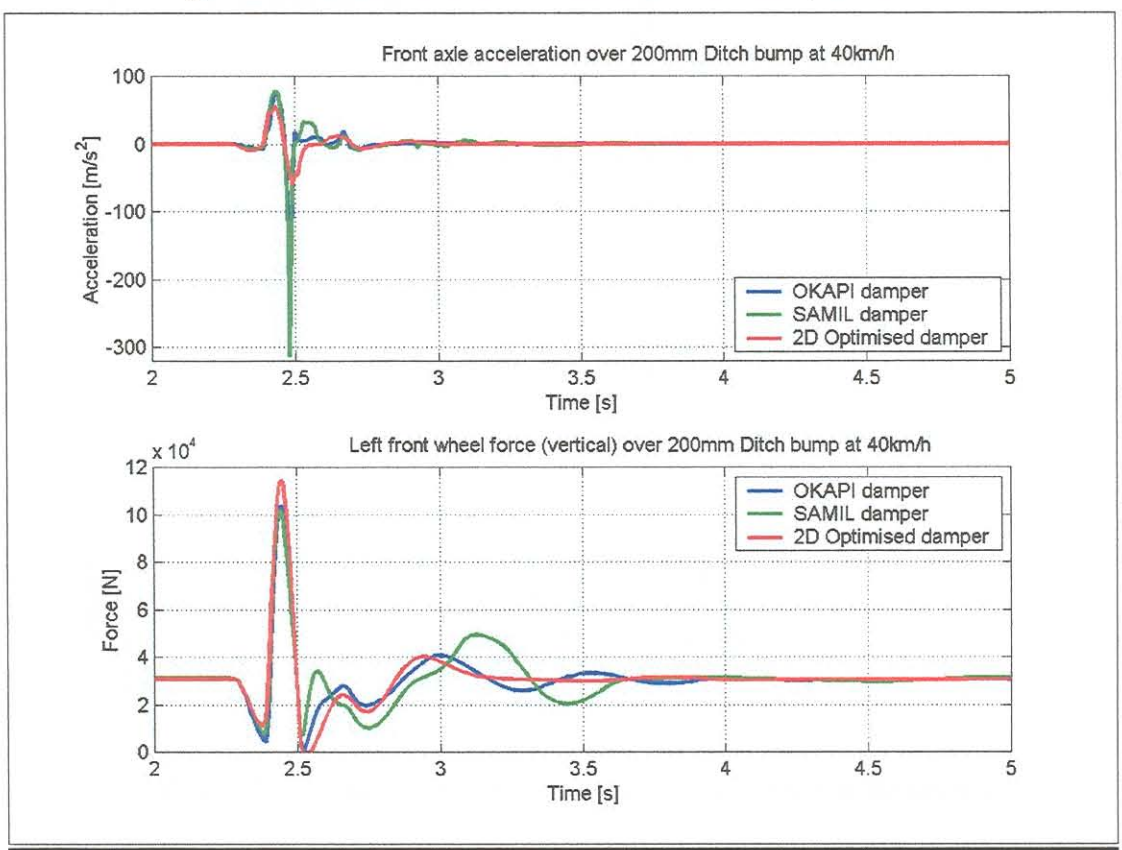

Figure 5.55: DADS simulation results for ditch bump at 40 km/h

5.7.2 Gravel track

DADS simulation results for a portion of the gravel track at 40 km/h simulations are shown in figures 5.56 to 5.59. From the simulation results the following can be seen:

i. The 2D Optimised damper produced lower PSD (power spectrum density) values for the axle accelerations in the frequency region 3 to 10 Hz - see figure 5.56.
ii. The total square root of the wheel force PSD and the RMS of the dynamic wheel force for the 2D Optimised damper compares well with, and is often lower than those for the Okapi and Samil dampers - see figure 5.57.
iii. While the square root of the axle acceleration and RMS of axle accelerations of the 2D-Optimised damper are comparable to that of the Okapi damper, it also gives comparable ride comfort to that of the Samil damper (figures 5.58 and 5.59).
iv. The overall performance of the 2D Optimized damper over the gravel track, as was also found previously for the ditch bump, is significantly better than that of the other two dampers.

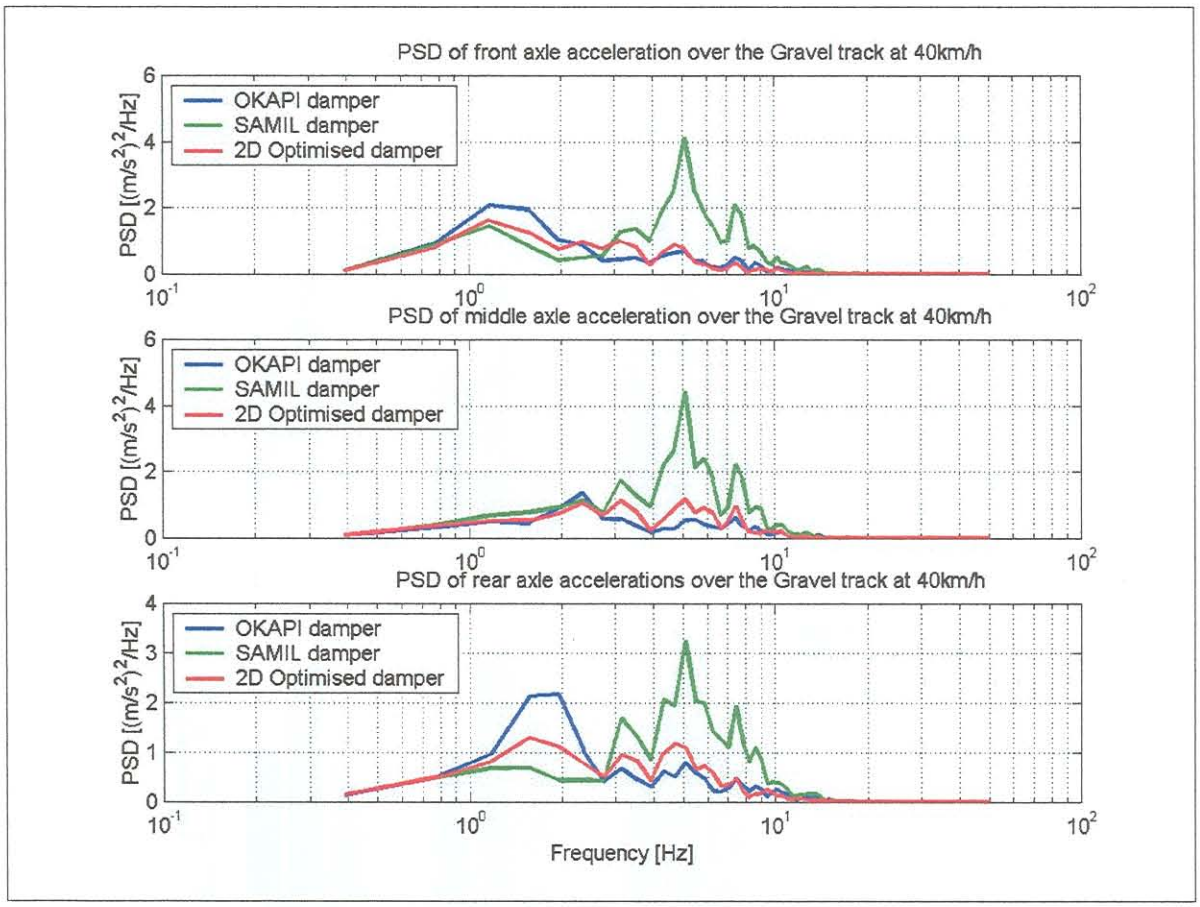

Figure 5.56: DADS simulation results for gravel track at 40 km/h

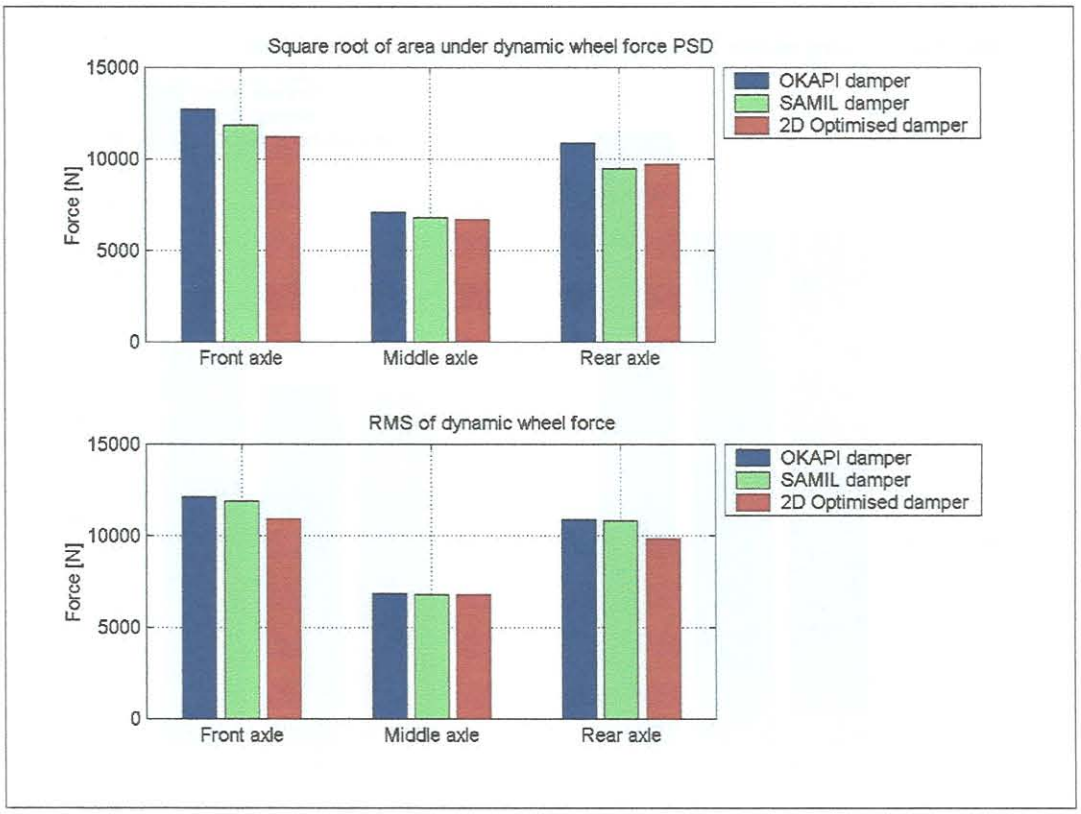

Figure 5.57: DADS simulation results for gravel track at 40 km/h

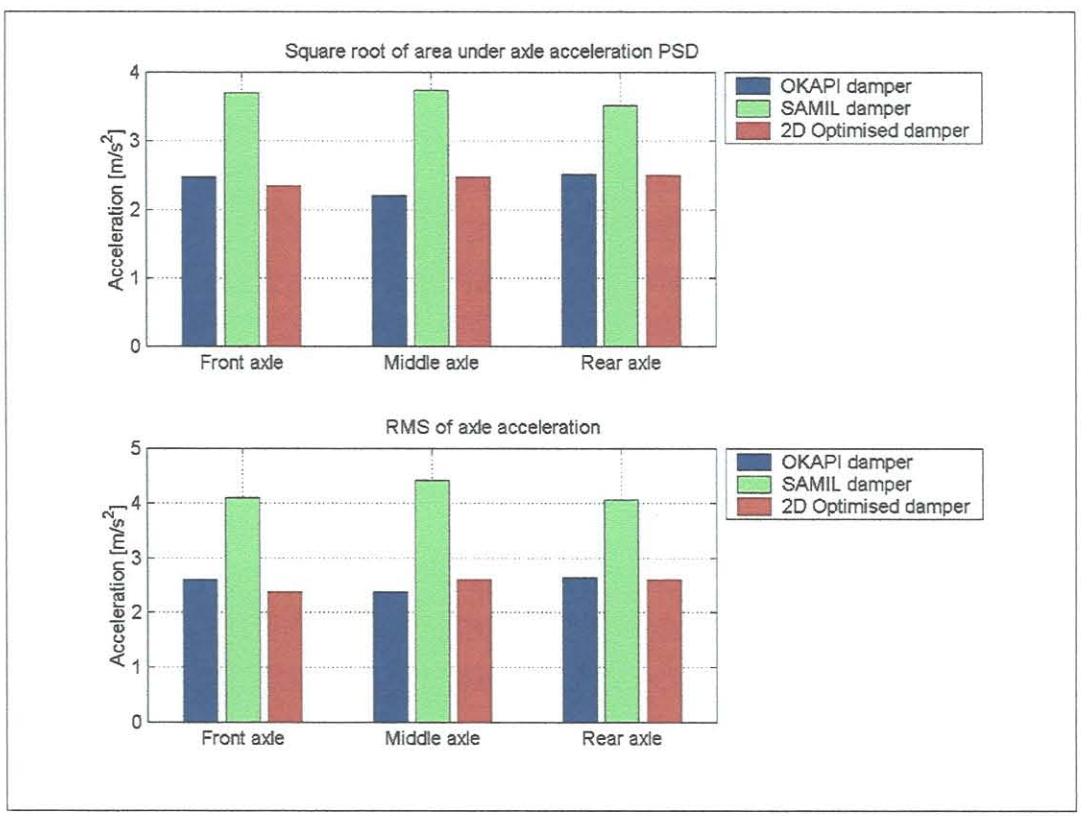

Figure 5.58: DADS simulation results for gravel track at 40 km/h

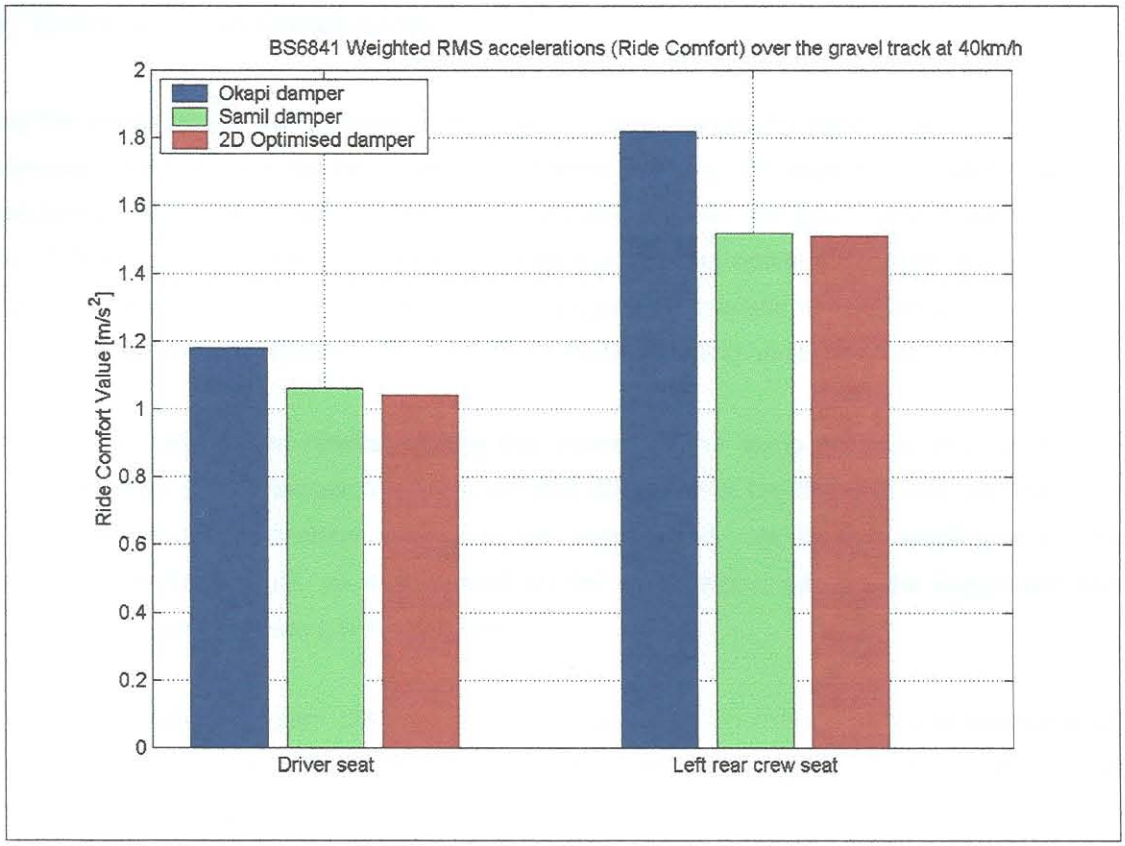

Figure 5.59: DADS simulation results for gravel track at 40 km/h

5.8 Summary and Conclusion

Using the simulation program Vehsim2d in conjunction with the LFOPC optimisation module, optimum suspension characteristics for the Okapi vehicle were obtained with regard to its performance over, respectively, the dirt road, the new Belgian paving and the 200 mm ditch bump route profiles. For each of these route profiles and prescribed speeds a different optimum damper characteristic was obtained. From these optimum characteristics a single characteristic was constructed and proposed as a suitable damper characteristic for the Okapi vehicle operating under general off-road conditions.

In general the optimisation results indicate that increasing the bump stiffness and decreasing the rebound stiffness of the damper, improves the ride comfort over the dirt road and ditch bump route profiles where large suspension deflections are experienced. At smaller amplitudes but higher frequency suspension input, as experienced on the new Belgian paving, the suggested damper characteristic gives a decrease in the ride comfort.

Using the simulation program DADS qualification was done on the damper characteristics of the damper suggested by the optimisation study. With this damper, simulation over the ditch bump profile showed a huge decrease in the driver seat and front axle accelerations compared to that of both the existing Okapi/Gabriel damper and the alternative Samil damper. On the gravel track the optimised damper also performed well by giving good ride comfort, low wheel forces as well as low axle accelerations. From this qualification it is clear that the Vehsim2d / LFOPC optimisation system provides realistic results that can successfully be used for the optimisation of suspension characteristics during vehicle development.

CHAPTER 6:

CONCLUSION

6. Conclusion

6.1 Concluding review

The need for a suspension optimisation system arose from difficulties experienced during the design of the Okapi 6x6 armoured personnel carrier. It was realised that an optimisation system is required for vehicle concept design, at which stage little information regarding the geometry of the vehicle and suspension is available. It was proposed that a two-dimensional vehicle dynamic simulation program would be sufficient for use during the initial design phase, at which stage it could also be coupled to a mathematical optimisation algorithm which could point to possible optimum designs.

From an overview of work done in the field of suspension optimisation it is apparent that first order optimisation has been done in the past in this area via parametric studies. The latest development is, however, the application of mathematical optimisation algorithms in conjunction with computer aided simulation of the vehicle system, to determine optimum values for the design variables through the minimisation of a suitably chosen objective function. This development is in keeping with the application of a multidisciplinary design optimisation approach in almost every other engineering field. The work that has been done to date in the area of vehicle optimisation all achieved specific design optimisation goals but the methods used are not general enough to be applied directly to the current problem. Furthermore the existing methods can be computationally intensive when applied to the design of multi-body systems and may require specialised hardware and software.

A number of classes of optimisation algorithms is available for design optimisation. Most of these algorithms have successfully been applied to engineering optimisation problems. One of the optimisation algorithms that stand out is the LFOPC algorithm. This algorithm is a proven robust method and is particularly suited for use in problems where numerical noise and discontinuities may occur as typically experienced in the computer-aided analysis of mechanical systems.

The overall objective of this study was therefore ***the application of a formal mathematical approach to the optimisation of vehicle suspension characteristics*** with the following specific goals being set:

i. The process should be general enough to be applied to different vehicles consisting of a single vehicle body and up to four axles.
ii. The optimisation process must be able to optimise non-linear suspension characteristics for the different suspension components, namely springs, dampers, bump-stops and tyres. The specific design variables to be used must be user configurable.
iii. The specific objective function used must be user configurable.

iv. The optimisation process should be suitable for use during the concept design stage of the vehicle. During this stage only limited information regarding the geometry of the specific vehicle and suspension is available.

v. The system should be usable by the project manager, who may have a limited knowledge and experience of vehicle dynamic analysis.

In order to achieve the above goals accurately, yet within acceptable economy, a two dimensional mathematical model for the simulation of the vehicle dynamics was developed. Six piece-wise continuous linear approximations were used to describe the non-linear suspension characteristics of each spring, damper, bump stop and tyre used in the simulation model. Basically the vehicle model consists of five solid bodies, one representing the vehicle body and one body for each of up to four axles on the vehicle. Six degrees of freedom are used to describe the motion of the system of bodies. The suspension is modelled by using an equivalent trailing arm approach. The governing equations of motion are derived via the application of Newton's second law. Accelerations are determined for each time instant once the forces acting on the bodies due to the prescribed road inputs are calculated. Using a fourth order Runga Kutta numerical integration scheme the velocities and displacements of the bodies are computed at uniformly spaced time intervals.

The application of the robust and reliable LFOPC optimisation algorithm in conjunction with the vehicle dynamics model is also described. Using the LFOPC algorithm a set of design variables, linked to vehicle parameters, can be determined that minimises a specific user defined objective function.

Although the literature overview warns against the difficulties of linking a multi-body code directly to a mathematical optimisation algorithm, this approach was nevertheless taken in this study. Recent advances in computer processing power and the use of a multi-body code that is simple yet realistic, made this route more attractive. Further motivations were the robustness and reliability of the LFOPC algorithm that was to be used for the optimisation.

The simulation program Vehsim2d implements the two-dimensional vehicle model and input to the program is kept as limited as possible. The simulation program Vehsim2d was qualified by comparing its results with that of the simulation program DADS and with experimental measurements of the actual behaviour of the Okapi vehicle. For the qualification the vehicle was simulated and driven over a 200 mm half round bump at a speed of 20 km/h. Comparison between simulated and measured data shows very good correlation. From this qualification it is concluded that the simulation program Vehsim2d gives realistic results and can be successfully used as a simulation program during vehicle concept design.

The robust LFOPC optimisation algorithm is linked to the Vehsim2d code. With this optimisation algorithm the user may select the required design variables and link them to certain vehicle / suspension characteristics. Constraints on the design variables can also be prescribed. By selecting suitable objective criteria and weights the user builds an appropriate objective function that is to be minimised. Using the LFOPC optimisation algorithm a systematic search is effectively done through the design space for the optimum sets of design variable that minimises the objective function.

To initially evaluate the optimisation system examples of optimisation runs were performed to optimise certain damper and spring characteristics. These examples are also used to explain and demonstrate the Vehsim2d/LFOPC optimisation system to the reader. For the specific example vehicle, a reduction of 24.4 % in the objective function, linked to ride comfort over a specified road profile and at a representative speed, was obtained by optimisation of the bump and rebound characteristics of the damper.

In a further and more comprehensive case study the Vehsim2d / LFOPC optimisation system was used to compute optimum suspension characteristics for the Okapi vehicle over, respectively, a dirt road, new Belgian paving and a 200 mm ditch bump route profile. For each of these route profiles and prescribed speeds, a different optimum damper characteristic was obtained. From these optimum characteristics a single characteristic was constructed as a preferred damper characteristic for the Okapi vehicle.

In general the optimisation results indicate that increasing the bump stiffness and decreasing the rebound stiffness of the damper improves the ride comfort over the dirt road and ditch bump route profiles where large suspension deflections are experienced. However, in the case of smaller amplitude but higher frequency suspension input, as experienced on the new Belgian paving, the suggested damper characteristic gives a decrease in the ride comfort.

Using the simulation program DADS a qualification was done of the damper characteristics for the damper suggested by the optimisation study. Simulation over the ditch bump profile with the optimised damper shows large decreases in the driver seat and front axle accelerations compared to that given by both the existing Okapi/Gabriel damper and the alternative Samil damper. On the gravel track the optimised damper also performed well by giving good ride comfort, low wheel forces and axle accelerations. The qualification proves that the Vehsim2d / LFOPC optimisation system may successfully be used for the optimisation of suspension characteristics during vehicle development.

In retrospect all the specific goals set at the start of this study have been achieved. The final product produced by this study, the Vehsim2d/LFOPC system, has indeed already proved its worth outside of academia, through its practical implementation by Land Mobility Technologies (Pty) Ltd, who have concluded that "The Vehsim2d software has proved to be a valuable tool for any vehicle designer" [62].

6.2 Future work and challenges

The biggest problem that remains is the fact that, for passive suspensions, each choice of road profile and speed yields a different set of optimum spring, bump stop and damper characteristics. In order to prescribe overall optimum characteristics, the optimisation should be done by simultaneously considering a wide range of profiles and speeds. The computational cost is, however, prohibitive. During this study this problem was addressed by selecting a few different road profiles, typical of those that will be encountered by the vehicle. For each profile a more or less arbitrary but appropriate speed value was assigned and the optimisation performed. The "overall optimum" was then obtained by averaging the different optimum characteristics. The challenge remains to refine the methodology such that the vehicle's specific mobility requirements can be used to determine the correct, appropriate and representative sets of road profiles and speed values to be used for the optimisation. This method should also prescribe the way in which the different "optimums" obtained should be combined to give a final preferred design.

Concurrent with the development of the Vehsim2d / LFOPC program a more efficient optimisation technique, called Dynamic-Q [67] was developed. The Dynamic-Q method consists of applying the existing dynamic trajectory optimisation algorithm (LFOPC) to successive spherical quadratic approximations of the actual optimisation problem. The Dynamic-Q algorithm has the advantage of having minimal storage requirements, thus making it suitable for problems with a very large number of variables and, even more importantly with regard to the current study, appears to require an order less number of iterations for convergence. The indications are therefore that this new method is robust and efficient, and particularly well suited for practical engineering optimisations problems where the functions are computed via time-consuming simulations. In a future version of Vehsim2d the Dynamic-Q method must be added as an alternative to the LFOPC method used in the current version. In summary, the advantage of the Dynamic-Q method should be the use of a dramatically less number of simulations and therefore quicker convergence to the optimum solution with a great resultant saving in computer time.

The ultimate challenge will be to use the Dynamic–Q method in conjunction with a full three dimensional vehicle dynamic simulation program such as, for instance, GENRIT, to enable optimisation of vehicle / suspension characteristics over a full three dimensional route profile.

6.3 Response to some questions raised at the defense of this disseratation

Why model suspension and tyre characteristics by piecewise linear functions? Why not use a cubic polynomial or spline function? This would make the function space much smoother with little, if any, increase in complexity.

Even using cubic polynomial functions will require dividing the characteristic range into at least two stages, for instance in the case of a damper into a bounce and rebound stage. For each stage at least three variables (three coefficients) need to be used. To account for both stages will require at least six variables. See the example in figure 6.1 for the bounce stage of a specific damper.

For the same stage, using the linear approximations, five variables are used. As can be seen from the example shown in figure 6.1 the linear approximations provide as good, if not a better model than the polynomial (albeit that the latter may be smoother).

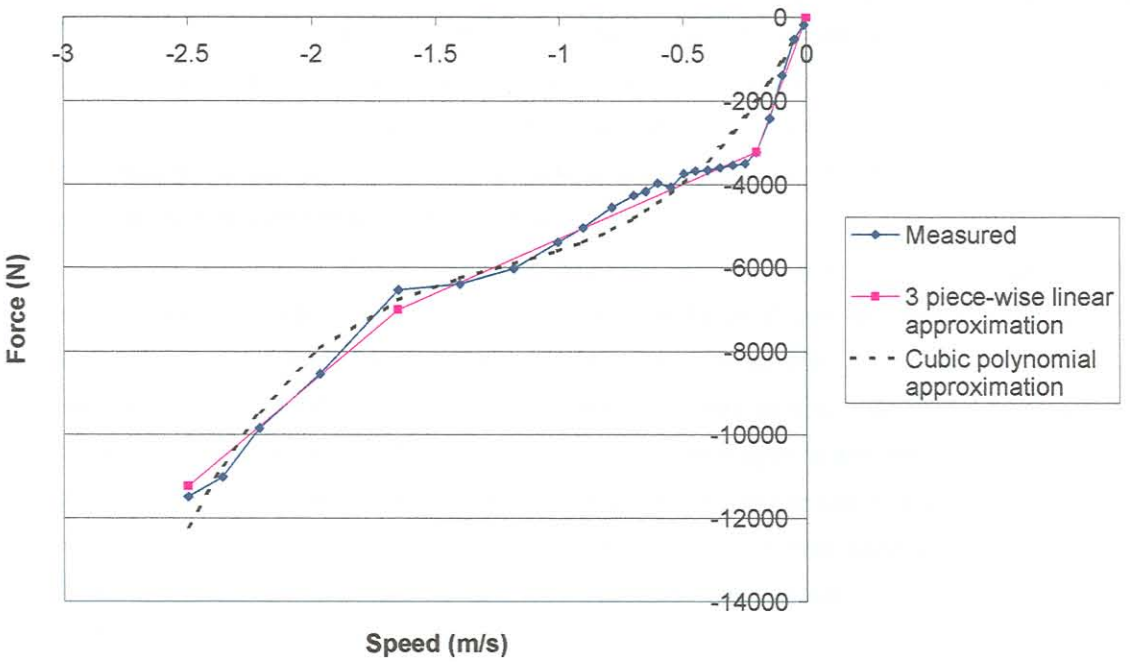

Figure 6.1: Comparison of different approximations for a specific damper characteristic

The second reason for using the piecewise linear approximation is that in reality most of the suspension force characteristics are normally piecewise linear, for example a two stage coil spring or a leaf spring with a helper spring that starts working at a certain deflection. Even damper characteristics can be divided into stages where certain valves open or close to give approximate linear damping in specific operating stages. Tyre characteristics show the same tendency, the first two stages are influenced by the carcass stiffness and tyre pressure and the last by the run-flat insert.

Thus, although the polynomial approximation provides a smoother characteristic, it was decided that using the linear approximations is more realistic and in addition the variables used can directly be linked to the damping stiffness, spring stiffness etc.

The argument for writing a new 2-d simulation program is not very compelling, though it's certainly a good learning exercise. For example, how much time does DADS require for a similar analysis? Is it necessary to write an optimisation friendly analysis? Why not just couple DADS with the optimiser?

The reasons for choosing a 2-d simulation program are as follows:

- Etman [5] states that using a full 3-d analysis complicates the identification of the design parameters that are critical. He suggests that using a 2-d analysis coupled to optimisation is preferable in order to understand the problem better.
- The 3-d program available to us is the locally developed GENRIT (comparable with DADS). The runtime for GENRIT for a similar simulation is only approximately 20% longer than that for the 2-d Vehsim2d analysis. Unfortunately DADS' runtime and the Vehsim2d runtime could not be compared due to the fact that both programs are not available on the same computer. Previous experience, however, shows that the GENRIT runtime is normally faster than that for DADS. This is due to the fact that GENRIT was developed as a dedicated vehicle dynamics package in comparison with the more general DADS package. Faster runtime was however, not the main reason for selecting a 2-d simulation.
- The main objective of this work was to enable optimisation during the early design stages (even during concept design) of a vehicle. At this stage all the required input for a vehicle model for a complete 3-d analysis are generally not yet available.
- As stated in the thesis, the 2-d simulations are only used for first order simulations and more advanced simulations should be performed during later stages in the vehicle design process.
- An additional objective was to provide a program that is easy to use by the project manager of the vehicle design project. Previous experience has shown that these project managers are often not qualified and/or do not have the necessary experience to use the more advanced and complicated packages.

The maximum optimisation time was under 20 minutes. This is trivial. We have clients who's analysis alone takes hours on a supercomputer. The issue is whether the time spent to optimise generates significant pay-off.

The important issue is certainly "significant pay-off". I believe that this study has shown that such goals can indeed be achieved by the modest modelling and optimisation system developed here. This is demonstrated by obtaining a 40% improvement in ride comfort after optimising the suspension under non-trivial conditions.

Further, the faster runtime of a simple 2-d vehicle analysis during vehicle concept is certainly of value. From my own experience, the more advanced simulations do give more accurate results but, by using first order simulations coupled to the optimisation, good "ball-park" starting designs may be obtained for further and more advanced simulations.

The optimisation problem is presented with general inequality and equality constraints (g and h), but it seems only bounds on the variables are actually considered. These are normally called side constraints and should never be allowed to be violated. For example, if we let a spring thickness be a design variable with a lower bound of 0.1, what's to prevent the optimiser from trying –0.1? This would rain havoc on the analysis.

Although the optimisation code allows for both types of constraints, indeed only the inequality constraints (side constraints) were used. The problem of entering a prohibited region of the design space is described in the thesis (see page 4-6). It was specifically noted that the lower bound should be such that, for example, a negative spring stiffness is not used during the simulations. The maximum violation allowed at the lower bound is two times the delta for the specific design variable. The code was accordingly modified in such a manner that a design variable, as it is changed along the optimisation trajectory, was not allowed to go below this value. The LFOPC code is robust enough so as not to fail as a result of such drastic "intervention".

100 plus optimisation iterations seem excessive for a modern optimiser, especially with so few variables.

In the majority of the examples given the objective function effectively converged to its optimum value, and to engineering accuracy, within the first ten iterations. The relatively sluggish convergence of the design variables, compared to that of the objective function is not due to a deficiency on the part of the optimiser, but due to the fact that in these types of optimisation problems the optimum is not unique but corresponds to a wide range of design variable values. The tight convergence tolerances set for the examples also led to a higher number of iterations than would normally be required for engineering accuracy – see the discussion on page 4-23.

Further, as stated in the conclusion, concurrent with this study a more efficient optimisation technique, called Dynamic-Q, was developed. In further work it is suggested that this technique should be added to the optimisation system as an alternative to the LFOPC method.

What about realistic constraints? For example, it's easy to imagine a case where the integrated ride quality is good, but includes unacceptable accelerations, displacements or forces. If we have overall good ride quality but break an axle due to one big bump, what have we gained?

Yes, this is certainly true. Therefore careful consideration should be given to the selection and weighting of the objective function criteria. For instance in the case study the "overall optimum" gives worse ride comfort over some of the road profiles selected. Further analysis of the simulation results for the "optimum configuration" should also be done to evaluate and to pick up other problems that may arise for the specific configuration. In the case study this was done by performing, for example, more advanced DADS simulations with the "optimum damper configuration".

To illustrate the need and value of additional analysis, the optimisation example in chapter 4, was redone with inclusion of the absolute value of the maximum tyre forces (that may break the axles) in the objective function, (see figure 6.2 and 6.3):

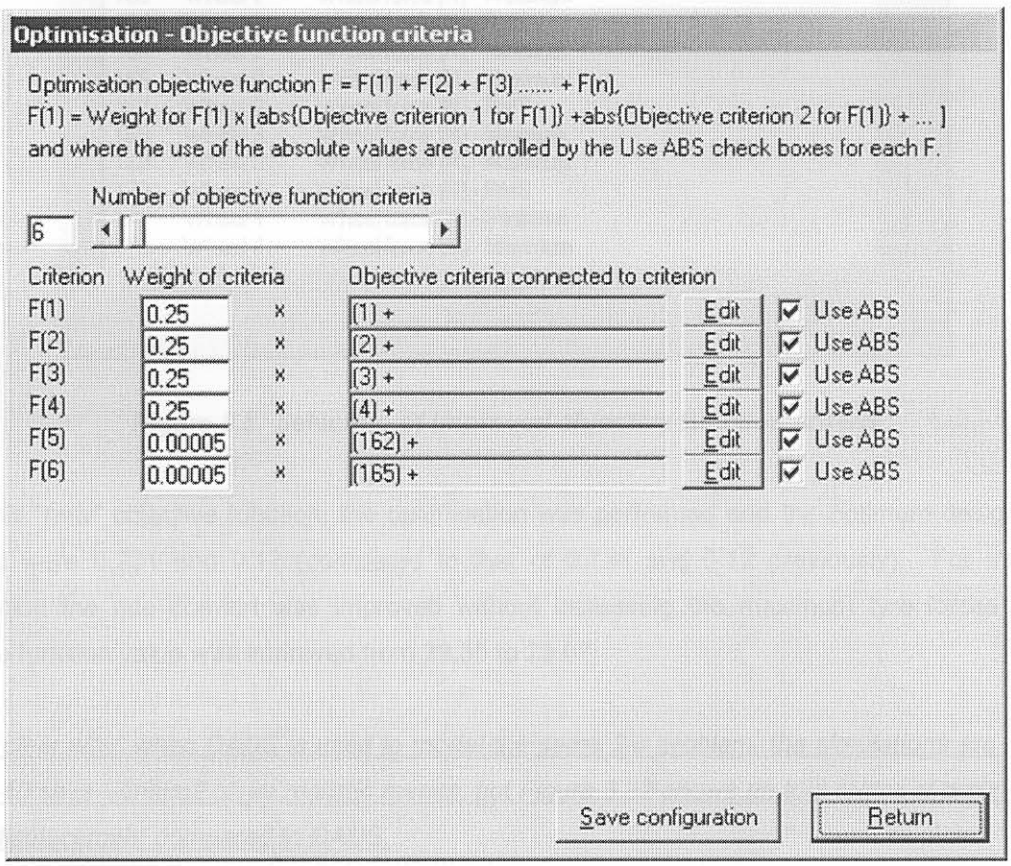

Figure 6.2: Selection of improved objective function criteria

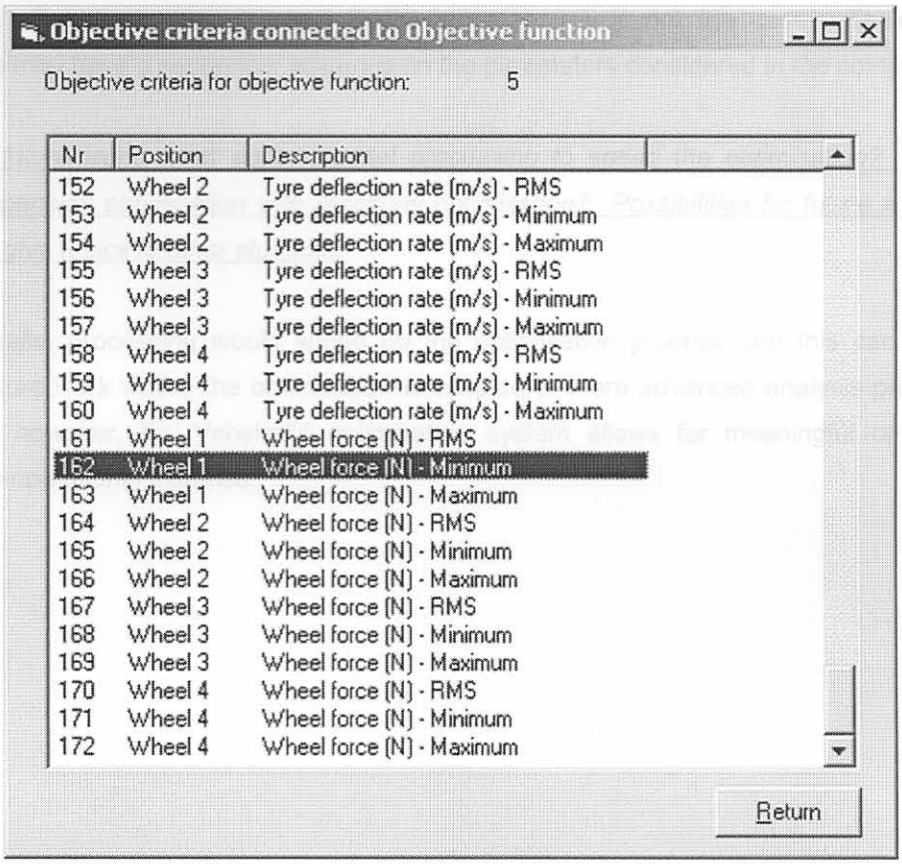

Figure 6.3: Selection of improved objective function criteria

Using this "new" objective function, the optimisation was performed and the optimum design values obtained were 0.731 and 0.12 (compared to that of 0.726 and 0.12 previously). For this "new" optimisation the ride comfort was improved without increasing the maximum tyre forces and the objective function value was improved from 29.55 to 25.07.

It is not clear why, when DADS is used to model the same 2-d problem, the simulations are different. Page 3-40 says Vehsim2 gives realistic results, but Figure 3.32 shows up to a factor of two difference with in displacement compared to DADS.

The main factor influencing the simulation results over such an extreme obstacle as the 200 mm bump used in this instance, is the specific tyre model used. The tyre model used in the Vehsim2d program is a tyre model developed for the GENRIT program and is different from the tyre model used by DADS. During the development of this tyre model measured and simulated tyre forces was used to qualify the tyre model. Even when comparing values obtained from the DADS model with the measured results, agreement between the simulation and measured values is not obtained.

Furthermore, in encountering such an extreme obstacle, the tyres also experience horizontal forces. The horizontal acceleration in the Vehsim2d program is neglected and the vehicle speed is simulated

as constant. For the more advanced DADS package this is not the case. These horizontal accelerations may have a secondary influence on the parameters considered in the comparison.

In terms of future work, what about parallel processing to speed the optimisation? What about coupling suspension optimisation with structural optimisation? Possibilities for future work could be expanded to give topics to other students.

Certainly parallel processing would speed up the optimisation process and this can certainly be applied in future work where the optimisation is coupled to more advanced analysis programs. For the present, however, the Vehsim2d optimisation system allows for meaningful optimisation at affordable computational expense.

REFERENCES

References

1. Niemand, L.J., Naudé, A.F., Raath, A.D., Fatigue investigation on Okapi axles, Report nr. VLG97/017, Laboratory for Advanced Engineering, Pretoria, South Africa, pp. 4-10, 1997.

2. Naudé, A.F., Ondersoek: Asfalings op Okapi ("Investigation of axle failures on the Okapi"), Report number VLG97/018, Laboratory for Advanced Engineering, Pretoria, South Africa, pp.1-9, 1997.

3. Genrit – 'n Algemene voertuigmodel vir die simulasie van ritdinamika ("Genrit – A general vehicle model for the simulation of ride dynamics), Report number 84/113, Laboratory for Advanced Engineering, Pretoria, South Africa, 1984.

4. Haug, E.J., Computer-aided kinematics and dynamics of mechanical systems, Allyn and Bacon, 1989.

5. Etman, P., Optimization of multibody systems using approximation concepts, Eindhoven Technische Universiteit, Eindhoven, 1997

6. Gillespie, T.D., Fundamentals of vehicle dynamics, Society of Automotive Engineers, 1992.

7. Sternberg, E.R., Heavy-duty truck suspensions, SAE Technical Paper 760369, Society of Automotive Engineers, Warrendale, U.S.A., 1976.

8. Nunney, M.J., Light and heavy vehicle technology, Heinemann Newnes, 1988.

9. Wong, J.Y., Theory of ground vehicles, John Wiley & Sons, 1978.

10. ISO 2631, Guide for the evaluation of human exposure to whole-body vibration, Second edition, International Organization for Standardization, 1978.

11. Nell, S., Evaluation of ride comfort criteria Phase 1: Literature study, Document number R0012498-0628, Reumech Ermetek, Elandsfontein, South Africa, pp. 1-36, 1997.

12. Pradko, F., Lee, R.A., Vibration Comfort Criteria, SAE Technical Paper 660139, Society of Automotive Engineers, Warrendale, U.S.A., 1966

13. British Standard Guide to Measurement and Evaluation of Human Exposure to Whole Body Mechanical Vibration and Repeated Shocks, BS6841, British Standard Institution, 1987.

14. Els, P.S., The application of ride comfort standards to off-road vehicles, Presented at: Human response to vibration 34th meeting of the UK group, 22-24 September 1999, Institute of Sound and Vibration Research, University of South Hampton, Dunton, Essex, England, pp. 281-292, 1999.

15. Barak, P., Magic numbers in design of suspensions for passenger cars, SAE Technical Paper 911921, Society of Automotive Engineers, Warrendale, U.S.A., pp. 1-36, 1991.

16. http://www.adams.com/solutions/auto/apps.htm#chassis, Automotive Industry Applications – Chassis: Vehicle Dynamics, 2000.

17. Heyns, P.S., Naudé. A.F., Bester, C.R., et.al, Ondersoek na aspekte van die ontwerp van 'n houersmobiliseringseenheid ("Investigation on aspects of the design of a container carrier"), Report number LGI92/023, Laboratory for advanced engineering, Pretoria, South Africa, pp. 1-64, 1992.

18. Naudé, A.F., Suspensie optimering van die Mingwe ("Suspension optimisation of the Mingwe vehicle"), Report nr. VLG89/109, Laboratory for advanced engineering, Pretoria, South Africa, 1989.

19. Lee, H., Lee, G., Kim, T., A study of ride analysis of medium trucks with varying the characteristics of suspension design parameters, SAE Technical Paper 973230, SP 1308, Society of Automotive Engineers, Warrendale, U.S.A., pp. 75-80, 1997.

20. Motoyama, K., Yamanaka, T., Hoshino, H., A study of automobile suspension design using optimization technique, 8th AIAA/USAF/NASA/ISSMC Symposium on Multidisciplinary Analysis and Design, 6-8 September 2000, Long Beach, California, pp.1-6, 2000.

21. Lee, T.H., Lee, K., Fuzzy multi-objective optimization of a train suspension using response surface model, 8th AIAA/USAF/NASA/ISSMC Symposium on Multidisciplinary Analysis and Design, 6-8 September 2000, Long Beach, California, pp. 1-7, 2000.

22. Botkin, M.E., Structural optimization of automotive body components based upon parametric solid modelling, 8th AIAA/USAF/NASA/ISSMC Symposium on Multidisciplinary Analysis and Design, 6-8 September 2000, Long Beach, California, pp.1-9, 2000.

23. Etman, L.F.P., Van Campen, D.H., Schoofs, A.J.G., Optimization of multibody systems using approximation concepts, IUTAM Symposium on optimization of mechanical systems, Kluwer Academic Publishers, pp. 81-88, 1996.

24. Park, T., Bang, W., Optimal design of a suspension using a mechanism analysis program, SAE Technical Paper 9530995, Society of Automotive Engineers, Warrendale, U.S.A., 1995.

25. Sanayama, M., Kobayashi, K., Satoh, Y., et.al., Improvement of ride comfort on motorway, SAE Technical Paper 9530931, Society of Automotive Engineers, Warrendale, U.S.A., 1995.

26. Esat, I., Optimisation of a double wishbone suspension system, Engineering Systems Design and Analysis, PD-Vol 81, Vol 9, ASME, pp. 93-98, 1996.

27. Emura, J., Kakizaki, S., Yamaoka, F., et.al., Development of the semi-active suspension system based on the sky-hook damper theory, SAE Technical Paper 940863, Vehicle suspension system advancements, SP 1031, Society of Automotive Engineers, Warrendale, U.S.A., pp. 17-26, 1994.

28. Moline, D., Floyd, S., Vaduri, S., et.al., Simulation and evaluation of semi-active suspensions, SAE Technical Paper 940864, Vehicle suspension system advancements, SP 1031, Society of Automotive Engineers, Warrendale, U.S.A., pp. 26-38, 1994.

29. Wilkinson, P.A., Advanced hydraulic suspension ride simulation using a 3-dimensional vehicle model, SAE Technical Paper 940866, Vehicle suspension system advancements, SP 1031, Society of Automotive Engineers, Warrendale, U.S.A., pp. 47-56, 1994.

30. Reybrouck, K., A non linear parametric model of an automotive shock absorber, SAE Technical Paper 940869, Vehicle suspension system advancements, SP 1031, Society of Automotive Engineers, Warrendale, U.S.A., pp. 79-86, 1994.

31. ElBeheiry, E.M., Karnopp, D.C., Optimization of active and passive suspensions based on a full car model, SAE Technical Paper 951063, Society of Automotive Engineers, Warrendale, U.S.A., 1995.

32. Saxon, N.L., Meldrum, W.R. Semi-active suspension: a field testing case study, SAE Technical Paper 981119, Society of Automotive Engineers, Warrendale, U.S.A., 1998.

33. Yu, F., Crolla, D.A. Analysis and benefits of an adaptive Kalman filter active vehicle suspension, SAE Technical Paper 981120, Tire, wheel, steering and suspension technology, SP 1338, Society of Automotive Engineers, Warrendale, U.S.A., pp. 195-200, 1998.

34. Roh, H-S., Park, Y., Preview control of active vehicle suspensions based on a state and input estimator, SAE Technical Paper 981121, Tire, wheel, steering and suspension technology, SP 1338, Society of Automotive Engineers, Warrendale, U.S.A., pp. 201-208, 1998.

35. Nicolas, C.F., Landaluze, J., Castrillo, M., et.al., Application of fuzzy logic control to the design of semi-active suspension systems, IEEE International Conference on Fuzzy Systems v 2, IEEE, pp. 987-983, 1997.

36. Kutche. T., Raulf, M., Becher, H-O., Optimized ride control of heavy vehicles with intelligent suspension control, SAE Technical Paper 973207, Society of Automotive Engineers, Warrendale, U.S.A., pp. 63-67, 1997.

37. Eiler, M.E., Hoogterp, F.B., Active suspension performance limits for cross-country operation, SAE Technical Paper 970383, Society of Automotive Engineers, Warrendale, U.S.A., 1997.

38. Saxon, N.L., Meldrum, R., Semi-active suspension: A mobility case study, SAE Technical Paper 970386, Society of Automotive Engineers, Warrendale, U.S.A., 1997.

39. Polston, R.K., Freeman, J.S., The influence of suspension modelling techniques on vehicle simulations, Presented at the ASME International Mechanical Engineering Congress & Exposition, Dallas, Texas, Nov 16-21, 1997.

40. Holdmann P., Köhn,P., Möller, B., Suspension kinematics and compliance – measuring and simulation, SAE Technical Paper 980897, Tire, wheel, steering and suspension technology, SP 1338, Society of Automotive Engineers, Warrendale, U.S.A., pp. 91-96, 1998.

41. Zhang, Y., Xiao, P., Palmer, K., et.al. Vehicle chassis/suspension dynamic analysis – finite element model vs rigid body model, SAE Technical Paper 980900, Tire, wheel, steering and suspension technology, SP 1338, Society of Automotive Engineers, Warrendale, U.S.A., pp. 113-126, 1998.

42. Renfroe, D.A., Fleniken, G.L., Designing for pitch and bounce motions of single-passenger off-road vehicles, http://www.renfroe.com/designptich.htm, pp.1-13, 1998.

43. Fleniken, G.L., Renfroe, D.A., Modeling of pitch and bounce motions of single-passenger off-raod vehicles, http://www.renfroe.com/modelptich.htm, pp. 1-18, 1998.

44. Chen. X., Lin, Y., Research on the dynamics of flexible multibody systems of passenger car suspensions, SAE Technical Paper 980899, Tire, wheel, steering and suspension technology, SP 1338, Society of Automotive Engineers, Warrendale, U.S.A., pp. 103-112, 1998.

45. Attia, H.A., Dynamic modelling of common suspension systems using point and joint coordinates, Engineering Systems Design and Analysis, PD-Vol 78, Vol 6, ASME, 1996.

46. Taheri, S. Bahrami, M., Kaynejad, F., Seventeen DOF non-linear vehicle dynamics simulation, Engineering Systems Design and Analysis, PD-Vol 81, Vol 9, ASME, pp. 25-30, 1996.

47. Hedrick, J.K., Butsuen, T., Invariant properties of automotive suspensions, International Conference: Advanced suspensions, The Institution of Mechanical Engineers, MEP, London, 1988.

48. Hastey, J.P., Baudelet, J., Gerard, E., et.al., Optimization on MacPherson Suspensions with a spring, SAE Technical Paper 970100, Steering and suspension technology, SP 1223, Society of Automotive Engineers, Warrendale, U.S.A., pp. 119-124, 1997.

49. Duym, S.M., Stiens, R., Baron, G.V., et.al., Physical modelling of the hysteretic behaviour of automotive shock absorbers, SAE Technical Paper 970101, Steering and suspension technology, SP 1223, Society of Automotive Engineers, Warrendale, U.S.A., pp. 125-138, 1997.

50. Chondros, T.G., Belokas, P.A. Vamvekeros, K., et.al. Vehicle dynamics simulation and suspension system design, SAE Technical Paper 970105, Steering and suspension technology, SP 1223, Society of Automotive Engineers, Warrendale, U.S.A., pp. 169-180, 1997.

51. Snyman, J.A., Craig, K., Proceedings of the International workshop on multidisciplinary design optimization, 7-10 August 2000, Pretoria, South Africa, pp. 1-298, 2000.

52. Papalambros, P.Y., Trends and challenges in system design optimization, Proceedings of the International workshop on multidisciplinary design optimization, 7-10 August 2000, Pretoria, South Africa, pp. 1-15, 2000.

53. Snyman, J.A., A new and dynamic method for unconstrained minimisation, *Appl. Math. Modelling*, Vol 6, pp. 449-462, 1982.

54. Snyman, J.A., An improved version of the original leap-frog dynamic method for unconstrained minimisation LFOP1(b), *Appl. Math. Modelling*, Vol 7, pp. 216-218, 1983.

55. Snyman, J.A., The LFOPC leap-frog method for constrained optimisation, *Computers & Mathematics with Applications*, Vol. 40, pp.1085-1096, 2000.

56. O'Niel, P.V., Advanced Engineering mathematics, Wadsworth Publishing Company, 1986.

57. Jeter, M.W., Mathematical programming: An introduction to optimization, Marcel Dekker Inc., 1986.

58. Snyman, J.A., Craig, K., Practical optimisation for engineers and scientists, Short course notes, Centre for Continuing Education, University of Pretoria, Pretoria, South Africa, 1999.

59. Naudé. A.F., Final Report: Decision making criteria for military vehicle suspension, Report number. AFNET 00/01, A.F. Naudé Engineering Technology, Pretoria, South Africa, pp. 1-18, 2000.

60. Naudé, A.F., Vehsim2d/LFOPC suspension optimisation of the Okapi, Report number. AFNET 00/02, A.F. Naudé Engineering Technology, Pretoria, South Africa, pp. 1-32, 2000.

61. Milliken, W.F., Milliken, D.L., Race car vehicle dynamics, SAE, 1995.

62. Gilliomee, C.L., Report: Okapi damper investigation, Report number R1/00064/1 Issue 1, Land Mobility Technologies (Pty) Ltd, Pretoria, South Africa, pp. 1-29, 2000.

63. Van Niekerk, N., Okapi upgrade DADS model input data file, Internal report, Reumech Ermetek, Elandsfontein, South Africa, 1999.

64. Jansen, B., Okapi: Detail design report on Okapi upgrade project, Report number: R0000495-A624, Vickers OMC, Benoni, South Africa, pp. 1-50, 1999.

65. O'Neil, P.V., Advanced Engineering Mathematics, Second Edition, Wadsworth Publishing Company, 1987.

66. Nocedal, J., Wright, S.J., Numerical optimization, Springer-Verlag, New York, 1999.

67. Snyman, J.A., Hay A.M., The Dynamic – Q optimisation method: An alternative to SQP?, Proceedings of the International Workshop on Multidisciplinary Optimisation, 7-10 August 2000, Pretoria, South Africa, pp.163-172, 2000.

68. Arora, J.S., Introduction to optimum design, McGraw-Hill, New York, U.S.A., 1989.

69. Haftka, R.T., Gürdal, Z., Elements of structural optimisation, Kluwer Academic Publishers, Dordrecht, The Netherlands, 1992.

70. Papalambros, P.Y., Wilde, D.J., Principles of optimal design, Modeling and Computation, Cambridge University Press, U.K., 2000.

71. Vanderplaats, G.N., Numerical optimisation techniques for engineering design, Vanderplaats Research and Development, Colorado springs, U.S.A., 1998.

72. Giliomee, C., Private communication, Land Mobility Technologies (Pty) Ltd, Pretoria, South Africa, 1998.

73. Chirtcow, B., Private communication, Gabriel, Cape Town, South Africa, 1999.

APPENDIX A:

SUPPLEMENT TO CHAPTER 2

Appendix A: Supplement to chapter 2

- **Section A.1**: List of parameters and variables used for vehicle model
- Detailed derivations of some important equations used in chapter 2:
  - **Section A.2**: Deflection of equivalent suspension (Eq. 2.29)
  - **Section A.3**: Total moment acting on vehicle body due to axle i (Eq 2.43)
  - **Section A.4**: Accelerations of different wheels (Eq 2.45 & 2.46)
- **Section A.5**: Snyman's dynamic trajectory optimization method

A.1 List of parameters and variables used for vehicle model

a_i = Distances between axles i and $i+1$ in the initial prescribed position, $i = 1,2,3$

(c_i, x_i) = Parameter pairs for six piece-wise continuous linear representation of force element data, $i = 1,2,...,6$

c^y = Vertical position of centre of gravity

c^x = Horisontal position of centre of gravity

d_i = Horisontal length of the equivalent trailing arm of axle i ,$i = 1,2,3,4$

d_i^w = Longitudinal distance d_i^w between the wheel centre of axle i, $i = 1,2,3,4$ and the centre of gravity as in the initial prescribed position

e_i = Vertical height of the equivalent trailing arm of axle i ,$i = 1,2,3,4$

f_i^a = Force in the equivalent trailing arm of axle i ,$i = 1,2,3,4$

f_i^b = Equivalent bump stop force on axle i ,$i = 1,2,3,4$

f_i^d = Equivalent damper force on axle i ,$i = 1,2,3,4$

f_i^e = Total equivalent suspension force on axle i ,$i = 1,2,3,4$

f_i^s = Equivalent spring force on axle i ,$i = 1,2,3,4$

f_i^w = Resultant tyre force on axle i ,$i = 1,2,3,4$

F^a = Total sum of the components of the trailing arm forces in the direction of q_1

F_i^b = Actual spring force at a deflection of Δ_i^b on axle i ,$i = 1,2,3,4$

F_i^d = Actual spring force at a deflection rate of $\dot{\Delta}_i^d$ on axle i ,$i = 1,2,3,4$

F^s = Sum of the suspension forces

F_i^s = Actual spring force at a deflection of Δ_i^s on axle i ,$i = 1,2,3,4$

F_i^{wd} = Wheel force due to the tyre deflection rate and damping on axle i ,$i = 1,2,3,4$

F_i^{ws} = Wheel force due to the tyre deflection and stiffness on axle i ,$i = 1,2,3,4$

h = Height of the centre of gravity with respect to the reference point 0,0 in the initial prescribed position

I = Pitch inertia of the sprung mass about its centre of gravity

L = Horisontal distance between the sprung mass centre of gravity and the centre of the front axle in the initial prescribed position

m_1 = Mass of the vehicle body (the sprung mass)

m_{i+1} = Mass of the unsprung mass associated with each axle i, $i = 1,2,3,4$

M_i = Moment applied on the vehicle body due to the forces at axle i ,$i = 1,2,3,4$

n_i^w = Number of wheels per axle on axle i ,$i = 1,2,3,4$

n_i^s = Number of springs on the axle on axle i ,$i = 1,2,3,4$

n_i^b = Number of bump stops per axle on axle i ,i = 1,2,3,4

n_i^d = Number of dampers per axle on axle i ,i = 1,2,3,4

q_1 = Vertical displacement at the centre of gravity of the vehicle body

q_2 = Pitch displacement of the vehicle body

q_{i+2} = Vertical displacement at the wheel centre of axle i, i = 1,2,3,4

$\dot{q}_i$ = Velocity associated with q_i, i = 1,2,...,6

$\ddot{q}_i$ = Acceleration associated with q_i, i = 1,2,...,6

$\ddot{q}_i^a$ = Accelerations of the different wheels (perpendicular to the equivalent trailing arm) of axle i, i = 1,2,3,4

r_i = Rolling radius of the tyres on axle i ,i = 1,2,3,4

t = Simulation time in seconds

t_i = Length of the equivalent trailing arm on axle i, i = 1,2,3,4

v = Horisontal (forward) vehicle speed at the centre of gravity of the vehicle body

w_i^x = Horisontal position of the wheel centre on axle i, i = 1,2,3,4 as measured from the reference point

w_i^y = Vertical position of the wheel centre on axle i, i = 1,2,3,4 as measured from the reference point

β_i = Angle of the equivalent trailing arm on axle i, i = 1,2,3,4

δ_i = Deflection of the equivalent suspension on axle i =1,2,3,4

δ_i^s = Initial spring deflection on axle i, i = 1,2,3,4

δ_i^b = Initial bump stop deflection on axle i, i = 1,2,3,4

δ_i^t = Initial tyre deflection on axle i, i = 1,2,3,4

δ_i^w = Resultant tyre deflection on axle i, i = 1,2,3,4

$\dot{\delta}_i^w$ = Resultant tyre deflection rate on axle i, i = 1,2,3,4

δ^t = Integration time step

Δ_i^a = Intermediate distance used to calculate the wheel position w_i^x for axle i, i = 1,2,3,4

Δ_i^b = Intermediate distance used to calculate the wheel position w_i^x for axle i, i = 1,2,3,4

Δ_i^c = Intermediate distance used to calculate the wheel position w_i^x for axle i, i = 1,2,3,4

Δ_i^s = Deflection at the actual spring on axle i, i = 1,2,3,4

Δ_i^b = Deflection at the actual bump stop on axle i, i = 1,2,3,4

$\dot{\Delta}_i^s$ = Deflection rate at the actual damper on axle i, i = 1,2,3,4

θ = Pitch angle of vehicle on a specific time instance

φ_i = Angle of the resultant tyre force on axle i, i = 1,2,3,4 and the vertical

κ_i^s = Ratio between the actual spring deflection on axle i, i = 1,2,3,4 and that for the

equivalent suspension

κ_i^b = Ratio between the actual bump stop deflection on axle i, $i = 1,2,3,4$ and that for the equivalent suspension

κ_i^d = Ratio between the actual damper deflection on axle i, $i = 1,2,3,4$ and that for the equivalent suspension

Λ_i = Tyre force factor on axle i, $i = 1,2,3,4$ determined by the shape of the tyre deflection

A.2 Deflection of equivalent suspension (eq. 2.29)

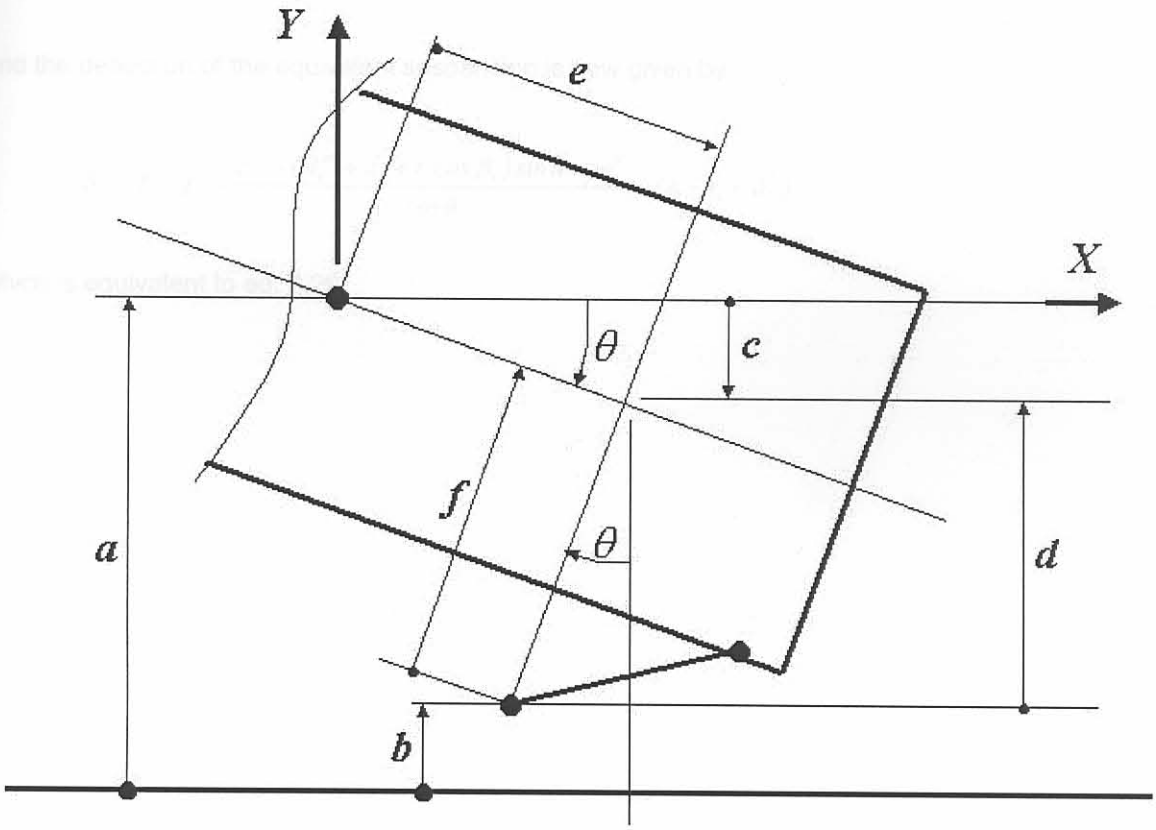

Figure A1: Schematic of vehicle body with one trailing arm for axle i

From figure A1 the value of f can be determined:

$$a = c^y$$

$$b = w^y$$

$$e = d_i^w + d_i + t_i \cos\beta_i \qquad (remember \cos\beta_i < 0)$$

$$c = e\sin\theta = (d_i^w + d_i + t_i \cos\beta_i)\sin\theta$$

$$d = a - c - b$$

$$f = \frac{d}{\cos\theta} = \frac{a-c-b}{\cos\theta} = \frac{c^y - (d_i^w + d_i + t_i \cos\beta_i)\sin\theta - w^y}{\cos\theta}$$

The original value for f (in the prescribed initial position), say f' is given by:

$$f' = h - (r_i + \delta_i^t)$$

and the deflection of the equivalent suspension is now given by:

$$\delta_i = f - f' = \frac{c^y - (d_i^w + d_i + t_i \cos\beta_i)\sin\theta - w_i^y}{\cos\theta} - (h - r_i - \delta_i^t)$$

which is equivalent to eq. 2.29.

A.3 Total moment acting on vehicle body due to axle *i* (eq. 2.43)

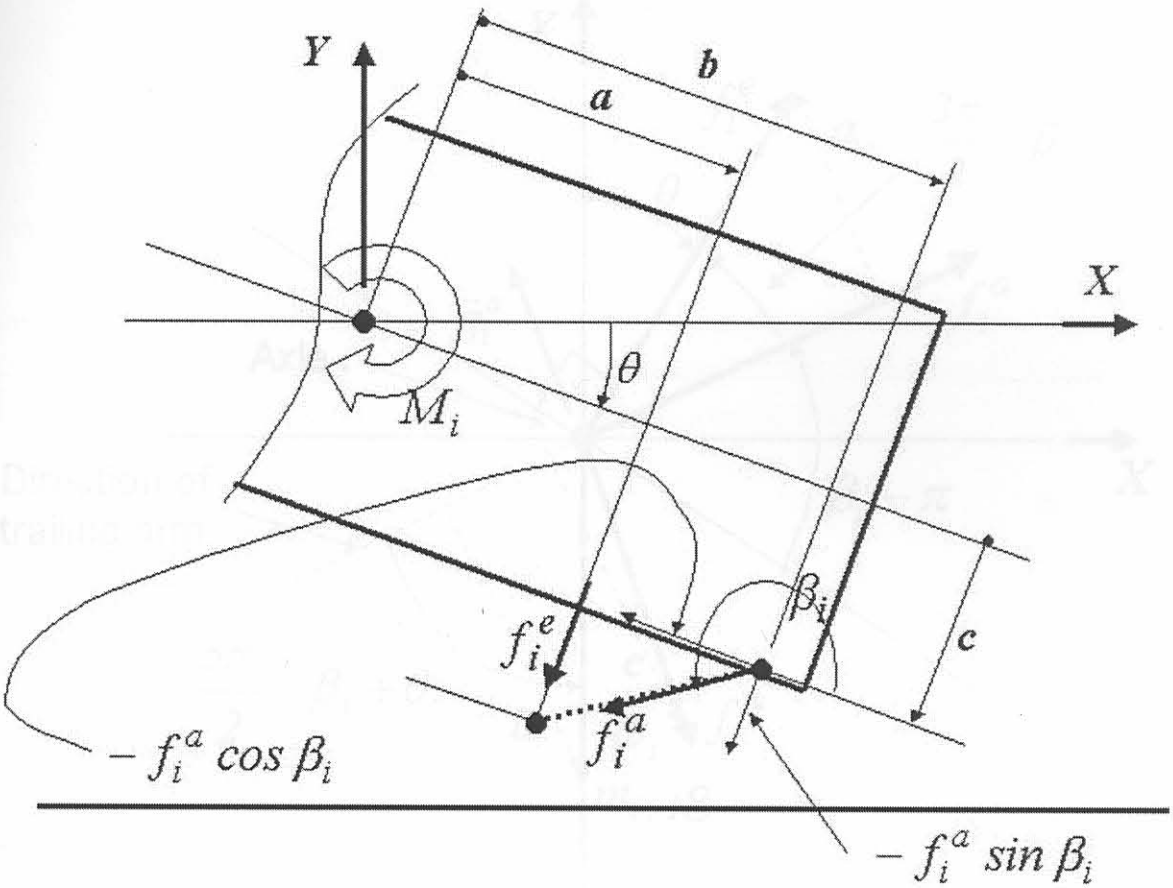

Figure A2: Schematic of vehicle body with one trailing arm for axle i

From figure A2 the moment acting on the vehicle can be determined as:

$$a = d_i^w + d_i + t_i \cos\beta_i \qquad (remember\ \cos\beta_i < 0)$$

$$b = d_i^w + d_i$$

$$c = h - (r_i + \delta_i^t + e_i)$$

$$M_i = a f_i^e + b(-f_i^a \sin\beta_i) + c(-f_i^a \cos\beta_i)$$

$$\Rightarrow M_i = f_i^e(d_i^w + d_i + t_i \cos\beta_i) - f_i^a(d_i^w + d_i)\sin\beta_i - f_i^a(h - r_i - \delta_i^t - e_i)\cos\beta_i$$

which is equivalent to eq. 2.43

A.4 Acceleration of axle center for axle i (eq. 2.45 & 2.46)

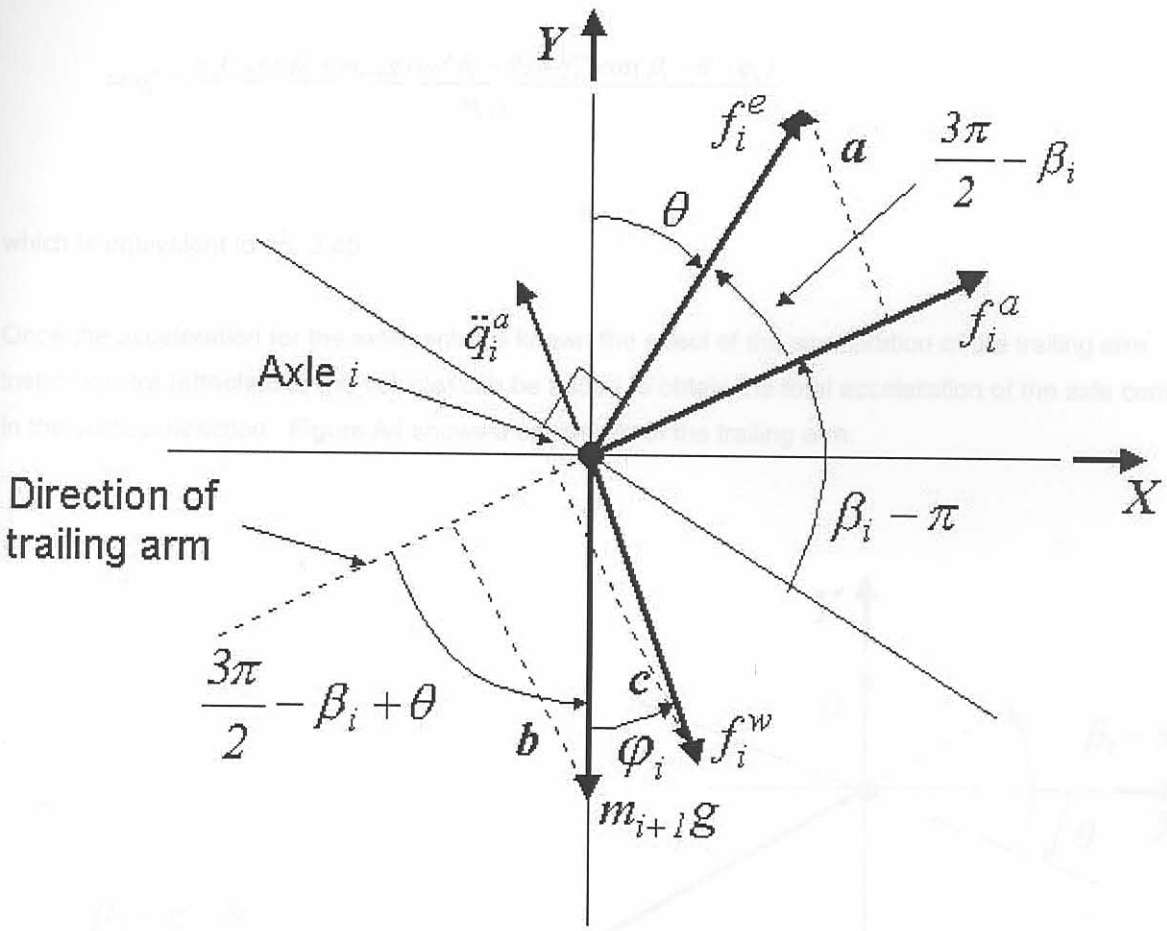

Figure A3: Schematic of axle i

From figure A3 the forces a,b and c is given by:

$$a = f_i^e \sin(\frac{3\pi}{2}-\beta_i) = -f_i^e \cos\beta_i$$

$$b = m_{i+1} g \sin(\frac{3\pi}{2}-\beta_i+\theta) = -m_{i+1} g \cos(-\beta_i+\theta) = -m_{i+1} g \cos(\beta_i-\theta)$$

$$c = f_i^w \sin(\frac{3\pi}{2}-\beta_i+\theta+\varphi_i) = -f_i^w \cos(\beta_i-\theta-\varphi_i)$$

According to Newton's second law the acceleration of the axle centre (perpendicular to the trailing arm) is now given by:

$$\ddot{q}_i^a = \frac{a+b+c}{m_{i+1}}$$

$$\Rightarrow \ddot{q}_i^a = \frac{-f_i^e \cos\beta_i + m_{i+1} g \cos(\beta_i - \theta) + f_i^w \cos(\beta_i - \theta - \varphi_i)}{m_{i+1}}$$

which is equivalent to eq. 2.45.

Once the acceleration for the axle centre is known the effect of the acceleration of the trailing arm instant centre (attached to the vehicle) can be added to obtain the total acceleration of the axle centre in the vertical direction. Figure A4 shows a schematic of the trailing arm.

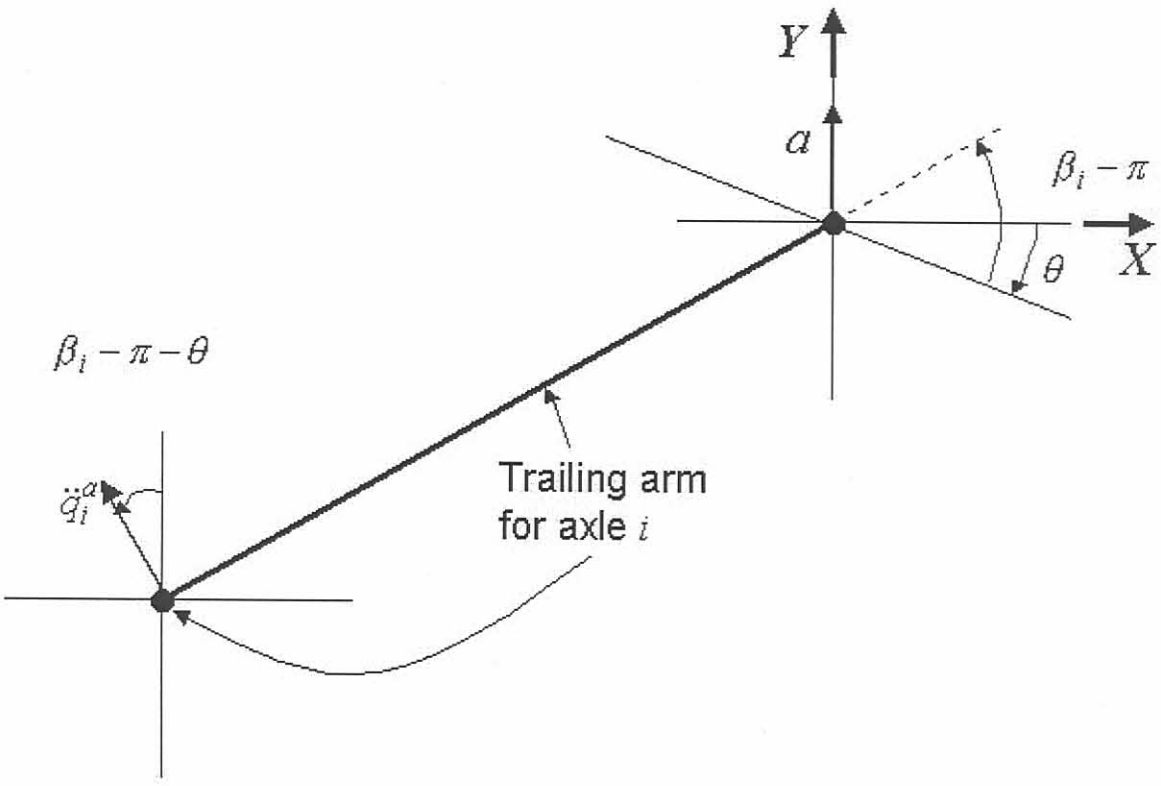

Figure A4: Schematic of trailing arm for axle i

The acceleration of the trailing arm centre (attached to the vehicle), due to the vehicle vertical acceleration and pitch acceleration is given by (also refer to figure A3):

$$a = \ddot{q}_1 - \ddot{q}_2[(d_i^w + d_i)\cos\theta - (h - r_i - \delta_i^t - e_i)\sin\theta]$$

and the vertical acceleration of the trailing arm centre due to $\ddot{q}_i^a$ is given by:

$$b = \ddot{q}_i^a \cos(\beta_i - \theta - \pi) = -\ddot{q}_i^a \cos(\beta_i - \theta)$$

The total acceleration of the wheel centre (vertically upwards) is then given by:

$$\ddot{q}_{i+2} = b + a = -\ddot{q}_i^a \cos(\beta_i - \theta) + \ddot{q}_1 - \ddot{q}_2[(d_i^w + d_i)\cos\theta - (h - r_i - \delta_i^t - e_i)\sin\theta]$$

which is eq. 2.46

A.5 Snyman's dynamic trajectory optimization method

Background

The dynamic trajectory method (also called the "leap-frog" method) for the unconstrained minimization of a scalar function $f(\boldsymbol{x})$ of n real variables represented by the vector $\boldsymbol{x}=(x_1,x_2,\ldots,x_n)^T$ was originally proposed by Snyman [A1,A2]. The original algorithm has recently been modified to handle constraints by means of a penalty function formulation. (Snyman et al [A3,A4]). The method possesses the following characteristics:

- It uses only function *gradient* information $\nabla f(\boldsymbol{x})$.
- *No* explicit *line searches* are performed.
- It is extremely *robust* and handles steep valleys and discontinuities in functions and gradients with ease.
- The algorithm seeks a *low local minimum* and can therefore be used as a basic component in a methodology for global optimization.
- It is not as efficient as classical methods on smooth and near-quadratic functions.

Basic dynamic model

The algorithm is modelled on the motion of a particle of unit mass in a n-dimensional conservative force field with potential energy at $\boldsymbol{x}$ given by $f(\boldsymbol{x})$. At $\boldsymbol{x}$, the force on the particle is given by

$$\boldsymbol{a} = \ddot{\boldsymbol{x}} = -\nabla f(\boldsymbol{x}) \tag{A.1}$$

from which it follows that for the time interval [0,t]

$$\begin{aligned} \tfrac{1}{2}\|\dot{\boldsymbol{x}}(t)\|^2 - \tfrac{1}{2}\|\dot{\boldsymbol{x}}(0)\|^2 &= f(\boldsymbol{x}(0)) - f(\boldsymbol{x}(t)) \\ T(t) - T(0) &= f(0) - f(t) \end{aligned} \tag{A.2}$$

or

$$f(t) + T(t) = \text{constant } \{\text{conservation of energy}\}$$

Note that since $\Delta f = -\Delta T$ *as long as* T *increases* f *decreases. This forms the basis of the dynamic algorithm.*

LFOP: Basic algorithm for unconstrained problems

Given $f(\boldsymbol{x})$ and a starting point $\boldsymbol{x}(0)=\boldsymbol{x}^0$

- Compute the dynamic trajectory by solving the initial value problem (IVP):

$$\ddot{\boldsymbol{x}}(t) = -\nabla f(\boldsymbol{x}(t))$$
$$\dot{\boldsymbol{x}}(0) = \mathbf{0}, \quad \boldsymbol{x}(0) = \boldsymbol{x}^0 \tag{A.3}$$

- Monitor $\boldsymbol{v}(t) = \dot{\boldsymbol{x}}(t)$. Clearly as long as $T = \frac{1}{2}\|\boldsymbol{v}(t)\|^2$ increases $f(\boldsymbol{x}(t))$ decreases as required.
- When $\|\boldsymbol{v}(t)\|$ decreases apply some interfering strategy to extract energy and thereby increase the likelihood of descent.
- In practice a numerical integration "leap-frog" scheme is used to integrate the IVP (A.3)

  Compute for k=0,1,2,… and time step Δt

$$\boldsymbol{x}^{k+1} = \boldsymbol{x}^k + \boldsymbol{v}^k \Delta t$$
$$\boldsymbol{v}^{k+1} = \boldsymbol{v}^k + \boldsymbol{a}^{k+1} \Delta t \tag{A.4}$$

  where $\boldsymbol{a}^k = -\nabla f(\boldsymbol{x}^k), \quad \boldsymbol{v}^0 = \frac{1}{2}\boldsymbol{a}^0 \Delta t$

- A typical interfering strategy is

  If $\|\boldsymbol{v}^{k+1}\| \geq \|\boldsymbol{v}^k\|$ continue

  else

  set $\boldsymbol{v}^k = \dfrac{\boldsymbol{v}^{k+1} + \boldsymbol{v}^k}{4}, \quad \boldsymbol{x}^k = \dfrac{\boldsymbol{x}^{k+1} + \boldsymbol{x}^k}{2}$ (A.5)

  compute new $\boldsymbol{v}^{k+1}$ and continue.
- Further heuristics are used to determine an initial Δt, to allow for the magnification and reduction of Δt, and to control the step size.

LFOPC: Modification for constrained problems

Constrained optimization problems are solved by the application, in three phases, of LFOP to a penalty function formulation of the problem [A3,A4]. Given a function $f(\boldsymbol{x})$, with equality constraints h_i=0 (i=1,2,…,r) and inequality constraints $g_j \leq 0$ (j=1,2,…,m) and penalty parameter $\mu >> 0$, the penalty function problem is to minimize

$$P(\boldsymbol{x},\mu) = f(\boldsymbol{x}) + \sum_{i=1}^{r} \mu h_i^2(\boldsymbol{x}) + \sum_{j=1}^{m} \beta_j g_j^2(\boldsymbol{x}) \tag{A.6}$$

$$\text{where } \beta_j = \begin{cases} 0 \text{ if } g_j(\boldsymbol{x}) \le 0 \\ \mu \text{ if } g_j(\boldsymbol{x}) > 0 \end{cases}$$

Phase 0: Given some $\boldsymbol{x}^0$, then with the overall penalty parameter $\mu = \mu_0 (= 10^2)$ apply LFOP to $P(\boldsymbol{x},\mu_0)$ to give $\boldsymbol{x}^*(\mu_0)$

Phase 1: With $\boldsymbol{x}^0 = \boldsymbol{x}^*(\mu_0)$, $\mu = \mu_1 (= 10^4)$ apply LFOP to $P(\boldsymbol{x},\mu_1)$ to give $\boldsymbol{x}^*(\mu_1)$ and identify active constraints $i_a = 1,2,\ldots,n_a$; $g_{i_a}(\boldsymbol{x}^*(\mu_1)) > 0$

Phase 2: With $\boldsymbol{x}^0 = \boldsymbol{x}^*(\mu_1)$, use LFOP to minimize

$$P_a(\boldsymbol{x},\mu_1) = \sum_{i=1}^{r} \mu_1 h_i^2(\boldsymbol{x}) + \sum_{i_a=1}^{n_a} \mu_1 g_{i_a}^2(\boldsymbol{x}) \tag{A.7}$$

to give $\boldsymbol{x}^*$.

REFERENCES

A1. J.A. Snyman, *'A new and dynamic method for unconstrained minimization'*, Appl. Math. Modeling. **6**, pp 449-462 (1982).

A2. J.A. Snyman, *'An improved version of the original leap-frog method for unconstrained minimization'*, Appl. Math. Modeling. **7**, pp 216-218 (1983).

A3. J.A. Snyman, W.J. Roux and N. Stander, *'A dynamic penalty function method for the solution of structural optimization problems'*, Appl. Math. Modeling. **180** (15), pp 371-386 (1994).

A4. J.A. Snyman, *'The LFOPC leap-frog algorithm for constrained optimization'*, Computers and Mathematics with Applications, **40**, pp 1085-1096 (2000).

APPENDIX B:

Compact disc with Vehsim2d (demonstration version)

Appendix B: Compact disc with Vehsim2d (demonstration version)

Note:

Vehsim2d uses a graphical user interface (GUI) operating in a ***Microsoft Windows 95/98/2K/NT*** environment. It was developed using Microsoft Visual Basic 6.0 (Enterprise edition).

Installation instructions:

Run the program Vehsim2d_Setup.exe that can be found on the CD. This will run the setup program for installation of the Vehsim2d/LFOPC program and the associated help files.